The Dissertation Committee for Charles Daniel Varnado Jr. Certifies that this is the approved version of the following dissertation:

Design, Synthesis, and Evaluation of New Organometallic and Polymeric Materials for Electrochemical Applications

Committee:

Christopher W. Bielawski, Supervisor

Allen J. Bard

Arumugam Manthiram

Jonathan L. Sessler

C. Grant Willson

Design, Synthesis, and Evaluation of New Organometallic and Polymeric Materials for Electrochemical Applications

by

Charles Daniel Varnado Jr., B. S.; M. A.

Dissertation

Presented to the Faculty of the Graduate School of

The University of Texas at Austin

in Partial Fulfillment

of the Requirements

for the Degree of

Doctor of Philosophy

The University of Texas at Austin

August 2013

Dedication

To my family, for their love and support.

Acknowledgements

First and foremost, I am grateful to my research advisor, Prof. Christopher W. Bielawski, for his passion and commitment to good science and hard work, for his unending patience, and for taking a chance with giving me place in his group. I would also like to thank my other committee members: Prof. Allen J. Bard, Prof. Arumugam Manthiram, Prof. Jonathan L. Sessler, and Prof. C. Grant Willson.

I am grateful to all of the Bielawski group members, past and present, from whom I have learned so much. Among these individuals I must specifically thank Dr. Dimitri Khramov for sharing his detailed knowledge of ferrocene chemistry, Dr. Evie Rosen and Dr. Kuppuswamy Arumugam, with whom I worked closely on multiple projects, and also others in the group who were friendly and helped me develop my skills as a chemist: Dr. Daniel Coady, Dr. Justin Kamplain, Dr. Brian Long, Daphne Sung, Dr. Kyle Williams, Dr. Brent Norris, Dr. Kelly Wiggins, Dr. Beth Neilson, Dr. Daniel Dreyer, Jonathan Moerdyk, Robert Ono, Johnathan Brantley, Garrett Blake, Alex Todd, Mary Collins, Lauren Kang, Andrea Carranza, Michael Ortiz, Dr. Andrew Tennyson, and Dr. Todd Hudnall. It has been a crazy ride.

I am also grateful to my collaborators in Dr. Arumugam Manthiram's research group from whom I was fortunate to learn about fuel cells and lithium ion batteries: Dr. Yongzhu Fu, Dr. Wei Li, Dr. Xinsheng Zhao, Dr. Zicheng Zuo, and Dr. Katharine Harrison.

Many thanks to Penny Kile who relentlessly cut through bureaucratic red tape with a heart full of love and fire. Thanks also to Betsy Hamblen, and all of the others in the graduate studies office who were very helpful along the way. Many thanks to Vince

Lynch and Steve Swinnea for help with X-ray techniques. Thanks also to Steve Sorey and Angela Spangenberg for helping with NMR analyses. Thanks also to Michael Ronalter for helping me to maintain structurally sound and intact apparatuses for conducting science.

I thank my undergraduate research advisors from Stephen F. Austin State University: Dr. Chunmei Li and Dr. Russell Franks and other professors who were an inspiration: Dr. Michael Janusa, and Dr. Alex Frantzen, Dr. Michele Harris, and Dr. Richard Langley, and especially Dr. Lu Yu who initially pushed me down this path.

I thank the friends in the scientific community I made along the way for their support and good conversation: Dr. Derek Laws, Dr. John Hardy, Dr. Brian Zaccheo, Pina Chesnut, and my close friends who tolerated my absence while I was attending graduate school: David Carson Fuls, Daniel Keesee, Dr. Yoshiharu Kobayashi, Mary and Phil McGehee, Kate Patchett, and Lisa Audiffred. I thank all the other people who I encountered a long the way for their various contributions.

I thank my entire family for their support. In particular, I thank Dana Varnado, Danny Varnado, Rachel Varnado, William Franklin, Christine Varnado, and Karen Hebert. I would not be who I am today without you all.

Finally, I give thanks to the Great Spirit for smiling upon my life and watching over my science.

Design, Synthesis, and Evaluation of New Organometallic and Polymeric Materials for Electrochemical Applications

Charles Daniel Varnado Jr., Ph.D.

The University of Texas at Austin, 2013

Supervisor: Christopher W. Bielawski

The efforts described in this thesis were bifurcated along two distinct projects, but generally were directed toward the development of new materials to solve outstanding issues in contemporary electrochemical applications. The first project involved the synthesis and application of redox-switchable olefin metathesis catalysts. N-heterocyclic carbenes (NHCs) bearing ferrocene and other redox-active groups were designed, synthesized, and incorporated into model iridium complexes to evaluate their intrinsic electrochemical and steric parameters. Using these complexes, the ability to switch the electron donating ability of the ligands via redox processes was quantified using a variety of electrochemical and spectroscopic techniques. The donicity was either enhanced or attenutated upon reduction or oxidation of the redox-active group, respectively. The magnitude of the change in donicity upon reduction or oxidation did not vary significantly as a function of the proximity of the redox-active group from the metal center. Thus, other factors, including synthetic considerations, sterics, and redox potential requirements, were determined to guide ligand design. Regardless, redox-active NHCs were adapted into ruthenium-based olefin metathesis catalysts and used to gain control control over various ring-opening metathesis polymerizations and ring-closing metathesis reactions.

The second project was focused on the development of new basic polymers for acid/base crosslinked proton exchange membranes intended for applications in direct methanol fuel cells. Polymers containing pendant pyridinyl and pyrimidinyl groups were obtained via the post polymerization functionalization of UDEL® poly(sulfone) and then blended with sulfonated poly(ether ether ketone) (SPEEK). Fuel cells containing these blends were found to exhibit reduced methanol crossover, higher open circuit voltages, and higher maximum power densities compared to plain SPEEK. The differences in fuel cell performance were attributed to the basicity and sterics of the pendant N-heterocycles.

Table of Contents

List of Figures

List of Schemes

List of Tables

Chapter 1: Introduction

OVERVIEW

This thesis describes two projects that focus on the development of new materials to address contemporary problems in electrochemistry. The first project focuses on the synthesis and study of redox-active N-heterocyclic carbenes (NHCs) and their applications in redox-switchable olefin metathesis. The second project describes the synthesis and characterization of new basic polymers and their incorporation into acid/base blend proton exchange membranes for application in direct methanol fuel cells.

REDOX SWITCHABLE CATALYSIS

Stimuli responsive catalysts[1,2] have the potential to impart improved control over the outcome of chemical reactions. Judicious incorporation of a group that responds to changes in pH, different wavelengths of light, the application of mechanical force, or an applied potential in a way that alters the intrinsic chemistry exhibited by a catalyst can enable the switching of activities and/or selectivities. Of the various choices of external stimuli, redox processes are particularly appealing because electrochemical conditions may be conveniently manipulated and are often orthogonal to chemical processes. Redox-switchable catalysis[3] (RSC) (Scheme 1.1) can utilize the sensitivity of many transition metal catalysts to minute differences in the amount of electron density at the metal center, which can be tuned by the choice of supporting ligands.[4] Incorporation of a redox-active group allows the electron donicity of the ligand, and consequently the electron richness of the ligated metal center, to be altered by electrochemically changing the redox state. Moreover, if the ligand-centered oxidation or reduction process is reversible, then the catalyst can be switched multiple times between two distinct states of catalytic activities.

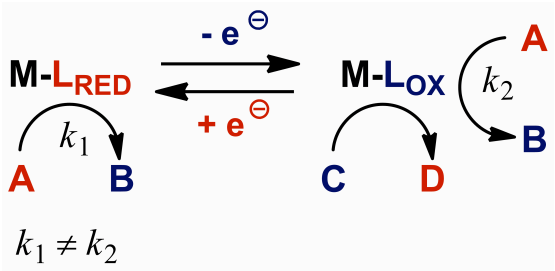

Scheme 1.1 Redox-Switchable Catalysis. A catalytically active metal center, M converts reactant A to product B at rate k_1 when the ligand is in the reduced state. Upon oxidation, the rate of conversion for A to B, k_2 may be altered and/or the resultant catalyst may facilitate an entirely different process (*e.g.*, C to D).

In 1995, Mark Wrighton and coworkers[5] reported a cobaltocene-containing rhodium complex that could be used to favor hydrosilations or hydrogenations depending on the oxidation state of the redox active moiety. Gibson and Long later reported a ferrocene-containing lactide polymerization catalyst that enabled the rate of the reaction to be reversibly switched by an order of magnitude by changing the oxidation state of the iron centers.[6] Although a handful of redox switchable catalysts have been reported,[5-7] the range of processes that can be controlled *via* RSC is ultimately limited by the choice of available ligands. For example, most redox-switchable ligands are multidentate, whereas many active catalysts require a monodentate ligand. A general solution to this limitation may be found within the N-heterocyclic carbenes (NHCs).

NHCs (Figure 1.1A) are an emerging class of ligands that have become relevant to many important catalytic processes (*e.g.* various Pd- and Ni-catalyzed cross coupling reactions[7e,8] and olefin metathesis[9]) due to enhanced performance over traditional ligands such as phosphines. The superior performance of NHCs is attributed to their strongly donating properties,[10] as well as their significant steric bulk that can stabilize a ligated metal center. Moreover, since NHCs coordinate in monodentate fashion to nearly all

transition metals, new developments in NHC design are expected to be broadly applicable.[11]

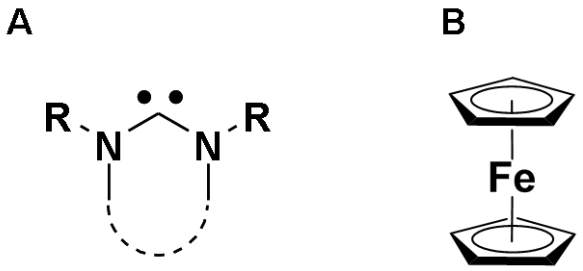

Figure 1.1 General structure of N-heterocyclic carbenes (A) and ferrocene (B)

Although there are a few reports of redox-active NHCs in the literature, these ligands have not yet been extensively investigated for RSC.[12] To impart redox-switchable functions to NHCs, we incorporated ferrocene (Figure 1.1B) or quinone groups. These two moieties exhibit reversible electrochemistry and participate in complimentary redox processes (*i.e* the ferrocene undergoes an oxidation; the quinone undergoes a reduction). Herein we discuss our investigation into the coordination chemistry and electrochemistry of a series of redox-active NHCs (see Figure 1.2 for examples and Chapters 2[13] and 3[14] for more details). The majority of the NHCs described herein contain ferrocene,[15] which was chosen for its electrochemical reversibility, chemical stability in both oxidation states, and because the cyclopentadienyl rings can be functionalized in a variety of ways to allow incorporation into the NHC scaffold. To evaluate the steric and electronic properties of the new NHCs, the ligands were incorporated into model iridium complexes. The resultant iridium complexes were subjected to a series of electrochemical and spectroelectrochemical experiments to quantify the donicities of the NHCs, as well as the change in their donicities in response to redox processes. As anticipated, donicity

increased upon ligand reduction and decreased in the cases of ligand oxidation. Unexpectedly, however, the magnitude of the change in donicity in response to reduction or oxidation did not vary significantly as a function of the proximity of the redox-active group to the metal center. Therefore, other factors should be considered when designing new redox-active NHC-based ligands, including synthesis sterics, and redox potential requirements.

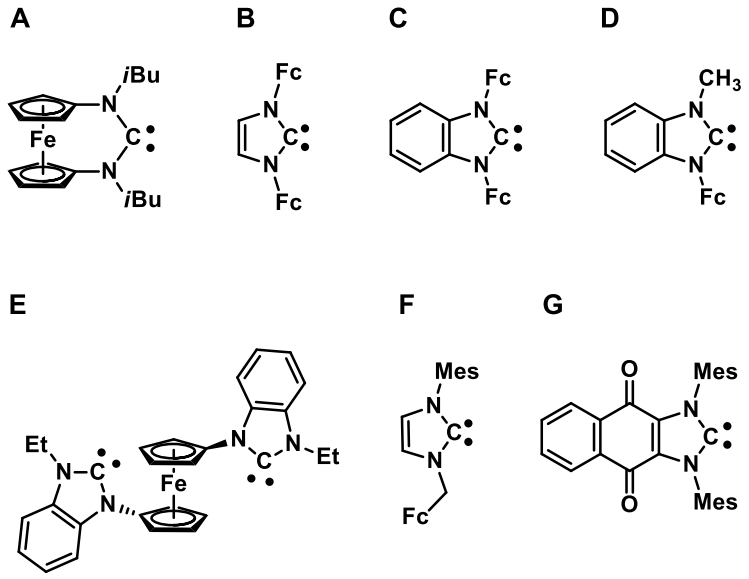

Figure 1.2 Examples of various redox-active NHCs studied herein.

OLEFIN METATHESIS

An ideal candidate for the application of RSC is olefin metathesis, a powerful synthetic method for which the 2005 Nobel Prize in chemistry was awarded.[16] Olefin metathesis catalysts facilitate the redistribution of C-C double bonds and have been used in a variety of applications.[17] Although multicomponent catalyst systems that are capable of performing such transformations have been known for decades,[18] the development of

single site homogenous catalysts based on tungsten, molybdenum[19] and ruthenium caused olefin metathesis to blossom as a broadly-applicable synthetic technique (see Figure 1.3 for catalysts and Scheme 1.2 for representative metathesis processes). A breakthrough in this regard was the development of the Ru-based Grubbs first generation catalyst (**G1**).[20] Moreover, it was later discovered that replacing one of the tricyclohexyl phosphine ligands with a more donating NHC resulted in a catalyst (**G2**)[9c] that exhibited enhanced activity without sacrificing functional-group tolerance.[9] Given this known trend in increasing activity as a function of the donicity of the supporting ligand,[17a] the Grubbs-type catalyst is an ideal candidate for controlling catalytic activity *via* a redox-switchable ligand.

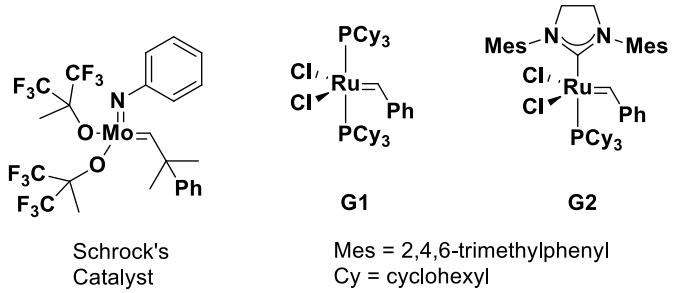

Figure 1.3 Examples of commercially available olefin metathesis catalysts.

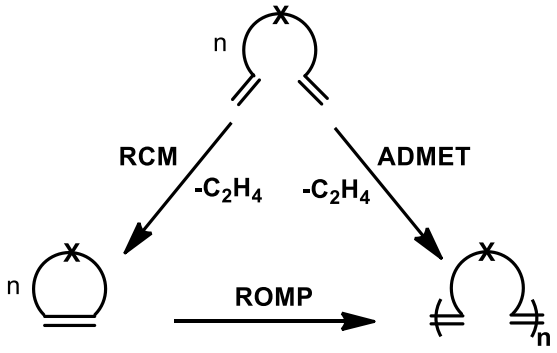

Scheme 1.2 Selected olefin metathesis processes.

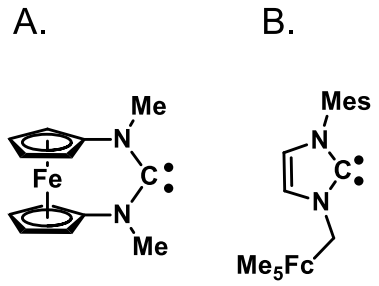

Figure 1.4 Examples of Ferrocenyl NHCs optimized for olefin metathesis catalysts.

REDOX SWITCHABLE OLEFIN METATHESIS CATALYSTS

Ligands containing ferrocene groups have previously been incorporated into Ru-based olefin metathesis catalysts as phase tags whereby ligand oxidation mediated a change in solubility and facilitated catalyst recovery.[21] Efforts toward using ligand oxidation as a means to bias the instrinsic E:Z selectivities displayed by a Ru catalyst bearing a ligand with pendant ferrocenyl substituents have also been reported.[22] In contrast, the use of a ferrocene-containing ligand to modify the activity of a Ru-based olefin metathesis catalyst by electrochemically tuning the donating ability of the ligand has not previously been reported.

Due to the strong electron donating ability and reversible electrochemistry of diaminocarbene[3]ferrocenophanes (FcDACs), a class of NHCs that contain a ferrocene moiety in the backbone of the NHC (See Figures 1.3A and 1.4A for specific examples, and Chapter 4 for full discussion), FcDACs were considered promising choices for preparing redox-switchable olefin metathesis catalysts. However, the first FcDACs,[23] bearing phenyl or *iso*-butyl N substituents were too bulky to allow isolation of stable ruthenium complexes. Therefore an optimized FcDAC bearing the smallest possible N-substituents, methyl groups (Figure 1.4A) was synthesized, and incorporated into a Grubbs second generation indenylidene-type complex[24] (Figure 1.5A). Gratifyingly, the rate of the ring-opening metathesis polymerization (ROMP) of *cis,cis*-1,5-cyclooctadiene

could be controlled by changing the redox state of the FcDAC (Chapter 4). Despite this successful proof of concept, however, catalyst stability and the degree of redox switchability were found to be limited, a result that was partially attributed to iron and ruthenium oxidation processes that occur at overlapping potentials.

Efforts were subsequently directed toward incorporating the ferrocene unit into a ligand class known to afford stable and active complexes, the imidazolylidenes. An imidazolylidene featuring a mesityl substituent, to shield the ruthenium center, and a ferrocenylmethyl group (Figure 1.2F) was incorporated into a Hoveyda-Grubbs type complex.[25] The performance of this catalyst was tested toward the ring-closing metathesis (RCM) of diethyl diallylmalonate. The rate of the reaction was attenuated by an order of magnitude upon oxidation of the pendent ferrocene group. After subsequent reduction of the tethered ferrocenium species with decamethylferrocene, the inital rate was partially restored. However, this ligand would not be applicable to other classes of ruthenium metathesis catalysts because in most other cases the Ru-centered oxidation occurs at a lower potential that would overlap with the ferrocene oxidation. Therefore, selective ligand oxidation and the consequent reversibility would be precluded.

Concomittant Ru-centered oxidation was a key challenge when attempting to use the $Fe^{II/III}$ redox couple to tune a ligated Ru center, as the $Ru^{II/III}$ couple often occurs at a similar or overlapping potential. To conduct RSC with this system, selective oxidation of the ferrocene was found to be critical as ruthenium oxidation can lead to decomposition. To increase the window between the two oxidation processes, efforts were directed to lowering the Fe^{II}/Fe^{III} oxidation potential by modifying the ferrocene. Specifically, pentamethylferrocene moieties were incorporated into a second generation ligand (Figure 1.4B). Since pentamethylferrocene compounds are known to exhibit reversible electrochemistry like the parent ferrocene but are easier to oxidize by ~300 mV,[26]

incorporating this modified ligand into an analogous catalyst (Figure 1.5B) would allow the use of a weaker oxidant to switch the rate of an RCM reaction and allow the entire process to be carried out with greater reversibility. Ultimately, it was found that oxidation with ferrocenium tetrafluoroborate attenuated the rate of RCM by an order of magnitude, and subsequent reduction restored activity to 96% of the initial state, demonstrating excellent reversibility. Furthermore, this ligand should provide a general solution to the overlapping oxidation potential problem and facilitate other redox switchable metathesis processes.

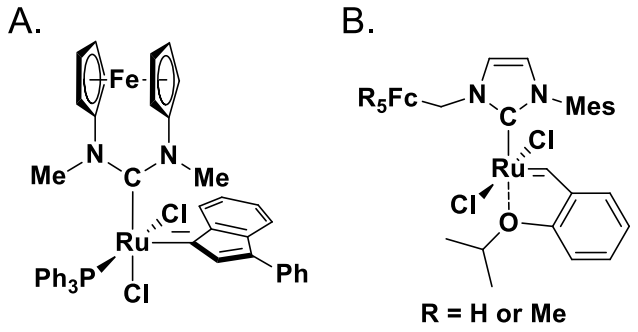

Figure 1.5 Redox-switchable metathesis catalysts studied herein.

NEW PROTON EXCHANGE MEMBRANES FOR METHANOL FUEL CELLS

Fuel cells convert the chemical energy stored in a fuel directly into electrical energy. Several different fuel cell technologies have been developed, utilizing different fuels (hydrogen, hydrocarbons, methanol), at different temperature ranges, and on different scales of energy output.[27] Proton exchange membrane fuel cells operate at low temperature (~65 to 90°C), and run on either hydrogen or methanol. Compared to hydrogen, aqueous methanol is nonflammable and easy to handle. Furthermore, liquid methanol has a high energy density. Collectively, these attributes render methanol an attractive choice for powering small electrical devices such as cell phones and laptops. In contrast to lithium ion batteries which require recharging cycles, a direct methanol fuel

cell (DMFC) is advantageous in that it would rely on an easily replaceable portable cartridge of liquid fuel.

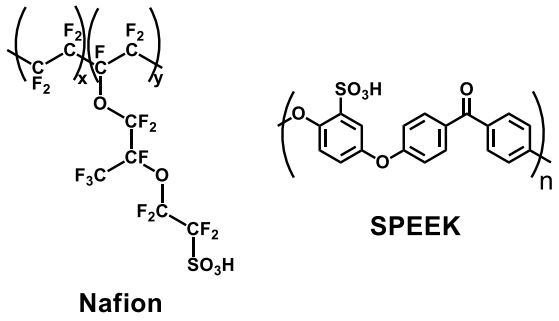

Figure 1.6 The structure of Nafion and SPEEK

A key challenge that currently impedes widespread commercialization of the DMFC is the lack of an inexpensive and sufficiently high-performing proton exchange membrane material. The role of this component is to conduct the protons generated by methanol oxidation at the anode to the cathode where they are consumed in the oxygen reduction reaction. Moreover, the membrane must also prevent methanol from crossing over from the anode to the cathode, which wastes fuel and poisons the cathode catalyst reducing cell voltage. Nafion® is the industry standard membrane material, and although expensive, performs well for hydrogen fuel cells on account of its excellent chemical stability and proton conductivity. However, Nafion is not suitable for the DMFC because the phase separated morphology results in high methanol permeability.

Sulfonated poly(ether ether ketone) (SPEEK) has been investigated as a low cost alternative to Nafion. SPEEK is less conductive but its morphology consists of hydrophilic regions that are smaller and more diffuse than those of Nafion, ultimately

resulting in reduced methanol crossover (Figure 1.6). Further improvements in methanol blocking ability are attainable through crosslinking (Figure 1.7). However, covalent crosslinks can result in brittle materials that are unsuitable for casting membranes. In contrast, ionic crosslinking *via* blending acid- and base-functionalized polymers can reduce methanol permeability while maintaining physical properties suitable for casting membranes.[28] Manthiram and coworkers have employed this approach successfully to generate high-performing membranes.[29] However, the reported syntheses of the basic polymers that were employed for crosslinking required cryogenic conditions and the use of a pyrophoric base. Collectively, these harsh and hazardous reaction conditions decreased the commercial viability of this approach. Thus, we pursued alternative syntheses of similar materials with the specific goal of finding reaction conditions that required neither cryogenic conditions nor pyrophoric bases.

Employing a two-step high temperature iridium-catalyzed C-H borylation followed by Suzuki coupling, allowed access to pyridine- and pyrimidine- functionalized poly(sulfone)s. These novel, basic polymers were blended with SPEEK to afford acid/base blend membranes. The properties and methanol fuel cell performance of the new membranes were evaluated (see Chapter 6). Compared to plain SPEEK membranes, the optimized blends gave lower methanol crossover, resulting in improved open circuit voltages and maximum power densities. Subtle differences in performance were attributed to variation in basicity and sterics of the basic groups. Collectively, these improvements will enhance the prospect of commercializing DMFCs.

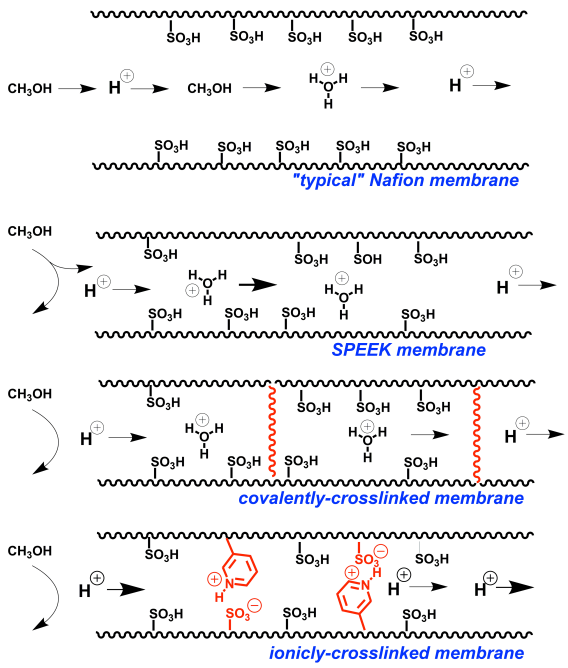

Figure 1.7 Illustration of differences in the ionic channels between various membranes.

ACKNOWLEDGEMENTS

Although this dissertation represents the author's thesis research, portions have been reprinted, with permission, from published works. Moreover, numerous individuals have contributed in some way to the work described herein. Their roles are respectfully acknowledged and their efforts are delineated at the beginning of each chapter. Chapter 1 was written entirely by the author.

REFERENCES

(1) Lüning, U. *Angew. Chem. Int. Ed.* **2012**, *51*, 8163.

(2) Leibfarth, F. A.; Mattson, K. M.; Fors, B. P.; Collins, H. A.; Hawker, C. J. *Angew. Chem. Int. Ed.* **2013**, *52*, 199.

(3) Allgeier, A. M.; Mirkin, C. A. *Angew. Chem. Int. Ed.* **1998**, *37*, 894–908.

(4) (a) Hadei, N.; Kantchev, E. A. B.; O'Brien, C. J.; Organ, M. G. *Org. Lett.* **2005**, *7*, 1991; (b) O'Brien, C. J.; Kantchev, E. A. B.; Chass, G. A.; Hadei, N.; Hopkinson, A. C.; Organ, M. G.; Setiadi, D. H.; Tang, T.-H.; Fang, D.-C. *Tetrahedron* **2005**, *61*, 9723; (c) Vorfalt, T.; Leuthäusser, S.; Plenio, H. *Angew. Chem., Int. Ed.* **2009**,

48, 5191–5194; (d) Khramov, D. M.; Rosen, E. L.; Er, J. A. V.; Vu, P. D.; Lynch, V. M.; Bielawski, C. W. *Tetrahedron* **2008**, *64*, 6853–6862.

(5) Lorkovic, I. M.; Duff, R. R., Jr.; Wrighton, M. S. *J. Am. Chem. Soc.* **1995**, *117*, 3617–3618.

(6) Gregson, C. K. A.; Gibson, V. C.; Long, N. J.; Marshall, E. L.; Oxford, P. J.; White, A. J. P. *J. Am. Chem. Soc.* **2006**, *128*, 7410–7411.

(7) (a) Broderick, E. M.; Guo, N.; Vogel, C. S.; Xu, C.; Sutter, J.; Miller, J. T.; Meyer, K.; Mehrkhodavandi, P.; Diaconescu, P. L. *J. Am. Chem. Soc.* **2011**, *133*, 9278–9281; (b) Broderick, E. M.; Guo, N.; Wu, T.; Vogel, C. S.; Xu, C.; Sutter, J.; Miller, J. T.; Meyer, K.; Cantat, T.; Diaconescu, P. L. *Chem. Commun.* **2011**, *47*, 9897–9899; (c) Ringenberg, M. R.; Kokatam, S. L.; Heiden, Z. M.; Rauchfuss, T. B. *J. Am. Chem. Soc.* **2008**, *130*, 788–789; (d) Boyer, J. L.; Cundari,T. R.; DeYonker, N. J.; Rauchfuss, T. B.; Wilson, S. R. *Inorg. Chem.* **2008**, *48*, 638–645; (e) Tennyson, A. G.; Lynch, V. M.; Bielawski, C. W. *J. Am. Chem. Soc.* **2010**, *132*, 9420.

(8) (a) Correa, A.; Marion, N.; Fensterbank, L.; Malacria, M.; Nolan, S. P.; Cavallo, L. *Angew. Chem. Int. Ed.* **2008**, *47*, 718; (b) Fructos, M. R.; Belderrain, T. R.; de Frémont, P.; Scott, N. M.; Nolan, S. P.; Díaz-Requejo, M. M.; Pérez, P. J. *Angew. Chem. Int. Ed.* **2005**, *44*, 5284; (c) Gimeno, A.; Medio-Simón, M.; de Arellano, C. R. r.; Asensio, G.; Cuenca, A. B. *Org. Lett.* **2010**, *12*, 1900; (d) Kinder, R. E.; Zhang, Z.; Widenhoefer, R. A. *Org. Lett.* **2008**, *10*, 3157; (e) Marion, N.; de Fremont, P.; Lemiere, G.; Stevens, E. D.; Fensterbank, L.; Malacria, M.; Nolan, S. P. *Chem. Commun.* **2006**, 2048; (f) Nolan, S. P. *Acc. Chem. Res.*, null; (g) Organ, M. G.; Abdel-Hadi, M.; Avola, S.; Hadei, N.; Nasielski, J.; O'Brien, C. J.; Valente, C. *Chem. Eur. J.* **2007**, *13*, 150; (h) Seo, H.; Roberts, B. P.; Abboud, K. A.; Merz, K. M.; Hong, S. *Org. Lett.*, *12*, 4860; (i) Kantchev, E. A. B.; O'Brien, C. J.; Organ, M. G. *Angew. Chem. Int. Ed.* **2007**, *46*, 2768; (j) O'Brien, C. J.; Kantchev, E. A. B.; Valente, C.; Hadei, N.; Chass, G. A.; Lough, A.; Hopkinson, A. C.; Organ, M. G. *Chem. Eur. J.* **2006**, *12*, 4743.

(9) (a) Huang, J.-K.; Stevens, E. D.; Nolan, S. P.; Petersen, J. L. *J. Am. Chem. Soc.* **1999**, *121*, 2674; (b) Scholl, M.; Trnka, T. M.; Morgan, J. P.; Grubbs, R. H. *Tet. Lett.* **1999**, *40*, 2674; (c) Scholl, M.; Ding, S.; Lee, C. W.; Grubbs, R. H. *Org. Lett.* **1999**, *1*, 953; (e) Fernández, I.; Lugan, N.; Lavigne, G. *Organometallics* **2012**, *31*, 1155; (g) Grubbs, R. H.; Trnka, T. M. *Ruthenium-Catalyzed Olefin Metathesis*; Wiley VCH, Weinheim, Germany, 2005; (h) Jafarpour, L.; Nolan, S. P. *J. Organomet. Chem.* **2001**, *617-618*, 17; (f) Weskamp, T.; Schattenmann, W. C.; Spiegler, M.; Herrmann, W. A. *Angew. Chem. Int. Ed.* **1998**, *37*, 2490.

(10) (a) Scott, N. M.; Clavier, H.; Mahjoor, P.; Stevens, E. D.; Nolan, S. P. *Organometallics* **2008**, *27*, 3181–3186; (b) Jafarpour, L.; Stevens, E. D.; Nolan, S. P. *J. Organomet. Chem.* **2000**, *606*, 49–54.

(11) For excellent reviews, see: Hahn, F. E.; Jahnke, M. C. *Angew. Chem. Int. Ed.* **2008**, 47, 3122; Herrmann, W. A.; Köcher, K. Angew. Chem. Int. Ed. **1997**, *36*, 2163; N-Heterocyclic Carbenes in Transition Metal Catalysis, F. Glorius, ed., Springer-Verlag, Berlin, Germany, 2007; N-Heterocyclic Carbenes in Synthesis, S. P. Nolan, ed., Wiley-VCH, Weinheim, 2006

(12) (a) Arduengo III, A. J.; Bannenberg, T. P.; Tapu, D.; Marshall, W. J. *Tetrahedron Lett.* **2005**, *46*, 6847; (b) Arduengo, III, A. J.; Bannenberg, T. P.; Tapu, D.; Marshall, W. J. *Chem. Lett.* **2005**, *34*, 1010; (c) Arduengo, III, A. J.; Iconaru, L. I. *Dalton Transactions* **2009**, 6903; (d) Arduengo, III, A. J.; Tapu, D.; Marshall, W. J. *J. Am. Chem. Soc.* **2005**, *127*, 16400; (e) Arduengo, A. J.; Tapu, D.; Marshall, W. J. *Angew. Chem. Int. Ed.* **2005**, *44*, 7240; (f) Arduengo, A. J.; Tapu, D.; Marshall, W. J. *Angew. Chem.* **2005**, *117*, 7406; (g) Bertogg, A.; Camponovo, F.; Togni, A. *Eur. J. Inorg. Chem.* **2005**, *2005*, 347; (h) Bildstein, B.; Malaun, M.; Kopacka, H.; Ongania, K.-H.; Wurst, K. *J. Organomet. Chem.* **1998**, *552*, 45; (i) Bildstein, B.; Malaun, M.; Kopacka, H.; Ongania, K.-H.; Wurst, K. *J. Organomet. Chem.* **1999**, *572*, 177; (j) Bildstein, B.; Malaun, M.; Kopacka, H.; Wurst, K.; Mitterbock, M.; Ongania, K.-H.; Opromolla, G.; Zanello, P. *Organometallics* **1999**, *18*, 4325; (k) Bolm, C.; Kesselgruber, M.; Raabe, G. *Organometallics* **2002**, *21*, 707; (l) Debono, N.; Labande, A. s.; Manoury, E.; Daran, J.-C.; Poli, R. *Organometallics*, *29*, 1879; (m) Gischig, S.; Togni, A. *Organometallics* **2004**, *23*, 2479; (n) Jackstell, R.; Frisch, A.; Beller, M.; Röttger, D.; Malaun, M.; Bildstein, B. *J. Mol. Catal. A: Chem.* **2002**, *185*, 105; (o) Seo, H.; Kim, B. Y.; Lee, J. H.; Park, H.-J.; Son, S. U.; Chung, Y. K. *Organometallics* **2003**, *22*, 4783; (p) Seo, H.; Park, H.-j.; Kim, B. Y.; Lee, J. H.; Son, S. U.; Chung, Y. K. *Organometallics* **2003**, *22*, 618; (q) Siemeling, U.; Auch, T. C.; Kuhnert, O.; Malaun, M.; Kopacka, H.; Bildstein, B. *Z. Anorg. Allg. Chem.* **2003**, *629*, 1334; (r) Siemeling, U.; Farber, C.; Bruhn, C. *Chem. Commun.* **2009**, 98; (s) Siemeling, U.; Farber, C.; Bruhn, C.; Leibold, M.; Selent, D.; Baumann, W.; von Hopffgarten, M.; Goedecke, C.; Frenking, G. *Chemical Science* **2010**, *1*, 697; (t) Labande, A.; Daran, J.-C.; Manoury, E.; Poli, R. *Eur. J. Inorg. Chem.* **2007**, *2007*, 1205; (u) Siemeling, U.; Färber, C.; Leibold, M.; Bruhn, C.; Mücke, P.; Winter, R. F.; Sarkar, B.; von Hopffgarten, M.; Frenking, G. *Eur. J. Inorg. Chem.* **2009**, *2009*, 4607.

(13) Rosen, E. L.; Varnado, C. D., Jr.; Tennyson, A. G.; Khramov, D. M.; Kamplain, J. W.; Sung, D. H.; Cresswell, P. T.; Lynch, V. M.; Bielawski, C. W. *Organometallics* **2009**, *28*, 6695.

(14) Varnado Jr., C. D.; Lynch, V. M.; Bielawski, C. W. *Dalton Trans.* **2009**, 7253.

(15) (a) Kealy, T. J.; Pauson, P. L. *Nature* **1951**, *168*, 1039; (b) Miller, S. A.; Tebboth, J. A.; Tremaine, J. J. *J.Chem. Soc. (Resumed)* **1952**, 632; (c) Werner, H. *Angew. Chem. Int. Ed.* **2012**, *51*, 6052.

(16) (a) Chauvin, Y. *Adv. Synth. Catal.* **2007**, 349, 27; (b) Grubbs, R. H. *Adv. Synth. Catal.* **2007**, *349*, 34; (c) Schrock, R. R. *Adv. Synth. Catal.* **2007**, *349*, 41.

(17) (a) Trnka, T. M.; Grubbs, R. H. *Acc. Chem. Res.* **2001**, *34*, 18–29; (b) Ivin, K. J.; Mol, J. C. *Olefin Metathesis and Metathesis Polymerization*, 1st ed.; Academic Press: San Diego, CA, 1997; (c) Ivin, K. J. *J. Mol. Catal. A.: Chem.* **1998**, *133*, 1–16; (d) Grubbs R. H.; Chang, S. *Tetrahedron* **1998**, *54*, 4413–4450; (e) Grubbs, R. H. *Tetrahedron* **2004**, *60*, 7117–7140; (f) Buchmeiser, M. R. *Chem. Rev.* **2000**, *100*, 1565–1604; (g) Fürstner, A. *Angew. Chem. Int. Ed.* **2000**, *39*, 3012;

(18) (a) Eleuterio, H. S. Journal of Molecular Catalysis **1991**, *65*, 55-61. (b) Eleuterio, H. Chemtech, **1991**, *21*, 92-95. (c) Banks, R. L. *Chemtech* **1986**, *16*, 112-117. (d) Ivin, K. J.; Mol, J. C. Olefin Metathesis and Metathesis Polymerization, Acedemic Press: San Diego, 1997. (d) Crabtree, R. H. The Organometallic Chemistry of Transition Metal, 3rd ed.; Wiley and Sons: New York, 2001.

(19) (a) Schrock, R. R.; Depue, R. T.; Feldman, J.; Yap, K. B.; Yang, D. C.; Davis, W. M.; Park, L.; Dimare, M.; Schofiled, M.; Anhaus, J.; Walborsky, E.; Evitt, E.; Kruger, C.; Betz, P. *Organometallics*, **1990**, *9*, 2262-2275; (b) Schrock, R. R.; Murdzek, J. S.; Bazan, G. C.; Robbins, J.; Dimare, M.; Oregan, M. *J. Am. Chem. Soc.* **1990**, *112*, 3875-3886; (c) Schrock, R. R. *Science* **1983**, *219*, 13-18; (d) Schrock, R. R.; Depue, R. T.; Feldman, J.; Schaverien, C. J.; Dewan, J. C.; Liu, A. H. *J. Am. Chem. Soc.* **1988**, *110*, 1423-1435; (e) Sharp, P. R.; Holmes, S. J.; Schrock, R. R.; Churchill, M. R.; Wasserman, H. J. *J. Am. Chem. Soc.* **1981**, *103*, 965-966; (f) Feldman, J.; Schrock, R. R. Prog. *Inorganic Chem.* **1991**, *39*, 1.

(20) (a) Dias, E. L.; Nguyen, S. T.; Grubbs, R. H. J. Am. Chem. Soc. **1997**, *119*, 3887-3897; (b) Marsella, M. J.; Maynard, H. D.; Grubbs, R. H. *Angew. Chem. Int. Ed.* Engl. **1997**, *36*, 1101-1103; (c) Trnka, T. M.; Grubbs, R. H. *Accounts Chem. Res.* **2001**, *34*, 18-29; (d) Dias, E. L.; Grubbs, R. H. *Organometallics* **1998**, *17*, 2758-2767; (e) Schwab, P.; France, M. B.; Ziller, J. W.; Grubbs, R. H. *Angew. Chem. Int. Ed.* **1995**, *34*, 2039-2041; (f) Schwab, P.; Grubbs, R. H.; Ziller, J. W. *J. Am. Chem. Soc.* **1996**, *118*, 100-110.

(21) (a) Sußner, M.; Plenio, H. *Angew. Chem. Int. Ed.* **2005**, *44*, 6885–6888; (b) Liu, G.; He, H.; Wang, J. *Adv. Synth. Catal.* **2009**, *351*, 1610–1620.

(22) Peeck, L. H.; Leuthaüsser, S.; Plenio, H. *Organometallics* **2010**, *29*, 4339–4345.

(23) Khramov, D. M.; Rosen, E. L.; Lynch, V. M.; Bielawski, C. W. *Angew. Chem. Int. Ed.* **2008**, *47*, 2267.

(24) Varnado, C. D., Jr.; Rosen, E. L.; Collins, M. S.; Lynch, V. M.; Bielawski, C. W. *Dalton Trans.* **2013**, DOI: 10.1039/C3DT51278A.

(25) Arumugam, K.; Varnado, C. D., Jr.; Sproules, S.; Lynch, V. M.; Bielawski, C. W. *Chem. Eur. J.* **2013**, *19*, 10866.

(26) Bildstein, B.; Hradsky, A.; Kopacka, H.; Malleier, R.; Ongania, K.-H. *J. Organomet. Chem.* **1997**, *540*, 127.

(27) Carrette, L.; Friedrich, K. A.; Stimming, U. *Fuel Cells* **2001**, *1*, 5.

(28) Development and Understanding of New Membranes Based on Aromatic Polymers and Heterocycles for Fuel Cells. Ph.D. Dissertation, The University of Texas at Austin, August 2009.

(29) (a) Fu, Y.; Manthiram, A.; M. D., Guiver *Electrochem. Commun.* **2006**, *8*, 1386-1390; Fu, Y.; Manthiram, A. Guiver, M. D. *Electrochem. Commun.* **2007**, *9*, 905-910; (c) Lee, J. K.; Li, W.; Manthiram, A. *J. Electrochem. Soc.* **2009**, *156*, B46-B50; (d) Li, W.; Manthiram, A.; Guiver, M. D. *Electrochem. Solid State Lett.* **2009**, *12*, B180-184.

Chapter 2: Redox Active N-Heterocyclic Carbenes: Design, Synthesis, and Evaluation of Their Electronic Properties

Portions of this chapter were reprinted with permission from Rosen, E. L.; Varnado, C. D., Jr.; Tennyson, A. G.; Khramov, D. M.; Kamplain, J. W.; Sung, D. H.; Cresswell, P. T.; Lynch, V. M.; Bielawski, C. W. *Organometallics* **2009**, *28*, 6695. Copyright 2009 American Chemical Society. E. L. Rosen, D. M. Khramov, J. W. Kamplain, D. H. Sung, and P. T. Cresswell contributed to the synthesis and evaluation of the various complexes containing **2.2**, and **2.4**-**2.6**. V. M. Lynch assisted with the X-ray crystallography. E. L. Rosen, A. G. Tennyson, and C. W. Bielawski assisted with writing the aforementioned publication. I performed the multistep syntheses, characterization, and electrochemical studies of complexes containing **2.1** and **2.3**, and helped to write the aforementioned publication.

ABSTRACT

To investigate effects of redox active functional groups on the coordination chemistry and electronic properties of N-heterocyclic carbenes (NHCs), we prepared a series of complexes comprising 1,3-diferrocenylimidazolylidene and -benzimidazolylidene (**2.1** and **2.2**, respectively), 1-ferrocenyl-3-methyl and 1,3-diphenyl-5-ferrocenylbenzimidazolylidene (**2.3** and **2.4**, respectively), N,N'-diisobutyl-diaminocarbene[3]ferrocenophane (**FcDAC**), and 1,3-dimesitylnapthoquinoimidazolylidene (**NqMes**) ligands and coordinated [Ir(COD)Cl] (COD = 1,5-cyclooctadiene), $[Ir(CO)_2Cl]$ and $[M(CO)_5]$ (M = Cr, Mo, W) units. The coordination chemistry of the aforementioned NHCs was investigated by X-ray crystallography and their electronic properties were studied by NMR and IR spectroscopy, as well as electrochemistry. No significant variation in ν_{CO} was observed

among metal carbonyl complexes supported by **2.2**–**2.4** and **FcDAC**, indicating that the number (one vs. two) of redox-active groups, the location (N-atom vs. backbone) of the redox-active group, and carbene ring identities (strained 6-membered, non-aromatic vs. 5-membered, heteroaromatic) did not have a significant effect on ligand electron donating ability. Because the shifts in ν_{CO} upon oxidation of **2.1**–**2.3** and **FcDAC** were similar in magnitude but opposite in sign to **NqMes**, we conclude that the enhancement or attenuation of ligand donating is primarily Coulombic in origin (*i.e*. due to the molecule acquiring a positive or negative charge).

INTRODUCTION

Transition metal-based complexes containing redox active ligands have been used in diverse areas[1] including catalysis,[2,3] sensing,[4,5] and optical materials.[6,7] The appeal of ligands with redox active functional groups stems from their abilities to change the electronic properties of a metal without the need for further synthetic modifications. In many cases, these ligands exhibit reversible redox processes and therefore enable "switchable" control of the electronic properties of metals by chemical redox agents or bulk electrolysis. Examples of previously reported metal complexes with redox active ligands are shown in Figure 2.1.[2,3,8,9] It is important to note that these complexes, as well as many others, contain neutral ligands which are capable of adopting cationic states as well as those that transition to anionic states. Additionally, there are ligand classes where *multiple* oxidation states can be accessed.[10-13]

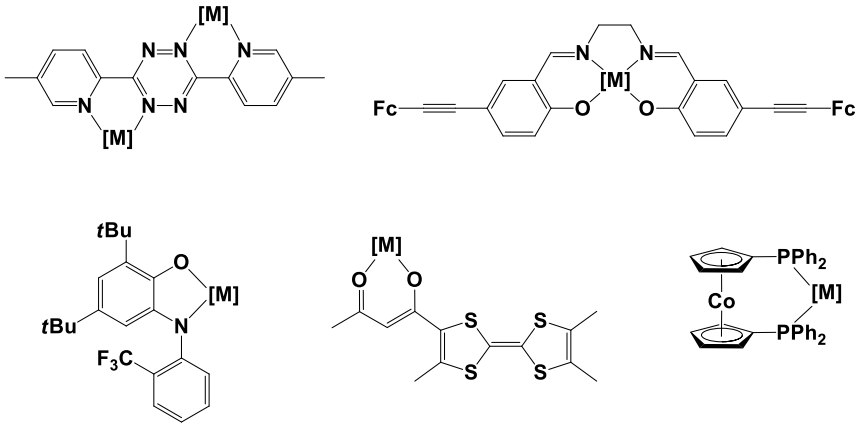

Figure 2.1 Examples of metal complexes supported by redox active ligands.

Oxidation or reduction of a substitutionally inert ligand can tune the electronic properties of a complex without changing the oxidation state of the metal or steric parameters.[14-16] These effects can be quantified *via* ligation to a transition metal–carbonyl complex followed by measurement of the carbonyl stretching frequency (ν_{CO}) as a function of ligand oxidation state. For example, the complexes shown in Figure 2.2 display shifts in carbonyl stretching energy ($\Delta\nu_{CO}$) of up to 35 cm^{-1}.[1,17-19] Although correlation between $\Delta\nu_{CO}$ and the characteristics of transition metal complexes is not well-understood,[20,21] ligands with a $\Delta\nu_{CO}$ value in the mid- to upper-end of this range often result an measurable influence. For example, a Re carbonyl complex containing a 1,1′-bis(diphenylphosphanyl)cobaltocene ligand shows $\Delta\nu_{CO}$ values from –11 to –17 cm^{-1}.[11] As a result, nucleophilic attack on the carbonyl groups was enhanced 200-fold upon oxidation of the metal center.

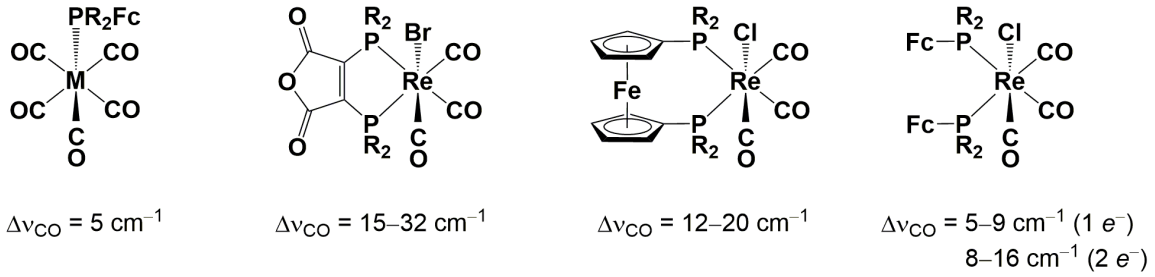

Figure 2.2 Selected examples of redox-switchable ligands. The absolute values of the change in metal–carbonyl stretching frequencies ($\Delta\nu_{CO}$) upon oxidation of the neutral ligands shown are indicated. R = Ph; M = Cr, Mo, W; Fc = ferrocene.

Despite their unique properties, many classes of redox active ligands suffer from a number of practical and fundamental limitations. A large majority of redox active ligands are either bi- or multidentate; monodentate analogues appear to be much less common.[18,22,23] Although multidentate ligands can afford stable complexes, the range of possible geometries is often restricted. Other limitations include difficulties associated with metal coordination and/or an inability to impart significant electronic changes at a metal center upon changing the oxidation state of its redox active ligand. Furthermore, some complexes exhibit irreversible electrochemical behavior, inhibiting widespread use in sensing and catalysis.[24,25] The development of new classes of redox active ligands could overcome these limitations.

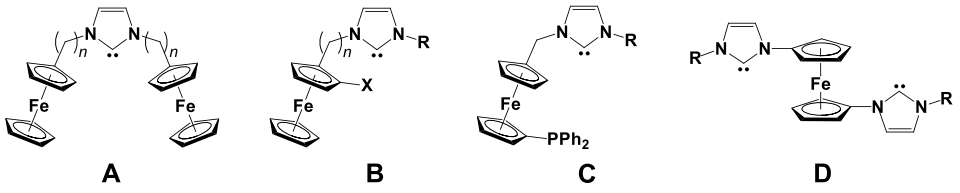

Figure 2.3 Examples of ferrocene-functionalized NHC-based ligands. n = 0, 1, or 2. X = donor group.

Over the past 50 years,[26-31] N-heterocyclic carbenes (NHCs)[32] and related compounds have become a versatile class of ligands for a broad range of transition metals.[33-43] One reason for this attention is the similarity of their coordination chemistry to phosphines.[38,44] However, due to their strong electron-donating abilities and unique steric parameters, NHCs often afford complexes that are relatively stable towards ligand displacement and show significantly improved catalyst activities.[45,46] Furthermore, NHCs can be synthesized from readily-available starting materials[47] using extensive metal complexation methodology via free NHCs[48] or transmetallation via Ag–NHC intermediates.[49] Despite these advantages, surprisingly few redox active NHCs and metal complexes thereof have been reported in the literature (see Figure 2.3 for examples).[50-59] Bildstein and co-workers reported[60,61] the first NHC containing N-ferrocenyl groups (**A** and **B**), but the ability of these redox active moieties to modulate electronic properties was not explored in detail. Although a $[W(CO)_5]$ complex supported by 1-ferrocenyl-3-methylbenzimidazolylidene has been prepared, its electronic properties were not studied as a function of the ferrocene oxidation state. A variety of NHC-supported complexes bearing N-ferrocenyl substituents have been reported, but these efforts have primarily focused on either chiral modification for asymmetric catalysis or to capitalize on the *steric* parameters of ferrocene rather than its *electrochemical* properties (*e.g.*, **C**),[56,58,59] with few exceptions (**D** in Figure 2.3, **FcDAC** in Figure 2.4).[62,63]

We recently introduced two classes of NHCs containing complementary redox active moieties. As shown in Figure 2.4, **FcDAC** is a N,N′-disubstituted diaminocarbene[3]ferrocenophane whereas **NqMes** features a naphthoquinone annulated to 1,3-mesitylimidazolylidene. The former can undergo oxidation (ferrocene ↔ ferrocenium), whereas the latter can undergo reduction (quinone ↔ semiquinone). Expanding the role of NHCs beyond simple phosphine analogues, we showed that both of

these ligands can adopt multiple oxidation states and alter the electron density of coordinated metals.[63,64,65]

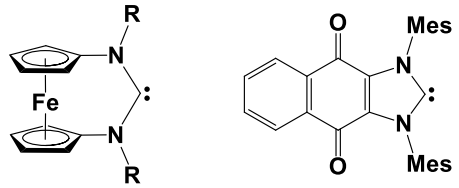

FcDAC **NqMes**

Figure 2.4 Complementary redox active carbenes. R = *iso*-butyl, Ph, or 2-Ad.[63,65] Mes = 2,4,6-trimethylphenyl.

Herein we report efforts to further explore how the incorporation of redox active functionalities into NHCs influences their coordination chemistry and electronic properties. As summarized in Figures 2.4 and 2.5, we sought to investigate the effects of various structural characteristics: (I) imidazolylidene vs. benzimidazolylidene frameworks (*e.g.*, **2.1** vs. **2.2**); (II) incorporating one vs. two ferrocene units (*e.g.*, **2.2** vs. **2.3**); (III) attaching a ferrocene unit to an NHC nitrogen atom vs. to the backbone of a benzimidazolylidene (*e.g.*, **2.3** vs. **2.4**); (IV) aromatic vs. non-aromatic cyclic NHCs (*e.g.*, **2.2** vs. **FcDAC**); and (V) oxidizable vs. reducible redox active functionalities (*e.g.*, **2** vs. **NqMes**). Fortunately, methodology has already been developed by us and others for preparing metal complexes of **2.1**,[57] **FcDAC**[63] and **NqMes**.[64] To access the remaining complexes, we improved the overall syntheses for **2.2**[60] and **2.3**[61] and developed a route to **2.4**. Given that the spectroscopic, structural and electrochemical properties of NHC-supported complexes of [Ir(COD)Cl] (COD = 1,5-cyclooctadiene) have been extensively explored,[66-70] analogous complexes containing **2.1**–**2.4**, **FcDAC** and **NqMes** were studied. Conversion of these complexes to $[Ir(CO)_2Cl]$ analogues was accomplished via treatment with CO (*g*), enabling more direct measurement of the metal electron density and ligand

donicity via IR spectroscopy.[66,67] We also pursued [M(CO)$_5$] (M = Cr, Mo, W) complexes supported by **2.1**–**2.4**, **FcDAC** and **NqMes**, given that analogous complexes supported by NHCs have been studied extensively by X-ray crystallography and IR spectroscopy.[61,71-85] Overall, we found that the NHC coordination chemistry and donating ability are most strongly influenced by the NHC backbone (*i.e.*, imidazolylidene vs. benzimidazolylidene vs. non-aromatic). We also discovered that the tunability of these redox active ligands is primarily determined by Coulombic factors: addition of a positive charge reduces NHC donating ability whereas a negative charge enhances it. Surprisingly, these effects are largely independent of the location of the redox active functionality so long as it is in reasonably close proximity to the carbene.

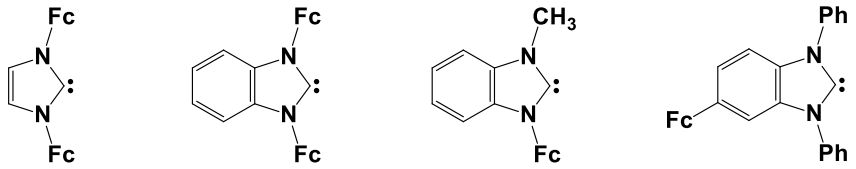

2.1 **2.2** **2.3** **2.4**

Figure 2.5 Redox active NHC-based ligands studied herein.

RESULTS AND DISCUSSION

Synthesis of N-Heterocyclic Carbene Precursors. Palladium-catalyzed coupling of aminoferrocene[60] with 1,2-dibromobenzene (Scheme 2.1A), followed by cyclization with triethylorthoformate and HCl (aq) afforded 1,3-diferrocenylbenzimidazolium chloride [**2.2**H][Cl] in excellent overall yield (91%). Alternatively, aminoferrocene underwent nucleophilic aromatic substitution with 2-fluoronitrobenzene (Scheme 2.1B) which, following subsequent formylative cyclization and alkylation produced 1-ferrocenyl-3-

methylbenzimidazolium iodide [**2.3**H][I] in 85% overall yield. To access [**2.4**H][Cl], we prepared 1,2-dichloro-4-diazoniumbenzene tetrafluoroborate[86] as a suitable precursor. Reaction of this salt with ferrocene under acidic conditions afforded 1,2-dichloro-4-ferrocenylbenzene (Scheme 2.1C), which was then subjected to Pd-catalyzed aryl amination and cyclization to give 1,3-diphenyl-5-ferrocenylbenzimidazolium chloride [**2.4**H][Cl] in 20% overall yield after 3 steps. The spectral properties for [**2.2**H][Cl] and [**2.3**H][I] obtained by these modified procedures were identical to literature values.[60,61] Similarly, the ^{1}H and ^{13}C NMR chemical shifts for the 2-position in [**2.4**H][Cl] (δ = 10.47 and 142.2 ppm, respectively, in DMSO-d_6) were consistent with analogous compounds reported in the literature.[87-89]

Scheme 2.1 Syntheses of Carbene Precursors.[a]

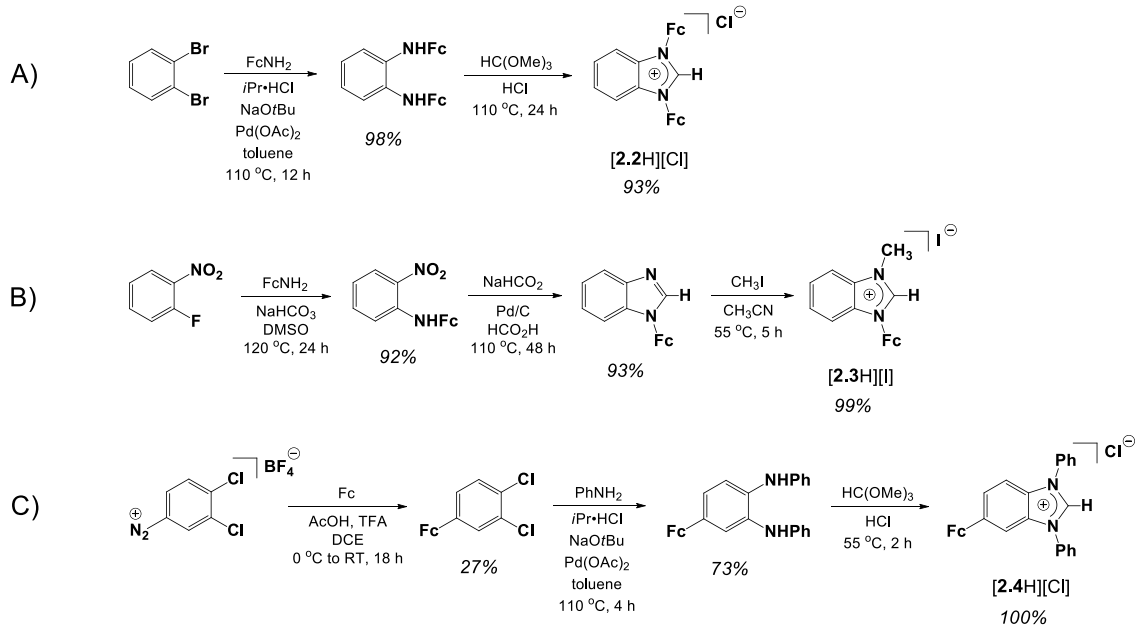

[a] *i*Pr•HCl = 1,3-bis(2,6-diisopropylphenyl)imidazolium chloride

Synthesis of Iridium Complexes. With the precursors to NHCs **2.1**–**2.4**, **FcDAC** and **NqMes** in hand, we pursued their respective [Ir(COD)Cl] (COD = 1,5-cyclooctadiene) complexes, given the abundance of spectroscopic, structural and electrochemical information available.[66-70] Additionally, the [Ir(COD)Cl] unit subsequently can be converted to $[Ir(CO)_2Cl]$ upon reaction with CO (*g*), enabling further interrogation of the complex's carbene ligand via IR spectroscopic analysis.[66,67] Two routes were employed for the preparation of the desired [Ir(COD)Cl] complexes supported by **2.1**–**2.4**, **FcDAC** and **NqMes**, depending on the stability of the free NHC. For NHCs that dimerize or decompose in free form (*i.e.*, **2.1**, **2.3** and **2.4**), deprotonation of the azolium was achieved with Ag_2O followed by transmetallation[49] to $[Ir(COD)(\mu\text{–}Cl)]_2$ (Route A, Scheme 2.2, 99–100% overall yield). Alternatively, the free NHCs **2.2**, **FcDAC** and **NqMes** were successfully generated upon treatment with KO^{t}Bu or NaHMDS and then coordinated[48] to iridium (Route B, 56–100% overall yield). For (**2.1**–

2.4)**a** and **2.6a**, the ^{13}C NMR chemical shifts for the 2-position were observed from δ = 182.2–194.6 ppm (Table B.3), within the range observed for other NHC-supported [Ir(COD)Cl] complexes (δ = 179.6–208.2 ppm).[68,90-93] Similarly, the analogous signal observed in the ^{13}C NMR spectrum of **2.5a** (δ = 213.2 ppm) was comparable to that observed in its rhodium congener (δ = 225.8 ppm),[63] but substantially different from (**2.1**–**2.4**)**a** and **2.6a**. Because the carbene nucleus is strongly influenced by the ring system comprising it, apparent by the markedly distinct ^{13}C NMR chemical shift of **2.5a** vs. (**2.1**–**2.4**)**a** and **2.6a**, we expected that the structural features of **2.5a** would be similarly unique.

Scheme 2.2 Syntheses of (**2.1**–**2.6**)**a** and (**2.1**–**2.6**)**b**.

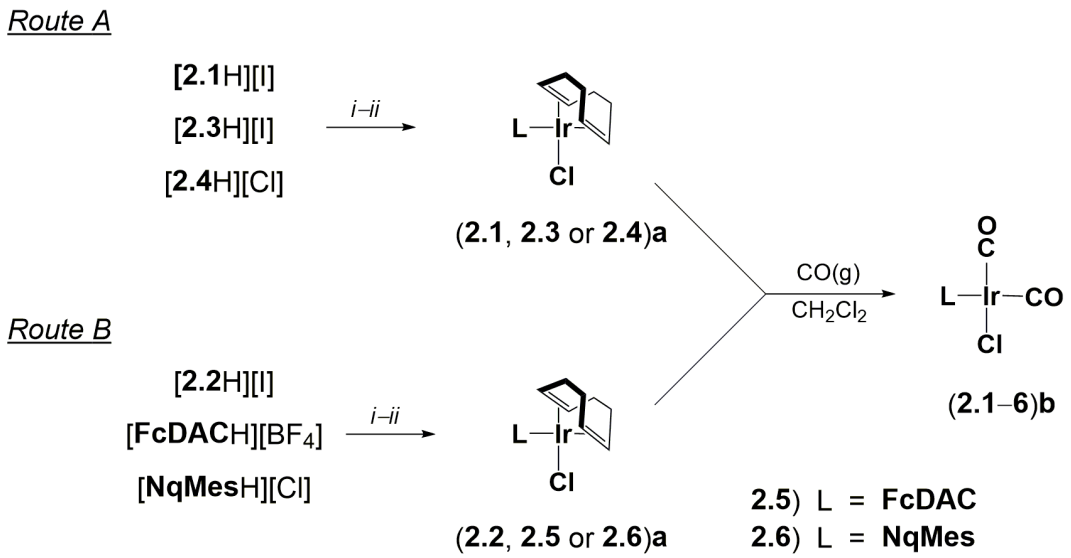

Route A. For **2.1**: (*i*) 0.5 equiv Ag_2O, 1,2-dichloroethane, 15 h, 94%; (*ii*) CH_2Cl_2, 6 h, 99%. For **2.3**: (*i*) CH_2Cl_2, 16 h, 91%; (*ii*) CH_2Cl_2, 12 h, 99%. For **2.4**: (*i*) CH_2Cl_2, 2 h, 100%; (*ii*) THF, 7 h, 60 °C, 100%. ***Route B.*** For **2.2**: (*iii*) KO^{t}Bu, THF, 12 h, 60 °C, 100%. For **FcDAC**: (*i*) NaHMDS, toluene, 20 min; (*ii*) 2 h, 71%. For **NqMes**: (*i*) NaHMDS, THF, 20 min; (*ii*) 12 h, 56%. The carbonylation reactions were performed by purging with CO (*g*) (see Experimental Section for details). Unless specified otherwise, all reactions were performed at ambient temperature. L = **2.1**–**2.4**, **FcDAC** (**2.5**) or **NqMes** (**2.6**).

Single crystals of (**2.1**–**2.3**)**a** and (**2.5**–**2.6**)**a** were obtained and analyzed by X-ray diffraction to obtain their respective structural parameters and enable comparison to crystallographically characterized analogues.[94] The iridium–NHC distances observed in these complexes (2.022(10) Å for **2.1a**, 2.020(5) Å for **2.2a**, 2.030(7) Å for **2.3a**, 2.068(3) Å for **2.5a**; 2.033(5) Å for **2.6a**; see Table 2.1) were consistent with other NHC-supported [Ir(COD)Cl] complexes (1.99 to 2.091 Å).[67,68,95-100] In these complexes, the Ir–COD bond distances *trans* to the NHC range from 2.134 to 2.227 Å, whereas the distances for the Ir–COD bonds in the *cis* position range from 2.081 to 2.155 Å. The corresponding lengths in (**2.1**–**2.3**)**a** and **2.6a** (2.189(4)–2.191(7) Å) agreed well with these structural features. Only **5a** appeared to deviate significantly from the other [Ir(COD)Cl] complexes, judging by ^{13}C NMR shifts and N–C–N angles (121.9(3) for **2.5a** vs. 102.8(8)–105.3(4) for (**2.1**–**2.3**)**a** and **2.6a**). In contrast, complexes (**2.1**–**2.4**)**a** and **2.6a** shared highly conserved spectroscopic and structural features. We conclude that the distinct coordination chemistry of **2.5a** compared to (**2.1**–**2.4**)**a** and **2.6a** reflects the fundamental structural differences between the 6-membered, non-aromatic, cyclic **FcDAC** and a 5-membered, heteroaromatic **2.1**–**2.4** and **NqMes**.

To gain additional insight into the electronic properties and donicity of **2.1**–**2.4**, **FcDAC** and **NqMes** via IR spectroscopic analysis, we prepared their metal carbonyl complexes. The [Ir(CO)$_2$Cl] complexes (**2.1**–**2.6**)**b** were obtained in excellent yields (88–100%) by bubbling 1 atm of CO (*g*) through CH_2Cl_2 solutions of the respective [Ir(COD)Cl] complexes (**2.1**–**2.6**)**a** (Scheme 2.2). Complexes (**2.1**–**2.4**)**b** and **2.6b** exhibited a range of values (δ = 180.7–186.9 ppm, $CDCl_3$),[94] consistent with known NHC-supported [Ir(CO)$_2$Cl] complexes (δ = 178.0–202.3 ppm).[67] A [Rh(CO)$_2$Cl] complex of **FcDAC** has been previously reported,[63] whose ^{13}C chemical shift (δ = 212.8 ppm in $CDCl_3$) was comparable to that observed in **2.5b** (δ = 202.4 ppm in $CDCl_3$).[94]

Interestingly, the ^{13}C NMR signals for the 2-position in (**2.1**–**2.6**)**b** (180.7–202.4 ppm) were upfield of their respective signals found in (**2.1**–**2.6**)**a** (182.2–213.2 ppm),[94] indicating greater shielding of the carbene nuclei in the $[Ir(CO)_2Cl]$ vs. [Ir(COD)Cl] complexes. Replacing COD with more electron withdrawing, π-acidic carbonyl ligands should decrease the overall metal electron density. As such, a coordinated NHC should donate more electron density to the metal. As the donation increases, the metal–NHC interaction will shift from a simple metal–carbene σ interaction to one that features more multiple-bond character. This phenomenom effectively results in an increase in the shielding of the carbene nucleus and an upfield shift in the ^{13}C NMR signal.

Crystal structures were obtained for (**2.1**–**2.3**)**b** and (**2.5**–**2.6**)**b**, thus enabling comparison to other NHC-supported $[Ir(CO)_2Cl]$ complexes (see Figures 2.6–2.10).[94] The iridium–NHC bond lengths in (**2.1**–**2.3**)**b** and (**2.5**–**2.6**)**b** (2.121(3) Å for **2.1b**, 2.080(4) Å for **2.2b**, 2.071(3) Å for **2.3b**, 2.121(3) for **2.5b**, 2.071(4) Å for **2.6b**)[94] agreed well with the values in analogous compounds (2.065–2.122 Å).[67,69,97] Additionally, the metal–carbonyl distances in (**2.1**–**2.3**)**b** and (**2.5**–**2.6**)**b** (*trans*: 1.877(4)–1.900(5) Å; *cis*: 1.827(4)–1.888(4) Å) were comparable to values observed in related $[Ir(CO)_2Cl]$ complexes (1.854–1.915 and 1.86–1.912 Å for the *trans* and *cis* positions relative to the NHC, respectively).[67,69,97] In general, the metal–carbon bonds *trans* to the NHC will be longer than those *cis* due to the strong *trans* effect of NHCs. Whereas the N1–C1–N2 angles in (**2.1**–**2.3**)**b** and **2.6b** varied minimally (105.5(3)–106.1(3)°), the corresponding value in **2.5b** was substantially more obtuse (122.4(2)°). Similarly, the chemical shifts for (**2.1**–**2.4**)**b** and **2.6b** were conserved, with the signal for **5b** significantly downfield (202.4 ppm for **2.5b** vs. 180.7–186.9 ppm for (**2.1**–**2.4**)**b** and **2.6b**).[94]

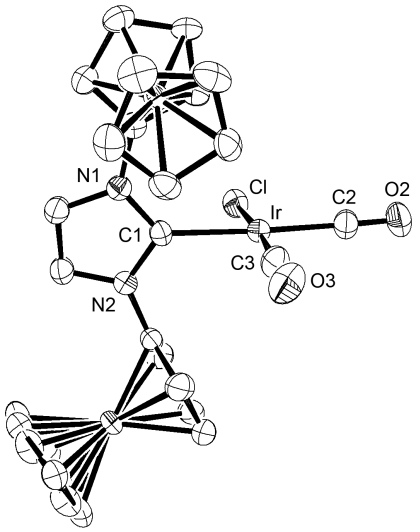

Figure 2.6 ORTEP diagram showing 50% probability thermal ellipsoids and selected atom labels for **2.1b**. Hydrogen atoms have been omitted for clarity. Selected bond lengths (Å) and angles (°): Ir–Cl, 2.367(2); Ir–C1, 2.089(6); Ir–C2, 1.892(8); Ir–C3, 1.859(11); C2–O2, 1.143(10); C3–O3, 1.091(12); N1–C1–N2, 105.9(5); N1–C1–Ir–Cl, 87.7(6).

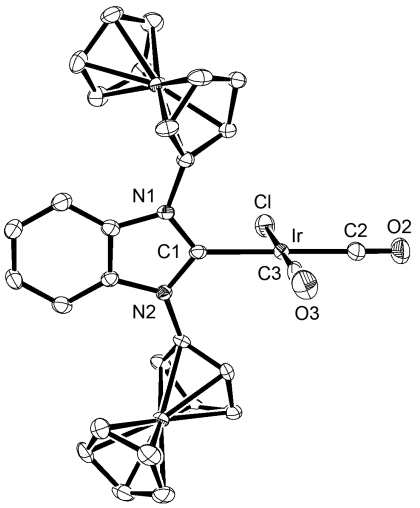

Figure 2.7 ORTEP diagram showing 50% probability thermal ellipsoids and selected atom labels for **2.2b**. Hydrogen atoms have been omitted for clarity. Selected bond lengths (Å) and angles (°):Ir–C1, 2.080(4); Ir–C2, 1.894(4); Ir–C3, 1.870(8); C2–O2, 1.127(5); C3–O3, 1.131(8); N1–C1–N2, 106.1(3).

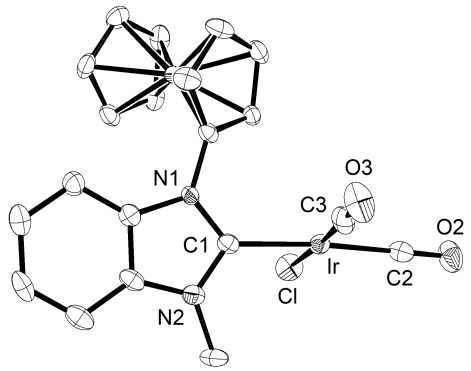

Figure 2.8 ORTEP diagram showing 50% probability thermal ellipsoids and selected atom labels for **2.3b**. Hydrogen atoms have been omitted for clarity. Selected bond lengths (Å) and angles (°):Ir–C1, 2.071(3); Ir–C2, 1.877(4); Ir–C3, 1.827(4); C2–O2, 1.141(5); C3–O3, 1.142(5); N1–C1–N2, 105.7(3).

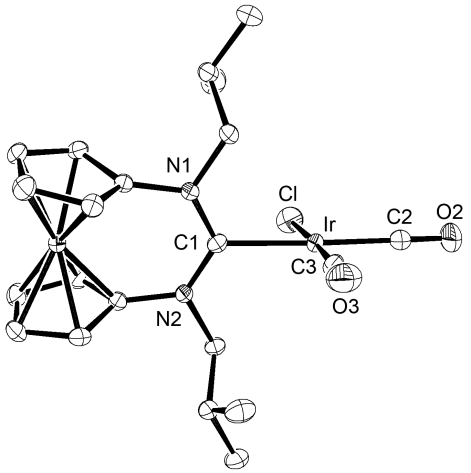

Figure 2.9 ORTEP diagram showing 50% probability thermal ellipsoids and selected atom labels for **2.5b**. Hydrogen atoms have been omitted for clarity. Selected bond lengths (Å) and angles (°): Ir–Cl, 2.3632(8); Ir–C1, 2.121(3); Ir–C2, 1.891(3); Ir–C3, 1.888(4); C2–O2, 1.136(4); C3–O3, 1.024(4); N1–C1–N2, 122.4(2); N1–C1–Ir–Cl, 78.71(18).

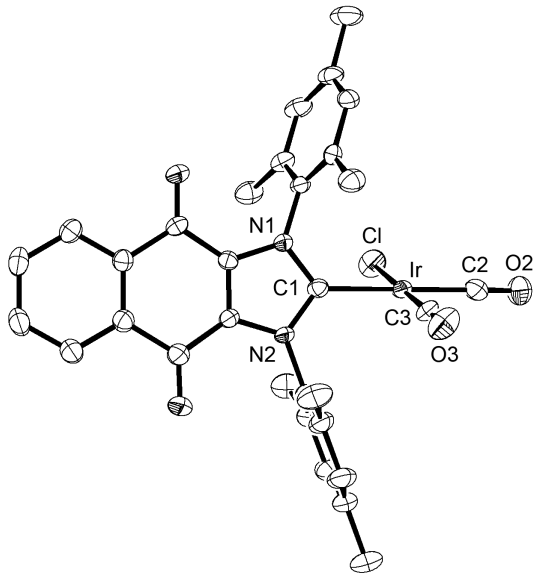

Figure 2.10 ORTEP diagram showing 50% probability thermal ellipsoids and selected atom labels for **2.6b**. Hydrogen atoms have been omitted for clarity. Selected bond lengths (Å) and angles (°):Ir–C1, 2.071(4); Ir–C2, 1.900(5); Ir–C3, 1.843(5); C2–O2, 1.120(5); C3–O3, 1.117(5); N1–C1–N2, 105.5(3).

Synthesis of Group 6 Complexes. To gain additional insight into the electron donating ability of these NHCs comprising redox active moieties, we prepared a series of $[M(CO)_5]$ complexes[72] supported by **2.1**–**2.4**, **FcDAC** and **NqMes**. Photolysis of the homoleptic carbonyl complexes $[M(CO)_6]$ (M = Cr, Mo, W) in THF afforded $[M(CO)_5(THF)]$,[101] where the coordinated THF was readily displaced with free NHC (Scheme 2.3). Unfortunately, the **FcDAC** complexes were very unstable and only the tungsten congener **5e** could be obtained. In contrast, **2.2c**–**e** and **2.6c**–**e** were purified via column chromatography and were found to be bench stable for days. The range of ^{13}C NMR chemical shifts for the 2-positions of the NHCs in **2.2c**–**e**, **2.5e** and **2.6c**–**e** (201.4–222.5 ppm, $CDCl_3$)[94] was consistent with those observed in previously reported group 6 $[M(CO)_5]$ complexes bearing NHC ligands (188.3–226.1 ppm).[61,71-85]

Scheme 2.3 Synthesis (top) and Structures (bottom) of Various Group 6 Complexes.[a]

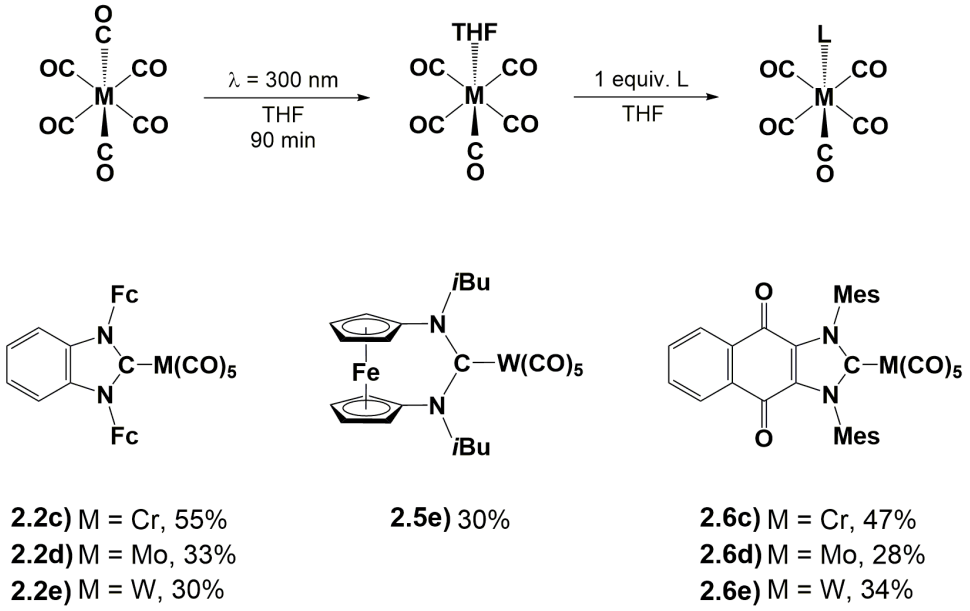

[a] For these complexes, L = **2.2**, **FcDAC** or **NqMes**.

Single crystals of the $[M(CO)_5]$ complexes supported by **2.2** and **NqMes** were obtained and subjected to X-ray diffraction.[94] The Cr–NHC distances in **2.2c** and **2.6c** (2.158(3) and 2.125(3) Å, respectively) were consistent with those observed in NHC-supported $[Cr(CO)_5]$ complexes (2.098–2.155 Å).[71-77] Additionally, the *trans* (1.852(4) and 1.857(3) Å) and *cis* (1.895 and 1.894 Å) chromium–carbonyl bond lengths fell within the range of values observed in analogous complexes (1.840–1.868 and 1.888–1.901 Å for *trans* and *cis*, respectively). Although no related structures of $[Mo(CO)_5]$ complexes are known, the metric parameters of **2.2d** and **2.6d** (Mo–C_{NHC} = 2.328(2) and 2.257(5) Å; Mo–C_{trans} = 1.975(3) and 1.999(7) Å; Mo–C_{cis} = 2.049 and 2.035 Å; respectively)[94] are similar to those of their tungsten congeners **2.2e** (W–C_{NHC} = 2.299(4) Å; W–C_{trans} =

1.978(4) Å; W–C_{cis} = 2.032 Å; see Figure 2.11) and **2.6e** (W–C_{NHC} = 2.259(5) Å; W–C_{trans} = 1.993(5) Å; W–C_{cis} = 2.039 Å; see Figure 2.12).

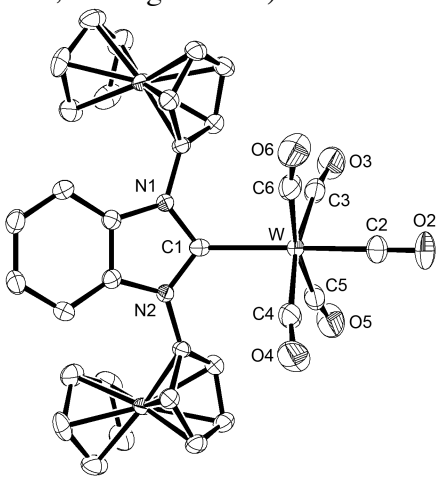

Figure 2.11 ORTEP diagram showing 50% probability thermal ellipsoids and selected atom labels for **2.2e**. Hydrogen atoms have been omitted for clarity. Selected bond lengths (Å) and angles (°): W–C1, 2.299(4); W–C2, 1.978(4); W–C3, 2.034(3); W–C4, 2.029(3); W–C5, 2.034(3); W–C6, 2.029(3); O2–C2, 1.164(5); O3–C3, 1.143(4); O4–C4, 1.157(4); O5–C5, 1.143(4); O6–C6, 1.157(4); N1–C1–N2, 103.9(3).

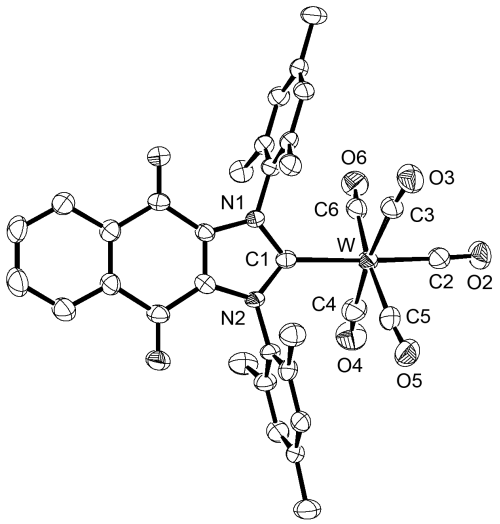

Figure 2.12 ORTEP diagram showing 50% probability thermal ellipsoids and selected atom labels for **2.6e**. Hydrogen atoms and solvent molecules have been omitted for clarity. Selected bond lengths (Å) and angles (°): W–C1, 2.259(5); W–C2, 1.993(5); W–C3, 2.048(5); W–C4, 2.036(6); W–C5, 2.029(6); W–C6, 2.042(6); O2–C2, 1.153(6); O3–C3, 1.128(6); O4–C4, 1.147(7); O5–C5, 1.149(7); O6–C6, 1.143(6); N1–C1–N2, 103.8(4).

A variety of complexes featuring an NHC coordinated to $[W(CO)_5]$ have been structurally characterized,[61,72,73,75,78-85] whose range of values for $W–C_{NHC}$ (2.242–2.296 Å), $W–C_{trans}$ (1.935–2.010 Å), and $W–C_{cis}$ (2.016–2.045 Å) encompass those exhibited by **2.2e** and **2.6e**. Overall, the ^{13}C NMR chemical shifts and structural features for **2.2c**–**e** and **2.6c**–**e** do not vary substantially beyond their different atomic radii of Cr vs. Mo and W. Surprisingly, the key structural and NMR spectroscopic features of the aforementioned NHC-supported $[M(CO)_5]$ complexes appear to be independent of the number or nature of the redox active functionalities present on the NHC scaffold (*e.g.*, two ferrocene units in **2.2** vs. one napthoquinone moiety in **NqMes**).

Although the ^{13}C NMR and crystallographic analyses of the $[Ir(CO)_2Cl]$ and $[M(CO)_5]$ complexes of the imidazolylidene-based NHCs **2.1**–**2.4** and **NqMes** displayed highly conserved features, the $Ir–C_{NHC}$ distance and N–C–N angle in **2.5b** were

significantly longer and more obtuse, respectively, than those observed in (**2.1**–**2.4**)**b** or **2.6b**. Based on these results, we conclude that the intrinsic electronic properties of the carbene nuclei in the aforementioned complexes (as determined by their respective ^{13}C NMR chemical shifts) as well as their coordination chemistry (as measured by their respective N1–C1–N2 angles and M–$C_{carbene}$ distances) are highly sensitive to the features of the cyclic system which comprises it. Compared to the imidazolylidene-derived **2.1**–**2.4** and **NqMes**, we believe the steric effects of the N-mesityl substituents and the 6-membered ring in **FcDAC** cause the carbene hybridization to adopt relatively greater *sp*-character, resulting in longer bonds to coordinated metals.[102,103]

Infrared Spectroscopy. Metal-bound carbonyls are useful spectroscopic handles for measuring the electron density at ligated metal centers. Increasing the electron density on a metal will increase its π-backbonding ability, thus reducing the C–O bond order and stretching frequency (ν_{CO}). For example, a more donating NHC will increase the electron density at the coordinated metal and thus lower the carbonyl stretching energy, allowing measurement of the ligand donicity. Many [$Ir(CO)_2Cl$] complexes supported by NHCs have been prepared for this reason, therefore we sought to determine and compare the donating abilities of **2.1**–**2.4**, **FcDAC** and **NqMes** to known NHCs.[67-70]

Complexes (**2.1**–**2.6**)**b** exhibited a range of *trans* (2058–2072 cm^{-1}) and *cis* (1982–1988 cm^{-1}) carbonyl stretching energies (see Table 2.1) consistent with those observed in known NHC-supported [$Ir(CO)_2Cl$] complexes (*trans*: 2055–2072 cm^{-1}, *cis*: 1971–1989 cm^{-1}).[67,69,93,97] Some remarkable trends become apparent upon examination of the average values exhibited by (**2.1**–**2.6**)**b** (ν_{av} = 2020.0–2030.0 cm^{-1}). The napthoquinone-annulated **NqMes** was less electron donating than the other imidazolylidene-based NHCs (**2.1**–**2.4**), suggesting that the quinone moiety decreased the donating ability of its fused carbene. Imidazolylidene **2.1** was more donating than

benzimidazolylidenes **2.2**–**2.4**, further evidence that annulation decreases the electron density at the carbene. Given the narrow range of ν_{av} values for **2.2**–**2.4**, we conclude that the electron donating ability of the benzimidazolylidene scaffold does not significantly vary with the number of the redox active groups present in the ligand or their position relative to the carbene atom. Because the carbonyl stretching energies for **2.1b** and **2.5b** are similar, no measurable alteration in carbene electron density is observable between the 5-membered aromatic and strained, 6-membered non-aromatic systems. Whereas the cyclic nature of **FcDAC** has a significant impact on *structural* features, it does not appear to greatly affect its ligand donating ability.

Table 2.1 Carbonyl Stretching Energies for Complexes (**2.1**–**2.6**)**b**, **2.2c**–**e** and **2.6c**–**e**.[a]

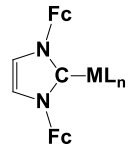

2.1

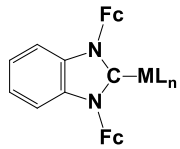

2.2

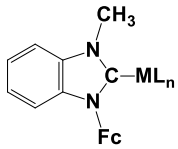

2.3

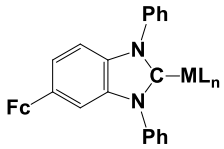

2.4

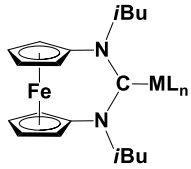

2.5

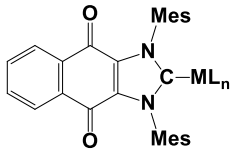

2.6

	[Ir(CO)$_2$Cl]				[M(CO)$_5$]
	ν_{CO}	ν_{av}	TEP		ν_{CO}
2.1b	2058, 1982	2020.0	2046.9	**2.2c**	2052, 1927, 1887*
2.2b	2064, 1984	2024.0	2050.3	**2.2d**	2052, 1926, 1889*
2.3b	2068, 1986	2027.0	2052.9	**2.2e**	2059, 1919, 1883*
2.4b	2068, 1985	2026.5	2052.4	**2.6c**[c]	2056, 1975*, 1933, 1678
2.5b	2062, 1982	2022.0	2048.6	**2.6d**	2063, 1980*, 1933, 1675
2.6b	2072, 1988	2030.0	2055.4	**2.6e**	2062, 1976*, 1928, 1676

[a] ML$_n$ = [Ir(CO)$_2$Cl] for (**2.1**–**2.6**)**b**, [Cr(CO)$_5$] for **2.2c** and **2.6c**, [Mo(CO)$_5$] for **2.2d** and **2.6d**, and [W(CO)$_5$] for **2.2e** and **2.6e**. For the [M(CO)$_5$] complexes, the $A_1^{(2)}$ mode is highest in energy and the $A_1^{(1)}$ mode is denoted with an asterisk (*). Measurements performed in CH_2Cl_2 or [c] $CHCl_3$.

To gain more insight into the donating abilities of the aforementioned NHCs, efforts turned toward evaluating their Tolman Electronic Parameters (TEPs), which can be derived from the metal–carbonyl stretching energies.[104,105] For [Ir(CO)$_2$Cl] complexes, Nolan enhanced an equation developed by Crabtree for determining the TEP from the observed ν_{av}, whereby TEP = $0.847 \times \nu_{av} + 336$ cm^{-1}.[67,70] The TEPs calculated for **2.1**–**2.4**,

FcDAC and **NqMes** (2046.9–2055.4 cm^{-1}) were consistent with the range observed in other NHC-supported [$Ir(CO)_2Cl$] complexes (2049.5–2057.3 cm^{-1}, see Figure 2.13 for representative examples).[67] For comparison, the TEP for **FcDAC** compares well to that for **IAd** (2048.6 vs. 2049.5 cm^{-1}, respectively) and **NqMes** to **IPrCl** (2055.4 vs. 2055.1 cm^{-1}, respectively). Similarly, there are other reported NHCs that exhibit comparable TEPs to the 2046.9 cm^{-1} measured for **2.1** (**IAd**, 2049.5 cm^{-1}), 2050.3 cm^{-1} for **2.2** (**ItBu**, 2050.1 cm^{-1}), 2052.4 and 2052.9 cm^{-1} for **2.4** and **2.3** (**SIPr**, 2052.2 cm^{-1}). When viewed in the context of previously reported NHCs (i.e., not including **2.2** – **2.4** or **2.6**), **2.1** and **FcDAC** were among the most electron-donating, **NqMes** was among the least, and **2.2**–**2.4** were intermediate in donicity.

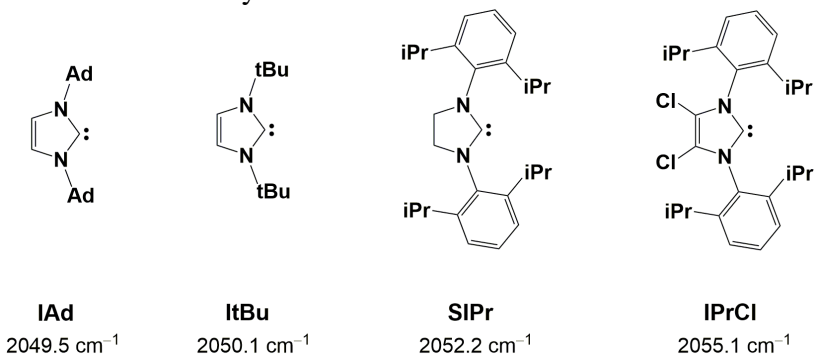

Figure 2.13 Representative NHCs with TEP values similar to **2.1**–**4**, **FcDAC** and **NqMes**.

Determination of ligand TEP values from group 6 [$M(CO)_5$] carbonyl stretching energies has not yet been detailed in the literature. Nonetheless, examination of the carbonyl stretching energies in **2.2c–e**, **2.5e**, and **2.6c–e** in comparison to previously reported analogues, should enable qualitative evaluation of the donating abilities of **2.1**–**2.4**, **FcDAC** and **NqMes**. Prior to this examination, a discussion regarding the number and symmetry of IR-active carbonyl stretching modes is helpful. In an idealized geometry, the C_{4v} [$M(CO)_5$(NHC)] scaffold has two sets of symmetry-inequivalent CO

groups in the equatorial (1) and axial (2) positions.[106] For CO_{ax}, the vibrational mode has A_1 symmetry and is IR and Raman active.[107] For CO_{eq}, the irreducible representation for the CO stretching modes is A_1, B_1 and E, where B_1 is not IR active. To distinguish between the equatorial and axial carbonyls, we will use superscripted (1) and (2) after the relevant Schönflies term symbol.

Because NHCs have a strong σ-donating effect, the CO trans to the NHC in the axial position will have the weakest π-backbonding interaction with the metal, thus the $A_1^{(2)}$ mode will be highest in energy.[106] However, the relative ordering of the $A_1^{(1)}$ + $E^{(1)}$ modes varies depending on the nature of the complex, where the $A_1^{(1)}$ mode can vary in energy greatly or be underneath the $E^{(1)}$ band. Correct identification can be achieved by comparing the relative intensities of the bands (in general, the $E^{(1)}$ mode is significantly more intense that the $A_1^{(1)}$ mode).[108-110] For the [M(CO)$_5$] (M = Cr, Mo, W) complexes supported by **2.2** and **NqMes**, the $A_1^{(2)}$ stretching energies (2052–2063 cm^{-1}, Table 1) coincided with the range of values observed in other NHC-supported analogues (2048–2064.1
cm^{-1}).[61,71-85] The $A_1^{(1)}$ modes for the pentacarbonyls supported by **2.2** (**2.2c**, 1887 cm^{-1}; **2.2d**, 1889 cm^{-1}; **2.2e**, 1883 cm^{-1}) and **NqMes** (**2.6c**, 1975 cm^{-1}; **2.6d**, 1980 cm^{-1}; **2.6e**, 1976 cm^{-1}) were consistent with other reported values (1882–1980 cm^{-1}). Similarly, the CO stretching energies for the $E^{(1)}$ modes in **2.2c–e** and **2.6c–e** (1919–1933 cm^{-1}) agreed well with those observed in other NHC-supported [M(CO)$_5$] complexes (1900–1966 cm^{-1}). These results suggest that either an oxidizable or a reducible functional group could be incorporated into an NHC without significantly altering its fundamental electron donating ability to [M(CO)$_5$] fragments comprising group 6 metals.

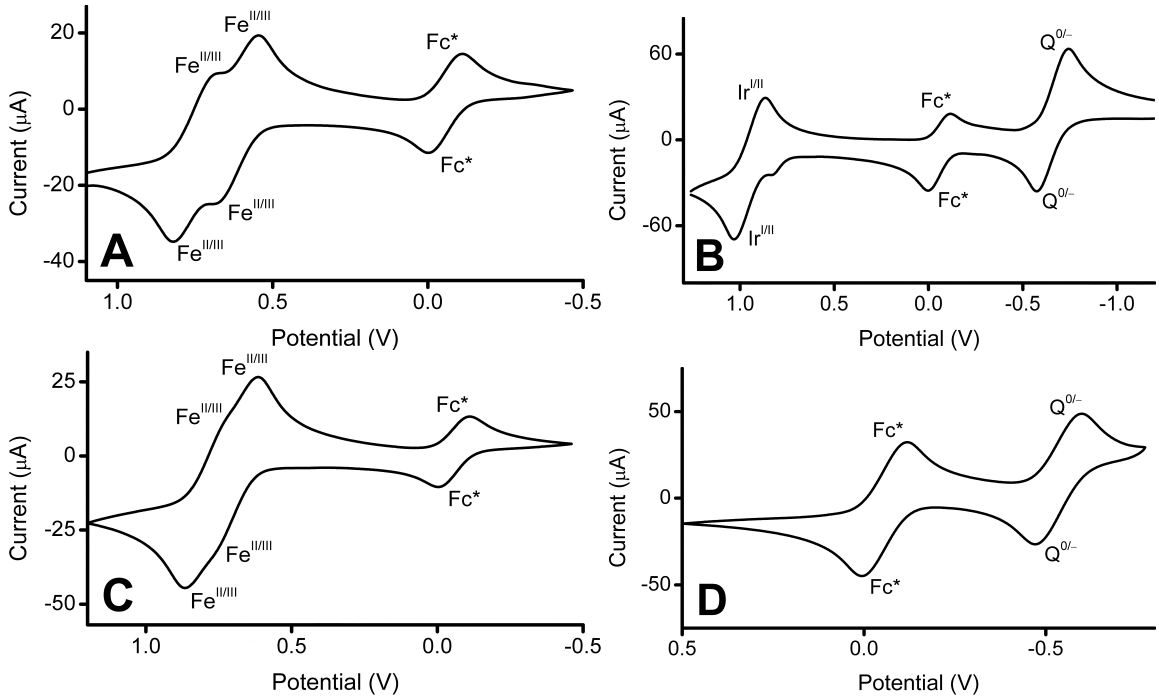

Figure 2.14 Representative cyclic voltammograms (100 mV s–1 scan-rate) with Fc* in CH_2Cl_2 with 0.1 M [Bu4N][PF6] and 1 mM (A) **2.2a**, (B) **2.6a**, (C) **2.2b**, (D) **2.6b**. Features are labelled according to metal oxidation ($Fe^{II/III}$ or $Ir^{I/II}$), quinone reduction ($Q^{0/-}$) or decamethylferrocene internal standard (Fc*).

Electrochemistry. Complexes **2.1a** and **2.2a**, comprising N,N'-diferrocenyl NHCs, exhibited two sets of quasi-reversible peaks (**2.1a**, +0.58 and +0.72 V; **2.2a**, +0.62 and +0.75 V; see Figures S10 and 14A of the original manuscript, respectively, as well as Table 2.2) in CH_2Cl_2,[94] which were attributed to the oxidation of their first and second ferrocene units, respectively. The potential separation between the two couples of 140 mV for **2.1a** and 130 mV for **2.2a** is consistent with other reported diferrocenyl-functionalized NHCs.[57,60,61,82] As expected, complexes **2.3a** and **2.4a**, supported by monoferrocenyl-functionalized NHCs, exhibited only one ferrocene based oxidation at

+0.62 and +0.53 V, respectively.[94] None of the iridium-based oxidations could be observed within the solvent window for (**2.1**–**2.4**)**a**.

Table 2.2 Electrochemical Properties of (**2.1**–**2.6**)**a** and (**2.1**–**2.6**)**b**.[a]

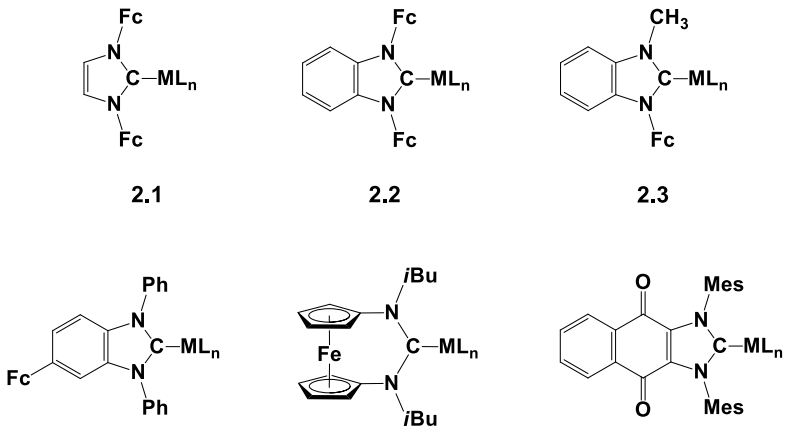

[Ir(COD)Cl]		[Ir(CO)$_2$Cl]		
	$E_{1/2}$ (V)		$E_{1/2}$ (V)	ΔE (mV)[b]
2.1a	0.72, 0.58	**2.1b**	0.78, 0.68 (sh)	60, 100 (80)
2.2a	0.75, 0.62	**2.2b**	0.79, 0.70 (sh)	40, 80 (60)
2.3a	0.62	**2.3b**	0.71	90
2.4a	0.53	**2.4b**	0.57	40
2.5a	1.02, 0.76	**2.5b**	0.94[c]	180
2.6a	0.95, –0.66	**2.6b**	–0.54[c]	120

[a] ML$_n$ = [Ir(COD)Cl] for (**2.1**–**2.6**)**a** and [Ir(CO)$_2$Cl] for (**2.1**–**2.6**)**b**. Measurements were performed in CH_2Cl_2 containing 0.1 M [Bu_4N][PF_6] at 100 mV s^{-1} scan-rate. [b] ΔE = $E_{1/2}$ (IrCO) – $E_{1/2}$ (IrCOD). Where two oxidations are present, the averaged value is also presented in parentheses. [c] The iridium-centered oxidation could not be observed within the solvent window.

In contrast, **2.5a** and **2.6a** exhibit quasi-reversible redox processes at +1.02 and +0.95 V (see Table 2.2)[94] that were attributed to Ir$^{I/II}$ couples, values that are consistent

with other NHC-suppoted [Ir(COD)Cl] complexes.[111,112] A reduction feature is also observed in **2.6a** at –0.66 V, similar with the quinone reduction observed in the previously reported [Rh(COD)Cl] analogue.[64] The ferrocene oxidation in **5a** occurs at +0.76 V, higher than the first oxidations in (**2.1**–**2.4**)**a**, reflecting the influence of the strained 6-membered ring and the inability of the orthogonal nitrogen lone pairs to donate electron density into the Cp rings to which they are linked. Additionally, the 90 mV difference between $Fc^{0/+}$ potentials in **2.3a** vs. **2.4a** revealed that an N-bound ferrocene was more electron deficient than a C-bound ferrocene. However, because the $Fc^{0/+}$ couple in **2.3a** occurs at an identical potential to the first oxidation observed in **2.2a** (+0.62 V), we conclude that the overall electron density does not depend on the number of ferrocene units within the NHCs. Furthermore, the small separation between ferrocene oxidations in **2.1a** and **2.2a** (<40 mV) suggests that the imidazolylidene- and benzimidazolylidene-based NHC scaffolds exert similar influences on the electronic environment at the iron centers.

The $Fe^{II/III}$ couples in (**2.1**–**2.4**)**b** exhibited anodic shifts of 40–100 mV relative to those observed in (**2.1**–**2.4**)**a**, reflecting the greater electron-withdrawing character of $[Ir(CO)_2Cl]$ compared to [Ir(COD)Cl] and agreeing with the ^{13}C NMR results. Similarly, the ferrocene oxidation in **2.5b** was observed at +0.94 V, a potential 180 mV higher than that observed for the analogous oxidation in **5a**. A greater shift for **2.5** than **2.1**–**2.4** is expected, given that the ferrocene unit in **FcDAC** is linked to the NHC at two positions instead of one. The quinone reduction in **2.6b** at –0.54 V was 120 mV higher than in **6a**, consistent with the reduced electron density at the metal.[64] Given the large shift in potentials for the NHC-based oxidations in **2.5b** and **2.6b**, it was not surprising that the $Ir^{I/II}$ couples were shifted beyond the solvent window and could not be observed. These

latter results were consistent with the electrochemical properties of related NHC-supported $[M(CO)_2Cl]$ complexes (M = Rh and Ir).[66,68,111]

As summarized in Table 2.3, a relatively narrow range of $M^{0/+}$ oxidation potentials was observed for the $[M(CO)_5]$ complexes supported by **2.2** (Cr: +0.67 V; Mo: +0.72 V; W: +0.69 V).[94] These values indicate that the electronic interactions between **2** and the $[M(CO)_5]$ fragments are nearly indistinguishable, presumably due to equivalent metal–NHC interactions. Overall, the range of metal-centered oxidation potentials observed in the $[M(CO)_5]$ complexes supported by **2.2** and **NqMes** (from +0.67 V to +1.15 V) were consistent with values measured in analogous complexes supported by other NHCs (+0.43 V to +1.2 V).[61,82] However, the $M^{0/+}$ couple in **2.6c** (+0.98 V) occurs at a potential substantially lower than its Mo and W congeners (+1.15 V for both **2.6d** and **2.6e**, respectively), in contrast to **2.2**.[94] In general, as the NHC and metal orbital energies converge, the extent of their interaction should increase. For a poorly-matched combination, the NHC should "experience" the influence from a generic n+ ion (which will not depend on the metal identity). Conversely, well-matched combinations should exhibit more significant interactions and greater dependence on metal identity and associated properties (*e.g.*, electronegativity, electron affinity, ionization potential, *etc*). Given that the metal oxidation potentials for **2.6d–e** are higher than **2.6c** and that Mo/W *d*-orbital energies are lower than Cr, we conclude that **NqMes** is a better energy match with $[Cr(CO)_5]$, whereby the greater interaction increases electron donation to the metal and thus reduces its oxidation potential.

Table 2.3 Electrochemical Properties of **2c–e** and **6c–e**.[a]

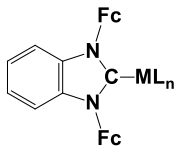

2.2

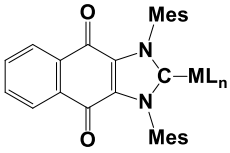

2.6

	$E_{1/2}$ (V)		$E_{1/2}$ (V)
2.2c	0.67	**2.6c**	0.98, –0.65
2.2d	0.72	**2.6d**	1.15, –0.68
2.2e	0.69	**2.6e**	1.15, –0.62

[a] ML_n = $[Cr(CO)_5]$ for **2.2c** and **2.6c**, $[Mo(CO)_5]$ for **2.2d** and **2.6d**, and $[W(CO)_5]$ for **2.2e** and **2.6e**. Measurements performed in CH_2Cl_2 containing 0.1 M $[Bu_4N][PF_6]$ at 100 mV s^{-1} scan-rate.

Interestingly, the quinone reductions in **2.6c–e** occurred at higher energies (from –0.62 V to –0.68 V) than the corresponding $[Ir(CO)_2Cl]$ complex **2.6b** (–0.54 V), consistent with a greater NHC–metal interaction in the latter case. Because the NHC ligand is conserved in these complexes, we conclude that the observed variation is due to the difference in *d*-orbital energy between the mid-transition group 6 metals and the late-transition group 9 iridium, as judged by the relative electron affinities of these metals (Cr: 64.3 kJ mol^{-1}; Mo: 71.9 kJ mol^{-1}; W: 78.6 kJ mol^{-1}; Ir: 151 kJ mol^{-1}).[113-115]

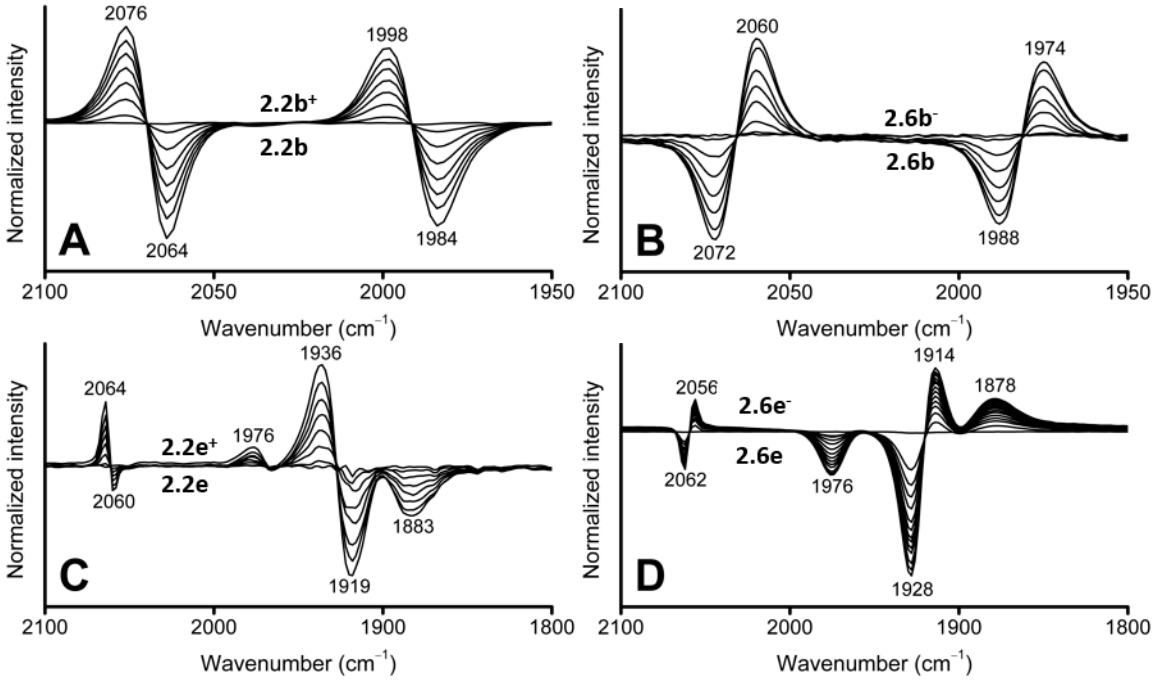

Figure 2.15 Normalized IR difference spectra at 60 s intervals showing the shift in metal carbonyl stretching energies upon oxidation (Eapp = +1.2 V) of **2.2b** (A) and **2.2e** (C) or reduction (Eapp = –1.2 V) of **2.6b** (B) and **2.6e** (D) in CH_2Cl_2 containing 10 mM analyte and 0.1 M [Bu4N][PF6].

Table 2.4 Spectroelectrochemical Results.[a]

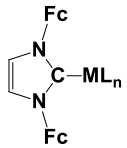

2.1

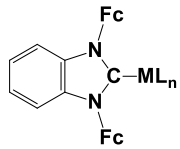

2.2

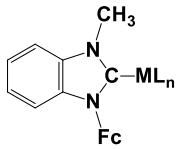

2.3

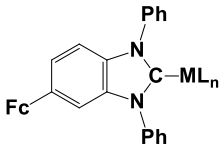

2.4

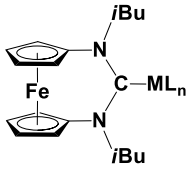

2.5

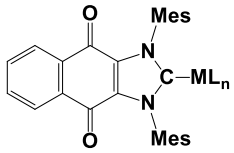

2.6

	[Ir(CO)$_2$Cl]						[M(CO)$_5$]	
	ν_{CO}*	ν_{av}*	TEP*	$\Delta\nu_{av}$	ΔTEP		ν_{CO}*	$\Delta\nu$ $A_1^{(1)}$
2.1b	2072, 1998	2035.0	2059.6	+15	+12.7	**2.2c**	2058, 1980*, 1944	+93
2.2b	2076, 1998	2037.0	2061.3	+13	+11.0	**2.2d**	2058, 1980*, 1944	+91
2.3b	2080, 2000	2040.0	2063.9	+13	+11.0	**2.2e**	2064, 1976*, 1936	+93
2.4b	—	—	—	—	—	**2.6c**	2048, 1916, 1882*	–93
2.5b	2074, 1996	2035.0	2059.6	+13	+11.0	**2.6d**	2058, 1920, 1878*	–102
2.6b	2060, 1975	2017.5	2044.8	–12.5	–10.6	**2.6e**	2056, 1914, 1878*	–98

[a] ML_n = [Ir(CO)$_2$Cl] for (**2.1** – **2.6**)**b**, [Cr(CO)$_5$] for **2.2c** and **2.6c**, [Mo(CO)$_5$] for **2.2d** and **2.6d**, and [W(CO)$_5$] for **2.2e** and **2.6e**. Measurements were performed in CH_2Cl_2 containing 0.1 M [Bu_4N][PF_6] under the conditions specified in Figure 2.15. Values with an asterisk (*) correspond to the in situ oxidized or reduced complex. Values of $\Delta\nu_{av}$, ΔTEP and $\Delta\nu$ $A_1^{(1)}$ were obtained by subtracting the values observed for the neutral complexes from those for the oxidized/reduced complexes.

Spectroelectrochemistry. A powerful method for determining the electronic influence of a redox active substituent within an NHC at a coordinated metal is IR spectroelectrochemistry.[17-19] Oxidation of the ferrocene units in **2.1**–**2.3** and **FcDAC** should decrease the donating abilities of the NHCs, thus lowering the electron density at the coordinated metal carbonyls and result in an increased ν_{av}. Alternatively, reducing the

quinone in complexes supported by **NqMes** should increase the carbenes electron donating ability, affording a more electron rich $[Ir(CO)_2Cl]$ or $[M(CO)_5]$ fragment with a concomitant decrease in carbonyl stretching energies. To explore the relationship between oxidation state of the redox active functionality and donicity of their respective NHCs, we sought to measure the shift in the average ν_{CO} of $[Ir(CO)_2Cl]$ and $[M(CO)_5]$ complexes upon oxidation of the ferrocene units in **2.1**–**2.3** and reduction of **NqMes**. Surprisingly, oxidation of (**2.1**–**2.3**)**b** and **2.5b** resulted in nearly identical shifts in ν_{av} (**2.1b**: +15 cm^{-1}; **2.2b**: +13 cm^{-1}; **2.3b**: +13 cm^{-1}; **2.5b**: +13 cm^{-1}; for **2.2b**, see Figure 2.15A; for the others, see Figures B.5, B.6, and the original manuscript; key features are summarized in Table 2.4)[94] that corresponded to ΔTEP values ranging from +11.0 to +12.7 cm^{-1}. These results suggest that the scaffold structure (i.e., imidazolylidene vs. benzimidazolylidene vs. non-aromatic) or the number of ferrocene units (i.e., one vs. two) do not obfuscate the redox tunability of NHC donicity when a redox active group is directly connected via an N substituent. Closely paralleling the ferrocene oxidation measurements, reduction of **2.6b** afforded a $\Delta\nu_{av}$ of –12.5 cm^{-1}, resulting in a decrease of the TEP by 10.6 cm^{-1} (see Figure 2.15B). Because the values of $\Delta\nu_{av}$ and ΔTEP for **2.6b** are nearly identical in magnitude but opposite in sign to those observed for (**2.1**–**2.3**)**b** and **2.5b**, we conclude that the redox tunability of these ligands do not strongly depend on the *specific* chemical identity of the redox active functional group. Rather, the overall charged imparted to the molecule upon redox change, appears to be the origin of the ligand's enhanced or attenuated donating ability.

Similar shifts were observed in the $A_1^{(1)}$ carbonyl stretching modes for the $[M(CO)_5]$ complexes of **2.2** and **NqMes**, albeit with dramatically greater magnitude. Oxidation of **2.2c**–**e** increased the $\nu A_1^{(1)}$ energies 91–93 cm^{-1} (for **2.2e**, see Figure 2.15C; for **2.2c**–**d**, see Figures S27–S28 in the original manuscript, also see Table 2.4),[94]

consistent with reduced metal electron density and consistent with shifts observed in complexes supported by ferrocene-functionalized phosphines.[17-19] Conversely, the $\Delta\nu\ A_1^{(1)}$ values for **6c**–**e** ranged from –93 to –102 cm^{-1} (for **2.6e**, see Figure 2.15D; for **6c**–**d**, see the original manuscript)[94] indicative of enhanced donicity upon reduction of **NqMes**. As observed with the $[Ir(CO)_2Cl]$ complexes, the magnitude of $\Delta\nu\ A_1^{(1)}$ was nearly identical for **2.2** vs. **NqMes**, albeit with opposite signs (positive for oxidation, negative for reduction).

Overall, the modulation of the ligand donating abilities of **2.1**–**2.3**, **FcDAC** and **NqMes** upon electrochemical switching of the redox active units (by oxidation or reduction) was largely *independent* of their molecular characteristics, contrary to expectations. No significant dependence on the presence (**FcDAC** vs. **2.1**–**2.3** and **NqMes**) or extent of an aromatic system (**2.1** vs. **2.2**) was observed. Oxidation of one or two the ferrocene units (**2.2** vs. **2.3**) afforded the same change in NHC electron donating ability, indicating that a second oxidation had marginal impact beyond the first. Furthermore, the magnitude of the enhanced donicity observed for **NqMes** upon reduction matched the attenuation observed for the ferrocene-functionalized NHCs upon oxidation. Collectively, these results suggest that the changes in electron donating ability of **2.1**–**2.3**, **FcDAC** and **NqMes** are largely due to Coulombic effects, where removal or addition of an electron alters the overall molecular charge.

CONCLUSIONS

In sum, we have developed families of [Ir(COD)Cl], $[Ir(CO)_2Cl]$, and $[M(CO)_5]$ (M = Cr, Mo, W) complexes supported by NHCs comprising redox active ferrocene (**2.1**–**2.4** and **FcDAC**) and quinone (**NqMes**) functionalities. Although the ^{13}C NMR spectroscopic and structural features of these complexes were consistent with previously

reported analogues, those comprising **FcDAC** were notably distinct from the other redox active NHCs studied (**2.1**–**2.4** or **NqMes**), presumably reflecting the greater *sp*-hybridization of the carbene nucleus in the former.

Measurement of the electron density at the metal, and thus the donating ability of the NHCs, via IR spectroscopic analysis of carbonyl stretching energies revealed different behavior than the X-ray diffraction or ^{13}C NMR spectroscopy results. Complexes **2.1b** and **2.6b** exhibited the lowest and highest ν_{av} values, respectively, demonstrating that the NHC backbone (imidazolylidene vs. benzimidazolylidene vs. napthoquinone) had a significant effect on the donating ability of the respective carbenes. However, the average carbonyl stretching energies for complexes (**2.2**–**2.5**)**b** were similar (differences of no more than 3 cm^{-1} were observed), suggesting the benzimidazolylidene scaffold could be functionalized with one or two redox active moieties at the N-atoms or backbone without significantly perturbing its donicity. Relative to previously reported NHCs, **2.1** and **FcDAC** were among the most electron-donating, **NqMes** was comparable with the least, and **2.2**–**2.4** were intermediate. Because electrochemical analyses revealed similar ferrocene oxidation potentials for the [Ir(COD)Cl] and $[Ir(CO)_2Cl]$ complexes supported by **2.1**–**2.3**, we conclude that neither the number of ferrocene units nor the identity of the aromatic backbone strongly influenced the electron density within the NHC. In contrast, the $Fc^{0/+}$ couples in **2.4a**–**b** and **2.5a**–**b** were distinct from those observed in **2.1**–**2.3**, evidence that both the attachment point of the redox active group (relative to the carbene nucleus) and the ring comprising the NHC affected the electronic environment at the iron centers in the respective complexes.

Spectroelectrochemical IR analyses revealed a narrow range of $\Delta\nu_{av}$ values for (**2.1**–**2.3**)**b** and **2.5b** (+13 to +15 cm^{-1}), corresponding to increases in TEPs from 11.0 to 12.7 cm^{-1}, upon oxidation of the ferrocene units. Reduction of the quinone in **2.6b**,

however, decreased its ν_{av} by 12.5 cm^{-1}, indicating enhanced donation by **NqMes** (ΔTEP = –10.6 cm^{-1}). Interestingly, the shift for **NqMes** was nearly equal in magnitude but opposite in sign to the shifts observed for **2.1**–**2.3** and **FcDAC**. Because the changes in ligand donating abilities did not depend significantly on the NHC characteristics, we surmise that the observed trends primarily reflect Coulombic effects, whereby addition of a positive or negative charge to the ligand alters its TEP by roughly +14 or –11 cm^{-1}, respectively.

Based on these results, NHCs with electrochemically-tunable electronic properties could be obtained via incorporating a redox active moiety by the most straightforward synthetic route available, without requiring extensive ligand design. For an NHC that can be electrochemically toggled to a less donating state, it need only feature a functionality that is (1) in close proximity to the carbene and (2) endows the molecule with a positive charge upon oxidation. Conversely, an analogous NHC bearing a redox active group that acquires a negative charge upon reduction could function as a ligand that can be redox-switched to a more donating state. Ultimately, we believe our findings will simplify the rational design of NHCs for use in redox-switchable applications that employ electrochemical control to attain both enhanced and attenuated electron donating states.

REFERENCES

(1) Allgeier, A. M.; Mirkin, C. A. *Angew. Chem. Int. Ed.* **1998**, *37*, 894–908.

(2) Gregson, C. K. A.; Gibson, V. C.; Long, N. J.; Marshall, E. L.; Oxford, P. J.; White, A. J. P. *J. Am. Chem. Soc.* **2006**, *128*, 7410–7411.

(3) Lorkovic, I. M.; Duff Jr., R. R.; Wrighton, M. S. *J. Am. Chem. Soc.* **1995**, *117*, 3617–3618.

(4) Sibert, J. W.; Forshee, P. B.; Lynch, V. *Inorg. Chem.* **2005**, *44*, 8602–8609.

(5) Beer, P. D. *Chem. Soc. Rev.* **1989**, *18*, 409–450.

(6) Liu, Z.; Yasseri, A. A.; Lindsey, J. S.; Bocian, D. F. *Science* **2003**, *302*, 1543–1545.

(7) Mori, H.; Miyoshi, E. *J. Theor. Comp. Chem.* **2005**, *4*, 333–344.

(8) McNitt, K. A.; Parimal, K.; Share, A. I.; Fahrenbach, A. C.; Witlicki, E. H.; Pink, M.; Bediako, D. K.; Plaisier, C. L.; Le, N.; Heeringa, L. P.; Griend, D. A. V.; Flood, A. H. *J. Am. Chem. Soc.* **2009**, *131*, 1305–1313.

(9) Ringenberg, M. R.; Kokatam, S. L.; Heiden, Z. M.; Rauchfuss, T. B. *J. Am. Chem. Soc.* **2008**, *130*, 788–789.

(10) Boyer, J. L.; Cundari, T. R.; DeYonker, N. J.; Rauchfuss, T. B.; Wilson, S. R. *Inorg. Chem.* **2009**, *48*, 638–645.

(11) Zanello, P.; Corsini, M. *Coord. Chem. Rev.* **2006**, *250*, 2000–2022.

(12) Ward, M. D.; McCleverty, J. A. *J. Chem. Soc., Dalton Trans.* **2002**, 275–288.

(13) Downs, H. H.; Buchanan, R. M.; Pierpont, C. G. *Inorg. Chem.* **1978**, *18*, 1736–1740.

(14) Higuchi, M.; Ikeda, I.; Hirao, T. *J. Org. Chem.* **1997**, *62*, 1072–1078.

(15) Yeung, L. K.; Kim, J. E.; Chung, Y. K.; Rieger, P. H.; Sweigart, D. A. *Organometallics* **1996**, *15*, 3891–3897.

(16) Lorkovic, I. M.; Wrighton, M. S.; Davis, W. M. *J. Am. Chem. Soc.* **1994**, *116*, 6220–6228.

(17) Yang, K.; Bott, S. G.; Richmond, M. G. *Organometallics* **1995**, *14*, 2387–2394.

(18) Miller, T. M.; Ahmed, K. J.; Wrighton, M. S. *Inorg. Chem.* **1989**, *28*, 2347–2355.

(19) Kotz, J. C.; Nivert, C. L.; Lieber, J. M.; Reed, R. C. *J. Organomet. Chem.* **1975**, *91*, 87–95.

(20) Allgeier, A. M.; Slone, C. S.; Mirkin, C. A.; Liable-Sands, L. M.; Yap, G. P. A.; Rheingold, A. L. *J. Am. Chem. Soc.* **1997**, *119*, 550–559.

(21) Sassano, C. A.; Mirkin, C. A. *J. Am. Chem. Soc.* **1995**, *117*, 11379–11380.

(22) Blackmore, K. J.; Lal, N.; Ziller, J. W.; Heyduk, A. F. *Eur. J. Inorg. Chem.* **2009**, 735–743.

(23) Shu, C.-F.; Wrighton, M. S. *Inorg. Chem.* **1988**, *27*, 4326–4329.

(24) Guerro, M.; Pham, N. H.; Massue, J.; Bellec, N.; Lorcy, D. *Tetrahedron* **2008**, *64*, 5285–5290.

(25) Traill, P. R.; Bond, A. M.; Wedd, A. G. *Inorg. Chem.* **1994**, *33*, 5754–5760.

(26) Bourissou, D.; Guerret, O.; Gabbaï, F. P.; Bertrand, G. *Chem. Rev.* **2000**, *100*, 39–91.

(27) Cardin, D. J.; Cetinkaya, B.; Cetinkaya, E.; Lappert, M. F. *J. Chem. Soc., Dalton Trans.* **1973**, 514–522.

(28) Wanzlick, H.-W.; Schönherr, H.-J. *Angew. Chem. Int. Ed.* **1968**, *7*, 141–142.

(29) Öfele, K. *J. Organomet. Chem.* **1968**, *12*, P42–P43.

(30) Winberg, H. E.; Coffman, D. D. *J. Am. Chem. Soc.* **1965**, *87*, 2776–2777.

(31) Breslow, R. *J. Am. Chem. Soc.* **1957**, *79*, 1762–1763.

(32) Arduengo III, A. J.; Harlow, R. L.; Kline, M. *J. Am. Chem. Soc.* **1991**, *113*, 361–363.

(33) Díez-González, S.; Nolan, S. P. *Topics Organomet. Chem.* **2007**, *21*, 47–82.

(34) Kantchev, E. A. B.; O'Brien, C. J.; Organ, M. G. *Angew. Chem. Int. Ed.* **2007**, *46*, 2768–2813.

(35) Marion, N.; Navarro, O.; Mei, J.; Stevens, E. D.; Scott, N. M.; Nolan, S. P. *J. Am. Chem. Soc.* **2006**, *128*, 4101–4111.

(36) Navarro, O.; Marion, N.; Oonishi, Y.; Kelly III, R. A.; Nolan, S. P. *J. Org. Chem.* **2006**, *71*, 685–692.

(37) Cavell, K. J.; McGuinness, D. S. *Coord. Chem. Rev.* **2004**, *248*, 671–681.

(38) Peris, E.; Crabtree, R. H. *Coord. Chem. Rev.* **2004**, *248*, 2239–2246.

(39) Herrmann, W. A. *Angew. Chem. Int. Ed.* **2002**, *41*, 1290–1309.

(40) Hillier, A. C.; Grasa, G. A.; Viciu, M. S.; Lee, H. M.; Yang, C.; Nolan, S. P. *J. Organomet. Chem.* **2002**, *653*, 69–82.

(41) Jørgensen, M.; Lee, S.; Liu, X.; Wolkowski, J. P.; Hartwig, J. F. *J. Am. Chem. Soc.* **2002**, *124*, 12557–12565.

(42) Gibby, J. L. J. E.; Farnworth, M. V.; Tekavec, T. N. *J. Am. Chem. Soc.* **2002**, *124*, 15188–15189.

(43) Trnka, T. M.; Grubbs, R. H. *Acc. Chem. Res.* **2001**, *34*, 18–29.

(44) Herrmann, W. A.; Mihalios, D.; Ofele, K.; Kiprof, P.; Belmedjahed, F. *Chem. Ber. Recl.* **1992**, *125*, 1795–1799.

(45) Scott, N. M.; Clavier, H.; Mahjoor, P.; Stevens, E. D.; Nolan, S. P. *Organometallics* **2008**, *27*, 3181–3186.

(46) Jafarpour, L.; Stevens, E. D.; Nolan, S. P. *J. Organomet. Chem.* **2000**, *606*, 49–54.

(47) Peris, E. *Topics Organomet. Chem.* **2007**, *21*, 83–116.

(48) Herrmann, W. A.; Köcher, K. *Angew. Chem. Int. Ed.* **1997**, *36*, 2163–2187.

(49) Wang, H. M. J.; Lin, I. J. B. *Organometallics* **1998**, *17*, 972–975.

(50) Arduengo III, A. J.; Iconaru, L. I. *Dalton Trans.* **2009**, 6903–6914.

(51) Arduengo III, A. J.; Tapu, D.; Marshall, W. J. *J. Am. Chem. Soc.* **2005**, *127*, 16400–16401.

(52) Arduengo III, A. J.; Bannenberg, T. P.; Tapu, D.; Marshall, W. J. *Chem. Lett.* **2005**, *34*, 1010–1011.

(53) Arduengo III, A. J.; Tapu, D.; Marshall, W. J. *Angew. Chem. Int. Ed.* **2005**, *44*, 7240–7244.

(54) Arduengo III, A. J.; Tapu, D.; Marshall, W. J. *Angew. Chem.* **2005**, *117*, 7406–7410.

(55) Arduengo III, A. J.; Bannenberga, T. P.; Tapu, D.; Marshall, W. J. *Tet. Lett.* **2005**, *46*, 6847–6850.

(56) Labande, A.; Daran, J.-C.; Manoury, E.; Poli, R. *Eur. J. Inorg. Chem.* **2007**, 1205–1209.

(57) Bertogg, A.; Camponovo, F.; Togni, A. *Eur. J. Inorg. Chem.* **2005**, 347–356.

(58) Gischig, S.; Togni, A. *Organometallics* **2004**, *23*, 2479–2487.

(59) Seo, H.; Kim, B. Y.; Lee, J. H.; Park, H.-J.; Son, S. U.; Chung, Y. K. *Organometallics* **2003**, *22*, 4783–4791.

(60) Bildstein, B.; Malaun, M.; Kopacka, H.; Wurst, K.; Mitterböck, M.; Ongania, K.-H.; Opromolla, G.; Zanello, P. *Organometallics* **1999**, *18*, 4325–4336.

(61) Bildstein, B.; Malaun, M.; Kopacka, H.; Ongania, K.-H.; Wurst, K. *J. Organomet. Chem.* **1999**, *572*, 177–187.

(62) Varnado Jr., C. D.; Lynch, V. M.; Bielawski, C. W. *Dalton Trans.* **2009**, 7253.

(63) Khramov, D. M.; Rosen, E. L.; Lynch, V. M.; Bielawski, C. W. *Angew. Chem. Int. Ed.* **2008**, *47*, 2267–2270.

(64) Sanderson, M. D.; Kamplain, J. W.; Bielawski, C. W. *J. Am. Chem. Soc.* **2006**, *128*, 16514–16515.

(65) Siemeling, U.; Färber, C.; Bruhn, C. *Chem. Commun.* **2009**, 98–100.

(66) Wolf, S.; Plenio, H. *J. Organomet. Chem.* **2009**, *694*, 1487–1492.

(67) Kelly III, R. A.; Clavier, H.; Giudice, S.; Scott, N. M.; Stevens, E. D.; Bordner, J.; Samardjiev, I.; Hoff, C. D.; Cavallo, L.; Nolan, S. P. *Organometallics* **2008**, *27*, 202–210.

(68) Leuthäußer, S.; Schwarz, D.; Plenio, H. *Chem. Eur. J.* **2007**, *13*, 7195–7203.

(69) Altenhoff, G.; Goddard, R.; Lehmann, C. W.; Glorius, F. *J. Am. Chem. Soc.* **2004**, *126*, 15195–15201.

(70) Chianese, A. R.; Li, X.; Janzen, M. C.; Faller, J. W.; Crabtree, R. H. *Organometallics* **2003**, *22*, 1663–1667.

(71) Kim, S.; Choi, S. Y.; Lee, Y. T.; Park, K. H.; Sitzmann, H.; Chung, Y. K. *J. Organomet. Chem.* **2007**, *692*, 5390–5394.

(72) Frey, G. D.; Öfele, K.; Krist, H. G.; Herdtweck, E.; Herrmann, W. A. *Inorg. Chim. Acta* **2006**, *359*, 2622–2634.

(73) Nonnenmacher, M.; Kunz, D.; Rominger, F.; Oeser, T. *J. Organomet. Chem.* **2005**, *690*, 5647–5653.

(74) Sakurai, H.; Sugitani, K.; Moriuchi, T.; Hirao, T. *J. Organomet. Chem.* **2005**, *690*, 1750–1755.

(75) Hahn, F. E.; Langenhahn, V.; Meier, N.; Lügger, T.; Fehlhammer, W. P. *Chem. Eur. J.* **2003**, *9*, 704–712.

(76) Tafipolsky, M.; Scherer, W.; Öfele, K.; Artus, G.; Pedersen, B.; Herrmann, W. A.; McGrady, G. S. *J. Am. Chem. Soc.* **2002**, *124*, 5865–5880.

(77) Bolm, C.; Kesselgruber, M.; Raabe, G. *Organometallics* **2001**, *21*, 707–710.

(78) Hahn, F. E.; Langenhahn, V.; Pape, T. *Chem. Commun.* **2005**, 5390–5392.

(79) Hahn, F. E.; Paas, M.; Van, D. L.; Fröhlich, R. *Chem. Eur. J.* **2005**, *11*, 5080–5085.

(80) Krahulic, K. E.; Enright, G. D.; Parvez, M.; Roesler, R. *J. Am. Chem. Soc.* **2005**, *127*, 4142–4143.

(81) Hahn, F. E.; Plumed, C. G.; Münder, M.; Lügger, T. *Chem. Eur. J.* **2004**, *10*, 6285–6293.

(82) Bildstein, B.; Malaun, M.; Kopacka, H.; Ongania, K.-H.; Wurst, K. *J. Organomet. Chem.* **1998**, *552*, 45–61.

(83) Ku, R.-Z.; Huang, J.-C.; Cho, J.-Y.; Kiang, F.-M.; Reddy, K. R.; Chen, Y.-C.; Lee, K.-J.; Lee, J.-H.; Lee, G.-H.; Peng, S.-M.; Liu, S.-T. *Organometallics* **1999**, *18*, 2145–2154.

(84) Herrmann, W. A.; Goossen, L. J.; Artus, G. R. J.; Köcher, C. *Organometallics* **1997**, *16*, 2472–2477.

(85) Herrmann, W. A.; Kocher, C.; Gooßen, L. J.; Artus, G. R. J. *Chem. Eur. J.* **1996**, *2*, 1627–1636.

(86) Doyle, M. P.; Bryker, W. J. *J. Org. Chem.* **1979**, *44*, 1572–1574.

(87) Vu, P. D.; Boydston, A. J.; Bielawski, C. W. *Green Chem.* **2007**, *9*, 1158–1159.

(88) Khramov, D. M.; Bielawski, C. W. *J. Org. Chem.* **2007**, *72*, 9407–9417.

(89) Khramov, D. M.; Boydston, A. J.; Bielawski, C. W. *Angew. Chem. Int. Ed.* **2006**, *45*, 6186–6189.

(90) Jeletic, M. S.; Jan, M. T.; Ghiviriga, I.; Abboud, K. A.; Veige, A. S. *Dalton Trans.* **2009**, 2764–2776.

(91) Peng, H. M.; Webster, R. D.; Li, X. *Organometallics* **2008**, *27*, 4484–4493.

(92) Zanardi, A.; Corberán, R.; Mata, J. A.; Peris, E. *Organometallics* **2008**, *27*, 3570–3576.

(93) Mas-Marzá, E.; Mata, J. A.; Peris, E. *Angew. Chem. Int. Ed.* **2007**, *46*, 3729–3731.

(94) Supporting Information Available from original manuscript: Synthetic and experimental details; tables spectroscopic and structural data (Tables S1–S7); ORTEP diagrams of (**2.1–3**)**a**, (**2.5–6**)**a**, **2.2c–d** and **2.6c–d** (Figures S1–S9); CVs of **2.1a**, (**2.3–5**)**a**, **2.1b**, (**2.3–5**)**b**, **2.2c–e** and **2.6c–e** (Figures S10–S23); spectroelectrochemical spectra for **2.1b**, **2.3b**, **2.5b**, **2.2c–d** and **2.6c–d** (Figures S24–S30); ^{1}H and ^{13}C NMR spectra; CIFs.

(95) Kownacki, I.; Kubicki, M.; Szubert, K.; Marciniec, B. *J. Organomet. Chem.* **2008**, *693*, 321–328.

(96) Chen, D.; Banphavichit, V.; Reibenspies, J.; Burgess, K. *Organometallics* **2007**, *26*, 855–859.

(97) Iglesias, M.; Beetstra, D. J.; Stasch, A.; Horton, P. N.; Hursthouse, M. B.; Coles, S. J.; Cavell, K. J.; Dervisi, A.; Fallis, I. A. *Organometallics* **2007**, *26*, 4800–4809.

(98) Herrmann, W. A.; Baskakov, D.; Herdtweck, E.; Hoffmann, S. D.; Bunlaksananusorn, T.; Rampf, F.; Rodefeld, L. *Organometallics* **2006**, *25*, 2449–2456.

(99) Viciano, M.; Poyatos, M.; Sanaú, M.; Peris, E.; Rossin, A.; Ujaque, G.; Lledós, A. *Organometallics* **2006**, *25*, 1120–1134.

(100) Vicent, C.; Viciano, M.; Mas-Marzá, E.; Sanaú, M.; Peris, E. *Organometallics* **2006**, *25*, 3713–3720.

(101) Schubert, U.; Friedrich, P.; Orama, O. *J. Organomet. Chem.* **1978**, *144*, 175–179.

(102) Arduengo III, A. J.; Dias, H. V. R.; Dixon, D. A.; Harlow, R. L.; Klooster, W. T.; Koetzle, T. F. *J. Am. Chem. Soc.* **1994**, *116*, 6812–6822.

(103) Arduengo III, A. J.; Dias, H. V. R.; Harlow, R. L.; Kline, M. *J. Am. Chem. Soc.* **1992**, *114*, 5530–5534.

(104) Tolman, C. A. *Chem. Rev.* **1977**, *77*, 313–348.

(105) Strohmeier, W.; Müller, F.-J. *Chem. Ber.* **1967**, *100*, 2812–2821.

(106) Cotton, F. A.; Kraihanzel, C. S. *J. Am. Chem. Soc.* **1962**, *84*, 4432–4438.

(107) Cotton, F. A. *Chemical Applications of Group Theory*; 3rd ed.; John Wiley & Sons: New York, 1990.

(108) Herrmann, W. A.; Roesky, P. W.; Elison, M.; Artus, G.; Öfele, K. *Organometallics* **1995**, *14*, 1085–1086.

(109) Öfele, K.; Herrmann, W. A.; Mihalios, D.; Elison, M.; Herdtweck, E.; Scherer, W.; Mink, J. *J. Organomet. Chem.* **1993**, *459*, 177–184.

(110) Öfele, K.; Roos, E.; Herberhold, M. *Z. Naturforsch. B* **1976**, *31*, 1070–1077.

(111) Tennyson, A. G.; Ono, R. J.; Hudnall, T. W.; Khramov, D. M.; Er, J. A. V.; Kamplain, J. W.; Lynch, V. M.; Sessler, J. L.; Bielawski, C. W. *Chem. Eur. J.* **2010**, *16*, 304.

(112) Tennyson, A. G.; Rosen, E. L.; Collins, M. S.; Lynch, V. M.; Bielawski, C. W. *Inorg. Chem.* **2009**, *48*, 6924–6933.

(113) Allen, L. C. *J. Am. Chem. Soc.* **1989**, *111*, 9003–9114.

(114) Allred, A. L. *J. Inorg. Nucl. Chem.* **1961**, *17*, 215–221.

(115) Pauling, L. *The Nature of the Chemical Bond*; 3rd ed.; Cornell University Press: Ithaca, 1960.

Chapter 3: 1,1′-Bis(N-benzimidazolylidene)ferrocene: Synthesis and Study of a Novel Ditopic Ligand and its Transition Metal Complexes†

Portions of this chapter were reprinted from Varnado, C. D., Lynch, V. M.; Bielawski, C. W. *Dalton Trans*. **2009**, 7253, and is reproduced with permissions from the Royal Society of Chemistry. V. M. Lynch assisted with the X-ray crystallography. C. W. Bielawski assisted with writing the aforementioned publication. I performed the syntheses, characterization, and study of all compounds and helped to write the aforementioned publication.

ABSTRACT

Diiridum complexes containing 1,1′-bis(N-benzimidazolylidene)ferrocene, a novel ditopic ligand comprised of two N-heterocyclic carbenes (NHCs) linked directly to each cyclopentadienyl ring of a ferrocene via their N-substituents, were synthesized. Crystallographic analyses of these C_2-symmetric complexes revealed the benzimidazolylidene moieties were intramolecularly stacked in nearly opposing orientations, effectively forming Janus-type bis(NHC) structures in the solid-state. Using a variety of electrochemical techniques, the oxidation potentials of the ferrocenyl moieties in these complexes were found to depend on the auxillary ligands coordinated to the Ir centers (i.e., 1,5-cyclooctadiene vs. carbonyl). Similarly, the ν_{CO} of carbonyls ligated to the Ir centers varied in accord with the oxidation state of the ferrocene moiety. These results suggest that the Ir and Fe centers in these complexes are electronically coupled and that the electron donating properties of the NHC ligands reported herein can be tuned electrochemically.

INTRODUCTION

N-heterocyclic carbenes (NHCs)[1] have emerged as a highly versatile class of ligands for a broad range of transition metals[2] They generally coordinate with higher affinities than phosphines[3] and, in many cases, greatly enhance the catalytic activities displayed by the metals to which they are ligated.[4] These effects are often amplified through the use of multi-topic NHCs, where a ligand containing multiple NHCs is coordinated to a single metal. A majority of these efforts have been directed toward bidentate derivatives (*e.g.*, **A**; Figure 3.1).[5] As a result of the chelate effect, these monometallic complexes are generally more stable than analogues containing two monodentate ligands.[6] In addition, such metal complexes often feature remarkable structural characteristics, such as unusual bite angles or asymmetry, which can result in pronounced catalytic activities or otherwise interesting physical properties.

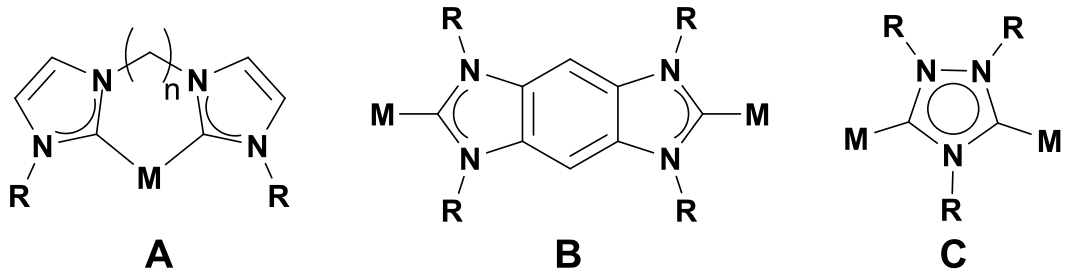

Figure 3.1 Representative examples of transition metal complexes containing ditopic N-heterocyclic carbenes.

We are generally interested in the development of multi-topic NHC scaffolds that are poised to bind multiple transition metals.[7] Capitalizing on the unique features inherent to NHCs and their transition metal complexes, we believe such materials hold tremendous potential in displaying novel physical and electronic properties. Our efforts

have focused primarily on Janus-type bis(NHC)s,[8] which feature two linearly-opposed NHCs annulated to a common arene backbone. These ditopic ligands have proven to be useful for the synthesis of new classes of bimetallic complexes (B)[9] as well as polymeric[10] and self-assembled[11] materials. Recently, Peris and co-workers demonstrated that triazolyldiylidenes[12] are also capable of binding two transition metals (C) and can be used to form homo- as well as hetero-binuclear complexes that exhibit useful catalytic properties.[13] One attractive feature of ditopic ligands such as B and C is that the two NHCs are connected via π-conjugated linkers, which creates opportunities for enabling electronic communication between coordinated metal centers.

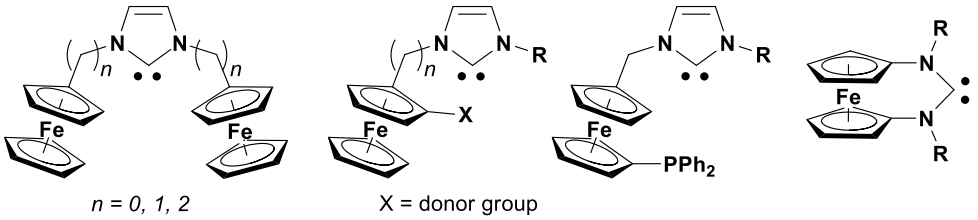

Figure 3.2 Representative examples of previously reported ferrocenyl-substituted NHCs and diaminocarbenes.

The key to growth in this field lies in the development of new molecular scaffolds for bridging transition metals. NHCs functionalized with ferrocenes hold considerable potential in such regard. Pioneered by Bildstein,[14] this burgeoning field[15] encompasses a broad range of NHCs,[16,17] including derivatives with additional donor groups[18] (i.e., phosphines, sulfides, etc.) that can be used as multi-dentate ligands. These ligands generally contain one NHC moiety and have been primarily used as sterically-encumbered or chiral groups to enhance the catalytic activities and/or selectivities displayed by various types of transition metals (see Figure 3.2 for examples).

The first example of a ferrocene-based ligand containing two NHCs was reported by Coleman and co-workers.[19] They synthesized a Pd^{II} chloride complex coordinated to 1,1′-bis(methyleneimidazolylidene) (**D**; Figure 3.3), which contains one imidazolylidene linked to each cyclopentadienyl (Cp) ring of a ferrocene via N-methylene spacers. Due to its unique geometry, this ditopic ligand was found to coordinate to a metal center in an unusual *trans* geometry. Notably, derivatives of these complexes were subsequently shown to be useful catalysts for facilitating the Heck and other coupling reactions.[20]

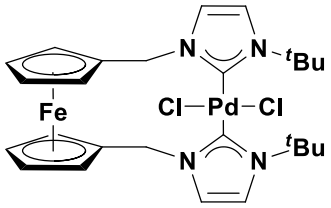

D

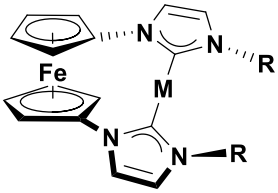

E

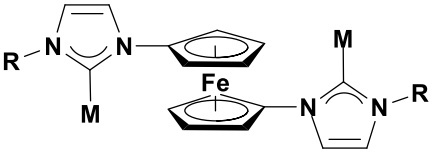

F

Figure 3.3 Selected examples of ditopic N-heterocyclic carbenes and their transition metal complexes.

Building upon these studies, we envisioned a new class of transition metal complexes containing a ditopic ligand that featured two NHCs connected directly to each Cp ring of a ferrocene unit via their N-substituents. As a result of the unique rotational processes exhibited by metallocenes, this ligand should be capable of binding to metals in two distinct ways. For example, coordination of the ligand to a single metal center should afford **E**, potentially as a C_2-symmetric complex. In this binding arrangement, the

ligand, like the one shown in **D**,[19] is an NHC analogue of 1,1'-bis(diphenylphosphino)ferrocene (dppf), a bisphosphine that has found tremendous utility in the synthesis of a variety of catalytically-active complexes.[21] Alternatively, coordination of the ditopic ligand to two metal centers should afford complex **F**. In this structure, the metal centers are proximally connected to a ferrocene moiety which may open new modes of electronic communication between the various groups.

Herein, we describe the synthesis and study of derivatives of complex **F**.‡ These efforts include the synthesis of a ditopic ligand analogous to the one shown as well as its binuclear $IrCl_2$(cod) (cod = 1,5-cyclooctadiene) and $IrCl_2(CO)_2$ complexes. These particular derivatives were selected because Ir-NHC complexes are typically stable and have been extensively used for evaluating the electron donating properties of a wide range of ligands,[22] facilitating comparison to others reported in the literature.[23] Finally, as part of our general interest in redox-active and functionalized NHCs,[17,24,25] we also probed whether the ferrocene moiety is electronically coupled to the NHC-metal centers using a range of electrochemical techniques.

RESULTS AND DISCUSSION

To prepare a ditopic ligand analogous to complex **E** (Figure 3.3), we initially envisioned synthesizing 1,1′-bis(N-imidazole)ferrocene via Ullmann coupling of 1,1′-dibromoferrocene[14] to imidazole, in accord with a literature report for an analogous reaction involving bromoferrocene,[26] followed by alkylation and metallation. Unfortunately, all attempts at the aforementioned coupling reaction resulted in a low yield of the desired product that was contaminated with 1-bromo-1′-(N-imidazole)ferrocene. As a result, a different synthetic pathway involving the amination of 2-fluoronitrobenzene with 1,1′-diaminoferrocene was developed.

As summarized in Scheme 3.1, treatment of 1,1′-diaminoferrocene[44] with 2-fluoronitrobenzene in DMSO under basic conditions afforded the desired S_NAr product, 1,1′-bis(2-nitroanilino) ferrocene (**3.1**), in 88% isolated yield. Guided by literature precedent,[10] Pd-catalyzed reductive cyclization of **3.1** using sodium formate in formic acid at 110 °C afforded bis(benzimidazole) **3.2** in 66% yield. Unfortunately, attempts to alkylate **3.2** with various alkyl iodides, including methyl iodide, did not yield the expected bis(benzimidazolium) iodide salt but rather afforded dimethylbenzimidazolium iodide and an intractable material. However, treatment of **3.2** with triethyloxonium tetrafluoroborate successfully afforded the desired bis(benzimidazolium) derivative, diethyl 1,1′-bis(N-benzimidazolium)ferrocene $(BF_4)_2$ (**3.3**), in 70% yield. The ^{1}H NMR signals for the benzimidazolium protons in **3.3** were found at δ = 9.8 ppm (DMSO-d_6), which was within the range expected for 1,3-disubstituted benzimidazolium salts.[27]

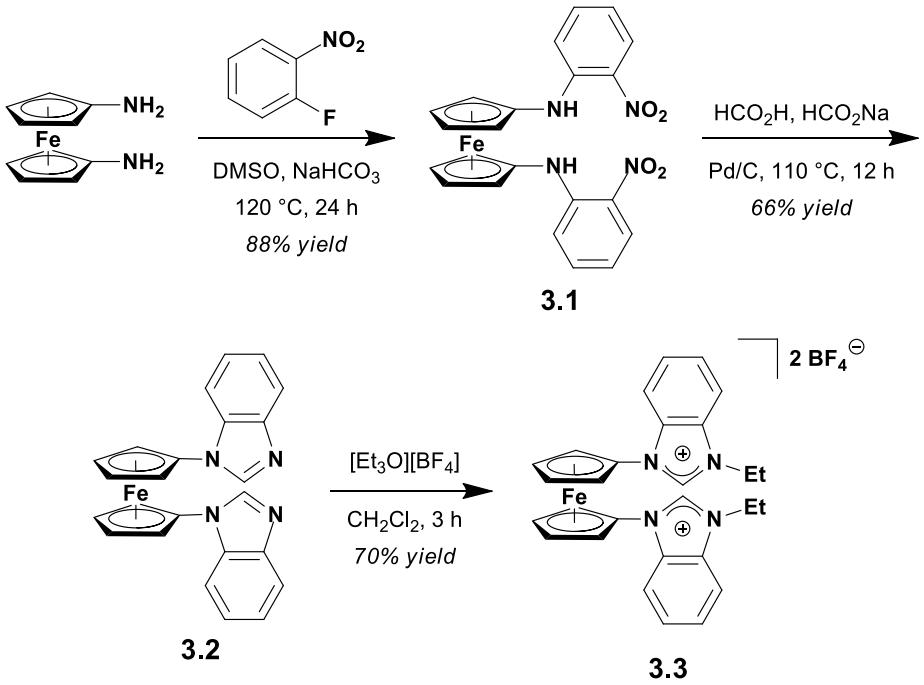

Scheme 3.1 Synthesis of bis(benzimidazolium) salt **3.3**.

X-ray analysis of a single crystal of **3.3** (obtained by slow diffusion of diethyl ether into an acetone solution saturated) confirmed the structure of this salt. As shown in Figure 3.4, the two benzimidazolium moieties were rotated out the plane of the Cp rings of the ferrocene moiety by approximately 31.4°. In addition, the Cp rings were slightly tilted toward each other by 1.6°, which may be due to crystal packing effects. The packing diagram of this structure (not shown) revealed that the benzimidazolium moieties were intermolecularly stacked in a coplanar arrangement and separated by a distance of 3.58 Å with a centroid-to-centroid offset distance of 1.18 Å. that was consistent with a π-π^* interaction.[28] The average distance between the Fe center in this salt and each carbon atom of its Cp rings was 2.040 Å. This distance was nearly identical to the analogous average distance found in ferrocene (2.045 Å).[29] Likewise, the key structural parameters of the benzimidazolium fragments were comparable to other known benzimidazolium salts.[27] Hence, despite direct attachment of two positively charged benzimidazolium groups to ferrocene, these components had only marginal effects on each other's molecular structures.

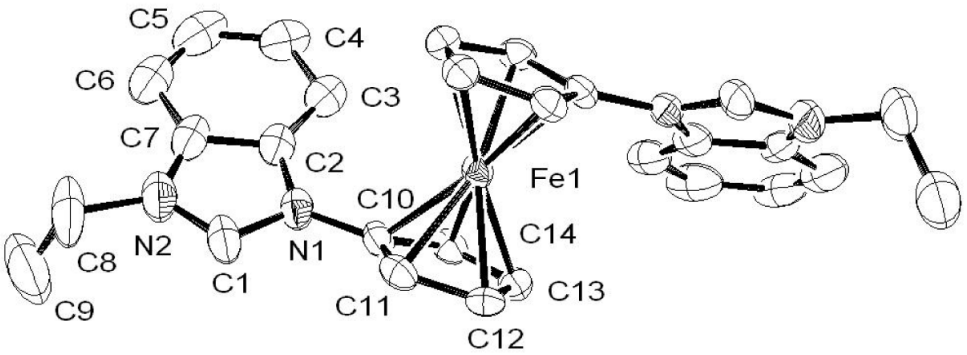

Figure 3.4 ORTEP diagram showing 50% probability thermal ellipsoids and selected atom labels for bis(benzimidazolium) salt **3.3**. Solvent molecules, counteranions, and hydrogen atoms have been removed for clarity. Selected bond lengths (Å) and angles (°): C1-N1, 1.351(5); C1-N2, 1.327(6); C2-N1, 1.401(6); C7-N2, 1.392(7); N1-C1-N2, 109.6(4). The distance between the Fe center and a Cp centroid is 1.647 Å. The angle between the planes of the two benzimidazolium moieties is 64.01°. The angle between the planes of the two Cp rings is 1.340°. The dihedral angle (φ) between the benzimidazolium moiety and the Cp ring (defined by torsion C1-N1-C10-C14) is 32.8(4)°.

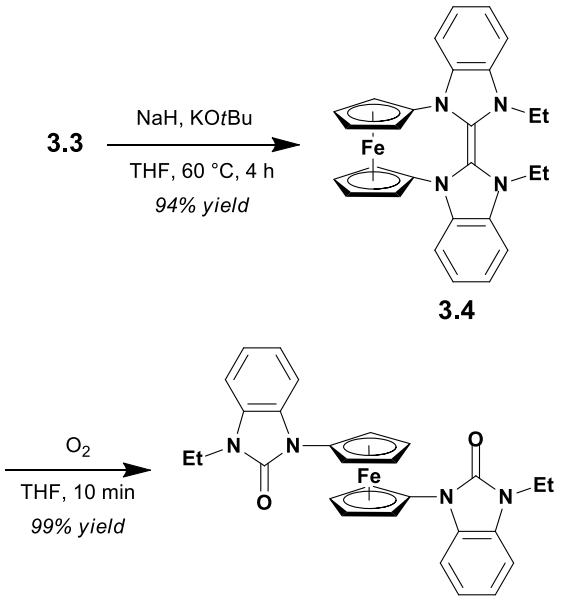

Scheme 3.2 Synthesis of enetetramine **3.4** and bis(urea) **3.5**.

As shown in Scheme 3.2, treatment of a THF solution of **3.3** with sodium hydride (and a catalytic amount of potassium *tert*-butoxide to facilitate deprotonation) afforded a dark red solid in 94% yield. This compound was tentatively assigned as enetetramine **3.4** and presumed to form via dimerization of the respective NHCs (generated in situ). In addition to a disappearance of the benzimidazolium proton in **3.3** (δ = 9.83 ppm; DMSO-d_6), a signal characteristic of an enetetramine[30] was observed at δ = 142.4 ppm (C_6D_6) in the ^{13}C NMR spectrum of **3.4**. Unfortunately, all attempts at obtaining a crystal of this compound suitable for X-ray diffraction analysis were unsuccessful. To verify its structure, a benzene solution of **3.4** was exposed to atmospheric oxygen which rapidly afforded bis(urea) **3.5** in nearly quantitative yield. It has been previously established that enetetramines react with oxygen to form bis(urea)s, whereas free NHCs do not.[8,31] Compared to **3.4**, a relatively downfield signal was found at δ = 152.4 ppm (C_6D_6) in the ^{13}C NMR spectrum of **3.5** and assigned to the carbon atoms of its carbonyl groups. As expected, the FT-IR spectrum of **3.5** displayed a carbonyl stretching frequency characteristic of an urea at ν_{CO} = 1709 cm^{-1} (KBr).

Enetetramines often exist in equilibrium with their free diaminocarbenes[32] and have been used to prepare NHC-metal complexes.[33] Hence, Ir complex **3.6** was synthesized by treating **3.4** with a molar equivalent of $[Ir(cod)Cl]_2$ in benzene (see Figure 3.7). After stirring the resulting mixture at ambient temperature for 12 h, excess hexanes was added which resulted in the formation of a yellow precipitate. Collection of this precipitate followed by further purification via column chromatography (eluent = 20:1 v/v CH_2Cl_2/CH_3OH) afforded **3.6** in 61% yield. Complex **3.6** was found to be stable toward both oxygen and water, and could be stored on the bench top for indefinite periods of time. The diagnostic ^{13}C signal for the metal ligated carbons of the NHC ligands was observed at δ = 189.9 ppm ($CDCl_3$), in accord with other Ir-NHC cod

complexes reported in the literature,[22,23] particularly those containing benzimidazolylidenes.[33]

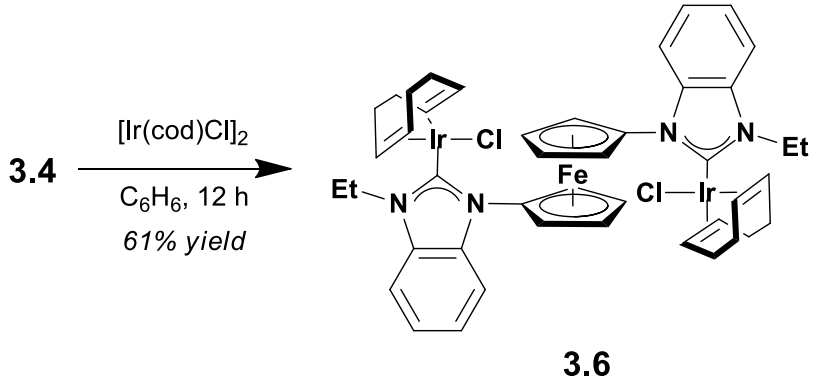

Scheme 3.3 Synthesis of binuclear Ir(cod) complex **3.6.**

The solid-state structure of complex **3.6** was determined by single-crystal X-ray diffraction analysis. X-Ray quality crystals were grown by slow diffusion of pentane into a saturated solution of $CHCl_3$. As shown in Figure 3.5, structure of **3.6** was found to adopt a C_2-symmetric structure with each Ir center featuring a distorted square planar geometry, as expected for Ir-NHC complexes of this type.[22,23,34] Likewise, the $C_{carbene}$-Ir and other bond lengths and angles of the Ir-NHC center were similar to those observed in other known NHC-Ir complexes. The benzene rings of the nearly coplanar (φ = 8.0°) benzimidazolylidene moieties were intramolecularly stacked upon each other and separated by a centroid-to-centroid distance of 3.46 Å with a centroid-to-centroid offset distance of 0.86 Å consistent with a favorable π-π^* interaction.[28,35] This unique structural characteristic may explain why the Cp rings were tilted toward each other by 6.08°. Presumably to minimize negative steric interactions, the angle between the two NHC-Ir segments was found to be approximately 117°. Surprisingly, these features resulted in a solid-state structure that resembled a Janus-type bis(NHC)[8] where, as illustrated in Figure 3.5, the two benzimidazolylidenes were held into nearly opposing positions via a

supramolecular interaction. As a result, the planes of the benzimidazolylidenes and Cp rings were twisted by approximately 42.5°.

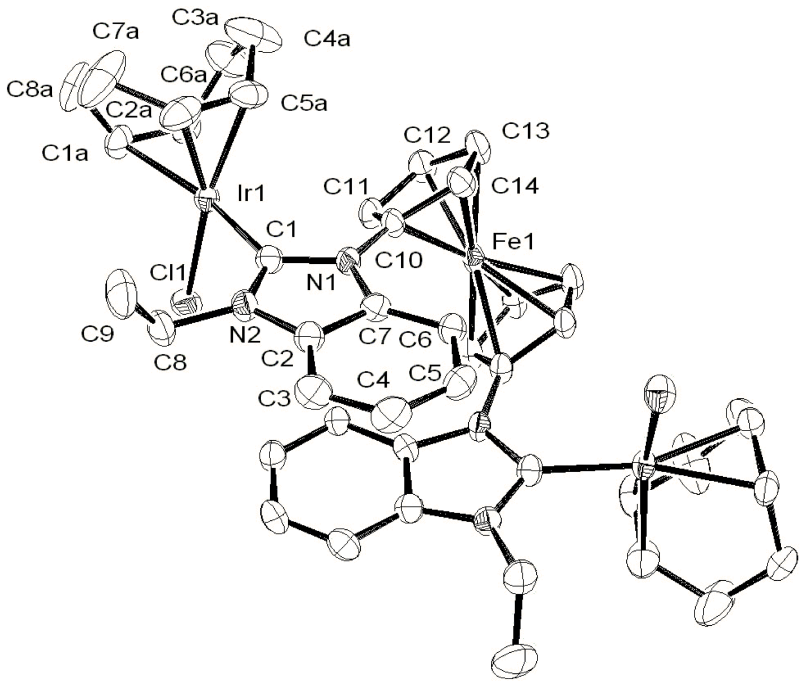

Figure 3.5 ORTEP diagram showing 50% probability thermal ellipsoids and selected atom labels for **3.6**. Solvent molecules and hydrogen atoms have been removed for clarity. Selected bond lengths (Å) and angles (°): Ir1-C1, 2.026(4); Ir1-C1a, 2.182(4); Ir1-C2a, 2.181(4); Ir1-C5a, 2.119(4); Ir1-C6a, 2.106(5); Ir1-Cl, 2.3772(10); C1-N1, 1.371(5); C1-N2, 1.355(5); N2-C2, 1.400(5); N1-C7, 1.395(5); C2-C7, 1.386(5); N1-C1-N2, 105.8(3). The distance between the centroids of the benzimidazolylidene benzene rings is 3.46 Å. The distance between Fe1 and a Cp centroid is 1.662 Å. The angle between the planes of the two benzimidazolylidenes is 8.00°. The angle between the planes of the two Cp rings is 6.08°. The dihedral angle (φ) between the benzimidazolylidene and the Cp ring (defined by torsion angle = C10-C14-N1-C7) is 42.5(6)°. Complex **3.6** sits on a crystallographic two-fold rotation axis along ½, y, ¼. The two-fold rotation axis passes through the iron atom.

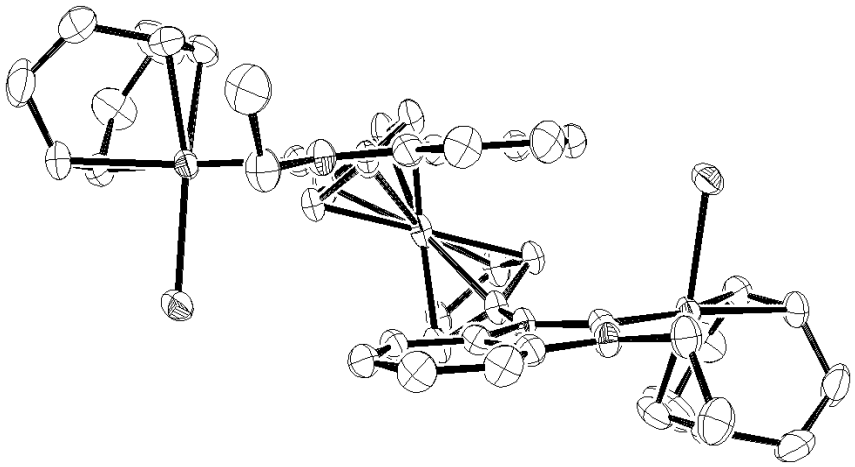

Figure 3.6 Alternate view of the ORTEP of **3.6** showing the coplanar benzimidazolylidenes and the nearly opposed NHC-Ir moieties.

As part of our evaluation of the electronic properties of complexes containing **3.4** (see below), derivatives containing ligands with diagnostic IR frequencies (*i.e.*, carbonyls) were also synthesized. Pressurizing a CH_2Cl_2 solution of **3.6** with carbon monoxide followed by stirring at ambient temperature for 1 h afforded **3.7** as a yellow solid in 95% yield, after removal of solvent and trituration with pentane (see Figure 3.10). Compared to **3.6**, the ^{13}C signal for the the carbene atoms of the NHC ligands in **3.7** was observed upfield at δ = 180.6 ppm ($CDCl_3$) and in accord with other NHC-Ir carbonyl complexes.[22,23] The ν_{CO}s for **3.7** were found at 1989 (asymmetric) and 2068 (symmetric) cm^{-1} in solution (CH_2Cl_2) (see below for further discussion).

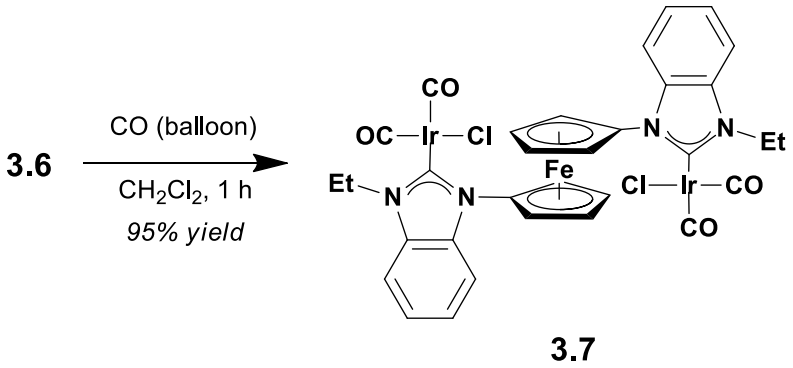

Scheme 3.4 Synthesis of binuclear Ir carbonyl complex 3.7.

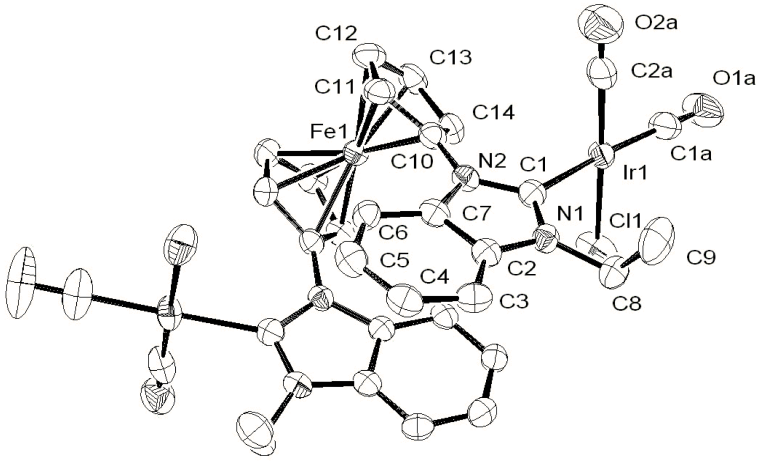

Figure 3.7 ORTEP diagram showing 50% probability thermal ellipsoids and selected atom labels for **3.7**. Solvent molecules and hydrogen atoms have been removed for clarity. Selected bond lengths (Å) and angles (°): Ir-C1, 2.084(4); Ir-C1a, 1.885(4); Ir-C2a, 1.883(5); Ir-Cl, 2.3466(12); C1-N1, 1.353(5); C1-N2, 1.359(5); N1-C2, 1.391(5); N2-C7, 1.407(5); C2-C7, 1.387(5); N1-C1-N2, 106.0(3)°. The distance between the centroids of the benzimidazolylidene benzene rings is 3.54 Å. The distance between Fe1 and a Cp centroid is 1.658 Å. The angle between the planes of the two benzimidazolylidenes is 12.04°. The angle between the planes of the two Cp rings is 8.03°. The dihedral angle (φ) between the benzimidazolylidene and Cp ring (defined by torsion C7-N2-C10-C11) is 37.2(5)°.

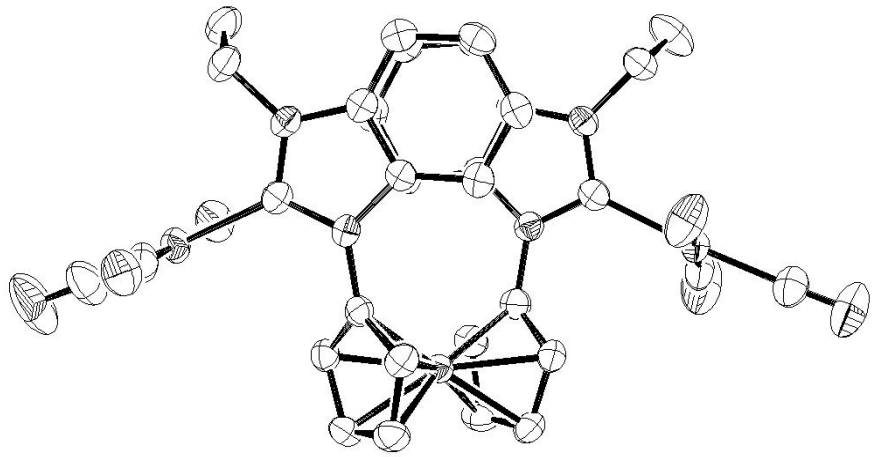

Figure 3.8 Alternate view of the ORTEP of **3.7** showing the wide angle (~128°) between the NHC-Ir moieties.

The structure of **3.7** was confirmed by single-crystal X-ray diffraction. X-ray quality crystals were grown by slow diffusion of pentane into a saturated solution of $CHCl_3$. As shown in Figure 3.7, complex **3.7** exhibited a similar solid-state structure as **3.6**. The benzene rings of the benzimidazolylidene fragments in **3.7** were stacked upon each other and separated by a centroid-to-centroid distance of 3.54 Å with a centroid-to-centroid offset distance of 1.07 Å. As noted above, this feature suggests a favorable π-π* interaction,[28,35] although the distance between the benzene rings in **3.7** was slightly longer compared to the analogous distance observed in **3.6** (3.46 Å) which also may be due to the electron deficient character inherent to the former complex. As observed in the solid-state structure of **3.6**, the two NHC-Ir units were positioned in a nearly directionally-opposed (~128°) orientation (see Figure 3.8). However, compared to **3.6**, the tilt of the planes of two Cp rings **3.7** slightly increased to 8.03° while the angle between the planes of the benzimidazolylidenes and the Cp rings decreased to 37.2°.

Upon synthesis and characterization, the electrochemical properties of Ir complexes **3.6** and **3.7** were evaluated using a variety of techniques. As shown in Figures 3.9a and 3.9b, the cyclic voltammograms of both complexes exhibited quasi-reversible redox processes, but at different potentials: $E_{1/2}$ = +0.75 V and +0.89 V for **3.6** and **3.7**, respectively (relative to SCE). Considering Ir carbonyl complexes containing NHC ligands typically show irreversible oxidations and bis(urea) **3.5** exhibited a redox couple at a similar potential ($E_{1/2}$ = +0.56 V), the aforementioned processes were attributed to the $Fe^{II/III}$ redox couple. The different redox potentials observed in these complexes suggested to us that the Ir centers were electronically coupled to the ferrocene moieties. Furthermore, the relative oxidation potentials of **3.6** and **3.7** were consistent with the greater π-acidity of carbonyl ligands compared to cod. These results were surprising in light of the solid-state structure of **3.3** which revealed that the benzimidazolium components of this salt had a near negligible effect on the key structural characteristics of its ferrocene moiety.

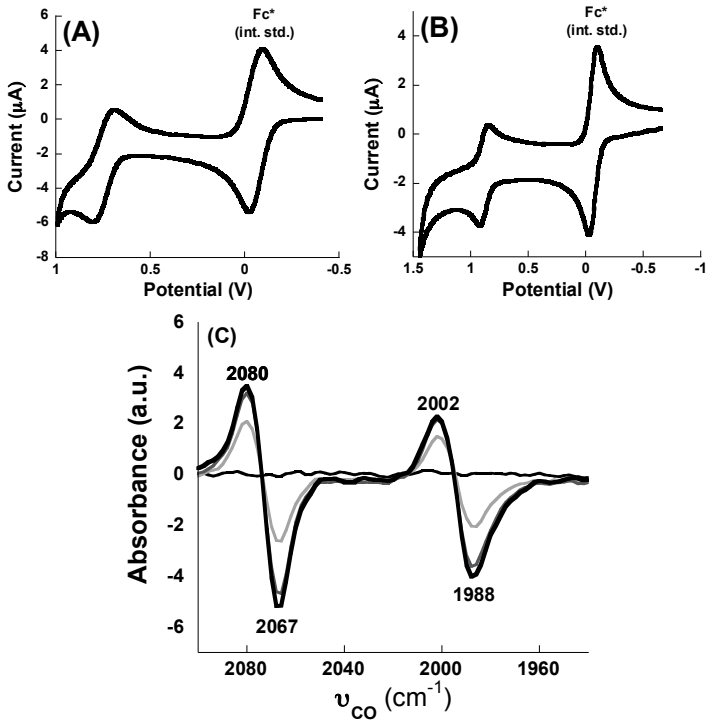

Figure 3.9 Cyclic voltammograms of **3.6** (A) and **3.7** (B) with Fc* added as an internal standard (referenced to –0.057 V vs. SCE). Conditions: CH_2Cl_2 as solvent, 0.1 M $[(Bu)_4N](PF_6)$ as electrolyte, 100 mV s^{-1} scan-rate. (C) Superimposed difference FT-IR spectra showing the disappearance of **3.7** (ν_{CO} = 2067, 1988 cm^{-1}) with concomitant formation of **3.7+** (ν_{CO} = 2080, 2002 cm^{-1}) upon oxidation (E = +1.0 V) over the duration of 30 s. Conditions: CH_2Cl_2 as solvent, $[\mathbf{3.7}]_0$ = 10 mM, 0.1 M $[(Bu)_4N](PF_6)$ as electrolyte.

It has been previously shown that the electron-donating nature of various ligands can be probed by analyzing the ν_{CO} of metal carbonyl complexes which contain them.[36] Hence, the ability of **3.4**'s redox-active ferrocene to modulate the donating properties of the NHCs and ultimately the ligated Ir centers to which it is connected was evaluated by examining the ν_{CO} of **3.7** as a function of the iron's oxidation state.[37] To accomplish this task, a spectroelectrochemical experiment§ that combined bulk electrolysis with time–resolved FT-IR spectroscopy was devised.[38] A thin-layer cell was assembled and a

solution of complex **3.7** was recorded as the background. To selectively oxidize the Fe center, a potential of +1.0 V was applied while FT-IR spectra were recorded over time. As shown in Figure 3.9c, signals attributable to **3.7** (ν_{CO} = 2067 and 1988 cm^{-1}) disappeared as a new material (assigned to **3.7**$^{+}$) exhibiting ν_{CO} = 2080 and 2002 cm^{-1} formed over the same time period.[39] These changes are consistent with diminished electron density at the Ir center induced by the development of positive charge at the redox-active Fe center (i.e., $Fe^{II} \rightarrow Fe^{III}$). To place these results into context, the Tolman electronic parameters (TEP)[40] of **3.7** and **3.7**$^{+}$ were calculated to be 2053.7 and 2064.7 cm^{-1}, respectively, using Nolan's method.[23] The former value is similar to TEPs displayed by weakly donating NHCs whereas the latter is similar to weakly donating phosphines.†† Collectively, these results further support the notion that the NHC ligated Ir centers and the ferrocenyl units in these complexes are electronically coupled and suggest that the electron donating properties of the the NHC ligands can be tuned electrochemically.

CONCLUSIONS

We report the synthesis and study of two new diiridium complexes linked together via 1,1′-bis(N-benzimidazol-ylidene)ferrocene, a novel ditopic ligand comprised of two N-heterocyclic carbenes linked directly to each Cp ring of a ferrocene via their N-substituents. These complexes were found to adopt Janus-like bis(NHC)s structures in the solid-state, which may be attributed to a favorable π-π* interactions formed between adjoining benzimidazolylidenes. It was determined that the oxidation potentials of the ferrocene moieties in complexes **3.6** and **3.7** were dependent on the electronic nature of the ligated Ir centers. Similarly, the electron donating properties of the NHC ligands in **3.7** were tuned by changing the oxidation state of its ferrocene moiety. Based on these

results, the ditopic ligand reported herein is poised for use in the formation of novel bimetallic complexes, including redox-active variants and those that may be used as bifunctional catalysts,[13,41] as well as connectable components in the growing fields of nano- and molecular electronics.[42]

EXPERIMENTAL

General Considerations. Unless otherwise noted, all manipulations were performed using standard Schlenk techniques under an atmosphere of nitrogen or in a nitrogen-filled glove box. THF was distilled from Na/benzophenone under nitrogen. Toluene was distilled from CaH_2 and degassed by three consecutive freeze-pump-thaw cycles. DMSO was distilled under nitrogen from calcium hydride. All other chemicals were used as received. ^{1}H NMR and ^{13}C NMR spectra were recorded on a Varian Mercury 400 MHz spectrometer and were referenced to residual protio solvent. ^{13}C NMR spectra were routinely run with broadband decoupling. Chemical shifts are reported in delta (δ) units, expressed in parts per million (ppm) downfield from tetramethylsilane using the residual solvent as an internal standard (^{1}H: $CDCl_3$, 7.24 ppm; C_6D_6, 7.15 ppm; DMSO-d_6, 2.49 ppm; ^{13}C: $CDCl_3$, 77.0 ppm; C_6D_6, 128.0 ppm; DMSO-d_6, 39.5 ppm). Infrared spectra were recorded using a Perkin-Elmer Spectrum BX FT-IR spectrometer in a solution cell equipped with CaF_2 windows. Unless otherwise noted, melting points were performed on a Mel-Temp apparatus under ambient atmosphere and are uncorrected. High-resolution mass spectra (HRMS) were obtained with a VG analytical ZAB2-E or a Karatos MS9 instrument and are reported as m/z (relative intensity). Microanalyses were performed at Midwest Microlab, LLC, Indianapolis, IN. Electrochemical analyses were performed on CH Instruments Electrochemical Workstations (series 660B and 700B) using an air-free three electrode cell under an

atmosphere of nitrogen. The electrochemical cell contained platinum working and counter electrodes and a silver wire as a quasi-reference electrode. All measurements were performed in dry CH_2Cl_2 using 1 mM analyte, 0.1 M $[(Bu)_4N](PF_6)$ as the electrolyte, and decamethylferrocene (Fc*) as the internal standard ($Fc^{*0/+}$ = –0.057 V vs. SCE).[43] The potentials listed were determined at 100 mV/s scan-rates and adjusted to saturated calomel electrode (SCE).

1,1′-Bis(2-nitroanilino)ferrocene (3.1). A 40 mL pressure tube was charged with 1,1′-diaminoferrocene[44] (1.55 g, 7.10 mmol), 2-fluoronitrobenzene (2.10 g, 15.0 mmol), sodium bicarbonate (1.80 g, 21.5 mmol), DMSO (6 mL) and a stirbar. The resulting mixture was then heated to 120 °C for 24 h. Upon cooling to ambient temperature, a black solid precipitated from solution. The filtrate was then poured into 500 mL of H_2O, causing additional precipitate to form. The precipitates were collected and combined, triturated with isopropanol in a sonicator, filtered, and then dried under vacuum to afford 3.0 g (88% yield) of the desired product as a black powder. m.p. = 177–182 °C. ^{1}H NMR ($CDCl_3$): δ 9.08 (s, 2H), 8.10 (d, J = 8.1 Hz, 2H), 7.28 (dd appearing as t, J = 7.5 Hz, 2H), 7.16 (d, J = 8.4 Hz, 2H), 6.67 (dd appearing as t, J = 7.5 Hz, 2H), 4.41 (br, 4H), 4.23 (br, 4H). ^{13}C NMR ($CDCl_3$): δ 144.4, 135.7, 132.6, 126.5, 116.9, 115.9, 95.6, 67.7, 66.5. HRMS: $[M]^+$ calcd for $C_{22}H_{18}O_4FeN_4$, 458.0675, found, 458.0672.

1,1′-Bis(N-benzimidazole)ferrocene (3.2). A 50 mL flask was charged with **3.1** (1.00 g, 2.20 mmol), sodium formate (3.2 g, 47 mmol), Pd/C (5% Pd, 500 mg, 0.23 mmol), formic acid (88% aqueous, 10 mL), and a stirbar, and then heated to 110 °C for 12 h. After cooling to ambient temperature, the reaction mixture was filtered through a PTFE filter into an aqueous solution containing 10% (w/v) sodium carbonate (400 mL). The resulting mixture was then extracted with ethyl acetate (3 x 150 mL). The combined organic extracts were washed with brine, and then dried over anhydrous sodium sulfate.

Removal of the residual solvent under vacuum afforded a hygroscopic yellow solid. The crude product was then purified via column chromatography (silica gel) using 20:1 CH_2Cl_2/CH_3OH as the eluent (r.f. = 0.32) to afford 0.60 g (66% yield) of the desired product as a yellow solid. m.p. = 169–172 °C. ^{1}H NMR ($CDCl_3$): δ 8.03 (s, 2H), 7.81 (d, *J* = 7.2 Hz, 2H), 7.50 (d, *J* = 7.2 Hz, 2H), 7.27 (t, *J* = 7.2 Hz, 2H), 7.23 (t, *J* = 7.2 Hz, 2H), 4.75 (t, *J* = 1.8 Hz, 4H), 4.40 (t, *J* = 1.8 Hz, 4H). ^{13}C NMR ($CDCl_3$): δ 144.2, 142.8, 133.7, 123.7, 122.9, 120.8, 110.9, 94.8, 67.8, 63.3. HRMS: $[M]^+$ calcd for $C_{24}H_{19}N_4Fe$, 419.0956; found, 419.09536.

Diethyl 1,1′-bis(N-benzimidazolium)ferrocene ($BF_4)_2$ (3.3). A 20 mL vial was charged with **3.2** (400 mg, 0.89 mmol), triethyloxonium tetrafluoroborate (600 mg, 3.0 mmol), CH_2Cl_2 (10 mL) and a stirbar, and then stirred for 4 h at ambient temperature. The reaction mixture was quenched with excess methanol (5 mL) and stirred at ambient temperature for an additional 12 h. The resulting mixture was poured into excess diethyl ether (50 mL), which caused yellow solids to precipitate. The solids were collected via filtration, washed with diethyl ether and then dried under vacuum to afford 480 mg (70% yield) of the desired product as a yellow powder. ^{1}H NMR (DMSO-d_6): δ 9.83 (s, 2H), 8.07 (d, *J* = 8.1 Hz, 2H), 7.83 (d, *J* = 8.4 Hz, 2H), 7.62 (dd appears as t, *J* = 7.2 Hz, 2H), 7.53 (dd appearing as t, *J* = 7.2 Hz, 2H), 5.47 (t, *J* = 1.8, 4H), 4.77 (t, *J* = 4.8, 4H), 4.28 (q, *J* = 7.2 Hz, 4H), 1.48 (t, *J* = 7.2, 6H). ^{13}C NMR (DMSO-d_6): δ141.5, 130.3, 129.6, 127.0, 126.6, 113.6, 92.9, 69.2, 64.5, 42.3, 13.7. HRMS: $[M - 2BF_4]^{2+} \div 2$ calcd for $C_{28}H_{28}FeN_4$, 238.0832; found, 238.0826.

Enetetramine 3.4. A 20 mL vial with a Teflon lined cap was charged with **3.3** (65 mg, 0.01 mmol), sodium hydride (10 mg, 043 mmol), potassium *tert*-butoxide (1 mg, 0.009 mmol), THF (2 mL), and a stirbar. The resulting red mixture was removed from the glovebox and heated to 60 °C for 6 h. After cooling to ambient temperature, the

mixture was returned to an inert atmosphere glovebox, diluted with hexanes (5 mL) and then filtered through a PTFE filter. Concentration of the resulting solution under reduced pressure afforded 45 mg (94% yield) of the desired compound as a red solid. m.p. = 155–160 °C (capillary tube sealed with vacuum grease). ^{1}H NMR (C_6D_6): δ 6.78 (m, 4H), 6.68 (d, *J* = 7.2 Hz, 2H), 6.59 (d, *J* = 6.8 Hz, 2H), 4.32 (t, *J* = 2.1, 4H), 3.93 (t, *J* = 1.8, 4H), 3.47 (q, *J* = 6.8, 4H), 0.90 (t, *J* = 6.8 Hz, 6H). ^{13}C NMR (C_6D_6): δ 142.4, 139.4, 121.1, 120.3, 118.3, 110.1, 107.2, 94.1, 68.6, 67.8, 41.3, 10.9. HRMS: $[M]^+$ calcd for $C_{28}H_{27}FeN_4$, 475.1581; found, 475.1580.

Bis(urea) 3.5. In a nitrogen-filled drybox, a 20 mL flask was charged with **3.4** (45 mg, 0.095 mmol), benzene (5 mL), and a stirbar. The resulting mixture was then removed from the drybox and stirred under an atmosphere of oxygen (balloon) for 10 min. The solution rapidly changed from cherry red to orange brown. Removal of the residual solvent under vacuum afforded 50 mg (99% yield) of the desired product as an orange solid. m.p. = 162–164 °C. ^{1}H NMR (C_6D_6): δ 7.41 (d, *J* = 7.6 Hz, 2H), 6.88 (t, *J* = 8.0 Hz, 2H), 6.83 (t, *J* = 7.6 Hz, 2H), 6.30 (d, *J* = 8.0 Hz), 5.01 (t, *J* = 1.6, 4H), 4.01 (t, *J* = 1.6, Hz, 4H), 3.33 (q, *J* = 7.2 Hz, 4H), 0.87 (t, *J* = 7.2 Hz, 6H). ^{13}C NMR (C_6D_6): δ 152.4, 129.1, 128.9, 121.1, 120.8, 109.8, 106.8, 93.8, 66.3, 63.9, 30.2, 13.3. HRMS: $[M + H]^+$ calcd for $C_{28}H_{27}N_4O_2Fe$, 507.1482; found, 507.1478. IR (CH_2Cl_2): 1708 cm^{-1}. IR (KBr): 1709 cm^{-1}. $E_{1/2}$ ($Fe^{II/III}$) = 0.56 V (quasi-reversible). E_{pa} = +0.60 V.

[$Ir_2(cod)_2Cl_2$](3.4) (3.6). A 20 mL vial was charged with **3.4** (48 mg, 0.10 mmol), $\{Ir(cod)Cl\}_2$ (75 mg, 0.11 mmol), benzene (2 mL), and a stir bar. The resulting mixture was stirred for 12 h at ambient temperature during which time its color changed from red to brown, and the mixture became cloudy. Addition of excess hexanes (10 mL) caused yellow solids to precipitate. The solids were then collected via filtration, dissolved in a mixture of CH_2Cl_2/CH_3OH (20:1 v/v), and then filtered through a plug of

silica gel. Removal of the residual solvent under vacuum to afforded 70 mg (61% yield) of the desired compound as a yellow powder. ^{1}H NMR ($CDCl_3$): δ 7.71 (d, *J* = 7.8 Hz, 2H), 7.34 (t, *J* = 7.8 Hz, 2H), 6.77 (t, *J* = 7.8 Hz, 2H), 6.74 (m, 2H), 6.78 (d, *J* = 7.8 Hz, 2H), 4.75-4.66 (br m, 6H), 4.53-4.19 (br m, 8H), 2.49 (br m, 2H), 2.10 (br m, 10H), 1.63 (br m, 8H), 1.49 (t, *J* = 7.2 Hz, 6H). ^{13}C NMR ($CDCl_3$): δ 189.9, 133.3, 132.9, 124.1, 121.6, 112.6, 111.5, 108.4, 98.1, 85.1, 84.7, 84.7, 70.2, 66.7, 65.0, 61.7, 53.4, 52.6, 43.3, 33.4, 32.7, 29.6, 28.9, 14.4. HRMS: $[M - Cl]^+$ calcd for $C_{44}H_{50}N_4FeIr_2Cl$, 1111.2316; found, 1111.2326. Elemental analysis: Calc. for $C_{44}H_{50}FeIr_2N_4$: C 46.11, H 4.40, N 8.40, found: C 46.39, H 4.62, N 4.94%. $E_{1/2}$ ($Fe^{II/III}$) = +0.75 V (quasi-reversible). E_{pa} ($Fe^{II/III}$) = +0.81 V. E_{pa} ($Ir^{I/II}$) = +1.05 V (irreversible).

[$Ir_2(CO)_4Cl_2$](3.4) (3.7). A 20 mL vial was charged with **3.6** (40 mg, 0.035 mmol), CH_2Cl_2 (2 mL), and a stir bar. The resulting solution was then stirred for 1 h under an atmosphere of carbon monoxide (balloon). After removal of the residual solvent under reduced pressure, the resulting yellow solid was triturated pentane (2 x 10 mL), filtered, and then dried under vacuum to afford 34 mg (95% yield) of the desired product as a yellow powder. ^{1}H NMR ($CDCl_3$): δ 7.75 (d, *J* = 8.4 Hz, 2H), 7.46 (t, *J* = 8.4 Hz, 2H), 6.95 (t, *J* = 8.1 Hz, 2H), 6.84 (d, *J* = 8.1 Hz, 2H), 6.27(br m, 2H), 4.65-4.35 (br m, 10H), 1.46 (t, *J* = 7.2 Hz, 6H). ^{13}C NMR ($CDCl_3$): δ 180.6, 180.6, 166.8, 132.7, 132.4, 125.1, 123.2, 112.2, 109.8, 97.2, 70.1, 67.8, 65.6, 62.6, 43.8, 14.2. HRMS: $[M - Cl]^+$ calcd for $C_{32}H_{26}N_4O_4FeClIr_2$, 1007.0245; found, 1007.0245. IR (CaF_2, CH_2Cl_2): 2068 (*trans* ν_{CO}), 1989 (*cis* ν_{CO}) cm^{-1}. IR (KBr): 2062 (*trans* ν_{CO}), 1979 (*cis* ν_{CO}) cm^{-1}. $E_{1/2}$ ($Fe^{II/III}$) = +0.89 V (quasi-reversible). E_{pa} ($Fe^{II/III}$) = +0.93 V.

X-ray Crystallography. Data were collected on a Nonius Kappa CCD diffractometer using a graphite monochromator with MoKα radiation (λ = 0.71073 Å) at 153 K using an Oxford Cryostream low temperature device. Key details of the crystal

and structure refinement data are summarized in Table 1. Data reduction were performed using DENZO-SMN.[45] The structures were solved by direct methods using SIR97[46] and refined by full-matrix least-squares on F^2 with anisotropic displacement parameters for the non-H atoms using SHELXL-97.[48] The hydrogen atoms were calculated in idealized positions. Neutral atom scattering factors and values used to calculate the linear absorption coefficient are from the International Tables for X-ray Crystallography (1992).[48] Further crystallographic details may be found in the respective CIF files, which were deposited at the Cambridge Crystallographic Data Centre, Cambridge, UK. The CCDC reference numbers for **3.3**, **3.6**, and **3.7** were assigned as 729832, 729834, and 729833, respectively.

Table 3.1 Summary of X-ray Diffraction Experimental Details for **3.3**, **3.6**, and **3.7**.

	3.3	**3.6**	**3.7**[a]
formula	$C_{28}H_{28}B_2F_8FeN_4$	$C_{44}H_{50}Cl_2FeIr_2N_4$	$C_{33}H_{27}Cl_5FeIr_2N_4O_4$
fw (g mol^{-1})	650.01	1146.03	1161.09
morphology	yellow block	orange prisms	yellow plate
dimensions (mm)	0.30 × 0.1 × 0.08	0.12 × 0.08 × 0.06	0.23 × 0.21 ×0.12
crystal system	monoclinic	monoclinic	monoclinic
space group	C2/c	C2/c	P21/c
a (Å)	28.853(2)	22.6278(6)	15.8100(2)
b (Å)	9.4328(12)	10.6387(4)	14.5490(2)
c (Å)	20.816(2)	18.5406(6)	17.1930(2)
α (deg)	90	90	90
β (deg)	98.506(2)	120.241(2)	110.5520(10)
γ (deg)	90	90	90
V (Å^3)	5603.1(10)	3855.9(2)	3703.02(8)
Z	8	4	4
ρ_{calc} (g cm^{-3})	1.541	1.974	2.083
μ (mm^{-1})	0.619	7.434	7.959
F(000)	2656	2224	2200
θ range (deg)	1.98 to 25.00	2.08 to 27.49	1.89 to 30.00
total / unique reflections	9421 / 4933	25726 / 4435	53217 / 10804
completeness to 2θ (%)	99.9	99.9	99.9
data / restraints / parameters	4933 / 309 / 428	4435 / 0 / 241	10804 / 0 / 411
GoOF	1.452	1.089	1.075
R_1[b], wR_2[c] [I > 2σ(I)]	0.0605, 0.1530	0.0274, 0.0604	0.0349, 0.0869
R_1[b], wR_2[c] (all data)	0.0744, 0.1592	0.0365, 0.0639	0.0508, 0.0913
Largest diff. peak & hole (*e* Å^{-3})	0.820 and −0.411	1.733 and −1.285	2.819 and −1.384

[a] A molecule of what appeared to be chloroform was disordered. Attempts to model the disorder were unsatisfactory. [b] $R_1 = \Sigma \mid |F_o| - |F_c| \mid / \Sigma |F_o|$. [c] $wR_2 = \{\Sigma [w(F_o^2 - F_c^2)^2] / \Sigma [w(F_o^2)^2]\}^{1/2}$. The contributions to the scattering factors due to the solvent molecule were removed by use of the utility SQUEEZE[49] in PLATON[50] PLATON was used as incorporated in WinGX.[51]

NOTES AND REFERENCES

¶ Irreversible oxidations were observed at E_{pa} = +1.05 V and approximately +1.50 V for **3.6** and **3.7**, respectively, and attributed to IrI/II redox couples.

§ The use of chemical oxidants to oxidize ferrocene containing NHC-metal complexes has been previously determined to be problematic; see ref. 17.

†† Similar results were obtained using methods reported by Crabtree and Plenio; see ref. 23.

(1) (a) Arduengo, A. J., III *Acc. Chem. Res.* **1999**, *32*, 913; (b) Wanzlick, H.-W. *Angew. Chem.* **1962**, *74*, 129; (c) Breslow, R. *J. Am. Chem. Soc.* **1958**, *80*, 3719–3726.

(2) For excellent reviews, see: Hahn, F. E.; Jahnke, M. C. *Angew. Chem. Int. Ed.* **2008**, *47*, 3122; Herrmann, W. A.; Köcher, K. *Angew. Chem. Int. Ed.* **1997**, *36*, 2163; N-Heterocyclic Carbenes in Transition Metal Catalysis, F. Glorius, ed., Springer-Verlag, Berlin, Germany, **2007**; N-Heterocyclic Carbenes in Synthesis, S. P. Nolan, ed., Wiley-VCH, Weinheim, **2006**.

(3) Scott, N. M.; Clavier, H.; Mahjoor, P.; Stevens E. D.; Nolan, S. P. *Organometallics*, **2008**, *27*, 3181; Scott, N. M.; Nolan, S. P. *Eur. J. Inorg. Chem.* **2005**, *10*, 1815–1828; J. K. Huang, H. J. Schanz, E. D. Stevens and S. P. Nolan, *Organometallics*, **1999**, *18*, 2370–2375.

(4) (a) Kantchev, E. A. B.; O'Brien, C. J.; Organ, M. G. *Angew. Chem. Int. Ed.* **2007**, *46*, 2768; (b) W. A. Herrmann, Angew. *Chem. Int. Ed.* **2002**, *41*, 1290–1309; (c) Herrmann, W. A.; Elison, M.; Fischer, J.; Köcher, C.; Artus, G. R. J. *Angew. Chem. Int. Ed.* **1995**, *34*, 2371.

(5) For excellent reviews, see: Normand, A. T.; Cavell, K. J. *Eur. J. Inorg. Chem.* **2008**, 2781; Mata, J. A.; Poyatos, M.; Peris, E. *Coord. Chem. Rev.* **2007**, 251, 841. For recent examples, see: Brown, D. H.; Nealon, G. L.; Simpson, P. V. Skelton, B. W.; Wang, Z. S. *Organometallics*, **2009**, *28*, 1965; Morgan, B. P.; Galdamez, G. A.; Gilliard, R. J., Jr.; Smith, R. C. *Dalton Trans.* **2009**, 2020.

(6) Crudden, C. M.; Allen, D. P. *Coord. Chem. Rev.* **2004**, *248*, 2247; Peris, E.; Crabtree, R. H. *Coord. Chem. Rev.* **2004**, *248*, 2239.

(7) Boydston, A. J.; Bielawski, C. W. *Dalton Trans.* **2006**, 4073.

(8) Khramov, D. M.; Boydston, A. J.; Bielawski, C. W. Angew. *Chem. Int. Ed.* **2006**, *45*, 6186.

(9) Er, J. A. V.; Tennyson, A. G.; Kamplain, J. W.; Lynch, V. M.; Bielawski, C. W. *Eur. J. Inorg. Chem.* **2009**, 1729; Mercs, L.; Neels, A.; Albrecht, M. *Dalton Trans.* **2008**, 5570.

(10) Kamplain, J. W.; Bielawski, C. W. *Chem. Commun.* **2006**, 1727; Boydston, A. J.; Rice, J. D.; Sanderson, M. D.; Dykhno, O. L.; Bielawski, C. W. *Organometallics* **2006**, *25*, 6087; Boydston, A. J., Williams, K. A.; Bielawski, C. W. *J. Am. Chem. Soc.* **2005**, *127*, 12496.

(11) Hahn, E.; Radloff, C.; Pape T.; Hepp, A. *Organometallics* **2008**, *27*, 6408.

(12) Guerret, O.; Sole, S.; Gornitzka, H.; Teichert, M.; Trinquier, G.; Bertrand, G. *J. Am. Chem. Soc.* **1997**, *119*, 6668.

(13) Mas-Marz, E.; Mata, J.; Peris E. *Angew. Chem. Int. Ed.* **2007**, *46*, 3729.

(14) B. Bildstein, M. Malaun and H. Kopacka, K.-H. Ongania, K. Wurst, *J. Organomet. Chem.*, **1998**, *552*, 45–61.

(15) For an excellent review, see: Bildstein, B. *J. Organomet. Chem.* **2001**, 617-618, 28.

(16) Bertogg, A.; Camponovo, F.; Togni, A. *Eur. J. Inorg. Chem.* **2005**, 347; Demirhan, F.; Yildirim, Ö.; Çetinkaya, B. *Transition Met. Chem.* **2003**, *28*, 558; Seo, H.; Kim, B. Y.; Lee, J. H.; Park, H.-J.; Son, S. U.; Chung, Y. K. *Organometallics*, **2003**, *22*, 4783; Jackstell, R.; Frisch, A.; Beller, M.; Röttger, D.; Malaun, M.; Bildstein, B. *J. Mol. Catal. A Chem.* **2002**, *185*, 105; Bolm, C.; Kesselgruber, M.; Raabe, G. *Organometallics* **2002**, *21*, 707; Broggini, D.; Togni, A. *Helv. Chim. Acta* **2002**, *85*, 2518; Bildstein, B.; Malaun, M.; Kopacka, H.; Wurst, K.; Mitterböck, M.; Ongania, K.-H.; Opromolla, G.; Zanello, P. *Organometallics*, **1999**, *18*, 4325.

(17) Khramov, D. M.; Rosen, E. L.; Lynch, V. M. Bielawski, C. W. *Angew. Chem. Int. Ed.* 2008, *47*, 2267; Siemeling, U.; Farber, C.; Bruhn, C. *Chem. Commun.* **2009**, 98.

(18) Gülcemal, S. G.; Labande, A.; Daran, J.-C.; Çetinkaya, B. Poli, R. *Eur. J. Inorg. Chem.* **2009**, 1806; Willms, H.; Frank, W.; Ganter, C. *Chem. Eur. J.* **2008**, *14*, 2719; Labande, A.; Daran, J.-C.; Manoury, E.; Poli, R. *Eur. J. Inorg. Chem.* **2007**, 1205; Shi, J.-C.; Yang, P.-Y.; Tong, Q.; Wu, Y.; Peng, Y. *J. Mol. Catal. A* **2006**, *259*, 7; Gischig, S.; Togni, A. *Organometallics* **2005**, *24*, 203; Gischig, S.; Togni, A. *Eur. J. Inorg. Chem.* **2005**, 4745; Yuan, Y.; Raabe, G.; Bolm, C. *J. Organomet. Chem.* **2005**, 690, 5747; Gischig, S.; Togni, A. *Organometallics*, **2004**, *23*, 2479; Seo, H.; Park, H.-J.; Kim, B. Y.; Lee, J. H.; Son, S. U.; Chung, Y. K. *Organometallics* **2003**, *22*, 618.

(19) Coleman, K. S.; Turberville, S.; Pascu, S. I. Green, M. L. H. *J. Organomet. Chem.* **2005**, *690*, 653.

(20) Dallas, A.; Kuhtz, H. A.; Farrell, B. Quilty; and Nolan, K. *Tetrahedron Lett.* **2007**, *48*, 1017.

(21) Bandoli, G.; Dolmella, A. *Coord. Chem. Rev.* **2000**, *209*, 161; Tan, K.-S.; Hor, T.S.A. In: Togni, A. and Hayashi, T. eds., Ferrocenes – Homogeneous Catalysis, Organic Synthesis and Material Science, VCH, Weinheim (1995); Hayashi, T.; Konishi, M.; Kobori, Y.; Kumada, M.; Higuchi, T.; Hirotsu, K. *J. Am. Chem. Soc.*, **1984**, *106*, 158.

(22) Wolf, S.; Plenio, H. *J. Organomet. Chem.* **2009**, *694*, 1487; Song, G.; Zhang, Y.; Li, X. *Organometallics* **2008**, *27*, 1936; Frey, G. D.; Rentzsch, C. F.; von Preysing, D.; Scherg, T.; Mühlhofer, M.; Herdtweck, E.; Herrmann, W. A. *J. Organomet. Chem.* **2006**, *691*, 5725; Altenhoff, G.; Goddard, R.; Lehmann, C. W.

Glorius, F. *J. Am. Chem. Soc.*, **2004**, *126*, 15195; Chianese, A. R.; Kovacevic, A.; Zeglis, B. M.; Faller, J. W.; Crabtree, R. H. *Organometallics*, **2004**, *23*, 2461.

(23) Kelly, R. A., III; Clavier, H.; Giudice, S.; Scott, N. M.; Stevens, E. D.; Bordner, J.; Samardjiev, I.; Hoff, C. D.; Cavallo, L.; Nolan, S. P. *Organometallics* **2008**, *27*, 202; Leuthäußer, S.; Schwarz, D.; Plenio, H. *Chem. Eur. J.* **2007**, *13*, 7195; Chianese, A. R.; Li, X.; Janzen, M. C.; Faller, J. W.; Crabtree, R. H. *Organometallics* **2003**, *22*, 1663.

(24) Sanderson, M. D.; Kamplain, J. W.; Bielawski, C. W. *J. Am. Chem. Soc.* **2006**, *128*, 16514.

(25) Khramov, D. M.; Rosen, E. L.; Er, J. A. V.; Vu, P. D.; Lynch, V. M.; Bielawski, C. W. *Tetrahedron* **2008**, *64*, 6853; Khramov, D. M.; Lynch, V. M.; Bielawski, C. W. *Organometallics* **2007**, *26*, 6042.

(26) Özcubukcu, S.; Schmitt, E.; Leifert, A.; Bolm, C. *Synthesis* **2007**, 389.

(27) Kühl, O.; Saravanakumar, S.; Ullah, F.; Kindermann, M. K.; Jones, P. G.; Köckerling, M.; Heinicke, J. *Polyhedron* **2008**, 27, 2825; Khramov, D. M.; Boydston, A. J.; Bielawski, C. W. *Org. Lett.* **2006**, *8*, 1831; Boydston, A. J.; Khramov, D. M.; Bielawski, C. W. *Tetrahedron Lett.* **2006**, *47*, 5123; Hahn, F. E. *Angew. Chem. Int. Ed.* **2006**, *45*, 1348; Hahn, F. E.; Langenhahn, V.; Lügger, T.; Pape, T.; Le Van, D. *Angew. Chem. Int. Ed.* **2005**, *44*, 3759; Hahn, F. E.; Langenhahn, V.; Meier, N.; Lügger, T.; Fehlhammer, W. P. *Chem. Eur. J.* **2003**, *9*, 704; Hahn, F. E.; Wittenbecher, L.; Le Van, D.; Fröhlich, R. *Angew. Chem., Int. Ed.* **2000**, *39*, 541; Hahn, F. E.; Wittenbecher, L.; Boese, R.; Bläser, D. *Chem. Eur. J.* **1999**, *5*, 1931; Hahn, F. E.; Foth, M. *J. Organomet. Chem.*, **1999**, *585*, 241.

(28) Hunter; C. A.; Sanders, J. K. M. *J. Am. Chem. S*oc. **1990**, *112*, 5525.

(29) Dunitz, J. D.; Orgel, L. E.; Rich, A. *Acta Cryst.* **1956**, *9*, 373; Dunitz, J. D.; Orgel, L. E. *Nature* **1953**, *171*, 121; Eiland, P. F.; Pepinsky, R. J. *Am. Chem. Soc.* **1952**, *74*, 4971.

(30) Kamplain, J. W.; Lynch, V. M.; Bielawski, C. W. O*rg. Lett.* **2007**, *9*, 5401; Taton, T. A.; Chen, P. *Angew. Chem. Int. Ed.* **1996**, *35*, 1011; Çetinkaya, E.; Hitchcock, P. B.; Küçükbay, H.; Lappert, M. F.; Al-Juaid, S. *J. Organomet. Chem.* **1994**, *481*, 89.

(31) Shi, Z.; R. P. Thummel, *J. Org. Chem.* **1995**, *60*, 5935; Winberg, H. E.; Downing, J. R.; Coffman, D. D. *J. Am. Chem. Soc.* **1965**, *87*, 2054.

(32) Poater, A.; Ragone, F.; Giudice, S.; Costabile, C.; Dorta, R.; Nolan, S. P.; Cavallo, L. *Organometallics*, **2008**, *27*, 2679; Alder, R. W.; Blake, M. E.; Chaker, L.; Harvey, L.; Paolini, F.; Schütz, J. *Angew. Chem. Int. Ed.* **2004**, *43*, 5896.

(33) For an excellent review: Lappert, M. F.; *J. Organomet. Chem.* **2005**, *690*, 5467.

(34) Metallinos C.; Du, X. *Organometallics* **2009**, *28*, 1233; Chianese, A. R.; Mo, A.; Datta, D. *Organometallics* **2009**, *28*, 465.

(35) Based on NMR data, complexes **3.6** and **3.7** do not appear to adopt π-π* stacked structures in solution to a significant degree.

(36) Tolman, C. A. *J. Am. Chem. Soc.* **1970**, *9*, 2953; Strohmeier, W.; Müller, F.-J. *Chem. Ber.* **1967**, *100*, 2812.

(37) Lorkovic, I. M.; Wrighton, M. S.; Davis, W. M. *J. Am. Chem. Soc.* **1994**, *116*, 6220; Miller, T. M.; Ahmed, K. J.; Wrighton, M. S. *Inorg. Chem.* **1988**, *27*, 4326.

(38) Krejcik, M.; Danek, M.; Hartl, F. *J. Electroanal. Chem.* **1991**, *317*, 179.

(39) For examples of monitoring νCO in carbonyl complexes as a function of metal oxidation state, see: Szesni, N.; Drexler, M.; Maurer, J.; Winter, R. F.; de Montigny, F.; Lapinte, C.; Steffens, S.; Heck, J.; Weibert, B.; Fischer, H. *Organometallics*, **2006**, *25*, 5774; Scheiring, T.; Fiedler, J.; Kaim, W. *Organometallics* **2001**, *20*, 1437; Weinberger, D. A.; Higgins, T. B.; Mirkin, C. A.; Liable-Sands, L. M.; Rheingold, A. L. *Angew. Chem. Int. Ed.* **1999**, *38*, 2565.

(40) Tolman, C. A. *Chem. Rev.* **1977**, *77*, 313.

(41) Ajamian, A.; Gleason, J. L. *Angew. Chem. Int. Ed.* **2004**, *43*, 3754; Lee, J. M.; Na, Y.; Han, H.; Chang, S. *Chem. Soc. Rev.* **2004**, *33*, 302; Fogg, D. E.; dos Santos, E. N. *Coord. Chem. Rev.* **2004**, *248*, 2365.

(42) Robertson, N.; McGowan, C. A. *Chem. Soc. Rev.* **2003**, *32*, 96.

(43) Noviandri, I.; Brown, K. N.; Fleming, D. S.; Gulyas, P. T.; Lay, P. A.; Masters, A. F.; Phillips, L. *J. Phys. Chem. B* **1999**, *103*, 6713; Connelly, N. G.; Geiger, W. E. *Chem. Rev.* **1996**, *96*, 877.

(44) Shafir, A.; Power, M. P.; Whitener, G. D. Arnold, J. *Organometallics*, **2000**, *19*, 3978.

(45) Otwinowski, Z.; Minor, W. *Methods in Enzymology in Macromolecular Crystallography*, Part A, *276*, 307–326, C. W. Carter, Jr. and R. M. Sweets, Eds., Academic Press, 1997.

(46) Altomare, A.; Burla, M. C.; Camalli, M.; Cascarano, G. L.; Giacovazzo, C.; Guagliardi, A.; Moliterni, A. G. G; Polidori, G.; Spagna, R. *J. Appl. Cryst.* **1999**, *32*, 115.

(47) Sheldrick, G. M. SHELXL97, program for the refinement of crystal structures, University of Gottingen, Germany, 1994.

(48) International Tables for X-ray Crystallography. Vol. C, Tables 4.2.6.8 and 6.1.1.4, A. J. C. Wilson, Ed., Kluwer Academic Press, Boston, MA, 1992.

(49) Sluis, P. V. D.; Spek, A. L. *Acta Cryst. A* **1990**, *46*, 194.

(50) Spek, A. L. PLATON, a multipurpose crystallographic tool, Utrecht University, The Netherlands, **2000**

(51) Farrugia, L. J. *J. Appl. Cryst.* **1999**, *32*, 837.

Chapter 4: Synthesis and Study of Olefin Metathesis Catalysts Supported by Redox-Switchable Diaminocarbene[3]ferrocenophanes†

Portions of this chapter were reprinted from Varnado, C. D., Jr.; Rosen, E. L.; Collins, M. S.; Lynch, V. M.; Bielawski, C. W. *Dalton Trans*. **2013**, DOI: 10.1039/c3dt51278a, and is reproduced with permissions from the Royal Society of Chemistry. E. L. Rosen synthesized, characterized, and studied the ruthenium complexes (**4.18**-**4.20**), and assisted with writing the aforementioned publication. M. S. Collins assisted with the synthesis of various intermediates. V. M. Lynch assisted with the X-ray crystallography. C. W. Bielawski assisted with writing the aforementioned publication. I synthesized and studied **4.5**, **4.9-4.13** and **4.15**, and helped to write the aforementioned publication.

ABSTRACT

A redox-switchable ligand, N,N'-dimethyldiaminocarbene[3]ferrocenophane (**4.5**), was synthesized and incorporated into a series of Ir- and Ru-based complexes. Electrochemical and spectroscopic analyses of (**4.5**)Ir$(CO)_2$Cl (**4.15**) revealed that **4.5** displayed a Tolman Electronic Parameter value of 2050 cm^{-1} in the neutral state and 2061 cm^{-1} upon oxidation. Moreover, inspection of X-ray crystallography data recorded for (**4.5**)Ir(*cis*,*cis*-1,5-cyclooctadiene)Cl (**4.13**) revealed that **4.5** was sterically less bulky ($\%V_{Bur}$ = 28.4) than other known diaminocarbene[3]ferrocenophanes, which facilitated the synthesis of (**4.5**)(PPh_3)Cl_2Ru(3-phenylindenylid-1-ene) (**4.18**). Complex **4.18** exhibited quasi-reversible electrochemical processes at 0.79 and 0.98 V relative to SCE, which were assigned to the Fe and Ru centers in the complex, respectively, based on UV-vis and electron pair resonance spectroscopic measurements. Adding 2,3-dichloro-5,6-dicyanoquinone over the course of a ring-opening metathesis polymerization of *cis*,*cis*-

1,5-cyclooctadiene catalyzed by **4.18** ([monomer]$_0$/[**4.18**]$_0$ = 2500) reduced the corresponding rate constant of the reaction by over an order of magnitude (pre-oxidation: k_{obs} = 0.045 s^{-1}; post-oxidation: k_{obs} = 0.0012 s^{-1}). Subsequent reduction of the oxidized species using decamethylferrocene restored catalytic activity (post-reduction: k_{obs} = up to 0.016 s^{-1}, depending on when the reductant was added). The difference in the polymerization rates was attributed to the relative donating ability of the redox-active ligand (i.e., strongly donating **4.5** versus weakly donating **4.5**$^+$) which ultimately governed the activity displayed by the corresponding catalyst.

INTRODUCTION

Redox-switchable catalysis[1] uses oxidation state changes to modulate catalytic activity. A recent example was reported by Matyjaszewski who demonstrated electrochemical control over an atom transfer radical polymerization reaction by regulating a Cu^I/Cu^{II} couple.[2] However, formally changing the oxidation state of metal centers can result in irreversible degradation or a loss in the desired catalytic activity due to coordination sphere changes. As such, attention has been directed toward the development of redox-switchable ligands as transition metal catalysts are typically sensitive to minute differences in ligand donicities.[3]

Redox-switchable ligands offer a means to impart unique selectivities and/or activities to supported catalysts through oxidation state changes and, in many cases, may be switched using chemical or electrochemical processes.[4,5] A seminal example was reported by Wrighton in 1995,[4] where it was shown that a 1,1′-bis(diphenylphosphino)cobaltocene Rh complex (Figure 4.1) facilitated hydrosilations or hydrogenations depending on the oxidation state of the redox active ligand (i.e., cobaltocene versus cobaltocenium). Gibson and Long later showed that the rate of the

ring opening polymerization (ROP) of lactide was dependent on the oxidation state of a ferrocene unit contained within a N,N'-ethylenebis(salicylimine) supported Ti catalyst.[5c] The use of ferrocene containing ligands to vary the rate of ROP reactions has since been elegantly expanded by Diaconescu[6] to include complexes of Y, In, and Ce. Similarly, ferrocene-containing ligands have have been utilized[7] by Plenio[7a] and Wang[7b] as "phase tags", for Ru-based olefin metathesis catalysts,[8] whereby ligand oxidation drives a change in solubility and facilitates catalyst recovery. Plenio also reported efforts toward using ligand oxidation as a means to bias the instrinsic E:Z selectivities displayed by a Ru catalyst containing a ligand bearing pendant ferrocenyl substituents.[9]

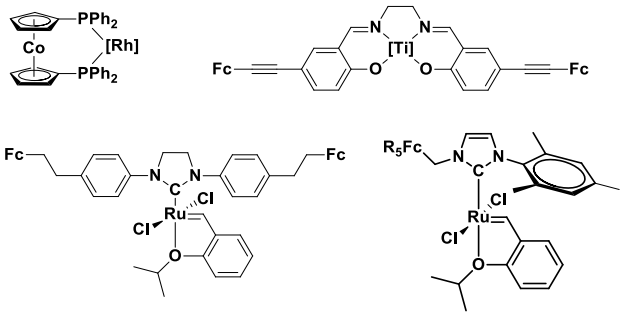

Figure 4.1 Representative examples of various complexes containing redox-switchable metallocenes. Fc = ferrocenyl.[4,5c,7a,24] Ph = phenyl. R = hydrogen or methyl.

Although a handful of redox-switchable ligands have been studied,[10,11] their utility in controlling catalytic reactions is still rather limited.[5,6,7,12,13] This deficiency may be, at least partially, due to the fact that many of the aforementioned ligands are bi- or multi-dentate, which confines their range of possible geometries and catalytically active transition metal complexes into which they may be incorporated. One solution to this limitation may be found within the N-heterocyclic carbenes (NHCs),[14] which are a class of ligands finding tremendous utility in catalysis.[15] As strong σ-donors,[16] they coordinate

numerous metals in a range of oxidation states and do so in a monodentate fashion.[15,17] Furthermore, compared to their phosphine counterparts, they often impart enhanced stability and/or catalytic activity upon coordination to a transition metal.[18] In light of these advantages, we have launched a program to explore redox-active NHCs as a general class of ligands for bestowing redox-switchable functions onto a broad range of transition metals.[19,20,21,22,23,24] For example, we recently disclosed a series of redox-switchable Ru-based olefin metathesis catalysts bearing N-ferrocenylated NHCs (Figure 4.2).[24] The activities displayed these catalysts in ring-closing metathesis reactions were found to depend upon the oxidation state of the redox-active ligand: catalysts supported by ferrocenium containing NHCs were significantly less active than their neutral analogues, which was attributed to the relative donating abilities of the respective ligands.

Previously, we[19] and others[25] reported the diaminocarbene[3]ferrocenophanes (FcDACs; Figure 4.2)[26] as a new class of redox-switchable ligands. The extent to which the associated redox processes impacted metals coordinated to the FcDACs were measured by analyzing $[(L)M(CO)_2Cl]$ (M = Rh or Ir) type complexes using IR spectroscopy, since the stretching frequencies displayed by the carbonyl groups are sensitive to the other ligands.[27] Indeed, the ν_{CO}s displayed by these complexes were measured to hypsochromically shift by 13-21 cm^{-1} upon oxidation of the FcDAC ligand.[9,25]

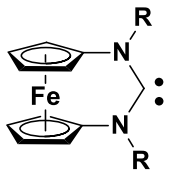

4.1 - 4.5

4.1: R = *iso*-Butyl
4.2: R = Phenyl
4.3: R = 2-Adamantyl
4.4: R = Neopentyl
4.5: R = Methyl

Figure 4.2 Structures of various N,N'-diaminocarbene[3]ferrocenophanes.[19,25]

Building on these results, we sought to investigate the ability of the FcDAC ligands to impart redox-switchable functions to catalytically-active transition metals and to faciliate comparisons to other redox-switchable catalysts containing ferrocene moieties. Attention was directed toward catalysts used to facilitate olefin metathesis, as this is a powerful reaction that has been used for the synthesis of small molecules as well as macromolecular materials.[28] In particular, Ru-based catalysts have garnered much success due to their high stabilities toward oxygen, moisture, and a broad range of functional groups.[29] Moreover, NHCs have played a prominent role in establishing the utility of Ru-based metathesis catalysts, as they often enhance activity and/or stability relative to other ligands, particularly phosphines.[18a,30,31] Representative examples of various Ru-based catalysts which have found widespread use in a variety of olefin metathesis reactions are shown in Figure 4.3 (**4.6**–**4.9**).[28b,32,33] Herein, we describe the synthesis and study of Ru-based olefin metathesis catalysts supported by redox-switchable FcDAC ligands.[34]

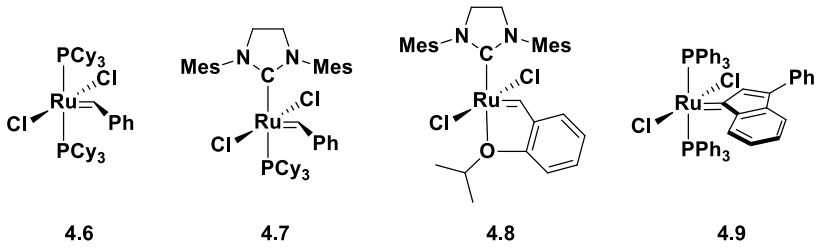

Figure 4.3 Structure of various Ru based olefin metathesis catalysts. Mes = 2,4,6-trimethylphenyl. Ph = phenyl. Cy = cyclohexyl.

RESULTS AND DISCUSSION

*Attempted synthesis of Ru complexes containing **4.1** or **4.2**.* We first attempted to synthesize (**4.1**)(PCy_3)Cl_2Ru=CHPh as an analogue to the Grubbs second generation catalyst (**4.7**). Although the respective free diaminocarbene (i.e., **4.1**) could

not be isolated,[35] *in situ* deprotonation of the known[19] salt [**4.1**H][BF_4] using NaHMDS followed by the addition of **4.6** appeared to result in the formation of the desired complex, as evidenced by diagnostic signals in the ^{1}H and ^{31}P NMR spectra recorded for the crude reaction mixture (Figure 4.4). For example, a new ^{1}H NMR signal attributed to the benzylidene proton was observed at 20.1 ppm (d, 1H, J = 6.3 Hz) and a ^{31}P NMR signal had appeared along with liberated PCy_3 (28.5 ppm and 12.3 ppm, respectively) ($CDCl_3$). Unfortunately, attempts to isolate (**4.1**)(PCy_3)Cl_2Ru=CHPh were unsuccessful, presumably due to its low stability in solution, even in the absence of air and moisture.[36] Attempts to deprotonate [**4.2**H][BF_4] in the presence of **4.6** under various conditions also resulted in decomposition.

We reasoned that the instability of (**4.1**)(PCy_3)Cl_2Ru=CHPh may be due to dissociation of the bulky phosphine ligand which renders the corresponding coordinatively unsaturated Ru complex susceptible to decomposition.[28e,37] Subsequent efforts were directed toward the Ru indenylidenes,[31f,33,38,39] as such complexes have gained attention for their high thermal stabilities and high activities in various olefin metathesis reactions.[40] We surmised that decreasing the steric bulk of the phosphine from PCy_3 to PPh_3 would also improve the stability of the resulting complex.[41] *In situ* deprotonation of [**4.1**H][BF_4] followed by the addition of (PPh_3)$_2$$Cl_2$Ru=(3-phenylindenylid-1-ene) (**4.9**) appeared to form the desired complex as determined by NMR spectroscopic analysis of the crude reaction mixture. Diagnostic ^{1}H and ^{31}P signals were observed at δ = 8.63 (d, 1H, J = 7.2) and 30.44 ppm ($CDCl_3$), respectively, which compared well to those observed for previously reported indenylidene complexes containing NHCs (^{1}H: 8.31–7.01 (d, J = 7.7–7.2) and ^{31}P: 30.51–27.3 ppm).[38a,40e,g] Additionally, free PPh_3 was observed at -4.3 ppm. Although small quantities of (**4.1**)(PPh_3)Cl_2Ru=(3-phenylindenylid-1-ene) were isolated, we were unable to access enough material for

further investigation, even after exploring a variety of purification techniques (*e.g.*, precipitation, trituration and column chromatography). Unfortunately, attempts to synthesize phosphine-free complexes containing **4.1**, such as (**4.1**)Cl_2Ru=CH(2-*iso*-propoxy-Ph)[42] or (**4.1**)(SIMes)Cl_2Ru=CHPh,[3c,43,44] (SIMes = 1,3-dimesitylimidazolin-2-ylidene) were also unsuccessful.

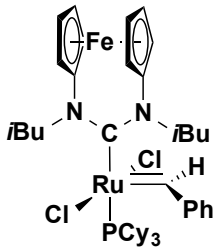

^{1}H NMR: 20.10 ppm (d, 1H, *J* = 6.3 Hz)
^{31}P NMR: 28.5 ppm

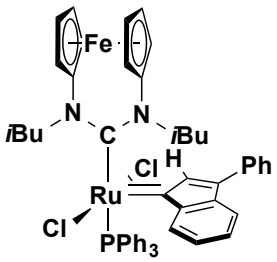

^{1}H NMR: 8.63 ppm (d, 1H, *J* = 7.2 Hz)
^{31}P NMR: 30.4 ppm

Figure 4.4 Diagnostic signals observed in the ^{1}H and ^{31}P NMR spectra recorded for (**4.1**)(PCy_3)Cl_2Ru=CHPh and (**4.1**)(PPh_3)Cl_2Ru=(3-phenylindenylid-1-ene) in $CDCl_3$.

*Synthesis and study of N-methyl FcDAC **4.5** and its transition metal complexes.* Although bulky N-substituents can often enhance the stability of Ru catalysts due to steric protection of the metal center, they may also hinder coordination in some cases. For example, attempts to prepare Ru complexes containing the bulky acyclic diaminocarbenes (ADCs), 1,3-di(1-adamantyl)-4-dihydroimidazol-2-ylidene or bis(*iso*-propylamino)-formamidin-2-ylidene were reported to be unsuccessful.[45,46] Although FcDACs feature N–C–N bond angles that are comparable to those displayed by the ADCs (approximately 120°),[25,47] a stable ADC-Ru complex, *N*,*N*'-dimesityl-*N*,*N*'-dimethylformamidin-2-ylidene)(SIMes)Cl_2Ru=CHPh, was synthesized and found to adopt a conformation where both *N*-methyl substituents were oriented towards the

coordinated Ru center.[43b] Thus, we hypothesized that an FcDAC bearing *N*-methyl substituents may enable isolation of a stable Ru complex supported by this ligand.

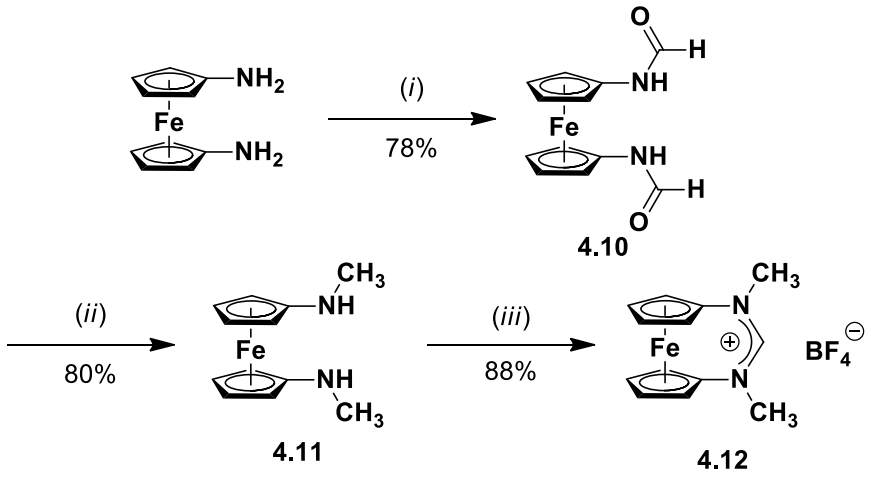

Scheme 4.1 Synthesis of **4.12**. (i) phenyl formate (2.2 equiv.) (ii) (a) $LiAlH_4$ (5 equiv.), THF, 0 °C → reflux, 1 h; (b) H_2O. (iii) HBF_4, $(MeO)_3CH$, 60 °C, 30 min.

As summarized in Scheme 4.1, the synthesis of [**4.5**H][BF_4] (**4.12**) began with 1,1'-diaminoferrocene which was formylated with phenyl formate to give *N,N'*-diformamidoferrocene **4.10**. Treatment of **4.10** with $LiAlH_4$ followed by an aqueous workup yielded *N,N'*-dimethylaminoferrocene **4.11**, which was formylatively cyclized with trimethylorthoformate in the presence HBF_4 to give **4.12**. The diagnostic ^{1}H NMR signal attributed to the C2 proton of this salt was observed at 8.71 ppm (DMSO-d_6) and was in good agreement with that previously recorded for [**4.1**H][BF_4] (8.80 ppm, DMSO-d_6). The solid state structure of **4.12** was elucidated by growing single crystals suitable for X-ray diffraction analysis via slow diffusion of diethyl ether into a saturated CH_2Cl_2 solution (Appendix C). The N–C–N bond angle (129.4(3)°) measured in the solid state structure was nearly identical to that observed for [**4.1**H][BF_4] (129.6(3)°)[19] and comparable to those reported for other crystalline formamidinium[3]ferrocenophanes

(129.7(2)–131.1(6)°).[25] Moreover, the cyclic voltammogram (CV) recorded for **4.12** in CH_2Cl_2 exhibited a reversible, one electron oxidation at $E_{1/2}$ = 1.03 V versus SCE, which was assigned to the Fe center (Table 4.1). The $E_{1/2}$ value recorded for **4.12** is similiar to those measured for [**4.1**H][BF_4] and [**4.2**H][BF_4] (1.10 V, and 1.14 V versus SCE, respectively) under otherwise identical conditions.[19] Deprotonation of **4.12** using NaHMDS in C_6D_6 afforded the free carbene **4.5**, as evidenced by the disappearance of the signal assigned to the C2 formamidinium proton.[48] Although we were unable to isolate **4.5**, it was found to be sufficiently stable in solution in the absence of air and moisture to record a ^{1}H NMR spectrum.

Prior to incorporating **4.5** into an olefin metathesis catalyst, the steric and electronic parameters of this ligand were evaluated. As mentioned above, complexes of the type (L)M(COD)Cl and (L)M$(CO)_2$Cl (L = NHC or phosphine, M = Rh, Ir) have proven to be useful for such purposes.[20,27] Furthermore, analogous complexes containing **4.1** have been previously reported, enabling subtle differences in the steric and electronic influences of the *N*-substituents to be deconvoluted.[20] As shown in Scheme 4.2, i*n situ* deprotonation of **4.12** using NaHMDS followed by the addition of $[Ir(COD)Cl]_2$ afforded **4.13** in 55% yield after isolation via column chromatography (media: SiO_2; eluent: 3:1 v/v hexanes/ethyl acetate). The ^{13}C NMR chemical shift assigned to the 2-position of **4.5** in **4.13** was observed at 215.6 ppm in $CDCl_3$, similar to that previously reported for (**4.1**)Ir(COD)Cl (**4.14**) (213.2 ppm).[20] The corresponding carbonyl complex (**5**)Ir$(CO)_2$Cl (**4.15**) was obtained upon stirring a CH_2Cl_2 solution of **4.13** under an atmosphere of CO. The IR spectrum of **4.15** (CH_2Cl_2) displayed ν_{CO}s at 2065 and 1983 cm^{-1}, similar to those previously recorded for (**4.1**)Ir$(CO)_2$Cl (**4.16**) (ν_{CO} = 2062 and 1982 cm^{-1}).[19]

The solid state structures of **4.13** and **4.15** were elucidated after growing X-ray quality crystals via slow evaporation of concentrated CH_2Cl_2 solutions (Figure 4.5)

and faciliated comparison to previously reported analogues. The N–C–N bond angles measured in the solid state structures of **4.13** and **4.14** (120.5(2) and 121.9(3)°,[20] respectively) as well as **4.15** and **4.16** (122.2(5) and 122.4(2)°,20 respectively) were similar, and comparable to those found for analogous complexes containing acyclic diaminocarbene ligands ((ADC)Ir(COD)Cl: 118.9(4)–119.1(4)° and (ADC)Ir$(CO)_2$Cl: 120.4(2)–122.2(2)°).49 Likewise, the Ir–C1 atom distances measured in the solid state structures of **4.13** and **4.14** (2.068(2) Å and 2.068(3) Å,20 respectively) were nearly identical and within the range previously reported for Ir(COD)Cl complexes supported by analogous NHCs and ADCs (2.041(3)–2.090(13) Å).[27d,50]Additionally, the Ir–C1 distances measured for **4.15** and **4.16** (2.112(6) and 2.121(3) Å[20]) were comparable to analogous complexes containing NHCs or ADCs (2.071(4)–2.121(14) Å).[27d,50] Collectively, the structural similarities found in the Ir complexes supported by **4.5** or **4.1** suggested to us that the N-substituents bestowed similar steric influences on the coordinated metal centers.

To quantify the steric properties of **4.5**, the buried volume ($\%V_{Bur}$), which provides the volume occupied by ligand atoms within a sphere centered on the metal, was calculated from the solid state structure of **4.13** using the method reported by Cavallo.[51] The $\%V_{Bur}$ calculated for **4.5** (28.4) was smaller than that reported for **4.1** (30.2)[20] as well as *N*,*N*'-dimesityl-*N*,*N*'-dimethylformamidin-2-ylidene (29.8; structure not shown).[49] Collectively, these results were encouraging as the aforementioned ADC had been successfully incorporated into stable Ru-based olefin metathesis catalysts.[43b]

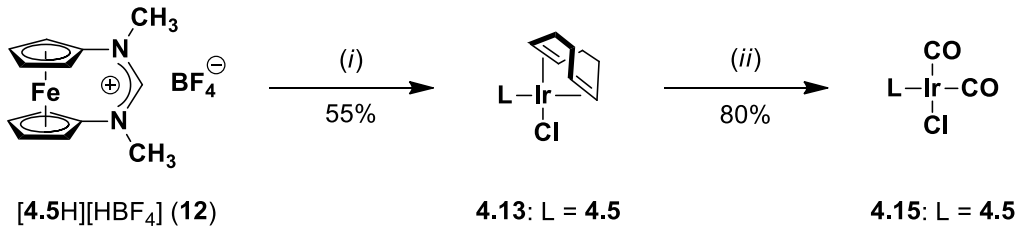

Scheme 4.2 Synthesis of Ir(COD)Cl and $Ir(CO)_2Cl$ complexes containing **4.5**. (i) (a) NaHMDS (1.0 equiv.), toluene, rt, 5 min; (b) $[Ir(COD)Cl]_2$ (0.5 equiv.), toluene, rt, 12 h. (ii) CO (1 atm), CH_2Cl_2, rt, 3 h. rt = room temperature.

We next investigated the electrochemical properties of **4.13** and **4.15** to evaluate the degree of electronic communication between the Fe and Ir centers. The CV recorded for **4.13** in CH_2Cl_2 exhibited two reversible oxidations at $E_{1/2}$ = 0.81 and 1.02 V versus SCE, which were assigned to the Fe and Ir metal centers, respectively (Table 4.1; see also Figure C.5). These values were comparable to those previously reported for **4.14** ($E_{1/2}$ = 0.76 and 1.02 V),[20] although the Ir centered oxidation measured for **4.13** occurred at a potential higher than those recorded for other Ir(COD)Cl complexes supported by NHCs ($E_{1/2}$ = 0.65–0.97 V).[20,27c,52] Upon ligand exchange of the cyclooctadiene ligand for two π-acidic CO ligands, a significant anodic shift was observed in the redox couple attributed to the Fe center ($E_{1/2}$ = 0.96 V, $\Delta E_{1/2}$ = 150 mV) and the Ir oxidation process was not observed within the solvent window (see appendix C), consistent with our prior report for the oxidation of **4.14** versus **4.16** ($\Delta E_{1/2}$ = 180 mV) and related complexes.[20,22,52,53] The 150 mV shift observed upon ligand exchange (i.e., **4.13** → **4.15**) suggested to us that the electronic communication between the Ir and Fe centers was significant and that the decrease of electron density on the Ir center was due to the π-acidic CO ligands, which consequently raised the oxidation potential of the ferrocene moiety.

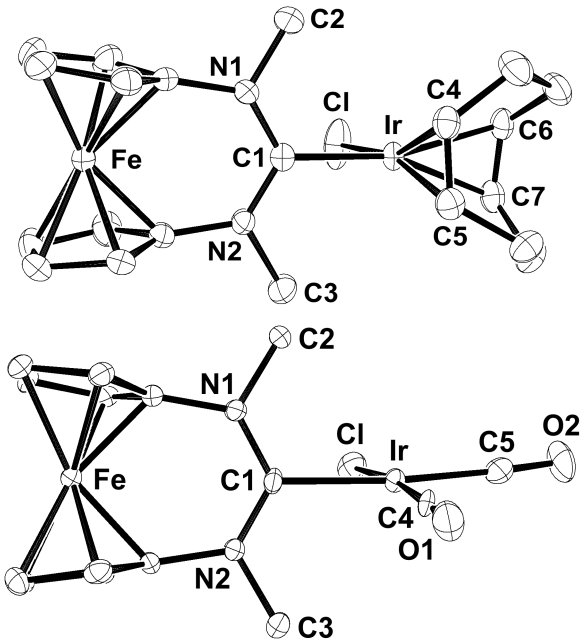

Figure 4.5 Top: ORTEP diagram of **4.13** showing ellipsoids at 50% probability. Hydrogen atoms have been omitted for clarity. Key atom distances (Å) and angles (°): Ir–C1, 2.068(2); N1–C1–N2, 120.5(2). Bottom: ORTEP diagram of **4.15** showing ellipsoids at 50% probability. Hydrogen atoms have been omitted for clarity. Key atom distances (Å) and angles (°): Ir–C1, 2.112(6); N1–C1–N2, 122.2(5).

The degree of electronic communication between the FcDAC ligand and the Ir center in **4.15** was also investigated using a spectroelectrochemical FT-IR analysis (Figure 4.6). Applying a potential of 1.2 V to a CH_2Cl_2 solution of **4.15** resulted in a decrease in the intensities of the signals associated with the starting material (1983 and 2065 cm^{-1}) and were accompanied with the appearance of new absorbances at higher frequencies (1998 and 2076 cm^{-1}), consistent with the formation of **4.15**$^+$. The spectroscopic shift reflected the formation of stronger CO bonds due to decreased π-backbonding from the Ir center resulting from a decrease in σ-donation from **4.5** upon oxidation.[20] To quantify the ligand donating abilities of **4.5** and **4.5**$^+$, the aforementioned ν_{CO}s were converted to their corresponding the Tolman Electronic Parameters (TEPs)[54]

using Nolan's modification[27d] of Crabtree's[27a] method.[55] In its neutral form, the TEP for **4.5** in **4.15** was calculated to be 2050 cm^{-1}; upon oxidation, the value shifted by 11 cm^{-1} to 2061 cm^{-1}. For comparison, the TEP of **4.5** in its neutral form is similar to that of strongly donating N,N'-diadamantylimidazolylidene (TEP = 2049.5 cm^{-1})[27d] but weakens to that of triethylphosphine (TEP = 2061.7 cm^{-1})[27d] upon oxidation. Given that the activities displayed by Ru-based olefin metathesis catalysts are strongly dependent on the donating abilities of their ligands,[24,28g,56] we anticipated that the activity displayed by an olefin metathesis catalyst supported by **4.5** would depend on the oxidation state of the redox-active FcDAC ligand.

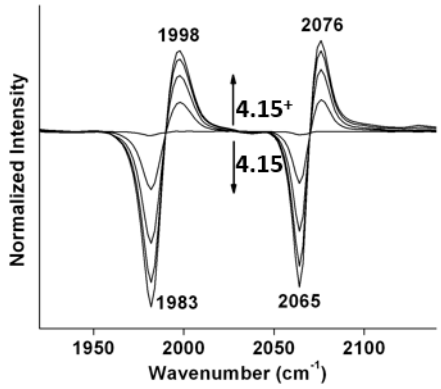

Figure 4.6 FT-IR difference spectra collected over time in CH_2Cl_2 showing the disappearance of **4.15** (1985 and 2065 cm^{-1}) with concomitant formation of **4.15**$^+$ (1998 and 2076 cm^{-1}) upon oxidation (applied voltage = +1.2 V). The arrows indicate the direction of the spectral changes over time.

*Synthesis of Ru complexes containing **4.5***. Upon verifying that the electronic communication between **4.5** and the coordinated Ir center was significant, efforts shifted toward synthesizing Ru alkylidenes thereof.[57] Given its relative stability compared to analogous Ru-benzylidenes,[40b] efforts were directed toward accessing a Ru-indenylidene

complex. The addition of bis-phosphine Ru-indenylidene **4.9** to a C_6D_6 solution of the diaminocarbene **4.5** (formed *in situ*) appeared to form a mixture of two new products by NMR spectroscopy. For example, diagnostic signals were observed at 9.18 (d, J = 7.2, α-C$H_{\text{indenylidene}}$) and 32.65 ppm (PPh$_3$) in the corresponding ^{1}H and ^{31}P NMR spectra (C_6D_6), respectively, of the crude reaction mixture, in addition to the formation of free PPh$_3$. These signals were similar to those reported for analogous NHC-containing Ru-indenylidene complexes (^{1}H NMR: 8.31–7.01 (d, J = 7.7–7.2) and ^{31}P NMR: 30.51–27.3 ppm)[38a,40e,g] and thus were tentatively attributed to the formation of the desired FcDAC indenylidene complex **4.17** (Scheme 4.3). Signals assigned to a second product were also observed at δ 10.47 (d, J = 7.6, α-C$H_{\text{indenylidene}}$) and 47.07 ppm. Over time, the mixture of products changed and the latter appeared to be favored.[58] Isolation of the major product (**4.18**) via column chromatography followed by ^{13}C NMR analysis (CD_2Cl_2) indicated that the complex adopted an unexpected geometry.[59] For example, doublets assigned to the $C_{\text{indenylidene}}$ (297.1 ppm, J = 16.1 Hz) and $C_{\text{diaminocarbene}}$ (215.7 ppm, J = 8.3 Hz) nuclei, respectively, were observed and accompanied with corresponding $J_{\text{C-P}}$ coupling constants. Collectively, these spectroscopic data suggested to us that the complex adopted a geometry in which the NHC was *cis* with respect to the phosphine nucleus rather than the commonly observed *trans* relationship (c.f., **4.17**).[40m,59,60] Additional support for the aforementioned structural assignment was gleaned from a single crystal X-ray diffraction analysis. X-ray quality crystals were obtained by vapor diffusion of hexanes into a saturated benzene solution, which revealed that the phosphine and diaminocarbene were indeed oriented in a *cis* fashion (Figure 4.7)

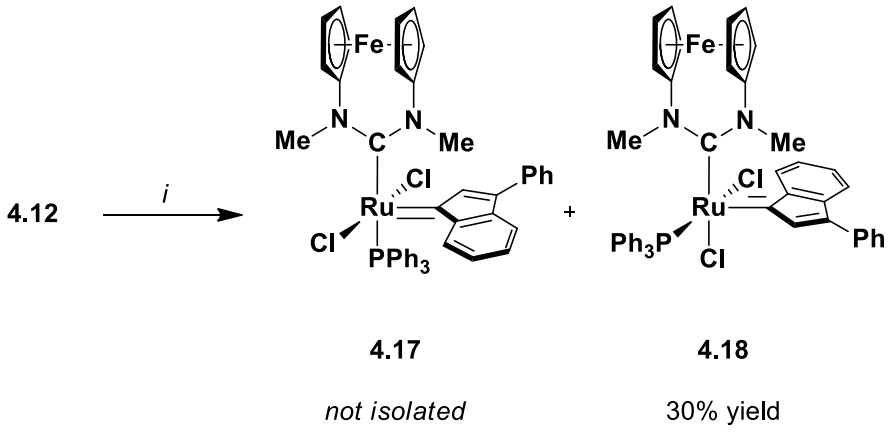

Scheme 4.3 Synthesis of Ru complexes containing **4.5**. (i) (a) NaHMDS (1.0 equiv.), toluene, rt, 5 min. (b) 4.9 (0.60 equiv.), toluene, rt, 1 h.

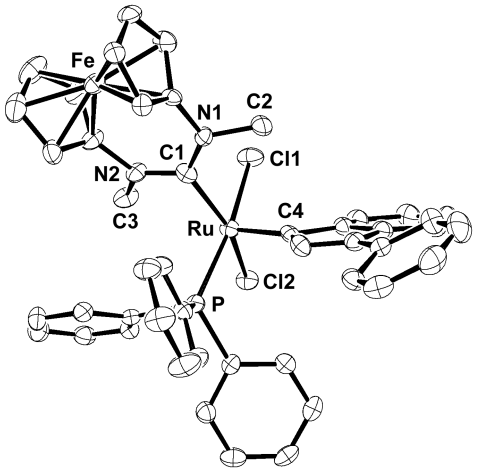

Figure 4.7 Left: ORTEP diagram of **4.18** showing ellipsoids at 50% probability. Hydrogen atoms have been omitted for clarity. Key atom distances (Å) and angles (°): Ru–C1, 2.063(3); Ru–C2, 1.862(4); Ru–P, 2.331(1); N1–C1, 1.358(5); N1–C2, 1.354(5); N1–C1–Ru, 111.4(2); N2–C1–Ru, 127.6(2); C1–Ru–C2, 102.2(1); C1–Ru–P, 97.9(1); Cl1–Ru–Cl2, 87.98(3); N1–C1–N2, 120.8(2).

Preliminary assessment of the catalytic activities displayed by FcDAC-Ru complexes. After the synthesis and characterization of **4.18**, a preliminary investigation of its ability to catalyze the ring-closing metathesis (RCM) of diethyl diallylmalonate and the ring-opening metathesis polymerization (ROMP) of COD was conducted. Although catalytic activity was not observed under the standardized conditions reported by Grubbs and co-workers (CD_2Cl_2, 30 °C),[61] enhanced activities were observed at 80 °C in toluene. For example, the RCM of DDM reached 20% conversion after 1 h ($[DDM]_0$ = 0.1 M, $[\mathbf{4.18}]_0$ = 1 mol%) and quantitative formation of poly(1,4-butadiene) was obtained from COD in less than 1 h ($[COD]_0$ = 0.5 M, $[\mathbf{4.18}]_0$ = 0.1 mol%).

*Evaluation of the electrochemical properties of **4.18***. Having established that **4.18** showed high activity toward the ROMP of COD at elevated temperatures, efforts shifted toward evaluating the redox-switchable characteristics of the complex. These efforts required a detailed examination of the electrochemical processes associated with the Fe and Ru centers present in **4.18**. As shown in Figure 4.8A, the cyclic voltammogram recorded for **4.18** in CH_2Cl_2 revealed two nearly overlapping quasi-reversible redox processes (E_{pa} = 0.79 and 0.98 V; Table 4.1). To assist with signal assignments, the differential pulse voltammogram (DPV) of **4.18** was recorded and compared to that obtained for the bis-phosphine Ru-indenylidene complex **4.9** (Figure 4.8B and 4.8C, respectively). Deconvolution of the former revealed two overlapping oxidations that were separated by approximately 100 mV. In contrast, only one signal was obtained upon deconvolution of the DPV for **4.9**, which was expected as this complex contains one redox-active metal center. We surmised that the oxidation of the Fe center in **4.18** occurred at a lower potential than the Ru center based on a comparison to other Ru complexes containing ferrocene moieties.[62] Moreover, upon oxidation of the ferrocene unit, the Ru center should experience a decrease in electron density due to the

introduction of positive charge.[20,62] Indeed, the redox couple attributed to the Ru center in **4.18** ($E_{1/2}$ = 0.98 V) occurred at a significantly higher potential than those recorded for other Ru-benzylidene[63] ($E_{1/2}$ = 0.45–0.54 V) and Ru-indenylidene[40j] ($E_{1/2}$ = 0.46–0.67 V) complexes supported by NHCs.

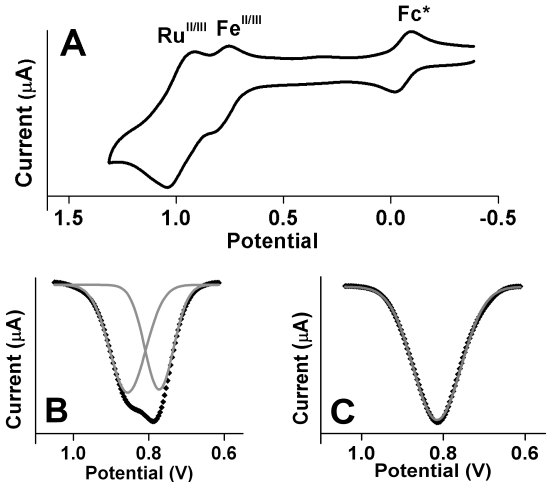

Figure 4.8 A) CV of **4.18** in CH_2Cl_2 showing quasi-reversible Fe and Ru redox processes. Conditions: 1 mM analyte, 0.1 M $[Bu_4N][PF_6]$ as the supporting electrolyte, and Fc* as an internal standard. B) DPV of **4.18** (black markers) and deconvolution of the signal (gray line). C) DPV of **4.9** (black markers) and deconvolution of the signal (gray line). Conditions for B) and C): CH_2Cl_2 solution containing 1 mM analyte and 0.1 M $[n\text{-}Bu_4N][PF_6]$ as the supporting electrolyte, 4 mV increment, 50 mV amplitude, 0.1 s pulse width, 0.0167 s sample width, 1 s pulse period.

Table 4.1 Summary of electrochemical properties for various Ir and Ru complexes.[a]

	$E_{1/2}$ (V)[b]
4.12	1.03
4.13	0.81, 1.02
4.15	0.96
4.18	0.79, 0.98
4.9	0.84

[a] Conditions: CH_2Cl_2 solution containing 1 mM analyte and 0.1 M $[Bu_4N][PF_6]$ as the supporting electrolyte. All redox processes were found to be reversible or quasi-reversible. [b] Values are reported relative to SCE through the addition of Fc* as an internal standard adjusted to –0.057 V.[73c]

*Evaluation of **4.18** and **4.18**$^+$ by UV/vis and EPR spectroscopy*. To support the relative Fe and Ru oxidation assignments, efforts were directed toward evaluating the oxidized product of **4.18** using UV/vis and EPR spectroscopy. Previous reports have shown that the oxidation products obtained by treating ferrocene and ferrocene-substituted derivatives with 2,3-dichloro-5,6-dicyanoquinone (DDQ) ($E_{1/2}$ = 0.58 V versus SCE in CH_2Cl_2/[Et_4N][ClO_4])[64] may be characterized using the aforementioned techniques.[64,65] To begin, a CH_2Cl_2 solution of **4.18** ([**4.18**]$_0$ = 0.13 mM) was treated with one equivalent of DDQ.[66] Subsequent analysis of the resulting solution by UV/vis spectroscopy revealed diagnostic absorption bands attributed to DDQ$^{\bullet-}$ (Figure 4.9A). For example, the absorption bands recorded at λ_{max} = 582, 542, and 347 nm were comparable to those reported for products obtained via the reaction of ferrocene with DDQ (λ_{max} = 587, 548, and 344 nm) and other literature values for the DDQ$^{\bullet-}$ ion.[65a,c] Although this result provided evidence that DDQ had been reduced, the strong absorbance in the expected region for ferrocenium (620 nm)[67,68] prevented unambiguous assignment of an Fe versus a Ru based oxidation.[69]

To determine the identity of the metal center (or centers) undergoing oxidation, the oxidized product of **4.18** (i.e., **4.18**$^+$) was also studied using EPR spectroscopy. The ferrocenium ion exhibits highly anisotropic *g*-tensors that typically result in a component at approximately g = 4.[70] Conversely, Ru^{III} exhibits broad signals with a relatively small *g*-anisotropy and individual *g*-values occurring between g = 1.5 and g = 2.5.[71] X-band EPR spectra of **4.18** after treatment with DDQ in CH_2Cl_2 were recorded at 110 K (Figure 4.9C). Oxidation of **4.18** using one or two equivalents of DDQ resulted in nearly identical spectra with two major features observed at g = 4.29 and 2.01. Given the high intensity and relative sharpness of the signal at g = 2.01, this signal was assigned to an organic-centered radical arising from DDQ$^{\bullet-}$; the weaker, broad signal at g

= 4.29 was consistent with that expected from an anisotropic Fe^{III}-centered radical. Since signals could not be attributed to the formation of a Ru^{III} species, the data were consistent with our above assessment that the Fe center oxidized at a lower potential than the Ru center in **4.18**. The EPR spectrum recorded after treating **4.18** with DDQ was also studied in toluene, as this solvent was found to facilitate catalytic activity at elevated temperatures. When an excess of DDQ was used (4 equiv. relative to **4.18**), signals were observed at g = 4.29 and 2.01, and assigned to Fe^{III} and semiquinone centered radical species centers, respectively. In addition, a weak broad signal was present at g = 2.01 (overlapping with the organic radical), which was consistent with a Ru-based paramagnetic species. Similar signals (g = 4.28 and 2.00) and assigments were reported by Kojima and co-workers for an oxidized Ru^{II} complex containing a ferrocene-substituted pyridylamine ligand.[72] As a control, an EPR spectrum was recorded in CH_2Cl_2 for **4.6** (which contains only one metal center) after treatment with DDQ (see supporting information). One strong signal was observed at g = 2.01 and assigned to the formation of $DDQ^{\bullet-}$; additionally, a broad signal attributed to a Ru^{III} species was recorded at g = 2.03.[70b,71]

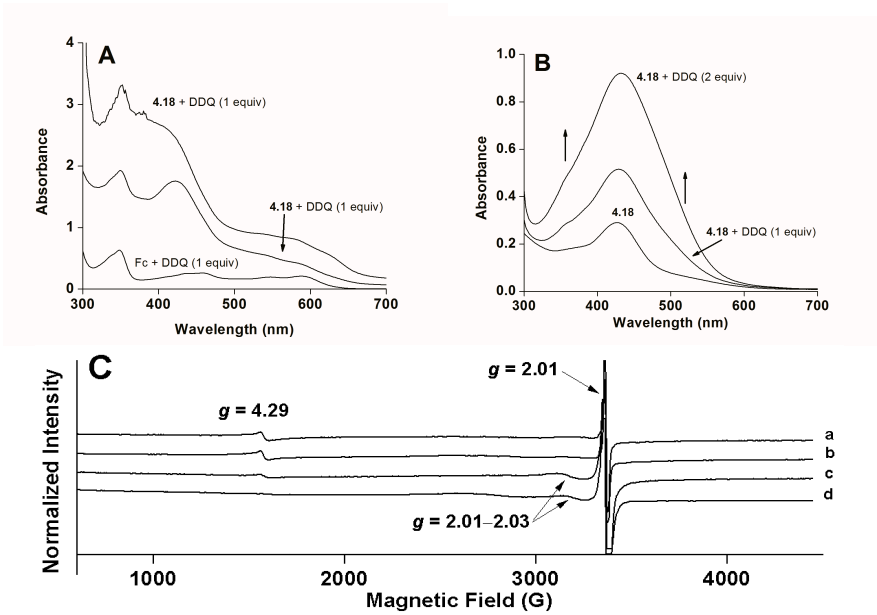

Figure 4.9 A) UV/vis absorption spectra of **4.18** ([**4.18**]$_0$ = 0.13 mM) after treatment with DDQ ([DDQ]$_0$ = 0.13 mM or 0.26 mM) in CH_2Cl_2 and ferrocene after treatment with DDQ ([ferrocene]$_0$ = ([DDQ]$_0$ = 0.12 mM). B) UV/vis absorption spectra of **4.18** ([**4.18**]$_0$ = 75 μM) and **4.18** ([**4.18**]$_0$ = 75 μM) after treatment with DDQ ([DDQ]$_0$ = 75 μM or 150 μM) in toluene/CH_2Cl_2 (79:1 v/v). C) X-band EPR spectra. Conditions: 110 K, 9.438 GHz frequency, 100 kHz modulation frequency, and 2.0 mW power. a) **4.18** ([**18**]$_0$ = 1 mM) after treatment with DDQ ([DDQ]$_0$ = 1 mM) in CH_2Cl_2; b) **4.18** ([**4.18**]$_0$ = 0.67 mM) after treatment with DDQ ([DDQ]$_0$ = 1.33 mM) in CH_2Cl_2; c) **4.18** ([**4.18**]$_0$ = 1 mM) after treatment with DDQ ([DDQ]$_0$ = 6.6 mM) in toluene; d) **4.6** ([**4.6**]$_0$ = 1 mM) after treatment with DDQ ([DDQ]$_0$ = 1 mM) in CH_2Cl_2. See Figures S10–S15 of the original manuscript for individual spectra and additional parameters.

Redox-switchable ring-opening metathesis polymerizations. Finally, the effect of ligand oxidation on the catalytic activity displayed by **4.18** was examined. Building on the aforementioned UV/vis and EPR studies, DDQ was selected as an oxidant for **4.18**. Decamethylferrocene (Fc*) was selected as the reductant on account of its appropriate oxidation potential ($E_{1/2}$ = –0.057 V in CH_2Cl_2 versus SCE)[73] and compatibility with the system under study (i.e., the oxidation product, decamethylferrocenium was expected to

be a spectator ion).[73] As summarized in Figure 4.10, the ROMP of 1,5-cyclooctadiene ($[COD]_0$ = 0.5 M) in toluene/CD_2Cl_2 (79:1 v/v)[74] at 60 °C using **4.18** as the catalyst (0.04 mol%) was monitored over time by NMR spectroscopy. When the conversion of monomer to polymer had reached approximately 25%, excess DDQ (4 equiv. relative to catalyst) was added,[75] which significantly reduced the rate constant of the polymerization reaction (pre-oxidation: k_{obs} = 0.045 s^{-1}; post-oxidation: k_{obs} = 0.0012 s^{-1}). Subsequent addition of Fc* (5 equiv. relative to catalyst) after either 30 min or 1 h restored the activity displayed by the catalyst. It appeared that the oxidized catalyst may slowly decompose over time, as the rate constant measured after reducing the catalyst after 1 h was lower than that observed after reduction after 30 min (k_{obs} = 0.0066 s^{-1} versus 0.016 s^{-1}, respectively). The premature catalyst decomposition may be due to the quasi-reversible nature of the Fe oxidation process. Moreover, from the aforementioned UV/vis and EPR studies involving **4.18**, it is feasible that the Ru center may also undergo oxidation, facilitating decomposition and contributing to the reduced catalytic activity. Regardless, the decreased rate of reaction observed upon the oxidation of **4.18** was consistent with the weaker ligand donating ability of **4.5**$^+$ (versus **4.5**) and thus generating a relatively less active catalyst. We believe that the subsequent reduction of the catalyst returned the ligand to its neutral, relatively strongly donating form and restored the catalytic activity intrinsic to **4.18**.[28g,56]

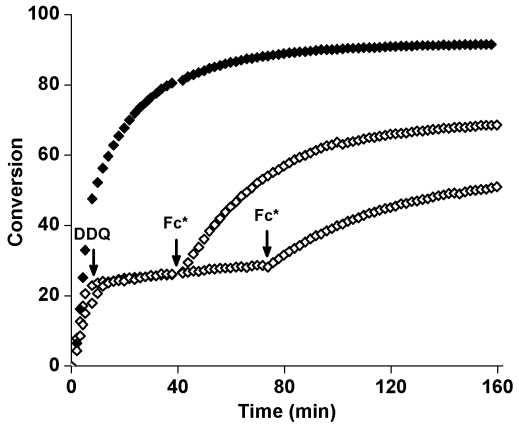

Figure 4.10 Redox-switchable ROMP of *cis,cis*-1,5-cyclooctadiene using **4.18**. All reactions were conducted in toluene-d_8/CD_2Cl_2 79:1 v/v at 60 ºC and the corresponding conversions were monitored by ^{1}H NMR spectroscopy. For the redox-switchable reactions (◊), DDQ (4 equiv. relative to **4.18**) was added after the conversion had reached approximately 25%. Subsequently, Fc* (5 equiv.) was added after an additional 0.5 h or 1 h. A control reaction where no oxidant or reductant was added over the course of the polymerization was also performed (♦). See main text and experimental section for additional details.

To confirm that the aforementioned changes in catalytic activity were driven by redox-induced changes in catalyst electronics rather than by precipitation driven phenomena,[7a] equimolar solutions of DDQ and **4.18** were analyzed by UV/vis spectroscopy in a solution of 79:1 v/v toluene/CH_2Cl_2. As shown in Figure 4.9B, increased absorption bands in the 500–600 nm region as well as the shoulder observed at 357 nm were consistent with those observed upon of the oxidation of **4.18** in CH_2Cl_2 (see above). The addition of 2 equiv. of DDQ relative to **4.18** lead to a further increase in absorbance and no precipitant was evident. Collectively, these observations reinforce the notion that adding an oxidant to the catalyst diminishes the donating ability of the FcDAC ligand rather than altering the solubility of the corresponding catalyst.

CONCLUSION

In summary, we report that FcDACs may be used as redox-switchable ligands to alter the performance displayed by olefin metathesis catalysts. The formation of various Ru-complexes incorporating *N,N'*-di-*iso*-butyl FcDAC **4.1** was observed but proved too difficult to isolate. A synthetic route to *N,N'*-dimethyl FcDAC **4.5** was developed, and this ligand was studied via its Ir(COD)Cl and $Ir(CO)_2Cl$ complexes. Compared to analogous Ir(COD)Cl and $Ir(CO)_2Cl$ complexes incorporating **4.1**, FcDAC **4.5** exhibited nearly identical electronic properties but reduced steric bulk. Building on these results, the first examples of Ru-based metathesis catalysts containing FcDAC ligands were synthesized and characterized in solution as well as in the solid state. The oxidation of (**4.5**)$(PPh_3)Cl_2$Ru(3-phenylindenylid-1-ene) (**4.18**) using DDQ as the oxidant was studied using UV/vis and EPR spectroscopy, which indicated that the oxidation of the FcDAC ligand had occurred preferentially over the Ru center. The ability of **4.18** to function as a redox-switchable catalyst was then demonstrated in the ROMP of *cis,cis*-1,5-cyclooctadiene. Chemical oxidation of the catalyst using DDQ resulted in a significant decrease in the observed rate of polymerization and subsequent reduction restored catalytic activity. UV/vis spectroscopy indicated that the catalyst was soluble upon oxidation and thus the changes in the observed rates were due to electronic tuning of the Ru center via ligand-centered oxidation rather than redox-induced precipitation. Collectively, these results underscore the potential of FcDACs to impart redox-switchable functions to transition metal catalysts. Due to the wide and growing applicability of NHC metal complexes in various synthetic processes,[76] we expect the FcDACs to be useful in outfitting a broad range of catalysts with redox switchable functions.

EXPERIMENTAL

General Considerations. Toluene and CH_2Cl_2 were dried and degassed using a Vacuum Atmospheres Company solvent purification system and then subsequently stored over 3 Å molecular sieves. Benzene-d_6 was distilled from sodium and benzophenone ketyl under an atmosphere of nitrogen then degassed by three, consecutive freeze-pump-thaw cycles. CD_2Cl_2 and toluene-d_8 (99.9%) were purchased from Cambridge Isotope Laboratories and stored over 3 Å molecular sieves. $(PCy_3)_2Cl_2Ru{=}CHPh$ (Cy = cyclohexyl) (**4.6**) was purchased from Aldrich. Diethyl diallylmalonate (DDM) was dried by stirring over 3 Å molecular sieves then degassed by three consecutive freeze-pump-thaw cycles. *cis*,*cis*-1,5-Cyclooctadiene (COD) was distilled from CaH_2 under an atmosphere of N_2 then degassed by three consecutive freeze-pump-thaw cycles. N,N′-Di-*iso*-butylformamidinium [3]ferrocenophane•BF_4 ([**4.1**H][BF4]),[19] N,N′-diphenylformamidinium[3]ferrocenophane•BF_4 ([**4.2**H][BF_4]),[19] $(PPh_3)_2Cl_2Ru$(3-phenylindenylid-1-ene),[33] (SIMes)(pyridine)$_2Cl_2Ru{=}CHPh$[77] (SIMes = 1,3-dimesitylimidazolin-2-ylidene) were synthesized according to literature procedures. Sodium hexamethyldisilazane (NaHMDS) (Acros) was purchased from Fisher Scientific and used as received. All other materials and solvents were of reagent quality and were used as received. Unless otherwise noted, all manipulations were performed under an atmosphere of nitrogen using standard drybox or Schlenk techniques.

Instrumentation. ^{1}H and ^{13}C {^{1}H} NMR spectra were recorded using a Varian 300, 400, 500 or 600 MHz spectrometer. Chemical shifts δ (in ppm) were referenced to tetramethylsilane using the residual solvent as an internal standard. For ^{1}H NMR: $CDCl_3$, 7.24 ppm; C_6D_6, 7.15 ppm; toluene-d_8, 2.09 ppm; CD_2Cl_2, 5.32 ppm; DMSO-d_6, 2.49 ppm. For ^{13}C NMR: $CDCl_3$, 77.0 ppm; CD_2Cl_2, 53.8 ppm; DMSO-d_6, 39.5 ppm. Coupling constants (J) are expressed in hertz (Hz). ^{31}P NMR spectra were recorded using a Varian

300 MHz spectrometer, with chemical shifts δ (in ppm) referenced externally to H_3PO_4. X-band EPR spectra were recorded on a Bruker EMX plus spectrometer equipped with a high sensitivity cavity and variable temperature unit accessory. Melting points (m.p.) were determined using a melt-temp apparatus and are uncorrected. Decomposition temperatures (T_d) were determined by thermogravimetric analyses (TGA) using a Mettler Toledo TGA/SDTA 851e instrument at a scan rate of 25 ºC/min under an atmosphere of air. UV-visible absorption spectra were recorded on a Perkin-Elmer Lambda 35 spectrometer. All measurements were made using matched 6Q Spectrosil quartz cuvettes (Starna) with 1 cm path lengths and 3.0 mL sample solution volumes. Electrochemical experiments were conducted on CH Instruments Electrochemical Workstations (series 630B and 700B) using a gastight, three-electrode cell under an atmosphere of dry nitrogen. The cell was equipped with gold working and tungsten counter electrodes as well as a silver wire quasi-reference electrode. Measurements were performed in dry CH_2Cl_2 with 0.1 M [*n*-Bu_4N][PF_6] as the electrolyte and $(Me_5Cp)_2Fe$ (Fc*) (Cp = cyclopentadienyl) as the internal standard. All potentials were determined at 100 mV s^{-1} scan rates and were referenced to saturated calomel electrode (SCE) by shifting $(Fc^*)^{0/+}$ to –0.057 V (CH_2Cl_2), unless otherwise noted.[73] IR spectra were recorded using a Perkin-Elmer Spectrum BX FT-IR instrument. High-resolution mass spectra (HRMS) were obtained with a VG analytical ZAB2-E or a Karatos MS9 instrument (ESI or CI) and are reported as m/z (relative intensity). Elemental analyses were performed by Midwest Microlabs, LLC (Indianapolis, IN).

1,1'-Diformamidoferrocene (4.10).[78] A 20 mL glass vial was charged with 1,1'-diaminoferrocene[79] (1.7 g, 7.9 mmol), phenyl formate (2.1 g, 95%, 17 mmol) and a stir bar. Upon addition of the phenyl formate, the reaction mixture instantly turned dark brown and generated an exotherm. The reaction mixture was subsequently stirred for 4 h

at ambient temperature and evaporated to dryness. The crude product was purified via column chromatography (media SiO_2, eluent 9:1 v/v CH_2Cl_2/MeOH) to afford the desired compound as an orange powder (1.7 g, 80% yield). m.p. 118–120 °C. ^{1}H NMR (400 MHz, DMSO-d_6): δ 9.46 (s, 0.4 H), 9.34 (s, 1H), 9.25 (m, 0.2H), 9.13 (m, 0.4H), 8.40 (m, 0.55H), 8.07 (m, 1.45H), 4.53 (t, J = 1.8, 0.85 H), 4.50 (t, J = 1.8, 2H), 4.28 (t, J = 1.8, 0.3 H), 4.24 (t, J = 1.8, 0.85 H), 4.01 (t, J = 1.8, 0.3 H), 3.99 (m, 1.6 H), 3.91 (t, J = 1.8 , 2.1 H). ^{13}C NMR (100 MHz, DMSO-d_6): δ 163.1, 159.4, 159.1, 95.9, 94.5, 94.3, 65.7, 65.4, 65.1, 65.1, 62.0, 61.8, 60.9, 60.6. m.p. 118–120 °C. HRMS: [M^+] Calcd for $C_{12}H_{12}N_2O_2Fe$ 272.02482; Found 272.02431. Anal. Calcd (%) for $C_{12}H_{12}N_2FeN_2O_2$: C, 52.97; H, 4.45; N, 10.30; Found: C, 53.20; H, 4.49; N, 10.30.

1,1'-Dimethylaminoferrocene (4.11). A 250 mL Schlenk flask was charged with lithium aluminum hydride ($LiAlH_4$) (0.30 g, 9.6 mmol), THF (20 mL) and a stir bar. The mixture was cooled to 0 °C in an ice bath. Under a constant stream of nitrogen, a degassed slurry of 1,1'-diformamidoferrocene (500 mg, 1.8 mmol) in THF (20 mL) was added drop-wise over 30 min via syringe. After stirring for an additional 30 min at 0 °C, the flask was fitted with a condenser and refluxed for 1 h. The reaction mixture was then cooled to 0 °C in an ice bath and the excess $LiAlH_4$ was quenched via dropwise addition of degassed water. Water (50 mL) and ether (50 mL) were then added which resulted in the formation of a white precipitate. After the white precipitate was allowed to settle, the ethereal phase was separated under nitrogen and evacuated at 20 millitorr for 24 h to give the desired compound as an oxygen-sensitive orange solid (350 mg, 78% yield). m.p. 68–70 °C. ^{1}H NMR (400 MHz, C_6D_6): δ 3.84 (t, J = 1.8, 4H), 3.72 (t, J = 1.8, 4H), 2.73 (s, 6H), 1.73 (br s, 2H). ^{13}C NMR (100 MHz, C_6D_6): δ 112.3, 63.2, 55.7, 33.8. HRMS: [M^+] Calcd for $C_{12}H_{14}N_2Fe$, 244.06629; Found, 244.06561. Due to its high sensitivity toward oxygen, elemental analysis of this compound was not performed.

***N,N'*-Dimethylformamidinium [3]ferrocenophane BF_4 (4.12).** 1,1'-Dimethylaminoferrocene (**4.11**) (639 mg, 2.61 mmol), degassed trimethylorthoformate (5 mL), tetrafluoroboric acid etherate (0.35 mL, 2.6 mmol) and a stir bar were added to a 25 mL Schlenk flask under nitrogen. The reaction mixture was heated for 30 min at 60 °C. After allowing the mixture to cool to room temperature, the solvent was removed under vacuum. The residue was extracted with CH_2Cl_2 (5 mL) and filtered through a 0.25 μm PTFE filter into hexanes (50 mL) to afford a golden precipitate, which was collected by filtration and washed with additional hexanes (100 mL). The solid was dried under vacuum to afford the desired compound as a gold powder (780 mg, 88% yield). Crystals suitable for X-ray structure determination were grown by slow diffusion of ether into a saturated CH_2Cl_2 solution of the compound. T_d 305 °C. ^{1}H NMR (400 MHz, DMSO-d_6): δ 8.71 (s, 1H), 4.67 (t, J = 1.8, 4H), 4.45 (t, J = 1.8, 4H), 3.50 (s, 6H). ^{13}C NMR (100 MHz, DMSO-d_6): δ 162.0, 93.7, 71.7, 67.2, 45.7. HRMS: [M^+-BF_4] Calcd for $C_{13}H_{15}N_2Fe$ 255.0575; Found 255.05792. Anal. Calcd (%) for $C_{13}H_{15}N_2FeBF_4$: C, 45.67; H, 4.42; N, 8.19; Found: C, 45.43; H, 4.42; N, 8.08.

(Dimethyldiaminocarbene[3]ferrocenophane)Ir(COD)Cl (4.13). A 7.5 mL glass vial equipped with a stir bar was charged with **4.12** (74 mg, 0.22 mmol), NaHMDS (98%, 42 mg, 0.22 mmol) and toluene (3 mL). The mixture was then stirred for 5 min. $[Ir(COD)Cl]_2$ (72 mg, 0.12 mmol) was added, and the resulting brown mixture was stirred for 12 h, after which point the work up was performed in air. The solvent was removed by evaporation under reduced pressure. The residue was taken up in a minimal amount of CH_2Cl_2 and purified using column chromatography (media SiO_2, eluent 3:1 v/v hexanes/ethyl acetate, R_f = 0.18). The yellow fraction was collected and the solvent was removed by evaporation under reduced pressure to give the desired product as a yellow powder (70 mg, 55% yield). ^{1}H NMR (400 MHz, $CDCl_3$): δ 4.47 (m, 2H), 4.18 (m, 12H),

3.91 (m, 2H), 2.96 (m, 2H), 2.20 (m, 4H), 1.75–1.50 (m, 4H). ^{13}C NMR (100 MHz, $CDCl_3$): δ 215.6, 100.2, 81.4, 71.0, 70.9, 66.3, 65.5, 53.2, 48.8, 33.1, 29.4. HRMS: [M^+-2H-Cl] Calcd for $C_{21}H_{24}N_2FeIr$ 553.09180; Found 553.09146. Anal. Calcd (%) for $C_{21}H_{26}ClN_2FeIr$: C, 42.75; H, 4.36; N, 4.94; Found: C, 42.87; H, 4.65; N, 4.65.

(*N,N'*-Dimethyldiaminocarbene[3]ferrocenophane)Ir(CO)$_2$Cl (4.15). A 20 mL glass vial equipped with a stir bar was charged with **4.13** (70 mg, 0.12 mmol) and CH_2Cl_2 (5 mL), and then sealed with a septum. The solution was then stirred under an atmosphere of CO (1 atm) for 3 h. The solvent was removed by evaporation under reduced pressure to give a yellow powder. Subsequent washing of the powder with a minimal amount of pentane followed by drying under vacuum for 48 h to remove the residual 1,5-cyclooctadiene afforded the desired product as a yellow solid (51 mg, 80% yield). ^1H NMR (400 MHz, $CDCl_3$): δ 4.27 (m, 4H), 4.23 (m, 2H), 4.16 (m, 2H), 3.98 (s, 6H). ^{13}C NMR (100 MHz, $CDCl_3$): δ 206.2, 180.5, 168.5, 99.4, 71.6, 71.5, 66.1, 65.6, 50.0. FT-IR (CH_2Cl_2): 2065, 1983 cm^{-1}. HRMS: [M^+-2H-Cl] Calcd for $C_{15}H_{14}N_2O_2FeIr$ 503.0034, Found 503.0029. Anal. Calcd (%) for $C_{15}H_{16}ClN_2O_2FeIr$: C, 33.37; H, 2.99; N, 5.19; Found: C, 33.84; H, 2.60; N, 5.00.

(*N,N'*-Dimethyldiaminocarbene[3]ferrocenophane)(PPh$_3$)Cl$_2$Ru(3-phenylindenylid-1-ene) (4.18). A 6 mL glass vial equipped with a stir bar was charged with **4.12** (103 mg, 0.301 mmol), NaHMDS (57.2 mg, 0.312 mmol) and toluene (6 mL), and then sealed with a Teflon lined cap. The reaction mixture was stirred for 5 min at ambient temperature. $(PPh_3)_2Cl_2Ru$(3-phenylindenylid-1-ene) (**4.9**) (158 mg, 0.178 mmol) was added and the vial was re-sealed with a Teflon lined cap. The solution was stirred at ambient temperature for 1 h and then concentrated under reduced pressure to afford a brown solid. The solid was then purified by column chromatography (media SiO_2, eluent 10:1 v/v hexanes/ethyl acetate) to elute a light red fraction (**4.17**). The

solvent was then switched to ethyl acetate to elute a dark red fraction (**4.18**). The second dark red fraction was evaporated to dryness by concentration under reduced pressure. Benzene was then added (3 mL) which caused a red microcrystalline solid to precipitate upon standing. The solid was recovered by vacuum filtration to yield the desired complex as a red microcrystalline solid (18.9 mg, 12% yield). The solvent was then removed from the first fraction by evaporation under reduced pressure. Subsequent purification of this fraction by chromatography using the aforementioned solvent system increased the overall combined yield of **4.18** to 30% (46.8 mg). X-ray quality crystals were grown by vapor diffusion of hexanes into a saturated benzene solution of the complex. ^{1}H NMR (300 MHz, CD_2Cl_2): δ 9.38 (d, 1H, J = 6.9), 7.59–7.25 (m, 23H), 6.13 (s, 1H), 4.35 (m, 2H), 4.26 (br s, 2H), 4.23 (br s, 2H), 4.17 (m, 1H), 4.05 (m, 1H), 3.38 (s, 3H), 2.71 (s, 3H). ^{13}C NMR (150 MHz, CD_2Cl_2): δ 297.1 (d, J = 16.1), 215.7 (d, J = 8.3), 145.01, 145.00, 141.8, 140.6, 140.5, 137.9, 135.5, 134.7, 131.5, 130.9, 130.81, 130.80, 130.4, 129.4, 129.1, 128.9, 128.71, 128.67, 128.6, 126.8, 118.3, 100.0, 99.5, 72.3, 72.2, 71.7, 71.5, 67.4, 66.5, 65.4, 64.4, 50.9, 46.9. ^{31}P NMR (121 MHz, CD_2Cl_2): δ 47.99. HRMS: [M^+-Cl] Calcd. for $C_{46}H_{39}ClFeN_2PRu$ 843.09420; Found 843.09268. Anal. Calcd (%) for $C_{46}H_{39}Cl_2FeN_2PRu\cdot(1/6)CH_2Cl_2$: C, 62.11; H, 4.44; N, 3.14. Found: C, 62.05; H, 4.48; N, 3.07.

General Procedure Used to Measure the Kinetics of the ROMP of *cis*,*cis*-1,5-Cyclooctadiene. Inside a drybox, an NMR tube was charged with either (i) 25 μL (0.40 μmol) of a 0.016 M stock solution of catalyst in CD_2Cl_2[74] and 0.78 mL of CD_2Cl_2 or (ii) 25 μL (0.40 μmol) of a 0.016 M stock solution of catalyst in CD_2Cl_2 and 0.78 mL of toluene-d_8. The tube was capped and shaken vigorously before COD (49.1 μL, 43.3 mg, 0.40 mmol; $[\text{monomer}]_0$ = 0.5 M) was added. The reaction was then removed from the drybox and allowed to proceed at either 30 or 80 °C in an oil bath. After 1 or 24 h, the

progress of the reaction was determined by comparing the integral of the signals attributed to the methylene protons of the *cis*,*cis*-1,5-cyclooctadiene monomer (δ = 2.17 ppm, m) versus the polybutadiene product (δ = 2.08 ppm, br m).

General Procedure Used to Monitor the RCM of Diethyl Diallylmalonate. Inside a drybox, an NMR tube was charged with either (i) 50 μL (0.80 μmol) of a 0.016 M stock solution of catalyst in CD_2Cl_2 and 0.75 mL of CD_2Cl_2 or (ii) 50 μL (0.80 μmol) of a 0.016 M stock solution of catalyst in CD_2Cl_2 and 0.75 mL of toluene-d_8. The tube was then capped and shaken vigorously before diethyl diallylmalonate (DDM) (19.3 μL, 19.2 mg, 0.080 mmol; $[DDM]_0$ = 0.1 M) was added. The tube was then re-capped, shaken, and sealed with parafilm. The reaction was then removed from the drybox and allowed to proceed at either 30 or 80 ºC in an oil bath. After 1 or 24 h, the progress of the reaction was determined by comparing the integral of the signals attributed to the methylene protons in DDM (δ = 2.61 ppm) with those found in the product (δ = 2.98 ppm).

General Procedure Used to Monitor Redox-Switchable ROMP of COD. In a nitrogen filled drybox, a stock solution of **4.18** in CD_2Cl_2 was prepared (0.016 M). Stock solutions of DDQ (0.02 M) and Fc* (0.02 M) were separately prepared in toluene-d_8. A screw-cap NMR tube was then charged with catalyst stock solution (10 μL, 0.16 μmol) and toluene-d_8 (0.79 mL), and then sealed with a septum-top screw-cap. The NMR tube was then equilibrated to 60 °C inside of an NMR spectrometer. The sample was ejected and COD (49.1 μL, 43.3 mg, 0.40 mmol; $[COD]_0$ = 0.5 M) was quickly added through the septum via microsyringe. NMR spectra were collected at 2 min intervals until the conversion had reached approximately 25%. The sample was again ejected and DDQ (32 μL, 0.64 μmol) was quickly added through the septum top via microsyringe. Data acquisition resumed at 2 min intervals until either 30 min or 1 h had

elapsed. At this point, the sample was again ejected and Fc* (40 μL, 80 μmol) was quickly added through the septum top via microsyringe. An NMR array function was then used to record a spectrum every 2 min for 3 h.

REFERENCES

(1) Allgeier, A. M.; Mirkin, C. A. *Angew. Chem. Int. Ed.* **1998**, *37*, 894–908.

(2) AMagenau, . J. D.; Strandwitz, N. C.; Gennaro A.; Matyjaszewski, K. *Science* **2011**, *332*, 81–84.

(3) (a) Hadei, N.; Kantchev, E. A. B.; O'Brien, C. J.; Organ, M. G. *Org. Lett.* **2005**, *7*, 1991; (b) O'Brien, C. J.; Kantchev, E. A. B.; Chass, G. A.; Hadei, N.; Hopkinson, A. C.; Organ, M. G.; Setiadi, D. H.; Tang, T.-H.; Fang, D.-C. *Tetrahedron* **2005**, *61*, 9723; (c) Vorfalt, T.; Leuthäusser, S.; Plenio, H. *Angew. Chem., Int. Ed.* **2009**, *48*, 5191–5194; (d) Khramov, D. M.; Rosen, E. L.; Er, J. A. V.; Vu, P. D.; Lynch, V. M.; Bielawski, C. W. *Tetrahedron* **2008**, *64*, 6853–6862.

(4) Lorkovic, I. M.; Duff, R. R., Jr.; Wrighton, M. S. *J. Am. Chem. Soc.* **1995**, *117*, 3617–3618.

(5) (a) Slone, C. S.; Mirkin, C. A.; Yap, G. P. A.; Guzei, I. A.; Rheingold, A. L. *J. Am. Chem. Soc.* **1997**, *119,* 10743–10753; (b) Hino, T.; Wada, T.; Fujihara, T.; Tanaka, K. *Chemistry Letters* **2004**, *33*, 1596–1597; (c) Gregson, C. K. A.; Gibson, V. C.; Long, N. J.; Marshall, E. L.; Oxford, P. J.; White, A. J. P. *J. Am. Chem. Soc.* **2006**, *128*, 7410–7411; (d) Ringenberg, M. R.; Kokatam, S. L.; Heiden, Z. M.; Rauchfuss, T. B. *J. Am. Chem. Soc.* **2008**, *130*, 788–789; (e) Muckerman, J. T.; Polyansky, D. E.; Wada, T.; Tanaka, K.; Fujita, E. *Inorg. Chem.* **2008**, *47*, 1787–1802; (f) Blackmore, K. J.; Lal, N.; Ziller, J. W.; Heyduk, A. F. *J. Am. Chem. Soc.* **2008**, *130*, 2728–2729; (g) Boyer, J. L.; Cundari,T. R.; DeYonker, N. J.; Rauchfuss, T. B.; Wilson, S. R. *Inorg. Chem.* **2008**, *48*, 638–645.

(6) (a) Broderick, E. M.; Guo, N.; Vogel, C. S.; Xu, C.; Sutter, J.; Miller, J. T.; Meyer, K.; Mehrkhodavandi, P.; Diaconescu, P. L. *J. Am. Chem. Soc.* **2011**, *133*, 9278–9281; (b) Broderick, E. M.; Guo, N.; Wu, T.; Vogel, C. S.; Xu, C.; Sutter, J.; Miller, J. T.; Meyer, K.; Cantat, T.; Diaconescu, P. L. *Chem. Commun.* **2011**, **47**, 9897–9899.

(7) (a) Sußner, M.; Plenio, H. *Angew. Chem. Int. Ed.* **2005**, *44*, 6885–6888; (b) Liu, G.; He, H.; Wang, J. *Adv. Synth. Catal.* **2009**, *351*, 1610–1620.

(8) Curran, D. P. *Angew. Chem.* **1998**, *110*, 1230–1255; *Angew. Chem. Int. Ed.* **1998**, *37*, 1174-1196.

(9) Peeck, L. H.; Leuthaüsser, S.; Plenio, H. *Organometallics* **2010**, *29*, 4339–4345.

(10) (a) Ward, M. D.; McCleverty, J. A. *J. Chem. Soc., Dalton Trans.* **2002**, 275–288; (b) Zanello, P.; Corsini, M. *Coord. Chem. Rev.* **2006**, *250*, 2000–2022; (c). Boyer, J. L.; Rochford, J.; Tsai, M.-K.; Muckerman, J. T.; Fujita, E. *Coord. Chem. Rev.* **2010**, *254*, 309–330.

(11) (a) Kotz, J. C.; Nivert, C. L.; Lieber, J. M.; Reed, R. C. *J. Organomet. Chem.* **1975**, *91*, 87–95; (b) Miller, T. M.; Ahmed, K. J.; Wrighton, M. S. *Inorg. Chem.* **1989**, *28*, 2347–2355; (c) Lorkovic, I. M.; Wrighton, M. S.; Davis, W. M. *J. Am. Chem. Soc.* **1994**, *116*, 6220–6228; (d) Yeung, L. K.; Kim, J. E.; Chung, Y. K.; Rieger, P. H.; Sweigart, D. A. *Organometallics* **1996**, *15*, 3891–3897; (e) Downs, H. H.; Buchanan, R. M.; Pierpont, C. G. *Inorg. Chem.* **1979**, *18*, 1736–1740; (f) Hartl, F.; Vlcek, A. *Inorg. Chem.* **1991**, *30*, 3048–3053; (g) Yang, K.; Bott, S. G. Richmond, M. G. *Organometallics* **1995**, *14*, 2387–2394; (h) Wada, T.; Fujihara, T.; Tomori, M.; Ooyama, D.; Tanaka, K. *Bull. Chem. Soc. Jpn.* **2004**, *77*, 741–749; (i) Bellec, N.; Massue, J.; Roisnel, T.; Lorcy, D. *Inorg. Chem. Commun.* **2007**, *10*, 1172–1176; (j) Blackmore, K. J.; Ziller, J. W.; Heyduk, A. F. *Inorg. Chem.* **2005**, *44*, 5559–5561.

(12) (a) Allgeier, A. M.; Slone, C. S.; Mirkin, C. A.; Liable-Sands, L. M.; Yap, G. P. A.; Rheingold, A. L. *J. Am. Chem. Soc.* **1997**, *119*, 550–559; (b) Sassano, C. A.; Mirkin, C. A. *J. Am. Chem. Soc.* **1995**, *117*, 11379–11380.

(13) Although metallocenes are commonly utilized, other types of redox-active ligands have been used to modulate catalytic reactions. For example, Rauchfuss reported[5d] that an Ir complex containing 2-(2-trifluoromethyl)anilino-4,6-di-*tert*-butylphenol activated H_2 upon oxidation; likewise, oxidation also increased the electrophilicity of a Pt complex containing the same ligand.[5g] We reported that Ni complexes containing 1,3-dimesitylnapthoquinimidazolylidene (**NQMes**)[23] modulate Kumada coupling reactions as a function of the ligand's oxidation state.[21]

(14) Arduengo, A. J. III; Harlow, R. L.; Kline, M. *J. Am. Chem. Soc.* **1991**, *113*, 361–363; (a) Arduengo, A. J., III; *Acc. Chem. Res.* **1999**, *32*, 913–921; (b) Crudden, C. M.; Allen, D. P. *Coord. Chem. Rev.* **2004**, *248*, 2247–2273; (c) Hahn, F. E.; Jahnke, M. C. *Angew. Chem., Int. Ed.* **2008**, *47*, 3122–3172.

(15) For reviews of catalytically-active transition metal complexes containing NHCs, see: (a) Herrmann, W. A. *Angew. Chem., Int. Ed.* **2002**, ***41***, 1290–1309; (b) Peris, E.; Crabtree, R. H. *Coord. Chem. Rev.* **2004**, *248,* 2239–2246; (c) Cavell, K. J.; McGuiness, D. S. *Coord. Chem. Rev.* **2004**, *248*, 671–681; (d) Kantchev, E. A. B.; O'Briend, C. J.; Organ, M. G. *Angew. Chem. Int. Ed.* **2007**, *46*, 2768–2813; (e) Colacino, E.; Martinez, J.; Lamaty, F. *Coord. Chem. Rev.* **2007**, *251*, 726–764; (f) Díez-González, S.; Marion, N.; Nolan, S. P. *Chem. Rev.* **2009**, *109*, 3612–3676; (g) Samojłowicz, C.; Bieniek, M.; Grela, K. *Chem. Rev.* **2009**, *109*, 3708–3742.

(16) (a) Scott, N. M.; Clavier, H.; Mahjoor, P.; Stevens, E. D.; Nolan, S. P. *Organometallics* **2008**, *27*, 3181–3186; (b) Jafarpour, L.; Stevens, E. D.; Nolan, S. P. *J. Organomet. Chem.* **2000**, *606*, 49–54.

(17) (a) Díez-González, S.; Nolan, S. in *N-Heterocyclic Carbenes in Transition Metal Catalysis*, Springer: Berlin Heidelberg, 2007, vol. 21, pp. 47–82; (b) Marion, N.; Navarro, O.; Mei, J.; Stevens, E. D.; Scott, N. M.; Nolan, S. P. *J. Am. Chem. Soc.* **2006**, *128*, 4101–4111; (c) Navarro, O.; Marion, N.; Oonishi, Y.; Kelly, R. A., III; Nolan, S. P. *J. Org. Chem.* **2006**, *71*, 685–692; (d) Hillier, A. C.; Grasa, G. A.; Viciu, M. S.; Lee, H. M.; Yang, C.; Nolan, S. P. *J. Organomet. Chem.* **2002**, *653*, 69–82; (e) Jörgensen, M.; Lee, S .; Liu, X.; Wolkowski, J. P.; Hartwig, J. F. *J. Am. Chem. Soc.* **2002**, *124*, 12557–12565; (f) Louie, J.; Gibby, J. E.; Farnworth, M. V.; Tekavec, T. N. *J. Am. Chem. Soc.* **2002**, *124*, 15188–15189.

(18) (a) Scholl, M.; Ding, S.; Lee, C. W.; Grubbs, R. H. *Org. Lett.* **1999**, *1*, 953–956; (b) O'Brien, C. J.; Kantchev, E. A. B.; Valente, C.; Hadei, N.; Chass, G. A.; Lough, A.;. Hopkinson, A. C.; Organ, M. G. *Chem. Eur. J.* **2006**, *12*, 4743–4748.

(19) Khramov, D. M.; Rosen, E. L.; Lynch, V. M.; Bielawski, C. W. *Angew. Chem., Int. Ed.* **2008**, *47*, 2267–2270.

(20) Rosen, E. L.; Varnado, C. D., Jr.; Tennyson, A. G.; Khramov, D. M.; Kamplain, J. W.; Sung, D. H.; Cresswell, P. T.; Lynch, V. M.; Bielawski, C. W. *Organometallics* **2009**, *28*, 6695–6706.

(21) Tennyson, A. G.; Lynch, V. M.; Bielawski, C. W. *J. Am. Chem. Soc.*, **2010**, *132*, 9420–9429.

(22) Varnado, C. D., Jr.; Lynch, V. M.; Bielawski, C. W. *Dalton Trans.* **2009**, 7253–7261.

(23) Sanderson, M. D.; Kamplain, J. W.; Bielawski, C. W. *J. Am. Chem. Soc.*, 2006, **128**, 16514–16515.

(24) Arumugam, K.; Varnado, C. D., Jr.; Sproules, S.; Lynch, V. M.; Bielawski, C. W. *Chem. Eur. J.* 2013, DOI: 10.1002/chem.201301247.

(25) (a) Siemeling, U.; Färber, C.; Bruhn, C. *Chem. Commun.* **2009**, 98–100; (b) Siemeling, U.; Färber, C.; Leibold, M.; Bruhn, C.; Mücke, P.; Winter, R. F.; Sarkar, B.; Hopffgarten, M. V.; Frenking, G. *Eur. J. Inorg. Chem.* **2009**, 4607–4612.

(26) Siemeling, U. *Eur. J. Inorg. Chem.* **2012**, 3523-2546.

(27) (a) Chianese, A. R.; Li, X.; Janzen, M. C.; Faller, J. W.; Crabtree, R. H. *Organometallics* **2003**, *22*, 1663–1667; (b) Altenhoff, G.; Goddard, R.; Lehmann, C. W.; Glorius, F. *J. Am. Chem. Soc.* **2004**, *126*, 15195–15201; (c) Leuthäusser, S.; Schwarz, D.; Plenio, H. *Chem. Eur. J.* **2007**, 13, 7195–7203; (d) Kelly, R. A., III; Clavier, H.; Giudice, S.; Scott, N. M.; Stevens, E. D.; Bordner, J.; Samardjiev,

I.; Hoff, C. D.; Cavallo, L.; Nolan, S. P. *Organometallics* **2008**, *27*, 202–210; (e) Wolf, S.; Plenio, H. *J. Organomet. Chem.* **2009**, *694*, 1487–1492.

(28) (a) Furstner, A. *Angew. Chem.* **2000**, *112*, 3140–3172; (b) Ivin, K. J.; Mol, J. C. *Olefin Metathesis and Metathesis Polymerization*, 1st ed.; Academic Press: San Diego, CA, 1997; (c) Ivin, K. J. *J. Mol. Catal. A.: Chem.* **1998**, *133*, 1–16; (d) Grubbs R. H.; Chang, S. *Tetrahedron* **1998**, *54*, 4413–4450; (e) Grubbs, R. H. *Tetrahedron* **2004**, *60*, 7117–7140; (f) Buchmeiser, M. R. *Chem. Rev.* **2000**, *100*, 1565–1604; (g) Trnka, T. M.; Grubbs, R. H. *Acc. Chem. Res.* **2001**, *34*, 18–29.

(29) (a) Schwab, P.; France, M. B.; Ziller, J. W.; Grubbs, R. H. *Angew. Chem.* **1995**, *107*, 2179–2181; *Angew. Chem. Int. Ed. Engl.* **1995**, *34*, 2039–2041; (b) Fraser, C. Grubbs, R. H. *Macromolecules* **1995**, *28*, 7248–7255; (c) Schwab, P.; Grubbs, R. H.; Ziller, J. W. *J. Am. Chem. Soc.* **1996**, ***118***, 100–110.

(30) (a) Staub, B. F. *Angew. Chem., Int. Ed.* **2005**, *44*, 5974–5978; (b) Weskamp, T.; Kohl, F. J.; Hieringer, W.; Gliech, D.; Herrman, W. A. *Angew. Chem. Int. Ed.* **1999**, *38*, 2416–2419.

(31) (a) Scholl, M.; Trnka, T. M.; Morgan, J. P.; Grubbs, R. H. *Tetrahedron Lett.* **1999**, *40*, 2247–2250; (b) Morgan, J. P.; Grubbs, R. H. *Org. Lett.* **2000**, *2*, 3153–3155; (c) Huang, J.; Stevens, E. D.; Nolan, S. P.; Peterson, J. L. *J. Am. Chem. Soc.* **1999**, *121*, 2674–2678; (d) Hermann, W. A.; Köcher, C. *Angew. Chem. Int. Ed.* **1997**, *36,* 2162–2187; (e) Chatterjee, A. K.; Morgan, J. P.; Scholl, M.; Grubbs, R. H. *J. Am. Chem. Soc.*, **2000**, *122*, 3783–3784; For selected examples with unsaturated imidazol-2-ylidenes, see: (f) Fürstner, A.; Thiel, O. R.; Ackermann, L.; Schanz, H. J.; Nolan, S. P. *J. Org. Chem.* **2000**, *65*, 2204–2207; (g) Briot, A.; Bujard, M.; Gouverneur, V.; Nolan, S. P.; Mioskowski, C. *Org. Lett.* **2000**, *2*, 1517–1519.

(32) Grubbs, R. H. *Handbook of Metathesis*; Wiley-VCH: Weinheim, Germany, 2003.

(33) Harlow, K. J.; Hill, A. F.; Wilton-Ely, J. D. E. T. *J. Chem. Soc., Dalton Trans.*, **1999**, 285–291.

(34) For a preliminary account of this work see: Rosen, E. L. PhD Thesis, University of Texas at Austin, 2009.

(35) The deprotonation of the respective hydrogen tetrafluorborate salts of **4.1** and **4.2** was studied under a variety of conditions. Although the formation of **4.2** was not observed in solution by ^{1}H NMR spectroscopy, **4.1** was characterized by ^{1}H and ^{13}C NMR spectroscopy despite undergoing decomposition upon concentration. See ref. 19 for additional details.

(36) Although a variety of purification techniques including precipitation, trituration, and column chromatography (neutral or basic Al_2O_3, and SiO_2) were investigated, the isolated product appeared to readily decompose in all cases; as such, more stable derivatives were pursued.

(37) Ulman, M.; Grubbs, R. H. *J. Org. Chem.* **1999**, *64,* 7202–7207.

(38) Fürstner, A.; Grabowski, J.; Lehmann, C. W. *J. Org. Chem.* **1999**, *64*, 8275–8280.

(39) For recent reviews, see: (a) Boeda, F.; Clavier, H.; Nolan, S. P. *Chem. Commun.* **2008**, 2726–2740; (b) Dragutan, V.; Dragutan, I.; Verpoort, F. *Platinum Met. Rev.* **2005**, *49*, 33–40.

(40) (a) Dorta, R.; Kelly, R. A.; Nolan, S. P. *Adv. Synth. Catal.* **2004**, *346*, 917–920; (b) Clavier, H.; Petersen, J. L.; Nolan, S. P. *J. Organomet. Chem.* **2006**, *691*, 5444–5477; (c) Clavier, H.; Nolan, S. P. *Chem. Eur. J.*, **2007**, *13*, 8029–8036; (d) Bieniek, M.; Michrowska, A.; Usanov, D. L.; Grela, K. *Chem. Eur. J.* **2008**, *14*, 806–818; (e) Boeda, F.; Bantreil, X.; Clavier, H.; Nolan, S. P. *Adv. Synth. Catal.* **2008**, *350*, 2959–2966; (f) Monsaert, S.; Drozdzak, R.; Dragutan, V.; Dragutan, I.; Verpoort, F. *Eur. J. Inorg. Chem.* **2008**, 432–440; (g) Clavier, H.; Urbina-Blanco, C. A.; Nolan, S. P. *Organometallics*, **2009**, *28*, 2848–2854; (h) Monsaert, S.; Canck, E. D.; Drozdzak, R.; Voort, P. V. D.; Verpoort, F.; Martins, J. C.; Hendrickx, P. M. S. *Eur. J. Org. Chem.* **2009**, 655–665; (i) Clavier, H.; Correa, A.; Escudero-Adán, E. C.; Benet- Buchholz, J.; Cavallo, L.; Nolan, S. P. *Chem. Eur. J.*, **2009**, *15*, 10244–10254; (j) Peeck, L. H.; Plenio, H. *Organometallics* **2010**, *29*, 2761-2766; (k) Urbina-Blanco, C. A.; Leitgeb, A.; Slugovc, C.; Bantreil, X.; Clavier, H.; Slawin, A. M. Z.; Nolan, S. P. *Chem Eur. J.* **2011**, *17*, 5045–5053; (l) Clavier, H.; Broggi, J.; Nolan, S. P. *Eur. J. Org. Chem.* **2010**, 937-943; (m) Bantreil, X.; Poater, A.; Urbina-Blanco, C. A.; Bidal, Y. D.; Falivene, L.; Randall, R. A. M.; Cavallo, L.; Slawin, A. M. Z.; Cazin, C. S. J. *Organometallics* **2012**, *31*, 7415–7426; (n) Luján, C. Nolan, S. P. *Catal. Sci. Technol.* **2012**, *2*, 1027–1032.

(41) The complex (**4.5**)(PCy_3)Cl_2Ru(2-phenylindenylid-1-ene) was found to decompose on silica gel and crystallization attempts were unsuccessful. The synthesis of (**4.1**)(PCy_3)Cl_2Ru(2-phenylindenylid-1-ene) has not yet been pursued in our laboratories.

(42) Garber, S. B.; Kingsbury, J. S.; Gray, B. L.; Hoveyda, A. H. *J. Am. Chem. Soc.* **2000**, *122*, 8168–8179.

(43) (a) Trnka, T. M.; Morgan, J. P.; Sanford, M. S.; Wilhelm, T. E.; Scholl, M.; Choi, T.-L.; Ding, S.; Day, M. W.; Grubbs, R. H. *J. Am. Chem. Soc.* **2003**, *125*, 2546–2558; (b) Rosen, E. L.; Sung, D. H.; Chen, Z.; Lynch, V. M.; Bielawski, C. W. *Organometallics* **2010**, *29*, 250–256; (c) Sashuk, V.; Peeck, L. H.; Plenio, H. *Chem. Eur. J.* **2010**, *16*, 3983–3993; (d) Bantreil, X.; Randall, R. A. M.; Slawin, A. M. Z.; Nolan, S. P. *Organometallics* **2010**, *29*, 3007-3011.

(44) For symmetric $(NHC)_2Cl_2$Ru=CHPh complexes, see: (a) Weskamp, T.; Schattenmann, W. C.; Spiegler, M.; Herrmann, W. A. *Angew. Chem., Int. Ed.* **1998**, *37*, 2490–2493; (b) Conrad, J. C.; Yap, G. P. A.; Fogg, D. E. *Organometallics* **2003**, *22*, 1986–1988; (c) Zhang, W.; Bai, C.; Lu, X.; He, R. *J.*

Organomet. Chem. **2007**, *692*, 3563–3567; (d) Ledoux, N.; Allaert, B.; Linden, A.; Van Der Voort, P.; Verpoort, F. *Organometallics* **2007**, *26,* 1052–1056.

(45) Dinger, M. B.; Nieczypor, P.; Mol, J. C. *Organometallics* **2003**, *22*, 5291–5296.

(46) Herrmann, W. A.; Öfele, K.; Preysing, D. V.; Herdtweck, E. *J. Organomet. Chem.* **2003**, *684*, 235–248.

(47) (a) Alder, R. W.; Allen, P. R.; Murray, M.; Orpen, A. G. *Angew. Chem.* **1996**, *108*, 1211–1213; *Angew. Chem. Int. Ed.* **1996**, *35***,** 1121–1123; (b) Alder, R.W.; Blake, M. E.; Chaker, L.; Harvey, J. N.; Paolini, F.; Schötz, J. *Angew. Chem.* **2004**, *116*, 6020–6036; *Angew. Chem. Int. Ed.* **2004**, *43*, 5896–5911; (c) Rosen, E. L.; Sanderson, M. D.; Saravanakumar, S.; Bielawski, C. W. *Organometallics* **2007**, *26*, 5774–5777.

(48) See Appendix C for deprotonation conditions and corresponding ^{1}H NMR data.

(49) Collins, M. S.; Rosen, E. L.; Lynch, V. M.; Bielawski, C. W. *Organometallics* **2010**, *29*, 3047–3053.

(50) (a) Binobaid, A.; Iglesias, M.; Beetstra, D. J.; Kariuki, B.; Dervisi, A.; Fallis, A. A.; Cavell, K. J. *Dalton Trans.* **2009**, 7099–7112; (b) Iglesias, M.; Beetstra, D. J.; Stasch, A.; Horton, P. N.; Hursthouse, M. B.; Coles, S. J.; Cavell, K. J.; Dervisi, A.; Fallis, I. A. *Organometallics* **2007**, *26*, 4800–4809.

(51) Parameters used for the calculation of $\%V_{Bur}$ were as follows: 3.5 Å sphere radius, 2.10 Å distance from the center of the sphere, and Bondii radii scaled by 1.17. In addition to removing the coordinates of the ligands and the coordinated Ir from the cif file prior to the calculation of the $\%V_{Bur}$, we found it necessary to remove the coordinates of the Fe atom. See: Poater, A.; Cosenza, B.; Correa, A.; Giudice, S.; Ragone, F.; Scarano, V.; Cavallo, L. *Eur. J. Inorg. Chem.* **2009**, 1759-1766.

(52) Tennyson, A. G.; Rosen, E. L.; Collins, M. S.; Lynch, V. M.; Bielawski, C. W. *Inorg. Chem.* **2009**, *48,* 6924–6933.

(53) Tennyson, A. G.; Ono, R. J.; Hudnall, T. W.; Khramov, D. M.; Er, J. A. V.; Kamplain, J. W.; Lynch, V. M.; Sessler, J. L.; Bielawski, C. W. *Chem. Eur. J.* **2010**, *16*, 304–315.

(54) Tolman, C. A. *Chem. Rev.* **1977**, *77*, 313–348.

(55) TEP = $0.847[\nu_{CO}(\text{average})] + 336\ \text{cm}^{-1}$

(56) The rates of RCM reactions catalyzed by Grubbs 2nd generation type catalysts increase with the electron donating ability of the NHC ligand, see: Leuthäußer, S.; Schmidts, V.; Thiele, C. M.; Plenio, H. *Chem. Eur. J.* **2008**, *14*, 5465–5481. For a more recent study, see: Borguet, Y.; Zaragoza, G.; Demonceau, A.; Delaude, L. *Dalton Trans.* **2013**, *42*, 7287–7296. The effect of varying NHC backbone electronics on the performance of Grubbs 2nd generation type indenylidene

complexes has also been explored, see: Urbina-Blanco, C. A.; Bantreil, X.; Clavier, H.; Slawin, A. M.; Nolan, S. P. *Beilstein J. Org. Chem.* **2010**, *6*, 1120-1126.

(57) We also synthesized and fully characterized complexes of the type (**4.5**)(PCy_3)Cl_2Ru=CHPh and (**4.5**)(SIMes)Cl_2Ru=CHPh (SIMes = 1,3-dimesitylimidazolinylidene) but did not study these catalysts for their redox-switchable properties, see Appendix C.

(58) Conditions which favored the formation of exclusively one product could not be found. After extended reaction times (12 h) at ambient temperature, the final molar ratio of **4.17** to **4.18** was approximately 1:5.

(59) It has been previously reported that the purification of Ru benzylidene complexes using column chromatography on silica gel may cause rearrangements to occur, although the isomerization of **4.17** → **4.18** was observed prior to purification. See: S. Prühs, C. W. Lehmann and A. Fürstner, *Organometallics***,** 2004, **23***,* 280-287.

(60) Slugovc, C.; Perner, B.; Stelzer, F.; Mereiter, K. *Organometallics*, **2004**, *23,* 3622-3626.

(61) Ritter, T.; Hejl, A.; Wenzel, A. G.; Funk, T. W.; Grubbs, R. H. *Organometallics* **2006**, *25*, 5740–5745.

(62) (a) Jones, N. D.; Wolf, M. O. *Organometallics* **1997**, *16,* 1352–1354; (b) Thomas, K. R. J.; Lin, J. T.; Lin, H.-M.; Chang, C.-P.; Chuen, C.-H. *Organometallics* **2001**, *20,* 557–563; (c) Maishal, T. K.; Mondal, B.; Puranik, V. G.; Wadgaonkar, P. P.; Lahiri, G. K.; Sarkar, A. *J. Organomet. Chem.* **2005**, *690*, 1018–1027.

(63) Süßner, M.; Plenio, H. *Chem. Commun.* **2005**, 5417–5419.

(64) Pal, S. K.; Alagesan, K.; Samuelson, A. G.; Pebler, J. *J. Organomet. Chem.* **1999**, *575*, 108–118.

(65) (a) Miller, J. S.; Krusic, P. J.; Dixon, D. A.; Reif, W. M.; Zhang, J. H.; Anderson, E. C.; Epstein, A. J. *J. Am. Chem. Soc.* **1986**, *108*, 4459–4466; (b) Murphy, V. J.; O'Hare, D. *Inorg. Chem.* **1994**, *33*, 1833–1841; (c) Salman, H. M. A.; Mahmoud, M. R.; Abou-El-Wafa, M. H. M.; Rabie, U. M.; Crabtree, R. H. *Inorg. Chem. Commun.* **2004**, *7*, 1209–1212.

(66) The use of stronger oxidants such as silver salts, [NO][BF_4], and [Ac_2Fc][BF_4] were also explored, but resulted in premature decomposition.

(67) (a) Lever, A. B. P. *Inorganic Electronic Spectroscopy*, 2nd ed., Elsevier, Amsterdam, 1984; (b) Prins, R. *J. Chem. Soc., Chem. Commun.* **1970**, 280b–281.

(68) Although oxidation of the Ru and the Fe centers in **4.18** were reversible (as determined from a scan-rate dependency study; see original manuscript, the neutral complex was found to decompose in solution over time. As the extinction

coefficient for the ferrocenium LCMT transition is relatively low (ε < 1000), the oxidized complex **4.18**$^{+}$ could not be formed in high enough concentration to be observed due to the competing decomposition of the starting material over the 30 min time scale of the experiment.

(69) (a) Hartmann, S.; Winter, R. F.; Brunner, B. M.; Sarkar, B.; Knödler, A.; Hartenbach, I. *Eur. J. Inorg. Chem.* **2003**, 876–891; (b) Das, N.; Arif, A. M.; Stang, P. *Inorg. Chem.* **2005**, *44*, 5798–5804; (c) Kaim, W.; Sixt, T.; Weber, M.; Fiedler, J. *J. Organomet. Chem.* **2001**, *637*, 167–171; (d) Gray, H. B.; Sohn, Y. S.; Hendrickson, D. N. *J. Am. Chem. Soc.* **1971**, *93*, 3603–3612.

(70) (a) Elschenbrolch, C.; Bilger, E. *Organometallics* **1985**, *4,* 2068–2071; (b) Sixt, T.; Fiedler, J.; Kaim, W. *Inorg. Chem. Commun.* **2000**, *3*, 80–82.

(71) Winter, R. F.; Hornung, F. M. *Organometallics* **1999**, *18,* 4005–4014.

(72) Kojima, T.; Noguchi, D.; Nakayama, T.; Inagaki, Y.; Shiota, Y.; Yoshizawa, K.; Ohkubo, K.; Fukuzumi, S. *Inorg. Chem.* **2008**, *47*, 886–895.

(73) Noviandri, I.; Brown, K. N.; Fleming, D. S.; Gulyas, P. T.; Lay, P. A.; Masters, A. F.; Phillips, L. *J. Phys. Chem. B*, 1999, **103**, 6713–6722.

(74) Complex **4.18** displayed limited solubility in non-polar solvents, including toluene and benzene.

(75) It was determined that the use of four equivalents of DDQ was necessary to significantly affect the rate of polymerization, which may be attributed to slow electron-transfer kinetics under the conditions studied.

(76) (a) Herrmann, W. A.; Köcher, C. *Angew. Chem., Int. Ed.* **1997**, *36*, 2163–2187; (b) *N-Heterocyclic Carbenes in Transition Metal Catalysis*, ed. F. Glorius, Springer-Verlag, Berlin, Germany, 2007; (c) *N-Heterocyclic Carbenes in Synthesis*; ed. S. P. Nolan, Wiley-VCH: Weinheim, 2006.

(77) Sanford, M. S.; Love, J. A.; Grubbs, R. H. *Organometallics* 2001, *20*, 5314–5318.

(78) 1,1'-Diformamidoferrocene (**4.10**) has been previously prepared *in situ* and used without additional characterization; see: Leusen D.; Hessen, B. *Organometallics* **2001**, *20*, 224–226. The NMR data recorded for this compound are complex and similar to those reported for the monoformamide of ferrocene; see: Knox, G. R.; Pauson, P. L.; Willison, D. *Organometallics* **1990**, *9*, 301–306.

(79) Shafir, A.; Power, M. P.; Whitener, G. D.; Arnold, J. *Organometallics* **2000**, *19*, 3978–3982.

Chapter 5: Redox Switchable Ring-Closing Metathesis: Catalyst Design, Synthesis, and Study

Portions of this chapter were reprinted with permission from Arumugam, K.; Varnado, C. D., Jr.; Sproules, S.; Lynch, V. M.; Bielawski, C. W. *Chem. Eur. J.* **2013**, *19*, 10866. Copyright 2013 John Wiley and Sons. K. Arumugam carried out the synthesis and study of compounds **5.1**-**5.6**. S. Sproules conducted EPR and Mössbauer spectroscopy and wrote the sections of the aforementioned publication that describe the aforementioned experiments. K. Arumugam and C. W. Bielawski assisted with writing the aforementioned publication. I synthesized and studied compounds **5.9**-**5.13** and helped to write the aforementioned publication.

ABSTRACT

High yielding syntheses of 1-(ferrocenylmethyl)-3-mesitylimidazolium iodide (**5.1**) and 1-(ferrocenylmethyl)-3-mesitylimidazol-2-ylidene (**5.2**) were developed. Complexation of **5.2** to $[Ir(COD)Cl]_2$ (COD = 1,5-cyclooctadiene) or $(PCy_3)Cl_2Ru(=CH\text{-}o\text{-}O\text{-}i\text{-}PrC_6H_4)$ afforded **5.3** ((**5.2**)Ir(COD)Cl) and **5.5** ((**5.2**)$Cl_2Ru(=CH\text{-}o\text{-}O\text{-}i\text{-}PrC_6H_4)$), respectively. Complex **5.4** ((**5.2**)$IrCO_2Cl$) was obtained by bubbling carbon monoxide through a CH_2Cl_2 solution of **5.3**. Spectroelectrochemical IR analysis of **5.4** revealed that the oxidation of the ferrocene moiety in **5.2** significantly reduced the electron donating ability of **5.2** (ΔTEP = 9 cm^{-1}; TEP = Tolman electronic parameter). The oxidation of **5.5** with $[Fe(\eta^5\text{-}C_5H_4COMe)Cp][BF_4]$ as well as the subsequent reduction of [**5.5**]$[BF_4]$ with decamethylferrocene each proceeded in greater than 95% yield. Mössbauer, UV/vis and EPR spectroscopy analysis confirmed that [**5.5**]$[BF_4]$ contained a ferrocenium species, indicating that the iron center was selectively oxidized over the ruthenium center. Complexes **5.5** and [**5.5**]$[BF_4]$ were found to catalyze the ring closing metathesis (RCM)

of diethyl diallylmalonate with observed pseudo-first-order rate constants (k_{obs}) of 3.1 × 10^{-4} s^{-1} and 1.2 × 10^{-5} s^{-1}, respectively. Adding suitable oxidants or reductants over the course of a RCM reaction, **5.5** was switched between different states of catalytic activity. A second generation *N*-heterocyclic carbene that featured a 1′,2′,3′,4′,5′-pentamethylferrocenyl moiety (**5.10**) was also prepared and metal complexes containing this ligand were found to undergo iron centered oxidations at lower potentials than analogous complexes supported by **5.2** (0.30 – 0.36 V vs. 0.56 – 0.62 V, respectively). Redox switching experiments using (**5.10**)$Cl_2Ru(=CH\text{-}o\text{-}O\text{-}i\text{-}PrC_6H_4)$ revealed that greater than 94% of the initial catalytic activity was restored after an oxidation-reduction cycle.

INTRODUCTION

Redox switchable catalysis (RSC) is a growing field of study that utilizes redox active ligands to influence the catalytic activities displayed by coordinated metals.[1] In a typical reaction (Scheme 5.1), a redox switchable catalyst facilitates a given transformation (*e.g.*, A→B) at a given rate, k_1, when the ligand on the catalyst is in a neutral state. However, upon oxidation or reduction, the activity or selectivity of the catalyst may change (i.e., $k_1 \neq k_2$), or the catalyst may facilitate a new transformation altogether (*e.g.*, C→D). Such redox switchable events frequently utilize a metallocene to influence the ligand's electron donating ability and, as a result, the catalytic activity displayed by the metal complex.[2] For example, in a seminal report, Wrighton elegantly demonstrated that a diphenylphosphinocobaltocene ligated rhodium complex (**A**; see Figure 5.1) catalyzed the hydrogenation of cyclohexene faster than its oxidized cobaltocenium analogue; conversely, the oxidized complex was found to catalyze hydrosilylations faster than its neutral percursor.[3] Gibson and Long later reported a

ferrocenyl-substituted titanium-based ring-opening polymerization catalyst (**B**) that showed a significantly decreased activity toward *rac*-lactide upon oxidation.[4] More recently, Diaconescu demonstrated that redox switchable ferrocene-containing alkoxide (M = Y or Ce, R = ^{t}Bu) and aryloxide phosfen (M = In, R = Ph) complexes (**C**) may be used to control the ring opening polymerization of L-lactide and trimethylene carbonate, respectively.[5]

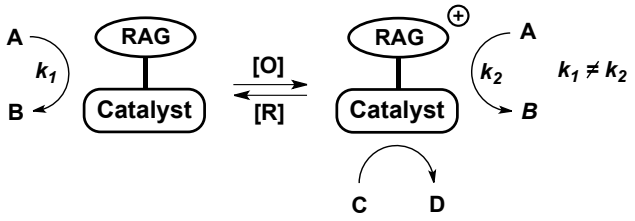

Scheme 5.1 General scheme for RSC. RAG = redox active group, [O] = oxidation, [R] = reduction, A and C = reactants, B and D = products and k_1, k_2 = rate constants.

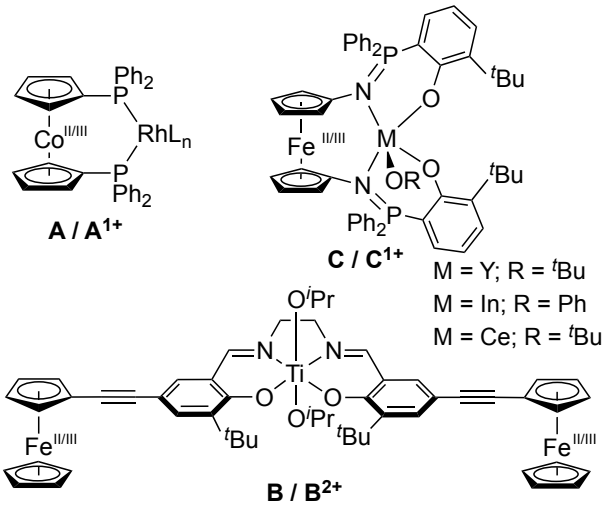

Figure 5.1 Representative examples of redox switchable catalysts.

Each of the aforementioned redox active ligands are multi-dentate, which contributes to the high stability of the corresponding complexes but also imposes restrictions on the types of catalysts that may be synthesized with redox switchable functionalities.[6] A general solution to this drawback may lie in the area of N-heterocyclic carbenes (NHCs), which are strongly coordinating, monodentate ligands[7] that have received widespread attention in broad range of applications,[8] particularly in organometallic catalysis.[9] Excellent examples of transformations that have benefitted from NHC-supported complexes include olefin metatheses,[10] hydrogenations,[11] and a sundry of coupling reactions.[12] An important subclass of NHCs are those which feature *N*-ferrocenyl groups, which are relatively straightforward to prepare, often display reversible electrochemistry, and coordinate to a wide range of transition metals.[13] Moreover, we and others have shown that the electron density at the metal centers ligated to *N*-ferrocenyl substituted NHCs directly correlated with the oxidation state of the ferrocene unit.[13w,13x] Since catalytic activity is often intimately tied to the electronic characteristics of ligated metals, RSC may provide new avenues for modulating the instrinsic chemo- and regioselectivities displayed by catalysts supported by redox-active NHCs. To explore the potential of ferrocene-containing NHCs in RSC, we describe herein a series of redox switchable olefin metathesis catalysts and demonstrate their utility in controlling ring-closing metathesis (RCM) reactions.[14]

RESULTS AND DISCUSSION

Our efforts began with the synthesis of a ferrocene containing NHC in conjunction with a detailed study of the electron donating ability of the ligand as a function of the oxidation state of the redox active group. To facilitate key electrochemical and spectroscopic measurements, a series of Ir based complexes that were supported by

the aforementioned NHC ligand were prepared and evaluated. Ultimately, the results from these studies helped to rationalize the activity displayed by a first generation redox switchable olefin metathesis catalyst and guided the development of second generation derivative which showed improved redox switchable functions.

Following a modified literature procedure,[15] *N*-mesityl imidazole was alkylated with (ferrocenylmethyl)-trimethylammonium iodide to afford **5.1** in 83% yield (Scheme 5.2). The salient spectroscopic characteristics (i.e., $C_{imidazolium}$–H, δ 9.48 ppm; DMSO–d_6) displayed by the isolated salt were consistent with the values reported for analogous compounds.[13h] Treatment of **5.1** with sodium hexamethyldisilazide (NaHMDS) in toluene afforded *N*-ferrocenylmethyl-*N′*-mesityl-imidazol-2-ylidene (**5.2**), as evidenced by the absence of the imidazolium ^{1}H NMR signal in conjunction with the appearance of a diagnostic ^{13}C NMR signal at 217.1 ppm (C_6D_6).[16] X-ray diffraction quality single crystals of **5.2** were grown from a saturated toluene solution at –35 °C.[17] The solid state structure of the free carbene (Figure 5.2) exhibited a longer average C1–N bond distance and a contracted N1–C1–N2 bond angle than its imidazolium precursor (see original manuscript). Moreover, the pendant *N*-ferrocenylmethyl group was oriented toward the carbenoid nucleus (C1–Fe1 = 4.298 Å) in **5.2** yet away in **5.1** (C1–Fe1 = 5.246 Å), presumably due to differential packing effects. As free NHCs are known to ligate to metallocenes,[18] the isolation and solid state elucidation of NHCs bearing *N*-ferrocenyl and *N*-ferrocenylmethyl groups is rare.[13x] Indeed, to the best of our knowledge, **5.2** is the first crystalline NHC bearing a pendant *N*-ferrocenyl group.

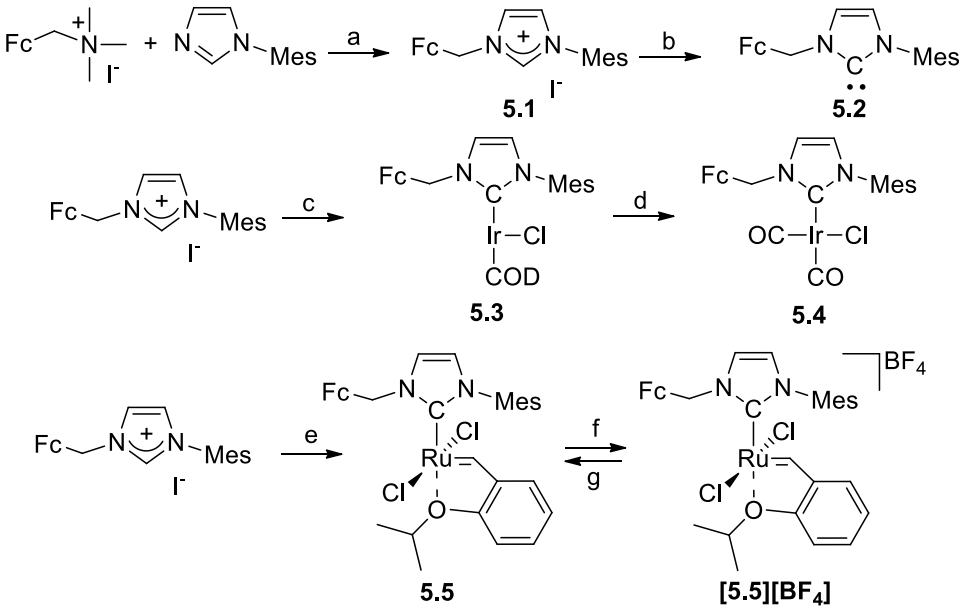

Scheme 5.2 Synthesis of **5.2** and various metal complexes (Fc = ferrocenyl, Mes = mesityl, COD = 1,5-cyclooctadiene): a.) CH_3CN, 80 °C, 24 h, 83% yield. b.) NaHMDS (1 equiv.), toluene, 25 °C, 1 h, 96% yield. c.) (i) NaHMDS (1 equiv.), toluene, 25 °C, 1 h; (ii) $[Ir(COD)Cl]_2$ (0.5 equiv.), 25 °C, 12 h, 85% yield. d.) CO (1 atm), CH_2Cl_2, 25 °C, 30 min, 93% yield e.) (i) NaHMDS (1 equiv.), toluene, 25 °C, 1 h; (ii) (PCy_3) Cl2Ru(═CH-o-O-i-PrC_6H_4) (0.9 equiv.), 25 °C, 12 h, 62% yield f.) (i) Fe(η5-C_5H_4COMe)Cp][BF_4] (1 equiv.), CH_2Cl_2, 25 °C, 2 h, 90% yield. g.) decamethylferrocene (1 equiv.), CH_2Cl_2, 25 °C, 1 h, 93% yield.

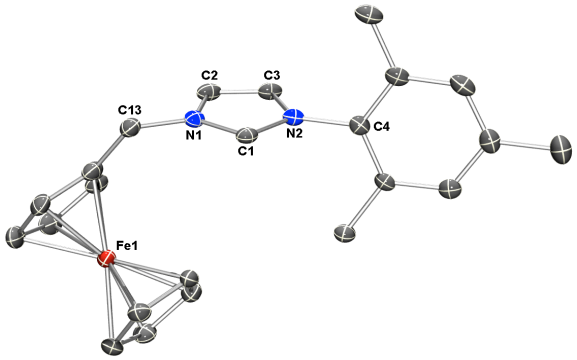

Figure 5.2 ORTEP diagram of **5.2** rendered using POV-Ray. Thermal ellipsoid plots were drawn at the 50% probability level. Hydrogen atoms and solvent molecules are omitted for clarity. Data are shown for one of two independent molecules in the asymmetric unit. Selected bond lengths (Å) and angles (°): C1–N1, 1.368(4); C1–N2, 1.369(4); C2–N1, 1.391(4); C3–N2, 1.393(4); C2–C3, 1.342(4), C4–N2, 1.443(4); C13–N1, 1.460(4); N1–C1–N2, 101.9(2); N1–C13–C14, 115.6(3).

The introduction of free NHC **5.2** (generated in situ) to 0.5 equiv. of $[Ir(COD)Cl]_2$ in toluene led to the formation of **5.3** (Scheme 5.2), which was subsequently isolated in 85% yield via filtration. Bubbling CO through a CH_2Cl_2 solution of **5.3** for 30 min followed by purification of the residue obtained upon evaporation using a series of n-pentane washes afforded **5.4** in 93% yield. X-ray quality crystals of **5.3** and **5.4** were grown by slow diffusion of n-pentane into a concentrated CH_2Cl_2 solution. As shown in Figures 5.3 and 5.4, the aforementioned Ir complexes adopted square planar coordination geometries as expected for d^8 metals in strong ligand field environments. The N1–C1–N2 bond angles and Ir1–C1 bond lengths measured in the solid state structures of **5.3** and **5.4** were in good agreement with data reported for analogous compounds.[13w,19]

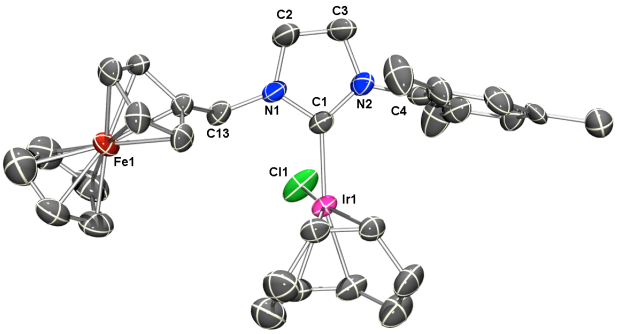

Figure 5.3 ORTEP diagram of **5.3** rendered using POV-Ray. Thermal ellipsoid plots were drawn at the 30% probability level. Hydrogen atoms are omitted for clarity. Selected bond lengths (Å) and angles (°): C1–N1, 1.363(11); C1–N2, 1.356(12); C2–N1, 1.382(13); C3–N2, 1.396(12); C2–C3, 1.354(15); C4–N2, 1.461(13); C13–N1, 1.441(12); C1–Ir1, 2.041(9); Cl1–Ir1, 2.358(3); N1–C1–N2, 103.9(8); N1–C13–C14, 112.2(8).

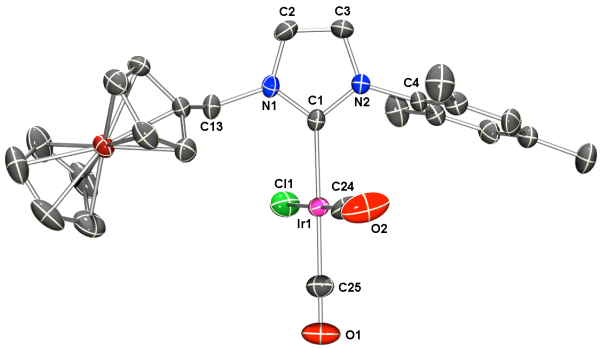

Figure 5.4 ORTEP diagram of **5.4** rendered using POV-Ray. Thermal ellipsoid plots were drawn at the 50% probability level. Hydrogen atoms are omitted for clarity. Selected bond lengths (Å) and angles (°): C1–N1, 1.350(5); C1–N2, 1.363(5); C2–N1, 1.372(5); C3–N2, 1.382(5); C2–C3, 1.336(6); C4–N2, 1.444(5); C13–N1, 1.483(5); C1–Ir1, 2.070(4); Cl1–Ir1, 2.3456(11); C24–Ir1, 1.821(5); C25–Ir1, 1.887(5); N1–C1–N2, 104.5(3); N1–C13–C14, 113.0(3).

Next, efforts were directed toward the synthesis of Ru-based complexes bearing **5.2**.[10g-i,20] Due to their high stability and high catalytic activities in RCM reactions,[21] efforts were directed toward the synthesis of a Hoveyda-Grubbs type[22] (HG-type)

analogue (i.e., **5.5**); an oxidized derivative ([**5.5**][BF_4]) was also prepared for comparative purposes. Treatment of **5.1** with NaHMDS in toluene followed by filtration and subsequent addition of 0.9 equiv. (PCy_3)Cl_2Ru(=CH-*o*-O-*i*-PrC_6H_4) to the filtrate lead to the formation of **5.5** (Scheme 5.2). The complex was isolated in 62% yield via precipitation from cold n-pentane (−35 °C) followed by filtration. Reflective of a more electron rich environment at the metal center due to the incorporation of the strongly donating NHC ligand,[22a] the diagnostic alkylidene signal (Ru=CH_α) displayed by (PCy_3)Cl_2Ru(=CH-*o*-O-*i*-PrC_6H_4) at 17.45 ppm shifted to 16.35 ppm in **5.5** (CD_2Cl_2). X-ray diffraction quality single crystals of **5.5** were grown by slow vapor diffusion of n-pentane into a saturated CH_2Cl_2 solution. As shown in Figure 5.5, the structure of the complex revealed a distorted square pyramidal geometry with the alkylidene unit oriented perpendicular to the C1–Ru1–Cl1–Cl2–O1 mean plane. The Cl1–Ru–Cl2 (151.42(6)°) and O1–Ru1–C1 (179.3(2)°) bond angles were in accord with data reported for other HG-type complexes.[22] Using a series of Nuclear Overhauser Enhancement Spectroscopy (NOESY) experiments, the solution state structure (CD_2Cl_2) of the complex was determined to be similar to the structure observed in the solid state (see original manuscript). Treatment of **5.5** with acetylferrocenium tetrafluoroborate ([Fe(η^5-C_5H_4COMe)Cp][BF_4]) in CH_2Cl_2 followed by the addition of Et_2O afforded a dark green precipitate (90% yield), which was subsequently identified as [**5.5**][BF_4] by elemental analysis, electron paramagnetic resonance (EPR) spectroscopy, and Mössbauer spectroscopy (see below). The complex [**5.5**][BF_4] was subsequently reduced to **5.5** in CH_2Cl_2 using decamethylferrocene (Fc*) and isolated in 95% yield, thus demonstrating that the two complexes were chemically interconvertable.

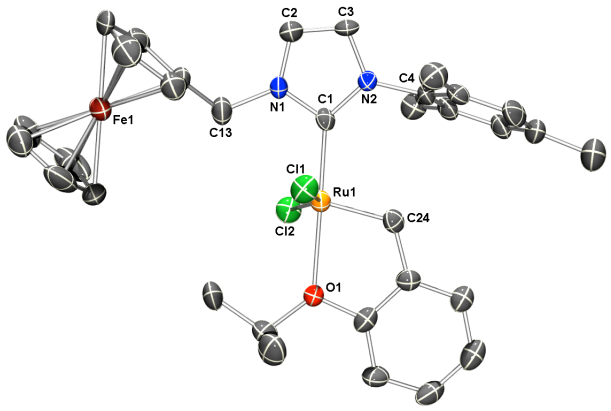

Figure 5.5 ORTEP diagram of **5.5** rendered using POV-Ray. Thermal ellipsoid plots were drawn at the 50% probability level. Hydrogen atoms are omitted for clarity. Selected bond lengths (Å) and angles (°): C1–N1, 1.353(7); C1–N2, 1.369(7); C2–N1, 1.382(7); C3–N2, 1.384(7); C2–C3, 1.333(8), C4–N2, 1.456(7); C13–N1, 1.482(7); Ru1–C1, 1.980(6); Ru1–C24, 1.822(6); Ru1–O1, 2.261(4); Ru1–Cl1, 2.3435(17); Ru1–Cl2, 2.3571(17); N1–C1–N2, 103.1(5); N1–C13–C14, 113.3(5); Cl1–Ru1–Cl2, 151.43(6); N2–C1–Ru1, 135.8(5).

To measure the electronic properties of the aforementioned compounds, a series of electrochemical measurements were conducted in CH_2Cl_2 with $[N(nBu_4)][PF_6]$ as the electrolyte; key data are summarized in Table 5.1 (see original manuscript for additional cyclic voltammograms (CVs) and the differential pulse voltammograms (DPVs)). Since the iodide counteranion in **5.1** was found to undergo oxidation along with the ferrocenyl substituent, the analogous hexafluorophosphate salt (**5.6**) was synthesized (via anion metathesis of **5.1** with $[CH_3CH_2)_3O][PF_6]$) and studied.[23] The CV of **5.6** revealed a single, reversible $Fe^{2+} \rightarrow Fe^{3+}$ oxidation process at 0.66 V (vs. saturated calomel electrode, SCE), which was comparable to the values reported in the literature for other *N*-

ferrocenylimidazolium salts.[13h] In contrast, complex **5.3** exhibited two oxidation processes at 0.56 V and 0.96 V (vs. SCE), which were attributed to the Fe^{2+}/Fe^{3+} and Ir^{1+}/Ir^{2+} redox couples, respectively. While one reversible Fe^{2+}/Fe^{3+} couple was measured at 0.59 V (vs. SCE) for **5.4**, the corresponding Ir^{1+}/Ir^{2+} couple was not observed within the solvent window, likely due to the electron withdrawing carbonyl groups present in the complex.

Table 5.1 Summary of the electrochemical data.[a]

Compound	$E_{1/2}$ (V)	$\Delta E_{1/2}$ (mV)
5.2	0.67 (qr)[b]	
5.3	0.56 (r), 0.96 (ir)	400
5.4	0.59 (r)	-
5.5	0.62 (r), 1.00 (r)	370
5.6	0.66 (r)	-

[a] Data obtained by CV and DPV in CH_2Cl_2 with 0.10 M [N(nBu4)][PF6] electrolyte and referenced vs. SCE. [b] In THF (decomposition of **5.2** was observed in CH_2Cl_2). r = reversible, ir = irreversible, qr = quasi-reversible.

Considering that the electron donating abilities of NHCs may be conveniently monitored by measuring the carbonyl stretching frequencies (υ_{CO}s) of NHC-supported $[Ir(CO)_2Cl]$ complexes, subsequent efforts were directed toward probing the change in electron density at the Ir center in **5.4** upon oxidation of the ferrocene containing ligand (i.e., **5.2**).[24] Compound **5.4** exhibited υ_{CO}s at 2064 cm^{-1} and 1980 cm^{-1}, which were intermediate of other NHC-supported $[Ir(CO)_2Cl]$ complexes (*trans*: 2055 – 2072 cm^{-1}, *cis*: 1971 – 1989 cm^{-1}) reported in the literature.[13w,19f,19g,25] The corresponding Tolman electronic parameter[26] (TEP) of **5.2** was calculated from the aforementioned υ_{CO}s using an equation developed by Crabtree[27] and later modified by Nolan[19g] (TEP = 0.847 × υ_{av} +

336 cm^{-1}) to be similar (2050.3 cm^{-1}) to the TEPs reported for 1,3-diadamantylimidazolylidene (2049 cm^{-1}) and 1,3-di(*tert*-butyl)-imidazolylidene (2050.1 cm^{-1}).[19g] Upon the bulk oxidation of **5.4** at 0.75 V (vs. SCE), an increase in the υ_{CO}s was observed (Figure 5.6) which resulted in a significant increase in the calculated TEP (2058 cm^{-1}). As a point of reference, the TEP measured for oxidized **5.2** (i.e., **5.2**$^{+}$) was greater than the analogous value calculated for tricyclohexylphosphine (2056.4 cm^{-1}).[19g] Regardless, the result suggested to us that **5.2** may be switched between two different states of ligand donating ability by changing the oxidation state of the ferrocene unit.

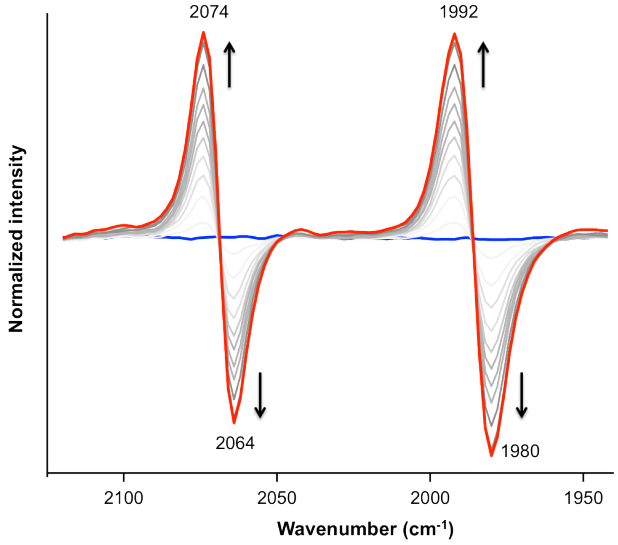

Figure 5.6 Normalized IR difference spectra showing the shift in the υ_{CO}s upon oxidation (E_{app} = +0.75 V) of **5.4** ([**5.4**]$_0$ = 1 mM) in CH_2Cl_2 with 0.1 M [N(*n*Bu$_4$)][PF$_6$] as the supporting electrolyte.

Building on the aforementioned results, the electrochemistry of the HG-type complex **5.5** was probed and found to exhibit two reversible oxidation processes at 0.62 V and 1.01 V (vs. SCE, Figure 5.7). The first oxidation was assigned to the Fe^{2+}/Fe^{3+}

couple while the second oxidation was attributed to a Ru^{2+}/Ru^{3+} oxidation process (vide infra). To gain additional insight into the electronic structure of **5.5**$^{+}$, controlled-potential coulometry at 0.75 V (vs. SCE) with concomitant UV-visible absorption spectroscopy was performed. As shown in Figure 5.8, new absorption maxima near 239 nm and ~600 nm were observed for the first oxidation process. The band at ~600 nm has been previously ascribed to the formation of a ferrocenium (Fc^{+}) species.[28] After the formation of **5.5**$^{+}$ from **5.5** was complete, controlled-potential coulometry was performed at 1.2 V (vs. SCE) to generate **5.5**$^{2+}$. A new band at 426 nm ($\varepsilon = 1.03 \times 10^{4}$ M^{-1} cm^{-1}), consistent with the oxidation of $Ru^{2+} \rightarrow Ru^{3+}$, was observed.[29]

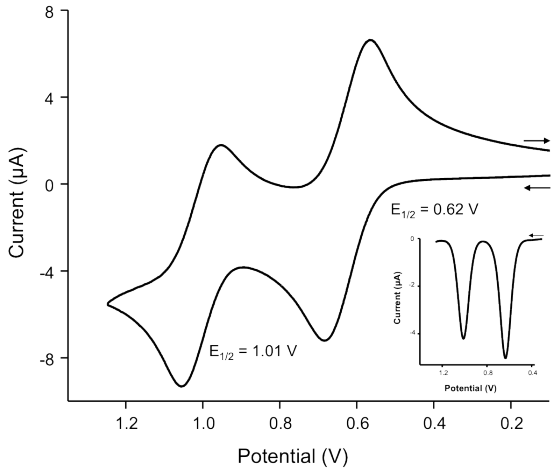

Figure 5.7 Cyclic voltammogram of **5.5** in CH_2Cl_2 with 1 mM of analyte and 0.1 M $[N(nBu_4)][PF_6]$, scan rate 100 mV s^{-1}. Inset: the differential pulse voltammogram of **5.5** under identical conditions (50 mV pulse amplitude).

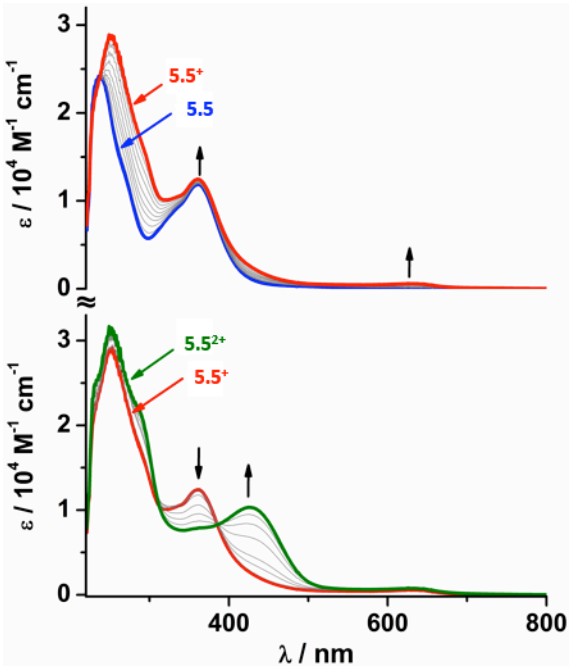

Figure 5.8 Electronic absorption spectra recorded during the bulk oxidation of **5** → **5**$^{1+}$ (top) (E_{app} = +0.75 V) and **5.5**$^{1+}$ → **5.5**$^{2+}$ (bottom) (E_{app} = +1.2 V) in CH_2Cl_2 with 0.1 M [N(*n*Bu)$_4$][PF$_6$] as the supporting electrolyte at –25 °C.

To support the electrochemical and spectroelectrochemical UV-vis assignments, a series of electron paramagnetic resonance (EPR) and Mössbauer spectroscopy experiments were performed. After oxidizing **5.5** with acetylferrocenium tetrafluoroborate ([Fe(η^5-C$_5$H$_4$COMe)Cp][BF$_4$]), the EPR spectrum of the corresponding product [**5.5**][BF$_4$] was recorded in a dichloromethane/toluene glass at 5 K. As shown in Figure 5.9, the EPR spectrum revealed a sharp feature at $g_{\parallel}$ = 4.24, a result consistent with the presence of a ferrocenium species.[28b,30] Moreover, the broadening of the $g_{\perp}$ feature was successfully modelled by including a large *g*-strain value (σ = 0.42) in the simulation which accounted for the microheterogeneity in the frozen glass. The line broadening was believed to arise from the bulky pendent arm of the Fc$^+$ group, which challenged the ability to observe the $g_{\perp}$ in the EPR spectrum of **5.5**$^+$ (Figure 5.9). However, the formation

of the ferrocenium species was supported by the large g-anisotropy ($\Delta g = g_{\parallel} - g_{\perp} = 2.95$), which stems from unquenched orbital angular momentum within the degenerate $^2E_{2g}$ ground state. Since this g-anisotropy cannot be generated by a Ru^{3+} d^5 ion ($S = {}^1/_2$) in this ligand field nor to a quartet ($S = {}^3/_2$) ground state, the signals were unambiguously assigned to a ferrocenium species.

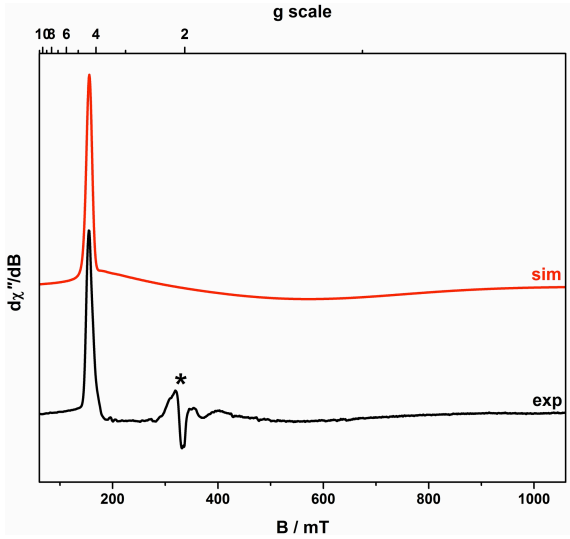

Figure 5.9 X-band EPR spectrum of **5.5**$^+$ (black line) in a CH_2Cl_2/toluene solution at 5 K and corresponding simulation (red line). Experimental conditions: frequency, 9.4361 GHz; power, 0.63 mW; modulation, 3.0 mT. Simulation parameters: g = 4.24, 1.29, 1.29; W = 110, 500, 500 × 10^{-4} cm^{-1}; g-strain, σ_x = 0.42. The asterisk denotes a Ru^{3+} impurity that accounted for <1% of the total signal intensity.

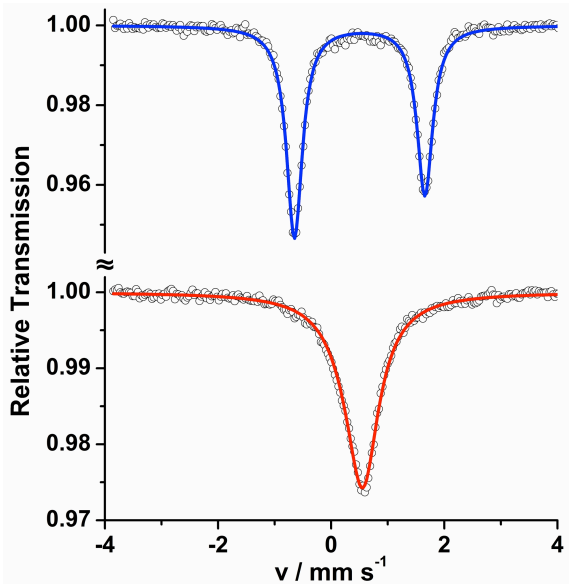

Figure 5.10 Zero-field Mössbauer spectra of **5.5** (blue, top) and [**5.5**][BF_4] (red, bottom) recorded using solid samples at 80 K. The open circles reflect the experimental data; the solid lines are the corresponding spectral fits.

To further support the notion that the ferrocene unit in **5.5** underwent oxidation upon the addition of [Fe(η^5-C_5H_4COMe)Cp][BF_4], **5.5** and [**5.5**][BF_4] were independently analyzed using Mössbauer spectroscopy. As shown in Figure 5.10,[31] complex **5.5** was characterized by an isomer shift at δ = 0.50 mm s^{-1} and a large quadrupole splitting at ΔE_Q = 2.31 mm s^{-1}, which were consistent with the low-spin Fe^{2+} d^6 center of ferrocene. The oxidized product **5.5**$^+$ exhibited the same isomer shift but the quadrupole splitting collapsed to ΔE_Q = 0.13 mm s^{-1}, a value characteristic of a ferrocenium species.[31] Collectively, the electronic absorption, EPR, and Mössbauer spectra unambiguously showed that the first oxidation process was ferrocene-based.

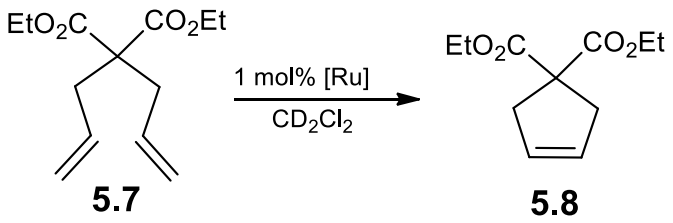

Having evaluated the ligand donating ability of **5.2** as a function of its oxidation state, efforts were directed toward exploring the utility of the latter in RSC. Using a modified literature procedure,[32] the ring closing metathesis (RCM) of diethyl diallylmalonate (**5.7**) ($[\mathbf{5.7}]_0$ = 0.1 M), eq. 1) to its respective cyclic product (**5.8**) was monitored by ^{1}H NMR spectroscopy at 30 °C in CD_2Cl_2 using 1 mol% **5.5** or [**5.5**][BF_4] as the catalyst. As shown in Figure 5.11, an 80% conversion of starting material to product was observed within 1 h when **5.5** was employed as the catalyst and the corresponding pseudo-first-order rate constant (k_{obs}) was calculated to be 3.1×10^{-4} s^{-1}. In contrast, the analogous reaction involving [**5.5**][BF_4] was measured to be significantly slower ($k_{obs} = 1.2 \times 10^{-5}$ s^{-1}) and the catalyst converted only 7% of **5.7** to **5.8** after 1 h. We hypothesized that the oxidation of the ferrocene moiety ($Fe^{2+} \rightarrow Fe^{3+}$) in complex **5.5** reduced the electron density at the ligated metal center and attenuated the catalytic activity accordingly.[10i]

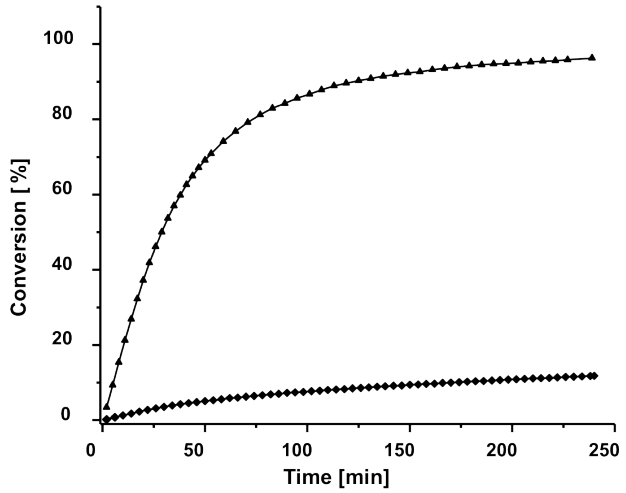

Figure 5.11 Plots of the percent conversion of **5.7** to **5.8** vs. time as catalyzed by 1 mol% of **5.5** (triangles) or [**5.5**][BF_4] (diamonds). Conditions: [**5.7**]$_0$ = 0.1 M, CD_2Cl_2, 30 °C.

Building on the observation that **5.5** and [**5.5**][BF_4] catalyzed the RCM of **5.7** with different rate constants, subsequent efforts were directed toward modulating the activity of the catalyst over the course of a reaction. Following the addition of **5.5** (1 mol %) to a CD_2Cl_2 solution of **5.7** ([**5.7**]$_0$ = 0.1 M), the resulting mixture was monitored at 30 °C by ^{1}H NMR spectroscopy (see Figure 5.12). After 10 min (~16% conversion of **5.7** to **5.8**; k_{obs} = 3.0 × 10^{-4} s^{-1}), 1.0 equiv. (with respect to **5.5**) of a chemical oxidant, [Fe(η^5-$C_5H_4COCH_3$)Cp][BF_4], was added to the reaction mixture. The addition resulted in the solution changing color from yellow to brown and was accompanied by a significant decrease in catalytic activity (k_{obs} = 0.98 × 10^{-5} s^{-1}), consistent with the in situ conversion of **5.5** → **5.5**$^+$. Subsequent addition of 1.1 equiv. (with respect to **5.5**) of a chemical reductant, decamethylferrocene (Fc*), to the mixture restored the initial yellow color and the relatively high catalytic activity (k_{obs} = 3.8 × 10^{-5} s^{-1}). As shown in Figure 5.12 (bottom), the aforementioned switching cycle was successfully repeated multiple times over the course of a single reaction.[33, 34]

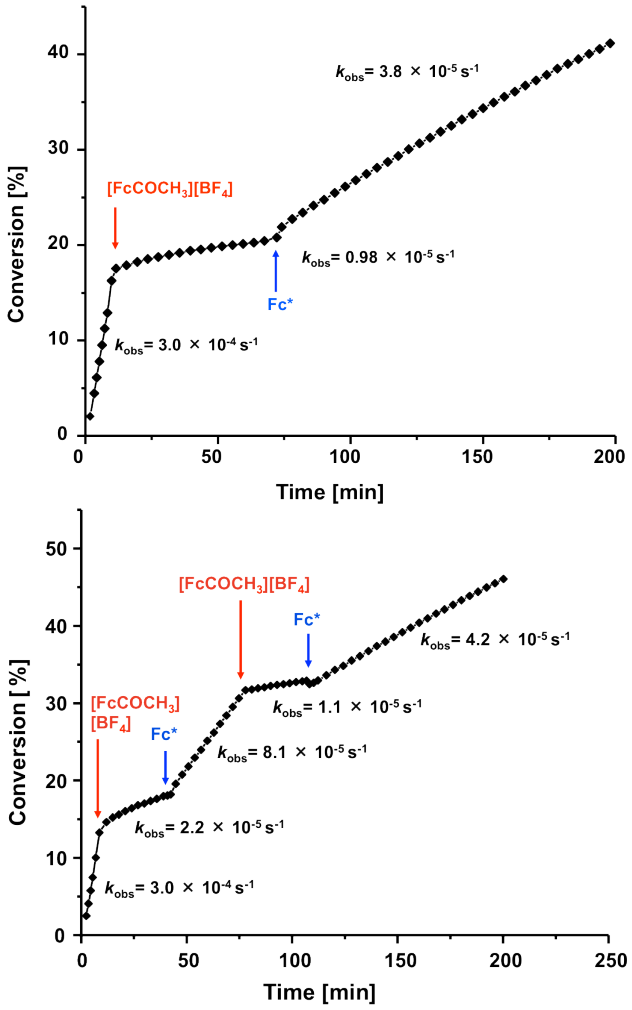

Figure 5.12 Plots of the percent conversion of **5.7** to **5.8** vs. time as catalyzed by 1 mol% of **5.5**; conditions: $[\mathbf{5.7}]_0 = 0.1$ M, CD_2Cl_2, 30 °C. The arrows indicate the time at which one equivalent of said reagent with respect to **5.5** was added. The corresponding rate constants over the given periods of time are indicated.

Close inspection of the redox switching data summarized in Figure 5.12 revealed that only ~13 % of the initial activity of the catalyst, as determined by the respective rate constants, was successfully restored.[35] Considering that the oxidation potentials of the iron and ruthenium centers in **5.5** differed by only 380 mV, we attributed the attenuated activity to partial ruthenium oxidation, which led to premature catalyst decomposition.

To develop a more robust catalyst, efforts were directed towards incorporating a 1′,2′,3′,4′,5′-pentamethylferrocene (Me_5Fc) moiety into an NHC scaffold, which was expected[36] to undergo oxidation at ca. 300 mV lower potential than the parent ferrocene analogue.

As summarized in Scheme 5.3, treatment of 1′,2′,3′,4′,5′-pentamethylferrocenylmethanol[37] with HBF_4 in the presence of mesitylimidazole led to formation of the imidazolium salt **5.9** as a crystalline product.[13v,36] In order to evaluate and compare electron donating ability of the corresponding NHC (i.e., **5.10**) to **5.2**, the iridium complex **5.11** was prepared in a similar manner to that described for the synthesis of **5.3** and subjected to electrochemical analysis.

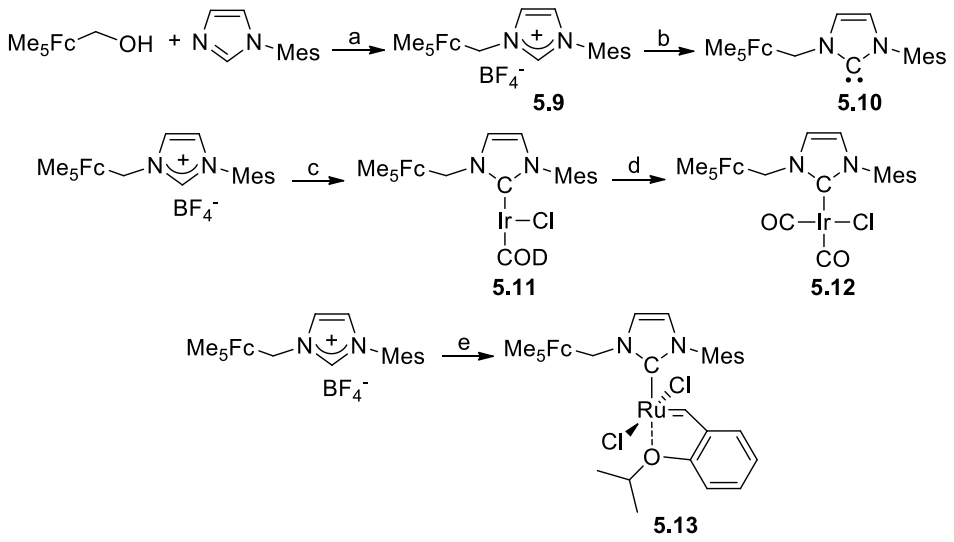

Scheme 5.3 Synthesis of **5.10** and various metal complexes (Me_5Fc = 1′,2′,3′,4′,5′-pentamethylferrocene, Mes = mesityl, COD = 1,5-cyclooctadiene). a) (i) HBF_4, CH_2Cl_2, 1 min; (ii) N-mesitylimidazole, 12 h, 41% yield. b.) NaHMDS (1 equiv.), benzene, 1 h. c.) (i) NaHMDS (1 equiv.), benzene, 25 °C, 15 min; (ii) $[Ir(COD)Cl]_2$ (0.5 equiv.), 25 °C, 12 h, 79% yield. d.) CO (1 atm), CH_2Cl_2, 25 °C, 2 h, 82% yield. e.) (i) 1 equiv. NaHMDS, toluene, 25 °C, 30 min; (ii) 0.5 equiv. $(PCy_3)Cl_2Ru(=CH\text{-}o\text{-}O\text{-}i\text{-}PrC_6H_4)$, 25 °C, 3 h; (iii) 2 equiv. S_8, 12 h, 48% yield.

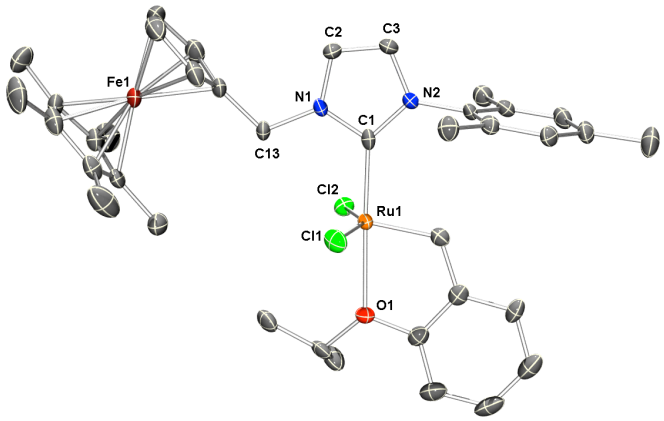

Figure 5.13 ORTEP diagram of **5.13** rendered using POV-Ray. Thermal ellipsoid plots were drawn at the 50% probability level. Hydrogen atoms are omitted for clarity. Selected bond lengths (Å) and angles (°): C1–N1, 1.364(4); C1–N2, 1.368(4); C2–N1, 1.382(4); C3–N2, 1.393(4); C2–C3, 1.340(5), C4–N2, 1.443(4); C13–N1, 1.479(4); Ru1–C1, 1.988(4); Ru1–C29, 1.822(4); Ru1–O1, 2.277(2); Ru1–Cl1, 2.3432(12); Ru1–Cl2, 2.3287(11); N1–C1–N2, 103.8(3); N1–C13–C14, 111.6(3); Cl1–Ru1–Cl2, 149.82(4); N2–C1–Ru1, 134.7(3).

Cyclic voltammetry of **5.11** (Figure D.3) in CH_2Cl_2 in the presence of $[N(nBu_4)][PF_6]$ as the electrolyte revealed that the iron-centered oxidation process occurred at 0.30 V (vs. SCE), which corresponded to a 260 mV cathodic shift as compared to the analogous oxidation process exhibited by **5.3**. However, the iridium oxidation processes displayed by **5.3** and **5.11** were found to occur at similar potentials (cf., 0.96 vs. 0.97 V, respectively) which suggested to us that even though the Me_5Fc containing ligand (**5.10**) underwent oxidation at a lower overall potential than its Fc parent (**5.2**), there was minimal difference in the donating ability of the two ligands.

To further characterize the steric and electronic properties of **5.10**, the (NHC)$IrCO_2Cl$ derivative **5.12** was prepared by stirring a solution of **5.11** under an atmosphere of CO (g) and isolated by precipitation. X-ray diffraction analysis of single crystals grown by the slow diffusion of n-pentane into a saturated chloroform solution of

5.12 were in accord with the recorded spectroscopic data and confirmed the identity of this complex (Figure D.2). As expected, **5.12** exhibited a square planar geometry with bond lengths and bond angles comparable to those measured in the solid state structure of **5.4**. Likewise, the percent buried volumes, a measure of steric bulk, displaced by ligands **5.2** and **5.10** were calculated to be similar (29.4% vs. 31.5%, respectively) using Cavallo's method.[38]

Table 5.2 Summary of electrochemical data.[a]

Compound	$E_{1/2}$ (V)	$\Delta E_{1/2}$ (mV)
5.11	0.30 (r) , 0.97 (ir)	670
5.12	0.34 (r)	-
5.13	0.36 (r), 1.02 (r)	660

[a] Data obtained by CV and DPV in CH_2Cl_2 with 0.10 M $[N(nBu_4)][PF_6]$ electrolyte and referenced vs. SCE. R = reversible, ir = irreversible.

With complex **5.12** in hand, the electron donating ability of **5.10** was measured and compared to that of **5.2**. The υ_{CO}s displayed by **5.12** were recorded at 2064 and 1979 cm^{-1}, and were nearly identical to those measured for **5.4**. Likewise, the TEP value of **5.10** (2048 cm^{-1}) was calculated to be similar to that of **5.2** (2049 cm^{-1}). The CV of **5.12** (Figure D.4) revealed that the first oxidation process occurred at 340 mV (vs SCE) which was 250 mV cathodically shifted when compared to the analogous process displayed by **5.4**. Even though the ligand oxidation occurred at lower potential, the resulting TEP difference between **5.12** and **5.12**$^+$ was nearly identical to that measured between **5.2** and **5.2**$^+$ (cf., 8 vs. 9 cm^{-1}, respectively), as determined by a spectroelectrochemical experiment (Figure D.6).

To test the performance of **5.10** in RSC, Ru complex **5.13** was prepared in an analogous manner to **5.5**. Unfortunately, treating **5.10** with $(PCy_3)Cl_2Ru(=CH\text{-}o\text{-}O\text{-}i\text{-}PrC_6H_4)$ yielded a mixture of products, one of which was a complex in which the phosphine ligand was coordinated to the Ru center yet the isopropyloxy group was dissociated, as evidenced by diagnostic ^{1}H NMR (a doublet at 20.95 ppm and a singlet at 16.68 ppm) and ^{31}P NMR (23.5 ppm and 10.9 ppm) signals. To maximize the yield of **5.13**, the aforementioned reaction mixture was stirred with 2 equiv. of elemental sulfur, an effective phosphine scavenger,[39] followed by silica column chromatography under an inert atmosphere which afforded the desired complex as a yellow solid in 48% isolated yield. X-ray quality crystals of **5.13** were obtained as red needles by vapor diffusion of pentane into a saturated benzene solution. The solid state structure of **5.13** exhibited a distorted square pyramidal geometry with bond lengths and angles similar to those measured for the analogous solid state structure of **5.5** (Figure 5.13).

The CV of **5.13** (Figure D.5) revealed an iron-centered oxidation at 0.36 V, a 260 mV cathodic shift when compared to the analogous oxidation process displayed by **5.5**. Consequently, the redox window measured between the Fe and Ru-centered oxidation processes exhibited by **5.13** was broadened to 660 mV, as opposed to the 380 mV window displayed by **5.5**. The wider electrochemical window facilitated the use of a weaker oxidant (i.e., $[Fc][BF_4]$; $E_{1/2} = 0.475$ V in CH_2Cl_2 vs. SCE)[40] to oxidize **5.13**.

A ring-closing reaction was initiated by adding **5.13** (1 mol%) to a CD_2Cl_2 solution of **5.7** ($[\mathbf{7}]_0 = 0.1$ M) and monitored at 30 °C by ^{1}H NMR spectroscopy. As shown in Figure 5.14, the neutral complex catalyzed the reaction with a rate constant (k_{obs}) of 4.5×10^{-5} s^{-1}. However, upon oxidation with $[Fc][BF_4]$, the rate constant was reduced to 0.86×10^{-5} s^{-1}. While the aforementioned rate constants were similar to those measured for **5.5** and **5.5**$^+$ respectively, the subsequent addition of decamethylferrocene

to the in situ generated **13**$^+$ restored greater than 94% of the catalytic activity displayed by its neutral precursor (k_{obs} = 4.25 × 10^{-5} s^{-1}).

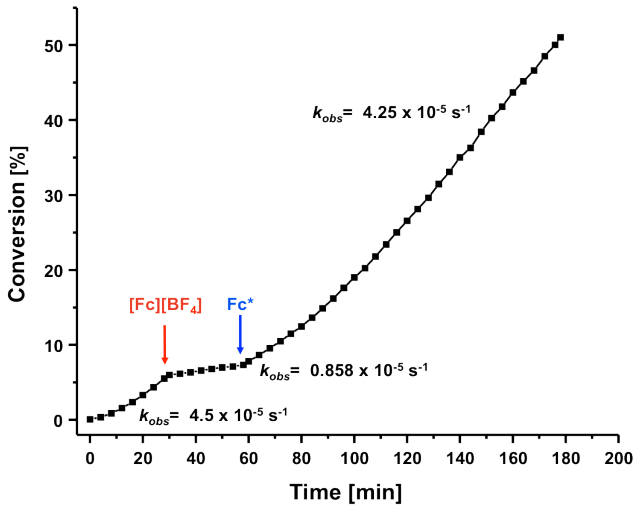

Figure 5.14 Plots of the percent conversion of **5.7** to **5.8** vs. time as catalyzed by 1 mol% of **5.13**, conditions: [**5.7**]$_0$ = 0.1 M, CD_2Cl_2, 30 °C. The arrows indicate the time at which one equivalent of said reagent with respect to **5.13** was added. The corresponding rate constants over the given periods of time are indicated.

CONCLUSION

In sum, we have developed straightforward syntheses of NHCs that feature redox active N-ferrocenyl substituents and ligated these compounds to a series of iridium and catalytically active ruthenium complexes. By measuring the υ_{CO}s of (**5.2**)Ir(CO)$_2$Cl, the ligand donating ability of **5.2** was found to decrease (ΔTEP = 9 cm^{-1}) upon selective oxidation of the ferrocene moiety. Electrochemical analysis of **5.5** (i.e., (**5.2**)Cl_2Ru(=CH-*o*-O-*i*-PrC_6H_4)) revealed two successive one-electron oxidations, corresponding to Fe^{2+} → Fe^{3+} followed by Ru^{2+} → Ru^{3+}, respectively, as confirmed using a series of electrochemical, spectroelectrochemical UV-vis absorption Mössbauer and EPR experiments. Complexes **5.5** and [**5.5**][BF_4] were found to catalyze the ring-closing

metathesis of diethyl diallylmalonate (**5.7**) at 30 °C, but at significantly different rates. Moreover, while the RCM reaction catalyzed by **5.5** was successfully attenuated through the addition of a chemical oxidant, the catalytic activity was only partial restored (~13%) upon subsequent chemical reduction, presumably due to premature catalyst decomposition. Regardless, these results corroborated the hypothesis that the oxidation of the ligand in **5.5** afforded a complex with diminished electron density at the metal center and therefore reduced catalytic activity. To increase the robustness of the catalyst and improve its redox switchable functions, an NHC bearing a 1′,2′,3′,4′,5′-pentamethylferrocene substituent was prepared (**5.10**). Complexes supported by **5.10** were found to oxidize at potentials that were at least 250 mV lower than the analogues that contained the parent ferrocene moieties. Moreover, greater than 94% of the initial RCM activity displayed by a Ru-based olefin metathesis catalyst supported by **5.10** was restored after a full redox switching cycle. To the best of our knowledge, these are the first homogeneous redox switchable NHC-supported Ru catalysts that have been used to control RCM reactions. More broadly, the results presented herein are expected to guide the development of other olefin metathesis and other NHC supported catalysts whose intrinsic chemo- and regioselectivities are determined by the oxidation state of the redox switchable ligand.

REFERENCES

(1) Allgeier, A. M.; Mirkin, C. A. *Angew. Chem. Int. Ed.* **1998**, *37*, 894.

(2) Lorkovic, I. M.; Wrighton, M. S.; Davis, W. M. *J. Am. Chem. Soc.* **1994**, *116*, 6220.

(3) Lorkovic, I. M.; Duff, R. R.; Wrighton, M. S. *J. Am. Chem. Soc.* **1995**, *117*, 3617.

(4) Gregson, C. K. A.; Gibson, V. C.; Long, N. J.; Marshall, E. L.; Oxford, P. J.; White, A. J. P. *J. Am. Chem. Soc.* **2006**, *128*, 7410.

(5) (a) Broderick, E. M.; Guo, N.; Vogel, C. S.; Xu, C.; Sutter, J. r.; Miller, J. T.; Meyer, K.; Mehrkhodavandi, P.; Diaconescu, P. L. *J. Am. Chem. Soc.* **2011**, *133*, 9278; (b) Broderick, E. M.; Guo, N.; Wu, T.; Vogel, C. S.; Xu, C.; Sutter, J.; Miller, J. T.; Meyer, K.; Cantat, T.; Diaconescu, P. L. *Chem. Commun.* **2011**, *47*, 9897.

(6) The coupling activities displayed by 1,4-naphthoquinone annulated N-heterocyclic carbene supported Group 10 metal complexes may be controlled by varying the oxidation state of the NHC ligand; see: Tennyson, A. G.; Lynch, V. M.; Bielawski, C. W. *J. Am. Chem. Soc.* **2010**, *132*, 9420.

(7) (a) Martin, D.; Melaimi, M.; Soleilhavoup, M.; Bertrand, G. *Organometallics* **2011**, *30*, 5304; (b) Tonner, R.; Heydenrych, G.; Frenking, G. *Chemistry – An Asian Journal* **2007**, *2*, 1555.

(8) (a) Arnold, P. L.; Casely, I. J. *Chem. Rev.* **2009**, *109*, 3599; (b) Back, O.; Donnadieu, B.; Parameswaran, P.; Frenking, G.; Bertrand, G. *Nat Chem*, *2*, 369; (c) Boydston, A. J.; Williams, K. A.; Bielawski, C. W. *J. Am. Chem. Soc.* **2005**, *127*, 12496; (d) Chi, Y.; Chou, P.-T. *Chem. Soc. Rev.* **2010**, *39*, 638; (e) Coady, D. J.; Khramov, D. M.; Norris, B. C.; Tennyson, A. G.; Bielawski, C. W. *Angew. Chem. Int. Ed.* **2009**, *48*, 5187; (f) Hahn, F. E.; Jahnke, M. C. *Angew. Chem. Int. Ed.* **2008**, *47*, 3122; (g) Lin, J. C. Y.; Huang, R. T. W.; Lee, C. S.; Bhattacharyya, A.; Hwang, W. S.; Lin, I. J. B. *Chem. Rev.* **2009**, *109*, 3561; (h) Masuda, J. D.; Schoeller, W. W.; Donnadieu, B.; Bertrand, G. *J. Am. Chem. Soc.* **2007**, *129*, 14180; (i) Norris, B. C.; Bielawski, C. W. *Macromolecules* **2010**, *43*, 3591; (j) Scheschkewitz, D. *Angew. Chem. Int. Ed.* **2008**, *47*, 1995; (k) Wolf, R.; Uhl, W. *Angew. Chem. Int. Ed.* **2009**, *48*, 6774.

(9) a) Díez-Gonzalez, S.; Marion, N.; Nolan, S. P. *Chem. Rev.* **2009**, *109*, 3612; (b) Enders, D.; Niemeier, O.; Henseler, A. *Chem. Rev.* **2007**, *107*, 5606; (c) Glorius, F. In *N-Heterocyclic Carbenes in Transition Metal Catalysis*; Springer Berlin / Heidelberg: 2007; Vol. 21, p 1; (d) He, M.; Bode, J. W. *J. Am. Chem. Soc.* **2007**, *130*, 418; (e) Kamber, N. E.; Jeong, W.; Waymouth, R. M.; Pratt, R. C.; Lohmeijer, B. G. G.; Hedrick, J. L. *Chem. Rev.* **2007**, *107*, 5813; (f) Phillips, E. M.; Wadamoto, M.; Chan, A.; Scheidt, K. A. *Angew. Chem. Int. Ed.* **2007**, *46*, 3107; (g) Read de Alaniz, J.; Rovis, T. *J. Am. Chem. Soc.* **2005**, *127*, 6284; (h) Sommer, W. J.; Weck, M. *Coord. Chem. Rev.* **2007**, *251*, 860.

(10) (a) Bieniek, M.; Samojłowicz, C.; Sashuk, V.; Bujok, R.; Śledź, P.; Lugan, N. l.; Lavigne, G.; Arlt, D.; Grela, K. *Organometallics* **2011**, *30*, 4144; (b) Fernández, I.; Lugan, N.; Lavigne, G. *Organometallics* **2012**, *31*, 1155; (c) Fürstner, A. *Angew. Chem. Int. Ed.* **2000**, *39*, 3012; (d) Grubbs, R. H.; Trnka, T. M. *Ruthenium-Catalyzed Olefin Metathesis*; Wiley VCH, Weinheim, Germany, 2005; (e) Jafarpour, L.; Nolan, S. P. *J. Organomet. Chem.* **2001**, *617-618*, 17; (f) Weskamp, T.; Schattenmann, W. C.; Spiegler, M.; Herrmann, W. A. *Angew. Chem. Int. Ed.* **1998**, *37*, 2490; (g) Huang, J.; Stevens, E. D.; Nolan, S. P.;

Petersen, J. L. *J. Am. Chem. Soc.* **1999**, *121*, 2674; (h) Scholl, M.; Ding, S.; Lee, C. W.; Grubbs, R. H. *Org. Lett.* **1999**, *1*, 953; (i) Trnka, T. M.; Grubbs, R. H. *Acc. Chem. Res.* **2000**, *34*, 18.

(11) (11) (a) Hillier, A. C.; Lee, H. M.; Stevens, E. D.; Nolan, S. P. *Organometallics* **2001**, *20*, 4246; (b) Lee, H. M.; Jiang, T.; Stevens, E. D.; Nolan, S. P. *Organometallics* **2001**, *20*, 1255; (c) Vazquez-Serrano, L. D.; Owens, B. T.; Buriak, J. M. *Chem. Commun.* **2002**, 2518; (d) Vazquez-Serrano, L. D.; Owens, B. T.; Buriak, J. M. *Inorg. Chim. Acta* **2006**, *359*, 2786; (e) Dobereiner, G. E.; Nova, A.; Schley, N. D.; Hazari, N.; Miller, S. J.; Eisenstein, O.; Crabtree, R. H. *J. Am. Chem. Soc.* **2011**, *133*, 7547.

(12) (a) Tennyson, A. G.; Lynch, V. M.; Bielawski, C. W. *J. Am. Chem. Soc.* **2010**, *132*, 9420; (b) Correa, A.; Marion, N.; Fensterbank, L.; Malacria, M.; Nolan, S. P.; Cavallo, L. *Angew. Chem. Int. Ed.* **2008**, *47*, 718; (c) Fructos, M. R.; Belderrain, T. R.; de Frémont, P.; Scott, N. M.; Nolan, S. P.; Díaz-Requejo, M. M.; Pérez, P. J. *Angew. Chem. Int. Ed.* **2005**, *44*, 5284; (d) Gimeno, A.; Medio-Simon, M.; de Arellano, C. R.; Asensio, G.; Cuenca, A. B. *Org. Lett.* **2010**, *12*, 1900; (e) Kinder, R. E.; Zhang, Z.; Widenhoefer, R. A. *Org. Lett.* **2008**, *10*, 3157; (f) Marion, N.; de Fremont, P.; Lemiere, G.; Stevens, E. D.; Fensterbank, L.; Malacria, M.; Nolan, S. P. *Chem. Commun.* **2006**, 2048; (g) Organ, M. G.; Abdel-Hadi, M.; Avola, S.; Hadei, N.; Nasielski, J.; O'Brien, C. J.; Valente, C. *Chem. Eur. J.* **2007**, *13*, 150; (h) Seo, H.; Roberts, B. P.; Abboud, K. A.; Merz, K. M.; Hong, S. *Org. Lett. 12*, 4860; (i) Kantchev, E. A. B.; O'Brien, C. J.; Organ, M. G. *Angew. Chem. Int. Ed.* **2007**, *46*, 2768; (j) O'Brien, C. J.; Kantchev, E. A. B.; Valente, C.; Hadei, N.; Chass, G. A.; Lough, A.; Hopkinson, A. C.; Organ, M. G. *Chem. Eur. J.* **2006**, *12*, 4743.

(13) (a) Arduengo Iii, A. J.; Bannenberg, T. P.; Tapu, D.; Marshall, W. J. *Tetrahedron Lett.* **2005**, *46*, 6847; (b) Arduengo, III, A. J.; Bannenberg, T. P.; Tapu, D.; Marshall, W. J. *Chem. Lett.* **2005**, *34*, 1010; (c) Arduengo, III, A. J.; Iconaru, L. I. *Dalton Transactions* **2009**, 6903; (d) Arduengo, III, A. J.; Tapu, D.; Marshall, W. J. *J. Am. Chem. Soc.* **2005**, *127*, 16400; (e) Arduengo, A. J.; Tapu, D.; Marshall, W. J. *Angew. Chem. Int. Ed.* **2005**, *44*, 7240; (f) Arduengo, A. J.; Tapu, D.; Marshall, W. J. *Angew. Chem.* **2005**, *117*, 7406; (g) Bertogg, A.; Camponovo, F.; Togni, A. *Eur. J. Inorg. Chem.* **2005**, *2005*, 347; (h) Bildstein, B.; Malaun, M.; Kopacka, H.; Ongania, K.-H.; Wurst, K. *J. Organomet. Chem.* **1998**, *552*, 45; (i) Bildstein, B.; Malaun, M.; Kopacka, H.; Ongania, K.-H.; Wurst, K. *J. Organomet. Chem.* **1999**, *572*, 177; (j) Bildstein, B.; Malaun, M.; Kopacka, H.; Wurst, K.; Mitterbock, M.; Ongania, K.-H.; Opromolla, G.; Zanello, P. *Organometallics* **1999**, *18*, 4325; (k) Bolm, C.; Kesselgruber, M.; Raabe, G. *Organometallics* **2002**, *21*, 707; (l) Debono, N.; Labande, A. s.; Manoury, E.; Daran, J.-C.; Poli, R. *Organometallics*, *29*, 1879; (m) Gischig, S.; Togni, A. *Organometallics* **2004**, *23*, 2479; (n) Jackstell, R.; Frisch, A.; Beller, M.; Röttger, D.; Malaun, M.; Bildstein, B. *J. Mol. Catal. A: Chem.* **2002**, *185*, 105; (o) Seo, H.; Kim, B. Y.; Lee, J. H.;

Park, H.-J.; Son, S. U.; Chung, Y. K. *Organometallics* **2003**, *22*, 4783; (p) Seo, H.; Park, H.-j.; Kim, B. Y.; Lee, J. H.; Son, S. U.; Chung, Y. K. *Organometallics* **2003**, *22*, 618; (q) Siemeling, U.; Auch, T. C.; Kuhnert, O.; Malaun, M.; Kopacka, H.; Bildstein, B. *Z. Anorg. Allg. Chem.* **2003**, *629*, 1334; (r) Siemeling, U.; Farber, C.; Bruhn, C. *Chem. Commun.* **2009**, 98; (s) Siemeling, U.; Farber, C.; Bruhn, C.; Leibold, M.; Selent, D.; Baumann, W.; von Hopffgarten, M.; Goedecke, C.; Frenking, G. *Chemical Science* **2010**, *1*, 697; (t) Khramov, D. M.; Rosen, E. L.; Lynch, V. M.; Bielawski, C. W. *Angew. Chem. Int. Ed.* **2008**, *47*, 2267; (u) Varnado Jr, C. D.; Lynch, V. M.; Bielawski, C. W. *Dalton Trans.* **2009**, 7253; (v) Labande, A.; Daran, J.-C.; Manoury, E.; Poli, R. *Eur. J. Inorg. Chem.* **2007**, *2007*, 1205; (w) Rosen, E. L.; Varnado, C. D.; Tennyson, A. G.; Khramov, D. M.; Kamplain, J. W.; Sung, D. H.; Cresswell, P. T.; Lynch, V. M.; Bielawski, C. W. *Organometallics* **2009**, *28*, 6695; (x) Siemeling, U.; Färber, C.; Leibold, M.; Bruhn, C.; Mücke, P.; Winter, R. F.; Sarkar, B.; von Hopffgarten, M.; Frenking, G. *Eur. J. Inorg. Chem.* **2009**, *2009*, 4607.

(14) Plenio previously reported a HG-type catalyst that featured a ferrocene-based NHC phase tag. The oxidation of this complex attenuated RCM activity through precipitation and facilitated catalyst recovery. See: M. Süßner, M.; Plenio, H. *Angew. Chem.* **2005**, *117*, 7045. More recently, Schanz reported that the activities displayed by Grubbs-type olefin metathesis catalysts bearing pH-responsive units were dependent on the degree of protonation. See: Balof, S. L., Yu, B., Lowe, A. B., Ling, Y., Zhang, Y., Schanz, H.-J. Eur. J. *Inorg. Chem.* **2009**, 1717; Dunbar, M. A., Balof, S. L., Roberts, A. N., Valente, E. J., Schanz, H.-J. *Organometallics* **2011**, *30*, 199. Dunbar, M. A., Balof, S. L., LaBeaud, L. J., Yu, B., Lowe, A. B., Valente, E.J., Schanz, H.-J. *Chem. Eur. J.* **2009**, *15*, 12435.

(15) Thomas, J.-L.; Howarth, J.; Hanlon, K.; McGuirk, D. *Tetrahedron Lett.* **2000**, *41*, 413.

(16) (a) Jahnke, M. C.; Hahn, F. E. *Top. Organomet. Chem* **2010**, *30*, 95; (b) Saravanakumar, S.; Kindermann, M. K.; Heinicke, J.; Kockerling, M. *Chem. Commun.* **2006**, 640.

(17) Free NHC **5.2** was stable under an inert atmosphere at –35 °C for several days, as determined by ^{1}H NMR spectroscopy (C_6D_6). The NHC was found to decompose over the course of 12 h at 25 °C in C_6D_6.

(18) Abernethy, C. D.; Clyburne, J. A. C.; Cowley, A. H.; Jones, R. A. *J. Am. Chem. Soc.* **1999**, *121*, 2329.

(19) (a) Chen, D.; Banphavichit, V.; Reibenspies, J.; Burgess, K. *Organometallics* **2007**, *26*, 855; (b) Herrmann, W. A.; Baskakov, D.; Herdtweck, E.; Hoffmann, S. D.; Bunlaksananusorn, T.; Rampf, F.; Rodefeld, L. *Organometallics* **2006**, *25*, 2449; (c) Kownacki, I.; Kubicki, M.; Szubert, K.; Marciniec, B. *J. Organomet. Chem.* **2008**, *693*, 321; (d) Leuthäußer, S.; Schwarz, D.; Plenio, H. *Chem. Eur. J.*

2007, *13*, 7195; (e) Viciano, M.; Poyatos, M.; Sanaú, M.; Peris, E.; Rossin, A.; Ujaque, G.; Lledós, A. *Organometallics* **2006**, *25*, 1120; (f) Iglesias, M.; Beetstra, D. J.; Stasch, A.; Horton, P. N.; Hursthouse, M. B.; Coles, S. J.; Cavell, K. J.; Dervisi, A.; Fallis, I. A. *Organometallics* **2007**, *26*, 4800; (g) Kelly Iii, R. A.; Clavier, H.; Giudice, S.; Scott, N. M.; Stevens, E. D.; Bordner, J.; Samardjiev, I.; Hoff, C. D.; Cavallo, L.; Nolan, S. P. *Organometallics* **2007**, *27*, 202.

(20) (a) Ackermann, L.; Fürstner, A.; Weskamp, T.; Kohl, F. J.; Herrmann, W. A. *Tetrahedron Lett*. **1999**, *40*, 4787; (b) Scholl, M.; Trnka, T. M.; Morgan, J. P.; Grubbs, R. H. *Tetrahedron Lett*. **1999**, *40*, 2247; (c) Weskamp, T.; Kohl, F. J.; Hieringer, W.; Gleich, D.; Herrmann, W. A. *Angew. Chem. Int. Ed*. **1999**, *38*, 2416.

(21) (a) Gessler, S.; Randl, S.; Blechert, S. *Tetrahedron Lett*. **2000**, *41*, 9973; (b) Hong, S. H.; Grubbs, R. H. *J. Am. Chem. Soc*. **2006**, *128*, 3508.

(22) (a) Garber, S. B.; Kingsbury, J. S.; Gray, B. L.; Hoveyda, A. H. *J. Am. Chem. Soc*. **2000**, *122*, 8168; (b) Kingsbury, J. S.; Harrity, J. P. A.; Bonitatebus, P. J.; Hoveyda, A. H. *J. Am. Chem. Soc*. **1999**, *121*, 791.

(23) Compound **5.6** was obtained via anion metathesis of **5.1** with triethyloxonium hexafluorophosphate (see ESI of original publication). See also: P. D. Vu, A. J. Boydston, C. W. Bielawski, *Green Chem*. **2007**, *9*, 1158-1159.

(24) (a) Kotz, J. C.; Nivert, C. L.; Lieber, J. M.; Reed, R. C. *J. Organomet. Chem*. **1975**, *91*, 87; (b) Miller, T. M.; Ahmed, K. J.; Wrighton, M. S. *Inorg. Chem*. **1989**, *28*, 2347; (c) Yang, K.; Bott, S. G.; Richmond, M. G. *Organometallics* **1995**, *14*, 2387.

(25) Altenhoff, G.; Goddard, R.; Lehmann, C. W.; Glorius, F. *J. Am. Chem. Soc*. **2004**, *126*, 15195.

(26) Tolman, C. A. *Chem. Rev*. **1977**, *77*, 313. For recent discussions regarding the validity of using TEPs to evaluate the ligand donicities of NHCs, see (a) Stevens, D.; Bordner, J.; Samardjiev, I.; Hoff, C. D.; Cavallo, L.; Nolan, S. P. *Organometallics* **2007**, *27*, 202; (b) Gusev, D. G. *Organometallics* **2009**, *28,* 763.

(27) Chianese, A. R.; Li, X.; Janzen, M. C.; Faller, J. W.; Crabtree, R. H. *Organometallics* **2003**, *22*, 1663.

(28) (a) Prins, R. *J. Chem. Soc. D: Chem. Commun*. **1970**, 280b; (b) Sixt, T.; Fiedler, J.; Kaim, W. *Inorg. Chem. Commun*. **2000**, *3*, 80.

(29) Spectroelectrochemical analysis of $(PCy_3)Cl_2Ru(=CH\text{-}o\text{-}O\text{-}i\text{-}PrC_6H_4)^{1+}$ showed a similar spectrum as **5.5**$^{2+}$ as well as an analogous isobestic point at ~380 nm (see original manuscript). See also: Kojima, T.; Noguchi, D.; Nakayama, T.; Inagaki, Y.; Shiota, Y.; Yoshizawa, K.; Ohkubo, K.; Fukuzumi, S. *Inorg. Chem*. **2008**, *47*, 886.

(30) (a) Horsfield, A.; Wassermann, A. *J. Chem. Soc., Dalton Trans.* **1972**, 187; (b) Prins, R.; Korswagen, A. R. *J. Organomet. Chem.* **1970**, *25*, C74; (c) Prins, R.; Reinders, F. J. *J. Am. Chem. Soc.* **1969**, *91*, 4929.

(31) Wertheim, G. K.; Herber, R. H. *J. Chem. Phys.* **1963**, *38*, 2106.

(32) For the performance of other Hoveyda-Grubbs type catalysts under identical conditions, see: Ritter, T.; Hejl, A.; Wenzel, A. G.; Funk, T. W.; Grubbs, R. H. *Organometallics* **2006**, *25*, 5740.

(33) For redox switching experiments performed over different timescales, see original manuscript

(34) Precipitation was not observed during any of the redox cycling events described herein. Moreover, no precipitate was collected upon passing any of the oxidized catalysts through 0.2 μm PTFE filters.[14]

(35) As controls, switching experiments were performed using the Hoveyda-Grubbs-type catalyst (1,3-bis-(2,4,6-trimethylphenyl)-2-imidazolylidene)dichloro (o-isopropoxyphenylmethylene)ruthenium (IMes-HG2) under conditions identical to those described above. While IMes-HG2 catalysed the conversion of **5.7** ($[\mathbf{5.7}]_0$ = 0.1 M) to **5.8** with a $k_{obs} = 2.8 \times 10^{-3}$ s^{-1} and the subsequent addition of $[Fe(\eta^5\text{-}C_5H_4COCH_3)Cp][BF_4]$ reduced the measured rate constant ($k_{obs} = 6.8 \times 10^{-5}$ s^{-1}), catalytic activity spontaneously and steadily increased over time (final $k_{obs} = 4.8 \times 10^{-4}$ s^{-1}), presumably due to a slow initiation process (see original manuscript). Moreover, the addition of Fc* to the mixture did not significantly alter the measured rate constant ($k_{obs} = 4.0 \times 10^{-4}$ s^{-1}).

(36) Bildstein, B.; Hradsky, A.; Kopacka, H.; Malleier, R.; Ongania, K.-H. *J. Organomet. Chem.* **1997**, *540*, 127.

(37) Poater, A.; Cosenza, B.; Correa, A.; Giudice, S.; Ragone, F.; Scarano, V.; Cavallo, L. *Eur. J. Inorg. Chem.* **2009**, *2009*, 1759.

(38) Poater, A.; Cosenza, B.; Correa, A.; Giudice, S.; Ragone, F.; Scarano, V.; Cavallo, L. *Eur. J. Inorg. Chem.* **2009**, *2009*, 1759.

(39) Donahue, J. P. *Chem. Rev.* **2006**, *106*, 4747.

(40) (a) Connelly, N. G.; Geiger, W. E. *Chem. Rev.* **1996**, *96*, 877; (b) Aranzaes, J. R.; Daniel, M.-C.; Astruc, D. *Can. J. Chem.* **2006**, *84*, 288.

Chapter 6: Pyridine- and Pyrimidine-Functionalized Poly(sulfone): Performance-Enhancing Crosslinkers for Acid/Base Blend Proton Exchange Membranes Used in Direct Methanol Fuel Cells

I intend to submit portions of this chapter to a peer-reviewed journal for publication. M. Ortiz assisted with the synthesis of SPEEK and characterization of the basic polymers. X. Zhao assisted with the MEA testing. Z. Zuo and Z. Jiang assisted with fabricating various membranes. C. W. Bielawski and A. Manthiram assisted with the writing of this chapter. I designed, synthesized and characterized the new basic polymers, fabricated membranes, and studied the properties and MEA performance of the membranes.

ABSTRACT

The direct methanol fuel cell (DMFC) is a promising energy conversion technology with potential to replace the lithium ion battery in portable electronic devices. At present, widespread commercialization is impeded in part by the absence of a suitable proton exchange membrane (PEM) material. Novel pyridine- and pyrimidine-functionalized polysulfones (PPS and PMPS) were prepared in two high yielding post-polymerization C–H borylation / Suzuki coupling steps from commercially available UDEL® poly(sulfone). Membranes comprised of crosslinking agents 2-PPS, 3-PPS or PMPS, blended with sulfonated poly(ether ether ketone) (SPEEK) were found to exhibit improved single cell performance and decreased methanol crossover in comparison to plain SPEEK and achieved higher power densities than Nafion® 112, an exchange membrane commonly used in DMFCs. Blend properties and single cell performances were found to be dependent on the basicity and steric parameters of the N-heterocycle incorporated into the polymeric material.

INTRODUCTION

Contemporary electronic devices, such as cellular telephones and portable computers, are ubiquitous conveniences but, because they are currently powered by lithium ion batteries, proximity to an electrical outlet for periodic recharging is required. This limitation could be transcended by replacing the lithium ion battery with a direct methanol fuel cell (DMFC). In the case of the latter, the power source (i.e., methanol) has a higher energy density and can be refreshed quickly and conveniently by switching out a portable cartridge of liquid fuel rather than connecting to an electrical outlet.[1]

The DMFC operates by converting the chemical energy stored in methanol directly into electricity. The overall process involves electrocatalytic methanol oxidation at the anode which generates electrons, protons, and carbon dioxide. The electrons and protons produced at the anode are consumed at the cathode where they participate in the electrocatalytic oxygen reduction reaction. The electrons travel from the anode to the cathode through the external circuit. The protons, however, must travel through a proton exchange membrane that is sandwiched between the two electrodes. The lack of sufficiently high-performing proton exchange membrane material remains a significant roadblock to the commercialization of DMFCs and related technologies.

Nafion® (Figure 6.1) is currently the industry standard for use in proton exchange membranes (PEMs), particularly for low temperature fuel cells which utilize hydrogen as a fuel. Although Nafion displays excellent chemical stability and high proton conductivity, the material is unsuitable for use in DMFCs. In addition to being prohibitively expensive, Nafion suffers from high methanol permeability. The resulting diffusion of methanol from the anode to the cathode is detrimental to overall fuel cell performance because it diminishes fuel efficiency and poisons the cathode catalyst, which results in a reduced cell operating voltage and performance. The successful development

of an inexpensive material that exhibits high proton conductivity but low methanol uptake, along with dimensional stability in both anhydrous and hydrated states is of intense interest. Attempts to prepare such materials are often challenged by the tendency of the same functionality that enhances proton conductivity to result in increased hydrophilicity which leads to higher liquid uptake, swelling, and liquid crossover.

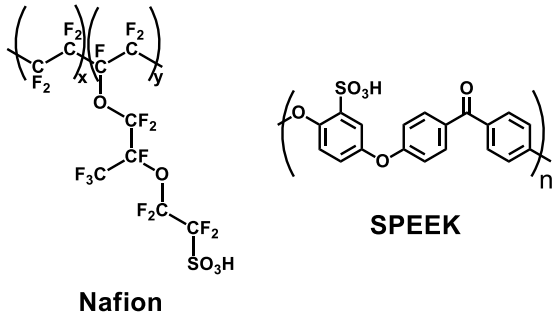

Figure 6.1 Proton conducting polymers Nafion and SPEEK

Nevertheless, recent years have seen much effort devoted to the development of new materials to overcome these deficiencies.[2-4] In particular, attention has been directed toward sulfonated aromatic polymers[5] such as sulfonated poly(ether ketone)s,[6] sulfonated poly(phenylene),[7] sulfonated poly(ether sulfone)[8-11] and sulfonated poly(ether ether ketone) (SPEEK).[12, 13] From a cost perspective, SPEEK stands out because it can be prepared conveniently in one scalable synthetic step from the bulk commodity polymer poly(ether ether ketone) (PEEK). Although its proton conductivity is lower than that of Nafion's, SPEEK displays a relatively reduced methanol crossover and has been investigated as a low cost alternative to Nafion for use as a PEM in DMFCs.

To further diminish liquid uptake, swelling, and methanol crossover, acid/base cross-linked blends[14, 15] comprised of SPEEK or other sulfonic acid functionalized aromatic polymers and a number of base-functionalized polymers have been investigated by others[16-19] and by us.[20-27] Specifically, we have studied blends of SPEEK with

poly(sulfone) functionalized with benzimidazole,[20] perimidine,[25] benzotriazole,[23] and 2-aminobenzimidazole[21] moieties. Insertion of the basic groups into the acidic domains is thought to facilitate proton conduction via a Grotthuss mechanism while blocking methanol via sterics imposed by the large aromatic moieties. The basic polymers that were previously reported are derived from UDEL® poly(sulfone), which was chosen because it is a low cost industrial polymer, has good mechanical and chemical stabilities, and is structurally similar to SPEEK that homogenous blends are often obtained. Overall, this has proved to be an effective strategy in improving fuel cell performance.

Unfortunately, the applicability of the basic polymers that we have previously investigated in DMFCs has been thwarted by their tedious and challenging-to-scale syntheses. For example, the synthetic routes used to prepare the aforementioned materials typically require a low temperature lithiation of poly(sulfone) with pyrophoric *n*-butyl lithium. With the goal of a safer and less expensive process that is more amenable to large scale manufacturing, we sought out a new synthetic strategy. The new route was planned specifically with the goals of minimizing the number of synthetic steps, employing only reactions that could be conducted at room temperature or above, and avoiding the use of pyrophoric bases.

Many functionalized poly(sulfone)s can be prepared via the polycondensation of bisphenols and dihalophenylsulfones. Poly(sulfone)s containing pyridinyl groups in the main chain have been prepared in this manner and were used to prepare phosphoric acid doped membranes for use in high temperature fuel cells.[28-30] In general, however, the direct synthesis of functionalized poly(sufone)s from functionalized monomers requires harsh reaction conditions that result in poor functional group tolerance. Furthermore, as a condensation polymerization, molecular weight and polydispersity can be difficult to control.

Alternatively, a few post-polymerization functionalization approaches to functionalizing poly(sulfone) are known. These have the advantage of starting from an inexpensive polymer precursor of specified molecular weight and polydispersity. The sulfone subunit can be lithiated with *n*-butyl lithium[31] and the resulting lithiated intermediate can be quenched with a variety of electrophiles to give derivatized poly(sulfone)s.[32, 33] Alternatively, the bisphenol A subunit is susceptible to electrophilic substitution.[34, 35] These methods were unappealing to us because they require multipe steps and/or harsh conditions to arrive at the base-functionilized final products.

Over the past decade, iridium-catalyzed C–H borylation[36-39] followed by Suzuki coupling[40, 41] has emerged as a powerful technique for accessing functionalized materials. We were inspired by a recent report on the functionalization of poly(sulfone) using this methodology to install a variety of functionalized phenyl substituents derived from commercially available aryl halides.[42, 43] Both steps were high yielding and the degree of functionalization could be controlled via the stoichiometry of the first step. We surmised that this strategy could similarly be utilized to tether N-heterocycles from the poly(sulfone) main chain. Furthermore, we envisioned that poly(sulfone)s decorated with these basic functionalities could be utilized as crosslinking agents for SPEEK membranes. We choose to incorporate the pyridine and pyrimidine functionalities which are sterically identical but differ in terms of the pKas (pyridinium: 5.25;[44] pyrimidinum: 1.1).[45] Furthermore, we prepared isomeric 2-pyridinyl and 3-pyridinyl containing polymers to compare how the proximity of the nitrogen atom with respect to the polymer main chain affects performance. Herein we report the synthesis and characterization of the first UDEL poly(sulfone) functionalized with pendant 2-pyridinyl (**2-PPS**), 3-pyridinyl (**3-PPS**), and 5-pyrimidinyl (**PMPS**) functionalities as well as the blend

properties and DMFC performance of membranes comprised of these new basic crosslinkers and SPEEK.

EXPERIMENTAL

Materials and Methods

All C–H activation and cross-coupling reactions were performed in a nitrogen purged glove box or under an atmosphere of nitrogen using standard Schlenk techniques. Tetrahydrofuran (THF) was dried using a Vacuum Atmospheres Company solvent purification system, and subsequently stored over 3 Å molecular sieves. Nafion 112 membrane was purchased from Fuel Cell Hub. PEEK (KetaSpire® KT-820FP) and UDEL poly(sulfone) were donated by Solvay Advanced Polymers. Borylated poly(sulfone) (PSfBpin) with a degree of functionalization of one boryl group per repeat unit was prepared from UDEL poly(sulfone) using a literature procedure.[42] All other reagents were commercially available and degassed before use. ^{1}H and ^{13}C NMR spectra were recorded using Varian 400, 500, or 600 MHz spectrometers. Chemical shifts δ (in ppm) are referenced to tetramethylsilane using the residual solvent as an internal standard: for ^{1}H-NMR, $CDCl_3$ 7.24; for ^{13}C, $CDCl_3$: 77.0 ppm. Thermogravimetric analysis was performed on a TA Instruments Q500 thermogravimetric analyzer. After drying under vacuum at 100 °C for at least 4 h, ~5 mg of the sample was loaded onto a Pt crucible. Samples were heated to 800 °C at rate of 20 °C min^{-1} under an atmosphere of nitrogen or oxygen. SEC was performed on a Viscotek GPCmax Solvent/Sample Module. Two fluorinated polystyrene columns (IMBHW-3078 and I-MBLMW-3078) were used in series and maintained at 24 °C. THF was used as the eluent at a flow rate of 1.0 mL/min. Detection was performed using a Viscotek VE 3590 Refractive Index

Detector or a Viscotek 2600 Phhotodiode Array Detector (tuned to 260 nm). Molecular weight and dispersity data are reported relative to polystyrene standards.

Synthesis of SPEEK

PEEK was sulfonated by stirring the material in 95% sulfuric acid at room temperature for 40 h according to a literature procedure.[12] The degree of sulfonation (DS) was determined to be 0.5 by NMR spectroscopy and the ion exchange capacity (IEC) of 1.5 mequiv. g^{-1} was determined by titration.

Synthesis of PMPS

In a glovebox, a 100 ml Shlenk flask was charged with pinacolatoboryl poly(sulfone) (PSfBpin) (1200 mg, 2.05 mmol), 5-bromopyrimidine (1300 mg, 8.22 mmol), potassium carbonate (1000 mg, 7.24 mmol), tetrakistriphenylphosphinopalladium(0) (100 mg, 0.087 mmol), a magnetic stir bar, and THF (30 ml). The flask was sealed with a septum, taken out of the glovebox, and put under positive pressure of nitrogen on a Schlenk line. Degassed and deionized water (3 mL) was added to the flask, which was then fitted with a reflux condenser and sealed. The reaction mixture was stirred at 75 °C for 12 h. After cooling to room temperature, the solution was filtered through a plug of silica into hexanes (200 mL). The resulting precipitate was collected via filtration, dissolved in THF (50 ml) and then precipitated by dropwise addition to methanol. The white precipitate was collected by filtration and then dried overnight under vacuum to yield 1.01 g (92%) of the desired polymer. ^{1}H NMR (400 MHz, $CDCl_3$, ppm): δ 9.16-8.75 (pyrimidine C–H), 7.92-7.77 (aromatic C–H), 7.29-7.18 (aromatic C–H), 7.01-6.87 (aromatic C–H), 1.72-1.59 (isopropylidene C–H). 13C NMR (100 MHz, CDCl3, ppm) δ = 162.3, 161.9, 159.2, 158.8, 157.9, 156.7, 156.4, 152.8, 152.7, 152.4, 150.4, 147.4, 147.2, 147.0, 136.8, 136.1, 135.5, 134.7, 132.1, 132.0,

130.1, 130.0, 129.9, 129.7, 128.6, 128.5, 128.5, 128.4, 126.0, 119.9, 119.8, 119.8, 119.6, 119.5, 117.7, 117.7, 42.6, 42.5, 31.0, 30.9, 29.7. T_d = 291 °C, M_n = 9.9 kg mol^{-1}, Đ = 4.6.

2.4 Synthesis of 2-PPS

In a glovebox, a 100 mL Shlenk flask was charged with PSfBpin (1000 mg, 1.76 mmol), 2-bromopyridine (2.0 mL, 21 mmol), potassium carbonate (1300 mg, 9.41 mmol), tetrakistriphenylphosphinopalladium(0) (80 mg, 0.069 mmol, 4 mol %), a magnetic stir bar, and THF (30 ml). The flask was sealed with a septum, taken out of the glovebox, and put under positive pressure of nitrogen on a Schlenk line. Degassed and deionized water (3 mL) was added to the flask, which was then fitted with a reflux condenser, sealed with a septum and kept under nitrogen (1 atm). The reaction mixture was stirred at 75 °C for 16 h. After cooling to room temperature, the solution was filtered through a plug of silica into hexanes (200 ml). The resulting precipitate was collected by vacuum filtration and washed with methanol (500 mL). The white precipitate was dried overnight under vacuum to yield 749 mg (82%) of the desired polymer. (400 MHz, $CDCl_3$, ppm) δ = 8.68–8.46 (pyridine C–H), 7.89–7.76, 7.68, 7.22–7.16, 6.98–6.91, 1.73–1.63; ^{13}C NMR (100 MHz, $CDCl_3$, ppm) δ = 162.0, 161.9, 159.0, 153.3, 153.1, 152.8, 149.5, 147.2, 147.1, 136.3, 135.4, 135.3, 131.5, 129.9, 129.7, 129.2, 128.4, 128.4, 125.0, 122.8, 119.8, 119.8, 119.6, 118.1, 118.0, 117.7, 117.7, 42.4, 31.0, 30.9; T_d = 394 °C, M_n = 15.4 kg/mol, Đ = 4.1.

Synthesis of 3-PPS

In a glovebox, a 100 mL Schlenk flask was charged with PSfBpin (1500 mg, 2.64 mmol), 5-bromopyrimidine (2.5 mL, 26 mmol), potassium carbonate (1050 mg, 7.5 mmol), tetrakistriphenylphosphinopalladium(0) (120 mg, 0.104 mmol, 4 mol%), a magnetic stir bar, and THF (30 mlL. The flask was sealed with a septum, taken out of the

glove box, and put under positive pressure of nitrogen on a Schlenk line. Degassed and deionized water (3 m) was added to the flask, which was then fitted with a reflux condenser, sealed with a septum and kept under nitrogen (1 atm). The reaction mixture was heated to 75 °C for 16 h. After cooling to room temperature, the solution was filtered through a plug of silica into hexanes (200 mL). The resulting white precipitate was collected by vacuum filtration, washed with methanol (200 ml) and dried overnight under vacuum to yield 1150 mg (83%) of the title polymer. ^{1}H NMR (400 MHz, CDCl3, ppm) δ = 8.80–8.46 (pyridine C–H), 7.99–7.70, 7.34–7.05, 7.03–6.87, 1.74–1.62; ^{13}C NMR (100 MHz, CDCl3, ppm) δ = 162.2, 162.0, 158.9, 159.0, 153.0, 152.9, 152.9, 152.7, 149.9, 149.7, 149.2, 149.1, 148.6, 147.2, 147.2, 147.0, 136.6, 136.5, 136.4, 136.0, 135.5, 135.4, 135.0, 131.9, 131.9, 130.5, 130.4, 129.8, 129.7, 129.1, 129.0, 128.5, 128.4, 128.4, 123.2, 123.2, 119.9, 119.7, 119.5, 119.4, 117.8, 117.8, 117.7, 117.6, 117.3, 117.2, 42.6, 42.4, 31.0, 30.9. T_d = 385 °C, M_n = 9.6 kg/mol , Đ = 4.1.

Nafion Pre-treatment

As received Nafion 112 was cut into small pieces, washed with with dionized water, boiled in 5% hydrogen peroxide solution for 1 hour, washed several times with deionized water, boiled in 0.5 M sulfuric acid solution, rinsed and boiled in dionized water. The pre-treated Nafion membranes were stored in dionized water before use.

Membrane Preparation

Plain SPEEK membrane and blend membranes consisting of SPEEK and basic polymer were prepared by casting from 10 wt.% N,N-dimethylacetamide (DMAc) solutions. The resulting membranes were dried at 80 °C overnight under vacuum. The membranes were soaked for 2 h in boiling, deionized water to remove the residual DMAc. Membranes with a thickness of 80 μm were employed in this study.

IEC Titration

After weighing, a dried slice of membrane was allowed to soak in 2 M NaCl for 48 h. Phenylphthalein (0.02 mL; 1 wt.% in methanol) was added. The membrane was then titrated with aqueous sodium hydroxide until the endpoint was reached. The IEC was determined by the following equation:

$$IEC = \frac{C \times V}{W} \qquad (6.1)$$

where C and V are respectively, the concentration and volume consumed of the sodium hydroxide solution, and W is the weight of membrane sample.

Liquid Uptake Measurement

The liquid uptake values for the membranes were calculated by the difference between the dry mass and the wet mass of a membrane sample. The dry weight was measured after drying the same sample at 100 °C under vacuum for 24 h. The samples were then allowed to equilibrate in deionized water or methanol solution for 2 h at 65 °C. The samples were then carefully dried with a paper towel and quickly weighed. The percent liquid uptake (W_{uptake}) was determined using the following equation:

$$W_{uptake}(\%) = \frac{W_{wet} - W_{dry}}{W_{dry}} \times 100\% \qquad (6.2)$$

where W_{wet} is the weight of the wet membrane and W_{dry} is the weight of the dry membrane.

Proton Conductivity Measurements

Proton conductivity values of the membranes were obtained from the impedance data collected with a computer interfaced HP 4192A LF Impedance Analyzer in the frequency range 5 Hz to 13 MHz with an applied voltage of 10 mV. Control of the equipment was obtained by means of the Z-Plot software. An open window-framed two-

platinum-electrode cell in the lateral direction (*i.e.* in-plan) was used to collect the impedance data. Temperature and relative humidity were controlled by a humidified oven. Measurements were obtained at 100% relative humidity and 65 °C. Before each measurement, membranes were presoaked in water at ambient temperature for 24 h and then at 65 °C for 1 hour. The resistance was used to determine conductivity according to the following equation:

$$\sigma = \frac{D}{R \times A} \qquad (6.3)$$

where D is the distance between the two electrodes, R is the resistance obtained from the impedance data, and A is the cross sectional area.

Small Angle X-Ray Scattering

In order to enhance the electron density contrast between the polymer matrix and the ionic clusters, membranes were first neutralized with Cs^+ ions by soaking in 2 M CsCl solution for 24 h, washed with deionized water, and oven dried at 90 °C for 48 h before each experiment. SAXS was carried out with 1.54 Å Cu Kα radiation and a multiwire gas-filled 2D detector (Molecular Metrology, Inc.) The experiments were carried out at room temperature for a duration of 90 min.

Membrane Electrode Assembly and Single Cell Test

Commercial PtRu/C (40 wt.% Pt and 20 wt.% Ru, Johnson Matthey) and Pt/C (60 wt.% Pt, Johnson Matthey) were used, respectively, as the anode and cathode catalysts. The catalysts were first wetted by a small amount of deionized water and then mixed with a required amount of solvent and Nafion solution (5 wt.% solution, EW1000, Dupont). The mixture was sonicated (Branson 1510) for 60 min for homogenizing at room temperature. The resultant ink was sprayed onto the gas diffusion layer (25 BC, SGL) on

a hot plate. The catalyst loadings on both the anode and cathode were 2.5 mg/cm^2. The Nafion content for the anode and cathode were 20 wt.% and 30 wt.%, respectively. The membrane-electrode assemblies (MEAs) were fabricated by uniaxially hot-pressing the anode and cathode onto the membrane at with a pressure of 50 kg/cm^2 at 135 ºC for 3 min. The MEAs were assembled in a single cell fixture (Electrochem Inc.) consisting of two graphite plates with serpentine channels. Electrical heaters and a thermocouple were embedded into the plates and connected to a fuel cell test station (Scribner, 850 C) to control the cell temperature, at 65 °C in this study. A peristaltic pump (Ismatec IPC4, Cole-Parmer Inst. Co.) was employed to supply aqueous methanol solution to the anode at the flow rate of 1.0 mL/min. O_2 was humidified by passing through the humidifier built in the test station and then fed to the cathode at the flow rate of 200 mL/min without backpressure. Current-voltage curves were automatically recorded with an electronic load bank.

Methanol Crossover Measurement

The methanol crossover was evaluated by a voltammetric method. As the anode side of the MEA was fed a 1 molar methanol solution, the cathode side was flushed with nitrogen. Application of a positive potential at the cathode and measuring the steady-state limiting current density allowed determination of the flux rate of permeating methanol.[46] The limiting current densities were used to calculate the methanol permeability P according to the following equation:

$$P = \frac{1}{k_{\mathrm{dl}} \mathrm{C_m}} \frac{J_{\mathrm{lim}} L_m}{6F} \qquad (4)$$

where L_m is the thickness of the membrane, $\mathrm{C_m}$ is the methanol concentration at the feed edge, J_{lim} is the steady state limiting current density, k_{dl} is the drag correction factor for J_{lim} (0.8829 for 1 M methanol), and F is the Faraday constant.

RESULTS AND DISCUSSION

Synthesis of Basic Polymers

As summarized in Scheme 6.1, iridium-catalyzed C–H borylation of UDEL poly(sulfone) with bispinacolatodiboron followed by Suzuki coupling with 5-bromopyrimidine, 2-bromopyridine, or 3-bromopyridine provided **PMPS, 2-PPS**, **3-PPS**, respectively, in high yields (90%, 82%, and 83%, respectively). The borylation reactions were done according to a literature procedure[42] and a reaction of time of 16 h was found to give a degree of boryation of one per repeat unit. The Suzuki coupling reactions were monitored by ^{1}H NMR spectroscopy via the disappearance of the C–H signal corresponding to the methyl groups of the pinacolboronate ester at 1.23 ppm ($CDCl_3$) along with a concomitant appearance of new signals in the downfield region corresponding to the C–H bonds of the respective N-heterocycle.

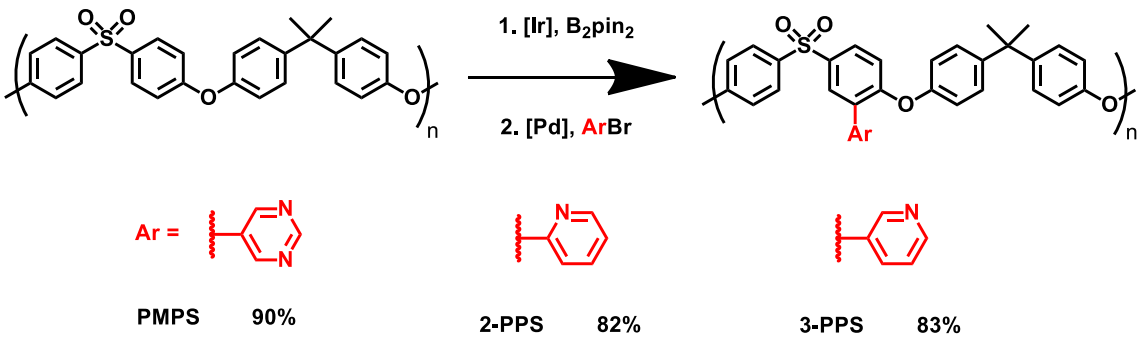

Scheme 6.1 Synthesis of **PMPS**, **2-PPS**, and **3-PPS**.

Table 6.1 Summary of the properties displayed by various blend membranes

Membrane Composition	**Proton-Conductivity ($mS\ cm^{-1}$) (65 °C, 100% rh)**	**IEC (experimental) ($meq.\ g^{-1}$)**	**IEC (theoretical) ($meq.\ g^{-1}$)**
SPEEK	72	1.52	1.50
SPEEK + 2.5% PMPS	74	1.40	1.45
SPEEK + 5.0% PMPS	61	1.36	1.41
SPEEK + 7.5% PMPS	57	1.31	1.37
SPEEK + 5.0% 2-PPS	30	1.36	1.37
SPEEK + 5.0% 3-PPS	45	1.36	1.36

Membrane Composition	**Liquid Uptake (65 °C, water) (%)**	**Liquid Uptake (65 °C, 1M MeOH) (%)**	**Liquid Uptake (65 °C, 2M MeOH) (%)**	**Liquid Uptake (65 °C, 5M MeOH) (%)**
SPEEK	40	42	73	170
SPEEK + 2.5% PMPS	38	46	62	544
SPEEK + 5.0% PMPS	31	36	54	460
SPEEK + 7.5% PMPS	24	32	40	310
SPEEK + 5.0% 2-PPS	26	26	29	54
SPEEK + 5.0% 3-PPS	25	27	31	172

Physical Properties of the Basic Polymers

The basic polymers, **PMPS**, **2-PPS**, and **3-PPS** all exhibited good solubility in common organic solvents, including: THF, CH_2Cl_2, DMSO, DMF, and DMAc. The thermal stabilities of the polymers were evaluated by thermogravimetric analysis. The onset of decomposition of **PMPS** under an atmosphere of oxygen was found to be 222 °C; **2-PPS** and **3-PPS** exhibited higher thermal stabilities, with onsets at 315 and 277 °C, respectively (see original manuscript for more details). Furthermore, the two step sequence of converting to the pyridine and pyrimidine functionalized poly(sulfone)s had a limited effect on M_n or polydispersity (see SI for GPC traces). For example, PSfBpin displayed a M_n of 11.9 kg mol^{-1} and a Đ of 4.8. While the M_n of **2-PPS** was slightly higher (15.4 kg mol^{-1}) with a similar Đ of 4.1, **PMPS** and **3-PPS** exhibited slightly lower M_n values of 9.9 and 9.6 kg mol^{-1} and similar polydispersities (4.6 and 4.1), respectively.

Combining solutions of SPEEK in DMAc with solutions of **2-PPS** or **PMPS** in DMAc resulted in slight turbidity but the solution rapidly homogenized upon stirring to give a transparent solution. Combining solutions of SPEEK and **3-PPS**, however, resulted in a suspension which may reflect a strong interaction between SPEEK and 3-PPS. However, heating the solution to 80 °C during membrane casting gave a homogenous membrane. All membranes were obtained as translucent films and successfully incorporated into membrane electrode assemblies (see below).

Liquid Uptake

Liquid uptake is an important parameter for evaluating PEMs because of its correlation to proton conductivity, dimensional stability, and methanol crossover. At 65 °C in deionized (DI) water, all blend membranes took up less water than plain SPEEK (Table 6.1). Comparing the series of **PMPS** blends, an increase in the wt.% of **PMPS** resulted in a corresponding incremental decrease in liquid uptake. Comparing the 5%

PMPS to the 5% **PPS** blends, both of the **PPS** additives were found to decrease water uptake than **PMPS**. Similar results were obtained for 1 M methanol, although the 2.5 % **PMPS** membrane exhibited a slightly higher liquid uptake than plain SPEEK. At higher methanol concentrations, the **PMPS** blends absorbed even more liquid than plain SPEEK and lost their mechanical integrity. In contrast, the **PPS** blends took up much less liquid than plain SPEEK and the **PMPS** blend at all methanol concentrations tested. These findings were consistent with Kerres' previous observation that using a weakly basic crosslinker does not substantially decrease liquid uptake in comparison to strongly basic crosslinkers due to incomplete protonation of the basic groups.[16-18] In all cases, the **2-PPS** membrane exhibited the lowest liquid uptake value illustrating the importance of the sterics of the basic moiety in reducing liquid uptake.

Ion Exchange Capacity

The ion-exchange capacity (IEC) is an important parameter for comparing PEM materials because of its strong relationship to proton-conductivity, liquid uptake, and dimensional stability. IEC is a function of the degree of incorporation of acidic sites and, in the case of SPEEK, can be controlled by the reaction conditions. SPEEK with too low of a degree of sulfonation exhibits low proton conductivity and poor solubility that leads to inhomogenous membranes unsuitable for use in fuel cells.[12] On the other hand, SPEEK with too high of a degree of sulfonation swells substantially and dissolves in warm aqueous methanol resulting in failure of the fuel cell.[12] We chose to employ SPEEK with an IEC of 1.5 meq g^{-1} because this level is sufficiently high to exhibit good proton-conductivity, but low enough to fabricate a membrane that will remain stable under the fuel cell operating conditions described below.

We found that blending SPEEK with **PMPS** had a small effect on IEC compared to the **2-PPS** and **3-PPS** (Table 6.1). This behavior was consistent with Kerres' observation that acid/base blend membranes comprised of a weak basic moiety have little impact on the observed IEC due to incomplete protonation.[16-18] In contrast, blends comprised of stronger bases result in a larger reduction in the IEC because the basic moieties are completely protonated which leads to stoichiometric consumption of acidic protons within the membrane.[17, 18]

Proton Conductivity

One of the most important parameters for evaluating PEMs is proton conductivity. The plain SPEEK membrane described above displayed a proton conductivity value of 72 mS cm^{-1} (Table 1) consistent with literature reports.[25-27] The 2.5% **PMPS** blend increased this value slightly, but membranes with 5% or 7.5% **PMPS** resulted in an incremental loss in proton conductivity. Although the acidic sites were not completely quenched, as determined by the IEC titration, the N-heterocycles may inhibit the migration of protonated water through the membrane due to microstructural changes and increased hydrophobicity of the membrane. The blends consisting of SPEEK and the more basic **2-PPS** and **3-PPS** exhibited a larger reduction in proton conductivity due to the stoichiometric quenching of acidic sites within the polymer matrix as a result of complete protonation of the pyridinyl groups. This loss of conductivity was greater for **2-PPS** than **3-PPS**, and attributed to the more pronounced insertion of the pendent N-heterocycle into the ionic clusters required to protonate the more sterically hindered basic nitrogen atoms. The resulting ionic domains are more diffuse and may block the passage of hydronium ions.

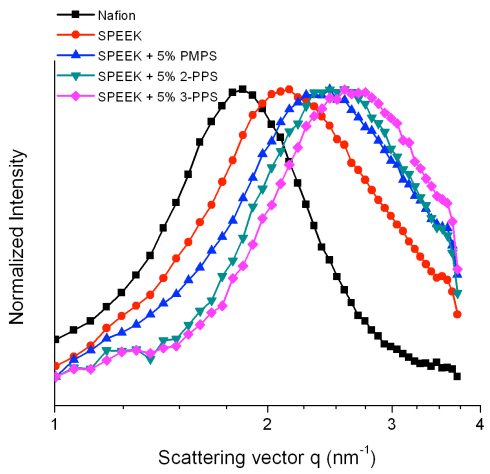

Figure 6.2 Normalized SAXS profiles for Nafion, SPEEK, and various blend membranes.

Morphology

Small angle X-ray scattering (SAXS) was used to investigate the microstructural differences between the membranes. The SAXS peak (i.e., the q value) is related to the average distance between the ionic clusters and their size.[26, 47] The addition of basic crosslinkers has been observed to increase the q value in the case of polymers that contain basic functionality within the main chain,[19] but decreases the q value in the case of polymers containing bulky pendant basic groups.[23-26] In these cases, a smaller q value indicates that the insertion of the basic groups into the ionic clusters and results in their expansion. Indeed, the methanol blocking ability of the blends described above was attributed to this phenomenon.

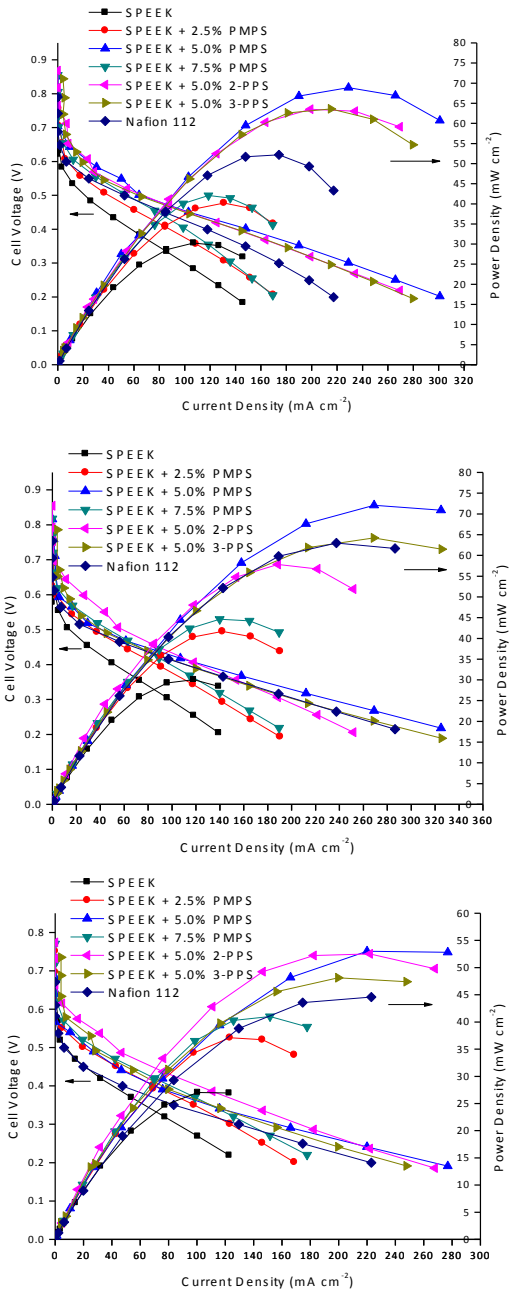

Figure 6.3 Comparison of the DMFC performances of various membranes at 65 °C and 1 M methanol (top) 2 M methanol (middle), and 5 M methanol (bottom).

The new crosslinked blends presented herein exhibited q values that were larger than the plain SPEEK (Figure 6.2) and increased in the order: **3-PPS** > **2-PPS** > **PMPS**. The **2-PPS** and **3-PPS** blends gave higher q values than the **PMPS** because the pyridinyl moieties are more basic than pyrmidinyl moieties resulting in complete protonation and thereby more effective ionic crosslinking. The **PMPS** crosslinker decreased cluster size to a smaller extent, presumably though a hydrogen bond interaction. A slightly smaller q value was observed for the **2-PPS** blend than the **3-PPS** blend indicating that the crosslinker with the more sterically hindered basic moiety results in slightly broader ionic clusters. The deeper penetration of the N-heterocycle into the hydrophilic domain required to facilitate the ionic interaction is believed to account for the decreased liquid uptake and proton-conductivity observed for the **2-PPS** blend.

Fuel Cell Performance

We next prepared a series of membranes comprised of varying percent compositions of **PMPS** blended with SPEEK and one comprised of plain SPEEK to find the optimal percent composition of this basic crosslinker to achieve the highest performance DMFC possible (Figure 6.3). The membranes were incorporated into membrane electrode assemblies (MEAs) using standard loadings of commercial catalysts and tested under various conditions. At 1 M methanol and 65 °C, the open circuit voltage was found to increase with increasing weight % of **PMPS** (Table 6.2) demonstrating that the addition of **PMPS** decreases the methanol permeability of the membrane. This was confirmed by measuring the methanol crossover current density (Figure 6.4) which showed that an incremental decrease in crossover current upon increasing the weight % of the **PMPS**. The maximum power density was found to increase up to 5 wt.% **PMPS** (69 mW cm^{-2}) which decreased upon further increase to 7.5 wt.% of the same material. At

this wt.% the decrease in proton-conductivity countered the benefit of reduced methanol permeability, resulting in an overall decrease in fuel cell performance. The performance of the blends changed very little upon increasing the concentration of methanol to 2 M but decreased slightly at 5 M. In all cases, the blend containing 5 wt.% **PMPS** gave the optimal maximum power density, approximately double that obtained for the plain SPEEK membrane tested for comparison, and slightly higher than the Nafion 112 membrane

To compare the **PMPS** containing membrane to the those containing the relatively more basic crosslinkers, **2-PPS** and **3-PPS**, we prepared and evaluated the MEA performance of blends of SPEEK + 5 wt.% **2-PPS** and **3-PPS**, respectively. At 65 °C and 1 M methanol, the addition of **2-PPS** and **3-PPS** improved fuel cell performance to nearly the same extent as **PMPS**, as both blends gave maximum power densities of 64 mW cm^{-2}. Furthermore, **2-PPS** gave the highest open circuit voltage (0.860 V) tested, consistent with the notion that a sterically hindered strongly basic crosslinker would most effectively block methanol crossover. The limiting current densities obtained from the methanol crossover determination were used to calculate methanol permeability values for the different membranes (Table 6.3). The SPEEK + 5 wt.% **2-PPS** membrane gave the lowest value (0.43×10^{-6} cm^2 s^{-1}) which is half of that obtained for SPEEK (1.01×10^{-6} cm^2 s^{-1}) and approximately one third of the value obtained for Nafion 112 (1.17×10^{-6} cm^2 s^{-1}), a result which corroborated the high OCV value.

At 65 °C and 5 M methanol, the blend containing **2-PPS** gave an better performance than **3-PPS**, and in the low current region also gave a better performance than the **PMPS** blend. However, at the high current region, the **PMPS** blend gave nearly equal performance on account of its higher proton conductivity. At 80 °C and 1 M methanol, similar results were obtained (Figure 6.5): the **3-PPS** blend gave the best

performance (89 mW cm^{-2}), followed closely by **PMPS** (87 mW cm^{-2}) and **2-PPS** (79 mW cm^{-2}).

Overall, the maximum power densities trended closely with proton conductivity. With the exception of the poorly conducting **2-PPS** blend, all + 5% blends gave higher maximum power densities and lower methanol crossovers under all conditions tested than Nafion 112, making these blends attractive candidates for use in DMFCs. However, the liquid uptake measurements suggest that the blends containing pyridne-based crosslinkers are more promising for long term performance.

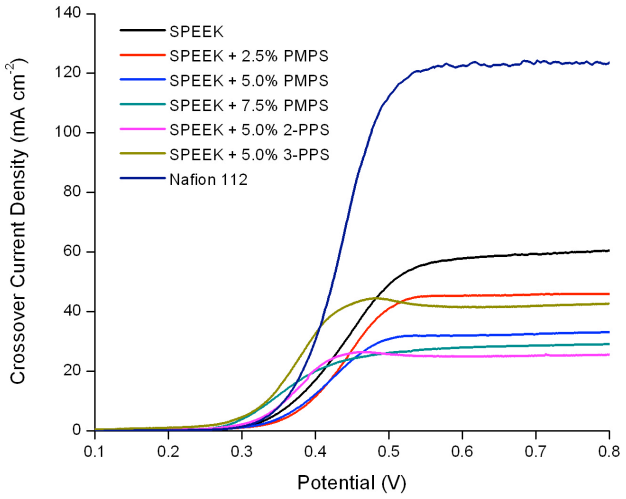

Figure 6.4 Comparison of methanol crossover current densities for plain SPEEK, Nafion® 112 and various blends at 65 °C and 1 M methanol.

Table 6.2 Methanol crossover current densities and methanol permeability values for SPEEK, various blend, and Nafion 112 membranes.

Membrane	Crossover Current Density (mA cm^{-2})	Methanol Permeability (cm^2 s^{-1})
SPEEK	61	1.01×10^{-6}
SPEEK + 2.5% PMPS	46	0.77×10^{-6}
SPEEK + 5.0% PMPS	33	0.55×10^{-6}
SPEEK + 7.5% PMPS	29	0.48×10^{-6}
SPEEK + 5.0% 2-PPS	26	0.43×10^{-6}
SPEEK + 5.0% 3-PPS	43	0.71×10^{-6}
Nafion 112	120	1.17×10^{-6}

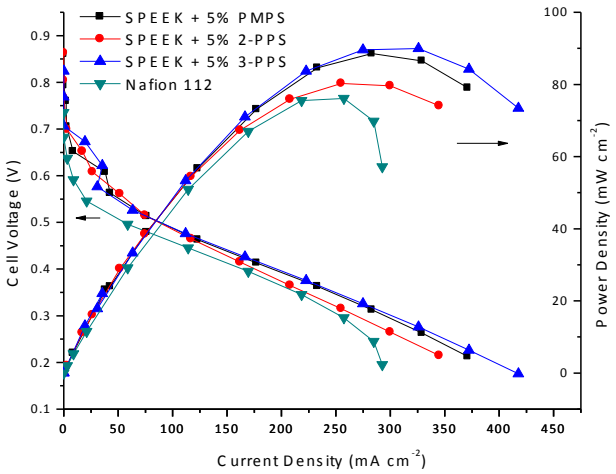

Figure 6.5 Polarization and power density curves for DMFCs with various blend and Nafion 112 membranes. Cell temperature: 80 °C. Methanol concentration: 1 M.

CONCLUSIONS

We have prepared three new poly(sulfone)s functionalized with basic pyridine and pyrimidine moieties in two high yielding (82 to 90%) steps from commercially available materials. The **PMPS**, **2-PPS**, and **3-PPS** crosslinkers were blended with SPEEK to fabricate membranes which, at the optimal composition (5 wt. %), were found to exhibit decreased methanol crossover by 46%, 58%, and 30%, respectively, compared to plain SPEEK and resulted in dramatically improved fuel cell performance (all blends

showed higher open circuit voltages, higher maximum power densities, and lower methanol crossover current densities than plain SPEEK) and compared favorably to Nafion 112.

Even though all three pendent basic functionalities are sterically identical, subtle variations in the identity of the N-heterocycle (weak base vs strong base; hindered base vs unhindered base) were found to have a significant impact on the membrane properties and fuel cell performance. The weakly basic but polar **PMPS** reduced the size of the ionic clusters which concomitantly reduced methanol crossover without sacrificing proton-conductivity, and afforded the highest maximum power density (69 mW cm^{-2} for SPEEK +5 wt.% **PMPS** *versus* 30 mW cm^{-2} for plain SPEEK at 65 °C and 1 M methanol). However, liquid uptake was also increased compared to plain SPEEK at high methanol concentration (460% for SPEEK + 5% **PMPS** versus 170% for SPEEK at 65 °C and 5 M methanol). The resulting swelling precludes this particular basic crosslinker from being a viable solution for long term fuel cell performance at high methanol concentration.

The more strongly basic pyridine based crosslinkers, **2-PPS** and **3-PPS** resulted in blends with smaller ionic clusters than **PMPS** with the **3-PPS** giving the smallest of the two. These favorable morphological changes resulted in reduced liquid uptake and methanol permeability with **2-PPS** taking up the smallest amount of liquid (54% at 65 °C and 5 M methanol), giving the lowest methanol crossover (0.43×10^{-6} cm^2 s^{-1}), and the highest open circuit voltage (0.860 V at 65°C and 1 M methanol). However, the stoichiometric loss of acidic sites due to quenching by the strongly basic pyridine moieties reduced the proton conductivity of the membranes which gave maximum power densities that were slightly lower than **PMPS** at 65 °C. The **3-PPS** with its intermediate conductivity and low liquid uptake gave the best performance at 80 °C (89 mW cm^{-2}). In

general, the these membranes are expected to give better long term fuel cell performance due better dimensional stability of the membranes arising from the reduced liquid uptake.

We believe our straightforward and scalable two-step approach toward the synthesis of basic crosslinkers that double the maximum power density of PEMs compared to plain SPEEK and give better performance than Nafion 112 under various conditions will enhance the propects for commercialization of the DMFC. Furthermore, we expect that the modularity of the approach described herein will spur the development of new classes of PEM materials.

NOTES AND REFERENCES

(1) Kleiner, K. *Nature* **2006**, *441*, 1046-1047.

(2) Hickner, M. A.; Ghassemi, H.; Kim, Y. S.; Einsla, B. R.; McGrath, J. E. *Chem. Rev.* **2004**, *104*, 4587-4612.

(3) Zhang, H.; Shen, P. K. *Chem. Rev.* **2012**, *112*, 2780-2832.

(4) DeLuca, N. W.; Elabd, Y. A. *J. Polym. Sci., Part B: Polym. Phys.* **2006**, *44*, 2201-2225.

(5) Scherer, G. N.; Maier, G.; Meier-Haack, J. Sulfonated Aromatic Polymers for Fuel Cell Membranes. In Fuel Cells II, Springer Berlin Heidelberg: 2008; Vol. *216*, pp 1-62.

(6) Liu, B.; Robertson, G. P.; Kim, D.-S.; Guiver, M. D.; Hu, W.; Jiang, Z. *Macromolecules* **2007**, *40*, 1934-1944.

(7) Ghassemi, H.; McGrath, J. E. *Polymer* **2004**, *45*, 5847-5854.

(8) Iojoiu, C.; Maréchal, M.; Chabert, F.; Sanchez, J. Y. *Fuel Cells* **2005**, *5*, 344-354.

(9) Harrison, W. L.; Hickner, M. A.; Kim, Y. S.; McGrath, J. E. *Fuel Cells* **2005**, 5, 201-212.

(10) Fu, Y. Z.; Manthiram, A. *J. Power Sources* **2006**, *157*, 222-225.

(11) Vernersson, T.; Lafitte, B.; Lindbergh, G.; Jannasch, P., A *Fuel Cells* **2006**, *6*, 340-346.

(12) Yang, B.; Manthiram, A. *Electrochem and Solid-State Lett.* **2003**, *6*, A229-A231.

(13) Iulianelli, A.; Basile, A. *International Journal of Hydrogen Energy* **2012**, *37*, 15241-15255.

(14) Kerres, J. A. *Fuel Cells* **2005**, *5*, 230-247.

(15) Zuo, Z.; Fu, Y.; Manthiram, A. *Polymers* **2012**, *4*, 1627-1644.

(16) Kerres, J.; Ullrich, A.; Häring, T.; Baldauf, M.; Gebhardt, U.; Preidel, W. *Journal of New Materials for Electrochemical Systems* **2000***, 3*, 229

(17) Tang, C. M.; Zhang, W.; Kerres, J. *Journal of New Materials for Electrochemical Systems* **2004**, *7*, 287-298.

(18) Kerres, J.; Ullrich, A.; Meier, F.; Häring, T. *Solid State Ionics* **1999,** *125*, 243-249.

(19) Min, S.; Kim, D. *Solid State Ionics* **2010**, *180*, 1690-1693.

(20) Fu, Y.; Manthiram, A.; Guiver, M. D. *Electrochem. Commun.* **2006**, *8*, 1386-1390.

(21) Fu, Y.; Manthiram, A.; Guiver, M. D. *Electrochem. Commun.* **2007**, *9*, 905-910.

(22) Lee, J. K., Li, W., Manthiram, A., Guiver, M. D. *J. Electrochem. Soc.* **2009**, *156*, B46-B50.

(23) Li, W. Devlopment and Understanding of New Membranes Based on Aromatic Polymers and Heterocycles for Fuel Cells. Univesity of Texas at Austin, 2009.

(24) Li, W., Fu, Y.-Z., Manthiram, A., Guiver, M. D. *J. Electrochem. Soc.* **2009**, *156*, B258-B263.

(25) Li, W.; Manthiram, A.; Guiver, M. D. *Electrochemical and Solid-State Letters* **2009**, *12*, B180-B184.

(26) Li, W.; Manthiram, A.; Guiver, M. D. *J. Membr. Sci.* **2010**, *362*, 289-297.

(27) Li, W.; Manthiram, A.; Guiver, M. D.; Liu, B. *Electrochem. Commun.* **2010**, *12*, 607-610.

(28) Gourdoupi, N.; Kallitsis, J. K.; Neophytides, S. *J. Power Sources* **2008**, *195*, 170-174.

(29) Gourdoupi, N.; Papadimitriou, K.; Neophytides, S.; Kallitsis, J. K. *Fuel Cells* **2008**, *8*, 200-208.

(30) Pefkianakis, E. K.; Morfopoulou, C.; Deimede, V.; Kallitsis, J. K. *Macromolecular Symposia* **2009**, *279*, 183-190.

(31) Guiver, M. D.; Apsimon, J. W.; Kutowy, O. *J. Polym. Sci. Part C: Polym. Lett.* **1988**, *26*, 123-127.

(32) Guiver, M. D.; Croteau, S.; Hazlett, J. D.; Kutowy, O. *British Polymer Journal* **1990**, *23*, 29-39.

(33) Guiver, M. D.; Robertson, G. P. *Macromolecules* **1995**, *28*, 294-301.

(34) Guiver, M. D.; Kutowy, O.; ApSimon, J. W. *Polymer* **1989**, *30*, 1137-1142.

(35) Warshawsky, A.; Kahana, N.; Deshe, A.; Gottlieb, H. E.; Arad-Yellin, R. *J. Polym. Sci. Part A: Polym. Chem.* **1990**, *28*, 2885-2905.

(36) Ishiyama, T.; Takagi, J.; Ishida, K.; Miyaura, N.; Anastasi, N. R.; Hartwig, J. F. *J. Am. Chem. Soc.* **2001**, *124*, (3), 390-391.

(37) Boller, T. M.; Murphy, J. M.; Hapke, M.; Ishiyama, T.; Miyaura, N.; Hartwig, J. F. *J. Am. Chem. Soc.* **2005**, *127*, 14263-14278.

(38) Cho, J.-Y.; Tse, M. K.; Holmes, D.; Maleczka, R. E.; Smith, M. R. *Science* **2002**, *295*, 305-308.

(39) Chotana, G. A.; Rak, M. A.; Smith, M. R *J. Am. Chem. Soc.* **2005**, *127*, 10539-10544.

(40) Miyaura, N.; Suzuki, A. *Chem. Rev.* **1995**, *95*, 2457-2483.

(41) Suzuki, A. *J. Organomet. Chem.* **1999**, *576*, 147-168.

(42) Jo, T. S.; Kim, S. H.; Shin, J.; Bae, C. *J. Am. Chem. Soc.* **2009**, *131*, 1656-1657.

(43) Chang, Y.; Lee, H. H.; Kim, S. H.; Jo, T. S.; Bae, C. *Macromolecules* **2013**, *46*, 1754-1764.

(44) Linnell, R. *J. Org. Chem.* **1960**, *25*, 290-290.

(45) Brown, H. C.; Baude, E. A.; Nachod, F. C. Determination of Organic Structures by Physical Methods. Academic Press: New York, 1955.

(46) Ren, X.; Springer, T. E.; Zawodzinski, T. A.; Gottesfeld, S. *J. Electrochem. Soc.* **2000**, *147*, 466.

(47) Choi, B. G.; Hong, J.; Park, Y. C.; Jung, D. H.; Hong, W. H.; Hammond, P. T.; Park, H. *ACS Nano* **2011**, *5*,5167-5174.

Appendix A: Benzo(bis)imidazolium Salts

INTRODUCTION

Benzo(bis)imidazolium salts (BBIs) were extensively developed by our group and have been found to have a variety of interesting properties.[1] The modular scaffold can be derivatized in numerous ways to give materials that can exhibit fluorescence and liquid crystallinity,[2] and serve as precursors to bis(carbene)s[3,4] and poly(enetetramine)s, which can in turn serve as precursors to bimetallic complexes, coordination polymers[2,5,6] and polyeletrolytes[7]

It had been previously been found that most simple BBI, with four methyl R groups, through supramolecular interaction can be utilized as a fluorescent sensor for a variety of analytes in aqueous media.[8] We sought to elaborate upon the scaffold in subtle ways to: A) tune binding affinites and B) include functional handles for subsequent derivatization. In pursuit of the former, an asymmetric BBI containing one methyl and three propyl N substituents, a BBI containing all methyl N substituents and also alkyl substituents from the C2 position, and a BBI containing two methyl and two tripeg substituents were pursued. In the case of the latter, a BBI with hydroxy terminated C2 alkyl substituents was pursued. Herein, the synthesis of the desired BBIs is disclosed.

RESULTS AND DISCUSSION

The starting point of our synthetic strategy for **BBI-1** (Scheme A.1) began with 1,5-dichloro-2,4-dinitrobeznene. Nucleophilic aromatic substitution (SNAr) with propylamine at room temperature (low temperature was required to avoid diamination) provided **A.1** in 88% yield. A second S_NAr reaction was carried out with **A.1** employing methylamine to furnish **A.2** in 94% yield. Reductive formylation provided N-methyl-N'-propylbenzobis(imidazole) **A.3**. Alkylation with methyl iodide provided our target

compound **BB-1** in yield and an overall yield of 31% from1,5-dichloro-2,4-dinitrobeznene.

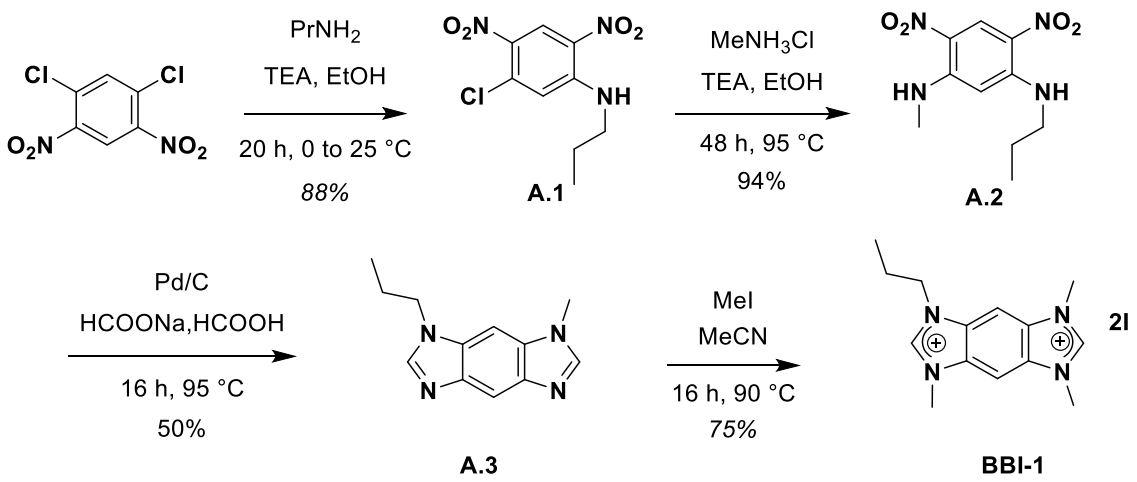

Scheme A.1 Synthesis of **BBI-1**

To access **BBI-2** (Scheme A.2) we needed to amidate 1,4-diamino-2,5-dinitrobenzene (**A.4**). Although the amine functionality on **A.4** is deactivated toward amidation due to the electron-withdrawing nitro groups and a number of standard amidation protocols were met with failure, amidation could be cleanly achieved by heating **A.4** in excess neat butyryl chloride for an extended period of time to give to condense HCl giving **A.5**. Subjecting **A.5** to catalytic hydrogenation employing palladium on carbon and one atmosphere of hydrogen provided the diamino-diamido compound **A.6**. Condensation at elevated temperature in neat acetic acid provided 2,2'-dipropylbenzobis(imidazole) (**A.7**) observed as two tautomers in the proton NMR. Alkylation of **A.7** was carried out with methyl iodide and stoichiometric sodium bicarbonate to provide the target **BBI-2**. The stoichiometricly generated sodium iodide

byproduct could then be removed by triturating with acetone. An overall yield of 39% was obtained from **A.4**.

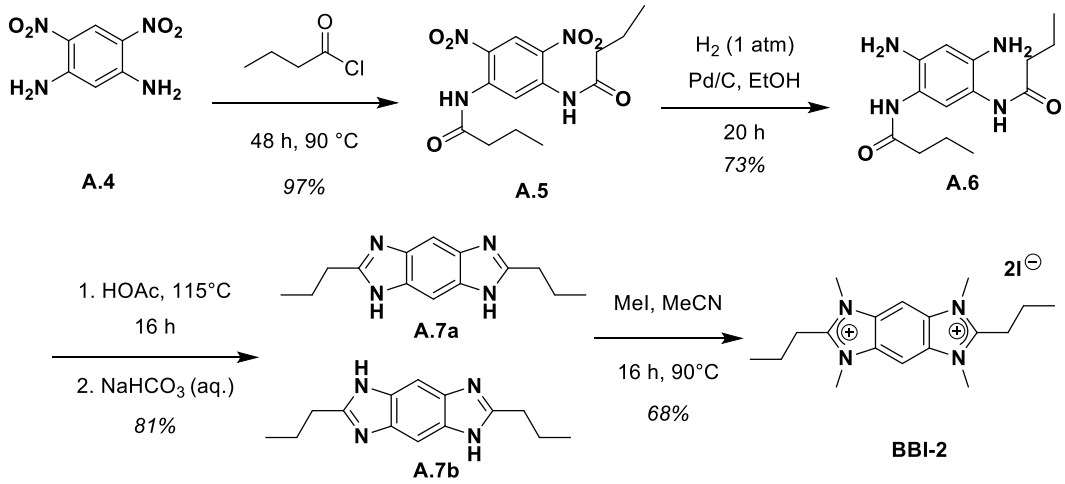

Scheme A.2 Synthesis of **BBI-2**

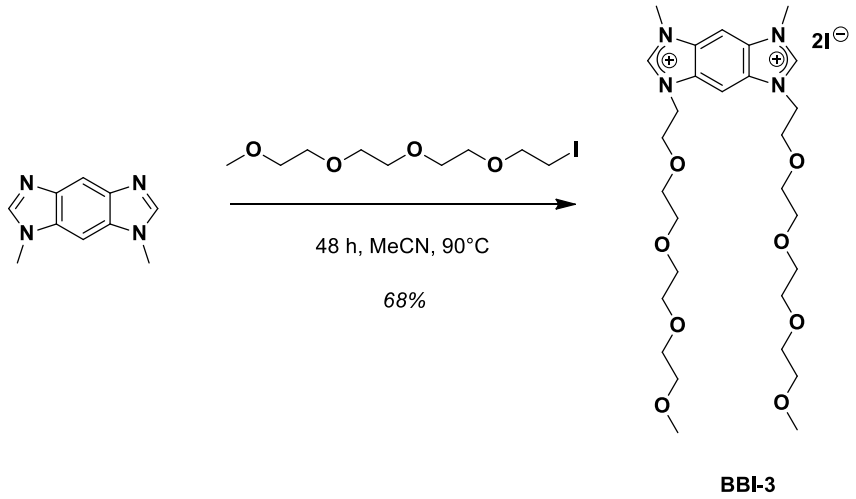

Scheme A.3 Synthesis of **BBI-3**

BBI-3 was prepared in 68% yield by alkylating dimethyl benzo(bis)imidazole with monomethyl terminated triethyleneglycol iodide (Scheme A.3). Interestingly, **BBI-3** was found to be a room temperature ionic liquid.

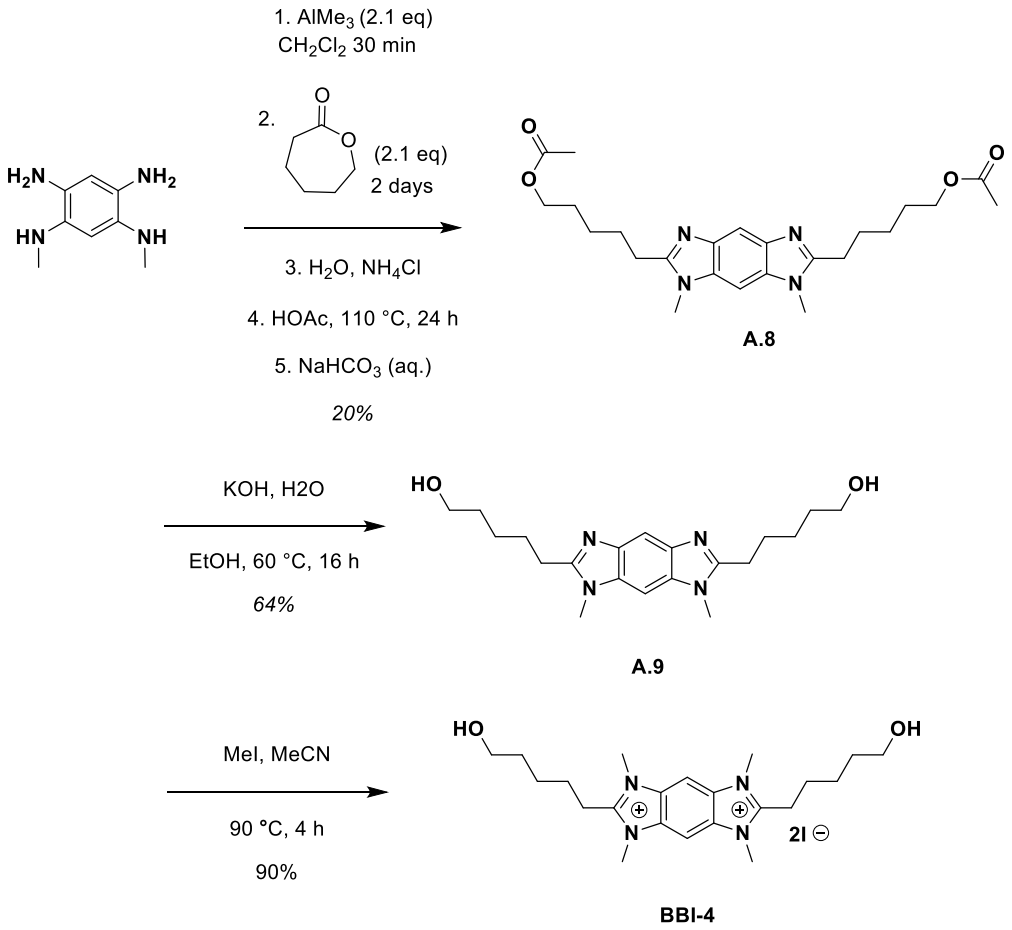

Scheme A.4 Synthesis of **BBI-4**

We wanted to obtain a BBI tethered from the C2 position with a pendant functional handle that would allow subsequent attachment to polymer chains or other groups. However, the route previously developed to install alkyl substituents (as in the case of **BBI-2**) would not be suitable in this case due to the incompatibility between between acid chlorides and alcohols precluding them from existing in the same molecule. However, it is known that esters and carboxylic acids can similarly react with amines to form amide linkages, albeit under harsher conditions. Many attempts were made along these lines resulting in no reactivity or poor yield, apparently due in part due to oxidation

of the tetramine precursor. We were inspired by a few reports in the literature of activating esters with trimethyl aluminum to facilitate amidation reactions.[9] By applying this technique to a lactone (Scheme A.4), we could form the amide and generate the tethered hydroxyl group. The crude reaction mixture contained various amides and also some cyclized benzo(bis)imidazole. Heating in acetic acid cleanly facilitated the cyclization, converting the residual amidated products to the benzo(bis)imidazole (**A.8**). Since this process was also found to esterify the alcohol end groups, a saponification reaction was required to remove them giving dialcohol **A.9**. Alkylation with methyl iodide could then cleanly furnish **BBI-4**. The overall yield from 1,5-dimethylamino-2,4-diaminobenzene was 22%.

BBI-1 and **BBI-2** have been employed to obtain binding constants for a number of receptors for the purpose of evaluating the predictive power of SAMPL3 software.[10]

EXPERIMENTAL

1-Chloro-5-propylamino-2,4-dinitrobenzene (A.1). A 250 mL flask was charged with 1,5-dichloro-2,4-dinitrobenzee (2.37 , 10 mmol), ethanol (30 mL) and a magnetic stir bar. The mixture was cooled to 0 °C and propylamine (0.9 mL, mmol) followed triethylamine (1.2 mL, mmol) were added dropwise, respectively, over 10 min. The flask was stoppered and the reaction mixture was stirred for 20 h at room temperature. The product was precipitated from water (500 mL), collected by vacuum filtration, and finally dried under vacuum to give 2.29 g (88%) of **A.3** as a yellow powder. M.p. = 89-92 °C. ^{1}NMR (400 MHz, $CDCl_3$): δ 9.04 (s, 1H), 8.39 (br, 1H), 6.93 (s, 1H), 3.32 (dt, J_1 = 5.6, J_2 = 7.2 , 2H), 1.79 (m, 2H), 1.07 (t, J = 7.2 , 3H); ^{13}C NMR (100 MHz, DMSO-d_6): δ 146.8, 135.9, 134.5, 128.9, 126.9, 116.0, 45.3, 22.0, 11.4. HRMS: $[M+H]^+$ calced for $C_9H_{11}ClN_3O_4$, 260.0433; found, 260.0432.

1-Methylamino-5-propylamino-2,4-dinitrobenzene (A.2). A pressure flask was charged with **A.1** (1.25 g, 4.8 mmol), methylammonium chloride (450 mg, 6.7 mmol), triethylamine (1.0 mL, 6.7 mmol), ethanol (30 mL) and a stirring bar. The flask was sealed, stirred, and heated in a 120 °C oil bath for 48 h. The reaction mixture was then allowed to cool to room temperature. Precipitation from water (500 mL) followed by filtration and drying under vacuum gave **A.2** in a yield of 1.14 g (94%) as a fluffy yellow powder. M.p. = 176.7-177.3 °C. ^{1}H NMR (400 MHz, $CDCl_3$): δ 9.22 (s, 1H), 8.35 (br s, 2H), 5.61 (s, 1H), 3.25 (tq, 2H). 3.01 (d, J = 5.2, 3H), 1.80 (tq, J = 5.2, J = 7.6, 2H), 1.07 (t, J = 7.6, 3H); ^{13}C NMR (100 MHz, $CDCl_3$): δ 149.5, 148.7, 129.5, 124.1, 89.8, 89.8, 45.1, 29.9, 21.8, 11.6. HRMS: $[M+H]^+$ calced for $C_{10}H_{15}N_4O_4$, 255.1088; found, 255.1089.

1-Methyl-5-propylbenzobis(imidazole) (A.3). To a 50 mL RBF in a fume hood was added **A.2** (648 mg, 2.55 mmol), Pd/C (5%, 340 mg, mol%), sodium formate (3 g, 44.1 mmol), and formic acid (10 mL, 88%). The flask was fitted with a reflux condenser and heated to 90°C for 16 h. The reaction mixture was cooled and then diluted with methanol (20 mL) and filtered through a pad of celite. The filtrate was added drop wise to a 200 mL of 10% sodium carbonate. The mixture was extracted with dichloromethane which was then condensed to give a purple residue. The solid was chromatographed on silica with CH_2Cl_2/MeOH (9:1). A yellow band eluted first (rf = 0.4) which was collected and evacuated to give **A.3** as a pale thick oil in a yield of 277 mg (50%). M.p. = 100.8-103.2 °C. ^{1}NMR (400 MHz, $CDCl_3$): δ 8.17 (s, 1H), 7.90 (s, 1H), 7.85 (s, 1H), 7.18 (s, 1H), 4.15 (m, 1H), 3.84 (m, 3H), 1.94 (m, 2H), 0.96 (t, 3H); ^{13}C NMR (100 MHz, $CDCl_3$): δ 144.1, 163.6, 141.1, 140.9, 132.8, 132.1, 110.3, 88.0, 46.9, 31.2, 22.7, 11.4. HRMS: $[M+Na]^+$ calced for $C_{12}H_{14}N_4Na$, 237.1111; found, 237.1112.

N,N',N''-Trimethyl-N'''-propylbenzobis(imidazolium) diiodide (BBI-1). A 20 mL vial with a teflon lined cap was charged with 1-methyl-5-propylbenzobis(imidazole) (**A.3**) (121 mg, 0.56 mmol), methyl iodide (1 mL) acetonitrile (5 mL) and a magnetic stir bar. The vial was sealed and heated to 95 °C for 16 h with stirring. The reaction mixture was allowed to cool and the white solids were collected by filtration. The solids were then washed with 20 mL diethyl ether and dried under vacuum to give **BBI-1** (215 mg, 75%) M.p. = 230°C (dec). ^{1}H NMR (400 MHz, DMSO-d_6): δ 10.00 (s, 1H), 9.19 (s, 1H), 8.92 (s, 1H), 8.85 (s, 1H), 4.55 (m, 2H), 4.18 (s, 9H), 2.00 (m, 2H), 0.98 (m, 3H); ^{13}C NMR (100 MHz, DMSO-d_6): δ 146.6, 146.0, 130.8, 130.7, 130.6, 129.8, 98.6, 48.6, 34.1, 34.0, 33.9, 21.8, 10.7. HRMS: $[M-H]^+$ calced for $C_{14}H_{19}N_4$, 243.1604; found, 243.1606.

1,5-Di(1-oxobutylamino)-2,4-dinitrobenzene (A.5): A 50-mL round bottom flask was fitted charged with **A.4** (3.20 g, 16.2 mmol), butyryl chloride (20 mL) and a stir bar. The flask was fitted with a condenser and the reaction mixture was heated to 90°C in an oil bath for 48 h. The reaction mixture was allowed to cool and excess butyryl chloride was removed via rotary evaporation in a well ventilated fume hood. The residual tan colored solid was collected (5.30 g, 97%) and was determined to be the title compound and required no further purification. M.p. = 103-108 °C. ^{1}H NMR (400 MHz, $CDCl_3$): δ 10.66 (s, 2H), 10.44 (s, 1H), 9.21 (s, 1H), 2.50 (m, 4H), 1.77 (m, 4H), 1.01 (m, 6 H); ^{13}C NMR (400 MHz, $CDCl_3$): 171.9, 140.7, 129.0, 125.5, 111.2, 40.6, 18.3, 13.6. HRMS: $[M+H]^+$ calced for $C_{14}H_{19}N_4O_6$, 339.1305; found, 339.1308. HRMS: $[M+H]^+$ calced for $C_{14}H_{19}N_4O_6$, 339.1305; found, 339.1308.

1,5-Diamino-2,4-di(1-oxobutyl)aminobenzene (A.6): A 50-mL RBF was charged with **A.5** (1 g, 2.16 mmol), Pd/C (5%, 200 mg, mol% Pd), ethanol (40 mL). The reaction mixture was stirred under hydrogen (1 atm) for 20 h. The reaction mixture was filtered through a 45 μm PTFE filter. The solution was condensed to 5 mL and chilled

overnight in a -40 degree freezer. The white resulting white crystalline solid was collected by filtration and rinsed with minimal cool ethanol and dried under vacuum to give **A.6** in a yield of 600 mg (73%). M.p. = 156.02 °C (dec.). ^{1}NMR (400 MHz, DMSO-d_6): δ 8.86 (s, 2H), 6.79 (s, 1H), 6.05 (s, 1H), 4.48 (s, 4H), 2.20 (m, 4H), 1.57 (m, 4H), 0.89 (m, 6H); ^{13}C NMR (100 MHz, DMSO-d_6): δ 170.9, 140.8, 123.5, 113.5, 102.3, 37.5, 18.8, 13.6.

2,2'-Dipropylbenzobis(imidazole) (A.7a and A.7b): A 100 mL RBF was charged with 1,5-diamino-2,4-di(1-oxobutyl)aminobenzene (**A.6**) (362 mg, 1.3 mmol) and glacial acetic acid (30 mL) and a stir bar. The reaction mixture was heated 115 °C for 16 h. The solution was allowed to cool to room temperature and then the acetic acid was stripped under vacuum to leave a tan-colored residue which was washed with aqueous sodium bicarbonate until the filtrate was neutral. The solid was then washed with water and finally dried under vacuum to give 255 mg (81%) of the title compound as a tan solid. Two tautomers were observed by ^{1}H-NMR. M.p. = 249.5 °C (dec.). (400 MHz, DMSO-d_6): δ 11.81 (br, 2H), 7.53-7.26 (br, 2H), 2.75 (m, 4H), 1.75 (m, 4H), 0.94 (m, 6H). HRMS: $[M+H]^+$ calced for $C_{14}H_{19}N_4$, 243.1604; found, 243.1608.

N,N',N'',-N'''-Tetramethyl-2,2'-dipropylbenzobis(imidazolium) diiodide (BBI-2): A 20-mL screw-cap vial was charged with 2,2'-dipropylbenzo(bis)imidazole (**A.7**)(412 mg, 1.7 mmol, 1 eq), MeI (1 mL), sodium bicarbonate (286 mg, 3.4 mmol, 2 eq.) and a stir bar. The reaction mixture was heated to 90 °C for 8 h. The resulting precipitate was isolated by filtration and triturated with methanol. The resulting white powder was finally dried under vacuum to give a yield of 665 mg (68 %). M.p. = 278 °C (dec.). (400 MHz, $CDCl_3$): δ 8.77 (s, 2H), 4.15 (s, 12H), 3.37 (m, 4H), 1.80 (m, 4H), 1.06 (m, 6H); ^{13}C NMR (100 MHz, DMSO-d_6): δ 157.0, 130.2, 97.4, 32.5, 25.4, 19.6, 13.5. HRMS: $[M-2I]^{2+}$ calced for $C_{18}H_{18}N_4$, 150.1000; found, 150.1000.

N,N-Di(TRIPEG)-N,N-dimethylbenzobis(imidazolium) diiodide (BBI-3). Triethylene glycol 2-iodoethyl methyl ether (2.24 mmol) was added to a vial containing 145 mg benzo(bis)imidazole and 5 mL acetonitrile and stirred at 80 °C for 16 h. The solvent was evaporated and the residual material was triturated with ether, filtered, and dried under vacuum to give an amorphous pale solid. Yield: 75% ^{1}H-NMR (DMSO, 400 MHz) δ (ppm) = 3.16 (m, 6H), 3.41 (m, 5H), 3.46 (m, 4H), 3.57 (m, 4H), 3.95 (m, 4H), 4.20 (s, 5H), 4.77 (m, 4H), 8.87 (s, 1H), 8.94 (s, 1H), 9.92 (s, 1H). (DMSO, 100 MHz) δ (ppm) 146.4, 130.7, 130.0, 104.2, 99.0, 71.1, 69.6, 69.5, 69.4, 67.1, 58.0, 47.2, 33.9. T_m = 18 °C.

2,2'-Di-6-acetoxyhexyllbenzobis(imidazole) (A.8) In a nitrogen-filled glovebox, a 240 ml Shlenk flask was charged with 1,2-diamino-4,5-dimethylaminobenzene (862 mg, 5.19 mmol), CH_2Cl_2, a stirbar, and fitted with a rubber septum. The flask was taken out of the glovebox and subsequent manipulations were conducted using standard Schlenk technique. The reaction mixture was cooled to 0 °C and 4.8 ml of a solution of trimethylaluminum (2.0 M in toluene, 10.6 mmol) was added drop wise resulting in a gradual color change of the solution from pale pink to pale yellow and the evolution of a methane gas. After the addition was complete, the solution was stirred for 20 min before ε-caprolactone was added drop wise resulting in the instanteous formation of a white precipitate. The mixture was allowed to warm to 25 °C and stirred for 12 hours. At this point water was carefully added dropwise to quench residual aluminum alkyl species. Finally, the mixture was acidified with 5% aqueous ammonium hydroxide. The crude mixture was heated in 20 ml HOAc for 16 h. After cooling the solution, it was slowly added to an aqueous sodium bicarbonate solution. The mixture was then extracted with CH_2Cl_2. The organic phase was pushed through a pad of celite and the solvent was stripped from the filtrate to give the 986 mg of title compound as a tan powder (42%

yield). ^{1}H-NMR (DMSO, 500 MHz) δ (ppm) = 7.60 (s, 1H), 7.45 (s, 1H), 4.0 (t, *J* = 6.5, 4H), 3.74 (s, 6H), 2.84 (t, *J* = 6.5, 4H), 1.82 (s, 6H), 1.79 (m, 4H), 1.64 (m, 4H), 1.42 (m, 4H). NMR (DMSO, 125 MHz): 170.4, 154.7, 138.7, 133.1, 105.9, 88.5, 63.7, 54.9, 29.5, 27.8, 26.6, 26.3, 25.2, 20.7.

2,2'-Di-6-hydroxyhexyllbenzobis(imidazole) (A.9) A 100 ml RBF was charged with **A.8** (986 mg, 2.23 mmol), KOH pellets (1.2 g, 21 mmol), ethanol (50 ml), and dionized water (20 ml). The solution was warmed to 60 °C with stirring for 16 h. After allowing to cool to ambient temperature, the solution was neutralized with 5% HCl (aq). Excess acid was then neutralized with $NaHCO_3$ (aq.) which resulted in the formation of a precipitate. After isolation by filtration, the precipitate was extracted with 19:1 CH_2Cl_2/MeOH and pushed through a short plug of silica. A yellow band eluted which was stripped of solvent giving 1.2 g of a ellow residue 64% ^{1}H-NMR (DMSO, 400 MHz) δ (ppm) = 7.60 (s, 1H), 7.45 (s, 1H), 4.37 (t, *J* = 5.5, 2H), 3.74 (s, 6H), 3.40 (q, *J* = 6, 4H), 2.83 (t, *J* = 7.5), 1.78 (m, 4H), 1.50-1.40 (m, 8H). ^{13}C-NMR (DMSO, 100 MHz): 154.8, 138.7, 133.1, 105.9, 88.6, 60.6, 32.3, 29.6, 26.8, 26.7, 25.4. HRMS: $[M+H]^+$ calced for $C_{20}H_{31}N_4O_2$, 359.2442; found, 359.2448.

N,N',N'',-N'''-Tetramethyl-2,2'-dihydroxypentylbenzobis(imidazolium) diiodide (BBI-4): A vial was charged with **A.8** (262 mg, 0.731 mmol), methyl iodide (2 ml), acetonitrile (10 ml), and a stirbar. The vial was sealed, and heated with stirring to 60 °C for 12 h, by which time a white precipitate had formed. The mixture was filtered and the white precipitate was washed with four sequential 20 ml portions of diethyl ether. The white powder was dried under vacuum to afford 388 mg (82% yield of the title compound. ^{1}H NMR (D_2O , 400 MHz) δ (ppm) = 8.30 (s, 2H), 4.13 (s, 12 H), 3.61 (t, *J* = 6 Hz, 4H), 3.37 (t, *J* = 8.4 Hz, 4H), 1.87 (m, 4H), 1.62-1.55 (m, 8H). ^{13}C NMR (100)

MHz, DMSO-d_6): δ 157.2, 130.2, 97.3, 60.4, 32.3, 31.9, 25.8, 25.3, 23.8 19.6 HRMS: $[M\text{-}2I]^{2+}$ calced for $C_{22}H_{36}N_4O_2$, 194.1419; found, 194.1412.

ACKNOWLEDGEMENTS

This author thanks his undergraduate research assistants Michael Ortiz for assistance with the characterization of **BBI-1, BBI-2**, and **BBI-3** and Andrea Carranza for assistance with the synthesis of **BBI-3**.

REFERENCES

(1) Khramov, D. M.; Boydston, A. J.; Bielawski, C. W. *Org. Lett.* **2006**, *8*, 1831.

(2) Boydston, A. J.; Pecinovsky, C. S.; Chao, S. T.; Bielawski, C. W. *J. Am. Chem. Soc.* **2007**, *129*, 14550. Boydston, A. J.; Vu, P. D.; Dykhno, O. L.; Chang, V.; Wyatt, A. R. II; Stockett, A. S.; Ritschdorff, E. T.; Shear, J. B.; Bielawski, C. W. *J. Am. Chem. Soc.* **2008,** *130*, 3143.

(3) Boydston, A. J.; Bielawski, C. W. *Dalton Trans.* **2006**, 4073.

(4) Khramov, D. M.; Boydston, A. J.; Bielawski, C. W. *Angew. Chem. Int. Ed.* **2006**, *45*, 6186.

(5) Boydston, A. J.; Rice, J. D.; Sanderson, M. D.; Dykhno, O. L.; Bielawski, C. W. *Organometallics* **2006**, *25*, 6087

(6) Williams, K. A.; Boydston, A. J.; Bielawski, C. W. *Chem. Soc. Rev.* **2007**, *36*, 729.

(7) Tennyson, A. G.; Kamplain, J. W.; Bielawski, C. W. *Chem. Commun.* **2009**, 2124.

(8) Biedermann, F.; Rauwald, U.; Cziferszky, M.; Williams, K. A.; Gann, L. D.; Guo, B. Y.; Urbach, A. R.; Bielawski, C. W.; Scherman, O. A. *Chem. Eur. J.* **2010**, *16*, 13716.

(9) Matsushita, H.; Lee, S.-H.; Joung, M.; Clapham, B.; Janda, K. D. *Tet. Lett.* **2004**, *45*, 313

(10) Muddana, H. S.; Varnado, C. D.; Bielawski, C. W.; Urbach, A. R.; Isaacs, L.; Geballe, M. T.; Gilson, M. K. *J. Comput. Aided Mol. Des.* **2012**, *26*, 475.

Appendix B: Supporting Information for Chapter 2

GENERAL INFORMATION AND SYNTHESES

Materials and methods. $[Ir(COD)Cl]_2$ was purchased from Strem Chemicals and used without further purification. Dichloromethane (CH_2Cl_2) and toluene were distilled from CaH_2. Tetrahydrofuran was distilled from Na/benzophenone. Solvents were degassed by three consecutive freeze-pump-thaw cycles. All other reagents were purchased from commercial sources and used without further purification. ^1H and $^{13}C\{^1H\}$ NMR spectra were recorded using a Varian 300, 400 or 500 MHz spectrometer. Chemical shifts δ (in ppm) are referenced to tetramethylsilane using the residual solvent as an internal standard. For ^1H NMR: $CDCl_3$, 7.24 ppm; CD_2Cl_2, 5.32 ppm; CD_3CN, 1.94 ppm; C_6D_6, 7.15 ppm; DMSO-d_6, 2.49 ppm. For ^{13}C NMR: $CDCl_3$, 77.0 ppm; CD_2Cl_2, 53.8 ppm; C_6D_6, 128.0 ppm; DMSO-d_6, 39.5 ppm. Coupling constants are expressed in hertz (Hz). FT-IR spectra were recorded using Perkin-Elmer Spectrum BX system. High-resolution mass spectra (HRMS) were obtained with a VG analytical ZAB2-E instrument (ESI or CI). Unless otherwise noted, all reactions were performed under an atmosphere of nitrogen using standard Schlenk or glovebox techniques.

Electrochemistry. Electrochemical experiments were conducted on CH Instruments Electrochemical Workstations (series 660D and 700B) using a gas-tight, three-electrode cell under an atmosphere of dry nitrogen. The cell was equipped with platinum working, platinum counter and silver quasi-reference electrodes. Measurements were performed in dry CH_2Cl_2 with 0.1 M [tetra-*n*-butylammonium][PF_6] (TBAP) as the electrolyte and decamethylferrocene (Fc*) as the internal standard. Unless otherwise noted, all potentials noted were determined at 100 mV s^{-1} scan rates and referenced to saturated calomel electrode (SCE) by shifting $(Fc^*)^{0/+}$ to –0.057 V (CH_2Cl_2).[1]

Crystallography. Data were collected on a Nonius Kappa CCD diffractometer using a graphite monochromator with MoKα radiation (λ = 0.71073 Å) at 153 K using an Oxford Cryostream low temperature device. Key details of the crystal and structure refinement data are summarized in Tables S1–S4 of the original manuscript. Data reduction were performed using DENZO-SMN.[2] The structures were solved by direct methods using SIR97[3] and refined by full-matrix least-squares on F^2 with anisotropic displacement parameters for the non-H atoms using SHELXL-97.[4] The hydrogen atoms were calculated in idealized positions. Neutral atom scattering factors and values used to calculate the linear absorption coefficient are from the International Tables for X-ray Crystallography (1992). Further crystallographic details may be found in the respective CIF files, which were deposited at the CCDC, Cambridge, UK.

Syntheses.

[Ag(2.1)(μ–I)]$_2$. A mixture of [**2.1**H][I] (340 mg, 0.60 mmol), Ag_2O (70 mg, 0.30 mmol), and 1,2-dichloroethane (10 mL) was stirred at ambient temperature for 15 h. Precipitated solids were collected by filtration and dried under high vacuum to afford 380 mg (94% yield) of the desired compound as a pale yellow powder. ^{1}H NMR ($CDCl_3$): δ 7.32 (s, 2H), 4.86 (s, 4H), 4.32 (s, 10H), 4.27 (s, 4H). ^{13}C NMR spectra could not be obtained due to the poor solubility of this compound. HRMS Calcd for $C_{46}H_{40}N_4AgFe_2$ [$(M–AgI_2)^+$]: 978.9703. Found: 978.9696.

[Ir(COD)Cl(1)] (2.1a). A mixture of [Ag(**2.1**)(μ–I)]$_2$ (48 mg, 0.36 mmol), [Ir(COD)(μ–Cl)]$_2$ (24 mg, 0.036 mmol), and CH_2Cl_2 (5 mL) was stirred at ambient temperature for 6 h. The reaction mixture was then filtered through a PTFE filter and concentrated under reduced pressure to afford 60 mg (99% yield) of the desired product as a yellow powder. ^{1}H NMR (CD_2Cl_2): δ 7.44–7.42 (m, 2H), 5.79 (s, 2H), 4.73–4.72 (m, 2H), 4.41 (s, 2H), 4.28 (s, 10H), 4.26-4.22 (m, 4H), 2.42 (s, 2H), 1.98 (br s, 2H), 1.71 (br

s, 2H), 1.51 (br s, 2H), 1.28 (br s, 2H). ^{13}C NMR ($CDCl_3$): δ 182.16, 121.83, 97.17, 82.45, 77.20, 69.60, 68.81, 65.89, 65.66, 62.54, 51.74, 32.88, 29.22. HRMS Calcd. for $C_{31}H_{32}N_2Fe_2Ir$: [(M–Cl)$^+$]: 737.0891. Found: 737.0888. CCDC: 742794.

[Ir(CO)$_2$Cl(1)] (2.1b). Complex **2.1a** (51 mg, 0.066 mmol) was dissolved in CH_2Cl_2 (5 mL) and stirred under an atmosphere of CO (g) for 1 h. Subsequent removal of the solvent under reduced pressure followed by trituration with pentane afforded 42 mg (88% yield) of the desired product as a yellow powder. ^{1}H NMR ($CDCl_3$): δ 7.55 (s, 2H), 5.26 (s, 2H), 4.80 (s, 2H), 4.29 (s, 10H), 4.26 (s, 4H). ^{13}C NMR ($CDCl_3$): δ 180.7, 174.9, 167.6, 123.2, 96.8, 69.8, 67.5, 66.41, 66.38, 64.9. FT-IR (CD_2Cl_2): ν = 2065 (CO, *trans*), 1983 (CO, *cis*) cm^{-1}. HRMS Calcd. for $C_{25}H_{20}N_2O_2Fe_2Ir$ [(M–Cl)$^+$]: 684.9854. Found: 684.9847. CCDC: 742795.

N,N'-Diferrocenyl-1,2-diaminobenzene. A pre-catalyst for mediating aryl amination coupling reactions was prepared by charging a 20 mL vial with 1,3-bis(2,6-diisopropylphenyl)imidazolium chloride (0.150 g, 0.34 mmol), NaO*t*Bu (0.033 g, 0.34 mmol), Pd(OAc)$_2$ (0.038 g, 0.17 mmol), toluene (5 mL), and a stir bar followed by stirring this mixture at ambient temperature for 10 min. This mixture was then added to a 100 mL flask containing 1,2-bromobenzene (2.0 g, 8.48 mmol) and toluene (30 mL). Aminoferrocene[5] (3.4 g, 17 mmol) and NaO*t*Bu (1.63 g, 17 mmol) were then added, and the resulting mixture was sealed and stirred at 110 ºC for 12 h. Precipitated solids were removed by hot filtration of the crude reaction under a cone of nitrogen and then washed with 10 mL of degassed THF. The organic fractions were combined and then dried under reduced pressure to afford 4.02 g (98% yield) of the desired product as a red oil that slowly crystallized upon standing. ^{1}H NMR ($CDCl_3$): δ 7.23–7.20 (m, 2H), 6.92–6.90 (m, 2H), 4.66 (br, 2H), 4.15 (s, 10H), 4.11 (t, J = 2, 4H), 3.98 (t, J = 2, 4H). ^{13}C NMR

($CDCl_3$): δ 134.8, 120.6, 117.2, 102.4, 68.9, 64.3, 60.5. HRMS Calcd. for $C_{26}H_{24}N_2Fe_2$ [M^+]: 476.0638. Found: 476.0641.

[1,3-Diferrocenylbenzimidazolium][Cl] [2.2H][Cl]. A 10 mL flask was charged with trimethylorthoformate (30 mL), N,N'-diferrocenyl-1,2-diaminobenzene (590 mg, 1.34 mmol), and 1 M HCl (1.5 mL). The reaction mixture was then heated to 55 °C for 24 h. The solids which precipitated from the reaction were collected by filtration, washed with Et_2O (15 mL), and dried under reduced pressure to afford 650 mg (93% yield) of the desired product as a brown-yellow powder. ^{1}H NMR (DMSO-d_6): δ 10.15 (s, 1H), 8.45 (br, 2H), 7.87 (br, 2 H), 5.19 (br, 4H), 4.56 (br, 4H), 4.39 (br, 10H). ^{13}C NMR (DMSO-d_6): δ 129.6, 125.9, 113.7, 89.9, 68.7, 61.7. HRMS Calcd. for $C_{27}H_{23}N_2Fe_2$ [$(M–Cl)^+$]: 487.0560. Found: 487.0559.

[Ir(COD)Cl(2)] (2.2a). A reaction vessel was charged with [**2.2**H][Cl] (79 mg, 0.15 mmol), $[Ir(COD)Cl]_2$ (50 mg, 0.075 mmol), KO*t*Bu (17 mg, 0.151 mmol), and THF (5 mL) and then stirred for 12 h at 60 °C. The resulting brown colored mixture with a suspension of fine yellow solids was diluted with an equal volume of CH_2Cl_2 to dissolve the yellow powder and then filtered through a 0.45 μm PTFE filter to remove the inorganic salts. Drying the filtrate under reduced pressure afforded 125 mg (100% yield) of the desired complex as dark yellow solid. ^{1}H NMR ($CDCl_3$): δ 8.37–8.35 (m, 2H), 7.45–7.43 (m, 2H), 6.26 (s, 2H), 4.62 (s, 2H), 4.54 (br, 2H), 4.41 (s, 4H), 4.37 (s, 10H), 2.15 (br, 2H), 1.98 (br, 2H), 1.47 (br, 2H), 1.2 (br, 2H). ^{13}C NMR ($CDCl_3$): δ 194.1, 135.3, 122.8, 112.9, 96.0, 83.4, 69.9, 68.8, 66.3, 65.2, 61.7, 52.3, 32.7, 28.9. HRMS: Calcd. for $C_{35}H_{34}N_2ClFe_2Ir$ [M^+]: 822.0739. Found: 822.0725. CCDC: 742796.

[Ir(CO)$_2$Cl(2.2)] (2.2b). Complex **2.2a** (0.1 g, 0.2 mmol) was dissolved in CH_2Cl_2 (5 mL) and stirred under an atmosphere of CO (g) for 1 h. The volume of the solution was reduced to 2 mL and 10 mL hexanes was added. The precipitated solids

were collected by filtration and triturated with 10 mL of hexanes. Removal of the residual solvent under reduced pressure afforded 80 mg (92% yield) of the desired complex as a yellow powder. ^{1}H NMR ($CDCl_3$): δ 8.51 (m, 2H), 7.55 (m, 2H), 5.54 (br, 2H), 4.95 (br, 2H), 4.38–4.36 (br, 4H), 4.31 (s, 10H). ^{13}C NMR ($CDCl_3$): δ 184.0, 180.4, 167.2, 134.6, 124.0, 114.1, 95.3, 69.8, 67.4, 66.3, 65.9, 64.2. FT-IR (CD_2Cl_2): ν = 2066 (CO, *trans*), 1984 (CO, *cis*) cm^{-1}. HRMS Calcd. for $C_{29}H_{22}N_2O_2ClFe_2Ir$ [M$^+$]: 769.9698. Found: 769.9691. CCDC: 742797.

N-Ferrocenyl-2-nitroaniline. A mixture of aminoferrocene[5] (402 mg, 2.2 mmol), 2-fluoronitrobenzene (282 mg, 2.0 mmol), sodium bicarbonate (184 mg, 2.2 mmol), and DMSO (10 mL) was stirred at 120 °C for 24 h. After allowing the mixture to cool to ambient temperature, it was poured into water (300 mL) and then filtered through a sintered glass frit. The brown filtered material was purified by column chromatography using 9:1 hexanes / ethyl acetate as the eluent and silica gel as the stationary phase (R_f = 0.55) to afford 592 mg (92% yield) of the desired product as a red solid. ^{1}H NMR ($CDCl_3$): δ 9.13 (s, 1H), 8.18–8.14 (m, 1H), 7.35 (br s, 1H), 7.12–7.09 (m, 1H), 6.72–6.68 (m, 1H), 4.38 (t, *J* = 1.8, 2H), 4.27 (s, 5H), 4.18 (t, *J* = 1.8, 2H). ^{13}C NMR ($CDCl_3$): δ 145.2, 135.6, 126.3, 116.4, 115.9, 94.2, 69.6, 66.1, 65.8. HRMS Calcd. for $C_{16}H_{14}N_2O_2Fe$ [M$^+$]: 322.0404. Found: 322.03992.

1-Ferrocenylbenzimidazole. A mixture of N-ferrocenyl-2-nitroaniline (493 mg, 1.53 mmol), sodium formate (1.0 g, 15 mmol), Pd/C (5 wt %, 0.09 mmol Pd, 0.06 equiv Pd), and formic acid (88%, 20 mL) was heated to 110°C with stirring for 48 h. Upon completion, the reaction mixture was allowed to cool to ambient temperature and then filtered slowly through a PTFE filter into aqueous solution of sodium carbonate (10% w/v, 150 mL). An orange solid precipitated obtained which was then extracted with ethyl acetate. The organic phase was washed with water, dried over Na_2SO_4, and concentrated

under reduce pressure to afford 430 mg (93% yield) of the desired product. Spectral data matched literature reports.[6]

[1-Ferrocenyl-3-methylbenzimidazolium][I] [2.3H][I]. A mixture of 1-ferrocenylbenzimidazole (200 mg, 0.66 mmol), methyl iodide (1.0 mL), acetonitrile (5.0 mL) and a stir bar were stirred at 50 °C for 5 h. Removal of the residual solvent under vacuum afforded 293 mg (99% yield) of the desired product. Spectral data matched literature reports.[7]

[Ag(2.3)(μ–I)]$_2$. A mixture of [**2.3**H][I] (116 mg, 0.26 mmol), Ag_2O (30 mg, 0.52 mmol), and CH_2Cl_2 (5.0 mL) and stirred in covered reaction vessel at ambient temperature for 16 h. Pentane (5 mL) was then added which caused yellow solids to precipitate. Collection of these solids by vacuum filtration afforded 130 mg (91% yield) of the desired product. Neither ^{1}H nor ^{13}C NMR spectra could be obtained due to the poor solubility of this compound. HRMS Calcd. for $C_{36}H_{32}N_4AgFe_2$ [(M–AgI$_2$)$^+$]: 739.0365. Found: 739.03712.

[Ir(COD)Cl(2.3)] (2.3a). A mixture of [Ag(**2.3**)(μ–I)]$_2$ (93 mg, 0.17 mmol), [Ir(COD)Cl]$_2$ (56 mg, 0.085 mmol) and CH_2Cl_2 (5 mL) was stirred at ambient temperature for 12 h in a covered reaction vessel. The mixture was then filtered through a PTFE filter and condensed to give an orange foam. Dissolution of this material in chloroform followed by precipitation from pentane afforded 110 mg (99% yield) of the desired product as a yellow powder. ^{1}H NMR ($CDCl_3$): δ 8.22–8.20 (m, 1H), 7.36–7.33 (m, 3H), 6.32–6.31 (m, 1H), 4.74–4.66 (m, 2H), 4.48 (s, 1H), 4.37 (s, 1H), 4.36 (s, 1H), 4.27 (s, 5H), 4.24 (s, 3H), 2.73 (br s, 1H), 2.31 (br s, 1H), 2.13 (br s, 3H), 1.70 (br s, 3H), 1.31 (br s, 2H). ^{13}C NMR ($CDCl_3$): δ 192.6, 135.7, 134.6, 122.9, 122.3, 112.5, 109.6, 96.0, 85.4, 84.8, 69.5, 69.0, 66.2, 65.8, 64.9, 61.0, 52.8, 52.2, 34.7, 33.6, 32.7, 29.6, 29.0. HRMS Calcd. for $C_{26}H_{28}N_2FeIr$ [(M–Cl)$^+$]: 617.1233. Found: 617.12257. CCDC: 742801.

[Ir(CO)$_2$Cl(2.3)] (2.3b). A solution of **2.3a** (60 mg, 0.088 mmol) in CH_2Cl_2 (5.0 mL) was stirred under an atmosphere of CO(g) for 30 min at ambient temperature. Concentration of the mixture produced a yellow powder that was triturated with pentane and dried under high vacuum to afford 52 mg (100% yield) the desired product. ^{1}H NMR ($CDCl_3$): δ 8.40–8.37 (m, 1H), 7.52–7.50 (m, 2H), 5.63 (s, 1H), 4.76 (s, 1H), 4.37 (br s, 2H), 4.29 (s, 5H), 4.18 (s, 3H). ^{13}C NMR ($CDCl_3$): δ 183.4, 180.8, 167.27, 135.14, 134.03, 124.42, 123.87, 113.80, 110.92, 95.32, 69.73, 68.03, 66.72, 65.52, 62.86, 35.58. FT-IR (CH_2Cl_2, NaCl): ν = 2068 (CO, *trans*), 1988 (CO, *cis*) cm^{-1}. HRMS Calcd. for $C_{20}H_{16}N_2O_2IrFe$ [(M–Cl)$^+$]: 565.0182. Found: 565.0185. CCDC: 742802.

X-RAY CRYSTALLOGRAPHY

Table B.1 Summary of Crystal Data, Intensity Collection, & Refinement Parameters for **2.1a–b** and **2.2a–b**.

	2.1a	**2.1b** [d]	**2.2a** [e]	**2.2b** [f]
CCDC No.	742883	742795	742796	742797
crystallization conditions [a]	pentane v.d. $CHCl_3$	pentane v.d. $CHCl_3$	pentane v.d. $CHCl_3$	pentane v.d. $CHCl_3$
formula	$C_{31}H_{32}ClN_2Fe_2Ir$	$C_{25}H_{20}ClN_2O_2Fe_2Ir$	$C_{37}H_{36}Cl_7N_2Fe_2Ir$	$C_{29}H_{22}ClN_2O_2Fe_2Ir$
MW (g mol^{-1})	771.96	719.80	1060.75	769.86
morphology	yellow needles	orange prisms	yellow needles	yellow laths
dimensions (mm)	0.26 × 0.06 × 0.05	0.22 × 0.12 × 0.11	0.22 × 0.07 × 0.04	0.30 × 0.12 × 0.04
crystal system	monoclinic	monoclinic	orthorhombic	monoclinic
space group	$P2_1/c$	$P2_1/c$	Pnma	$P2_1/n$
a (Å)	7.5690(3)	7.4024(4)	19.6920(1)	7.4270(1)
b (Å)	18.8851(9)	15.8832(8)	20.2716(3)	18.5130(3)
c (Å)	18.0949(12)	19.3124(12)	9.4088(4)	17.9910(3)
α (deg)	90	90	90	90
β (deg)	96.052(2)	91.036(3)	90	91.830(1)
γ (deg)	90	90	90	90
V (Å^3)	2572.1(2)	2270.3(2)	3755.88(17)	2472.43(7)
Z	4	4	4	4
ρ_{calc} (g cm^{-3})	1.993	2.106	1.876	2.068
μ (mm^{-1})	6.403	7.252	4.826	6.667
F(000)	1512	1384	2080	1488
θ range (deg)	2.71 – 25.00	2.11 – 27.48	1.00 – 27.49	2.20 – 27.49
total / unique reflections	8659 / 4489	18301 / 5193	39719 / 4417	11113 / 5678
completeness to 2θ (%)	99.4	99.7	99.7	99.9
data / restraints / parameters	4489 / 0 / 334	5193 / 212 / 345	4417 / 58 / 247	5678 / 4 / 348
GoOF	1.093	1.290	1.036	1.057
R_1 [b]	0.0531	0.0502	0.0322	0.0281
wR_2 [c]	0.1061	0.1206	0.0682	0.0633
Largest diff. peak, hole (*e* Å^{-3})	2.157, –1.474	1.803, –1.535	1.642, –0.621	0.936, –0.927

[a] v.d. = "vapor diffusion into a saturated solution in." s.e. = "slow evaporation of a saturated solution in." [b] $R_1 = \Sigma \mid |F_o| - |F_c| \mid / \Sigma |F_o|$; [c] $wR_2 = \{\Sigma [w(F_o^2 - F_c^2)^2] / \Sigma [w(F_o^2)^2]\}^{1/2}$. [d] One Cp ring displayed rotational disorder around the Cp centroid-Fe axis, which was modeled via partial occupancy. [e] The unit cell contained two molecules of $CHCl_3$. [f] The Cl and CO *cis* to the NHC exhibited positional disorder (w.r.t. each other) and were modeled via partial occupancy.

Table B.2 Summary of Crystal Data, Intensity Collection, & Refinement Parameters for **2.3a** and **2.3b**.

	2.3a [d]	**2.3b** [E]
CCDC No.	742801	742802
crystallization conditions [a]	pentane v.d. $CHCl_3$	pentane v.d. $CHCl_3$
formula	$C_{26}H_{28}ClN_2FeIr$	$C_{20}H_{16}ClN_2O_2FeIr$
MW (g mol^{-1})	652.02	599.87
morphology	yellow prisms	yellow prisms
dimensions (mm)	0.30 × 0.10 × 0.08	0.34 × 0.12 × 0.08
crystal system	triclinic	orthorhombic
space group	P_{-1}	$P2_12_12_1$
a (Å)	10.5057(7)	11.0906(6)
b (Å)	12.067(3)	12.0344(7)
c (Å)	18.0463(10)	14.1340(11)
α (deg)	92.810(2)	90
β (deg)	90.445(2)	90
γ (deg)	95.642(2)	90
V (Å^3)	2273.8(2)	1886.5(2)
Z	4	4
ρ_{calc} (g cm^{-3})	1.905	2.112
μ (mm^{-1})	6.619	7.975
F(000)	1272	1144
θ range (deg)	1.70 – 27.50	2.22 – 27.49
total / unique reflections	20296 / 20302	18802 / 4288
completeness to 2θ (%)	99.0	99.7
data / restraints / parameters	20302 / 0 / 562	4288 / 0 / 246
GoOF	1.171	1.065
R_1 [b]	0.0508	0.0230
wR_2 [c]	0.1328	0.0445
Largest diff. peak, hole (*e* Å^{-3})	1.703, –2.164	0.457, –0.790

[a] v.d. = "vapor diffusion into a saturated solution in." s.e. = "slow evaporation of a saturated solution in." [b] $R_1 = \Sigma \mid |F_o| - |F_c| \mid / \Sigma |F_o|$; [c] $wR_2 = \{\Sigma [w(F_o^2 - F_c^2)^2] / \Sigma [w(F_o^2)^2]\}^{1/2}$. [d] This crystal was twinned. [e] This crystal was a racemic twin.

Table B.3 Selected Spectroscopic and Structural Data for [Ir(COD)Cl] Complexes (**2.1**–**2.6**)a.

	δ (ppm) [a]	M–C_{NHC} (Å)	M–C_{trans} (Å) [b]	M–C_{cis} (Å) [b]	N–C–N (°)
1a	182.2	2.022(10)	2.200(9)	2.122(9)	102.8(8)
2a	194.1	2.020(5)	2.189(4)	2.112(4)	105.3(4)
3a	192.6	2.030(7)	2.191(7)	2.110(7)	105.4(5)
4a	191.9	—	—	—	—
5a	213.2	2.068(3)	2.167(3)	2.104(3)	121.9(3)
6a	194.6	2.033(5)	2.191(4)	2.102(4)	103.8(4)

[a] ^{13}C NMR shifts for the 2-position obtained in $CDCl_3$. [b] Averaged over the two equivalent positions.

Table B.4 Selected ^{13}C NMR Spectroscopic and Structural Data for $[Ir(CO)_2Cl]$ Complexes (**2.1**–**2.6**)**b**.

	δ (ppm) [a]	M–C_{NHC} (Å)	M–C_{trans} (Å)	M–C_{cis} (Å)	N–C–N (°)
1b	180.7	2.089(6)	1.892(8)	1.859(11)	105.9(5)
2b	184.0	2.080(4)	1.894(4)	1.879(9)	106.1(3)
3b	183.4	2.071(3)	1.877(4)	1.827(4)	105.7(3)
4b	182.3	—	—	—	—
5b	202.4	2.121(3)	1.891(3)	1.888(4)	122.4(2)
6b	186.9	2.071(4)	1.900(5)	1.843(5)	105.5(3)

[a] ^{13}C NMR shifts for the 2-position carbon obtained in $CDCl_3$.

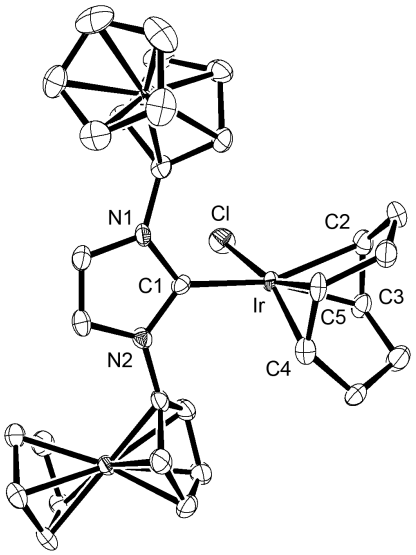

Figure B.1 ORTEP diagram showing 50% probability thermal ellipsoids and selected atom labels for **2.1a**. Hydrogen atoms have been omitted for clarity. Selected bond lengths (Å) and angles (°): Ir–Cl, 2.366(2); Ir–C1, 2.022(10); Ir–C2, 2.180(9); Ir–C3, 2.219(8); Ir–C4, 2.123(9); Ir–C5, 2.121(9); N1–C1–N2, 102.8(8). The COD bite angle is 86.2°.

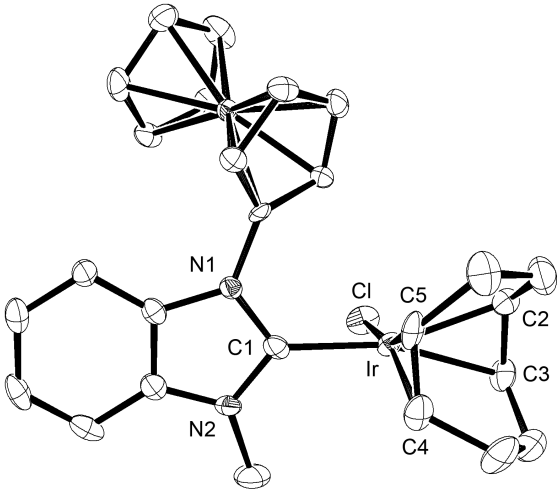

Figure B.2 ORTEP diagram showing 50% probability thermal ellipsoids and selected atom labels for **2.3a**. Hydrogen atoms have been omitted for clarity. Selected bond lengths (Å) and angles (°): Ir–Cl, 2.3755(17); Ir–C1, 2.028(6); Ir–C2, 2.194(6); Ir–C3, 2.177(6); Ir–C4, 2.106(7); Ir–C5, 2.109(6); N1–C1–N2, 105.4(5). The COD bite angle is 86.5°.

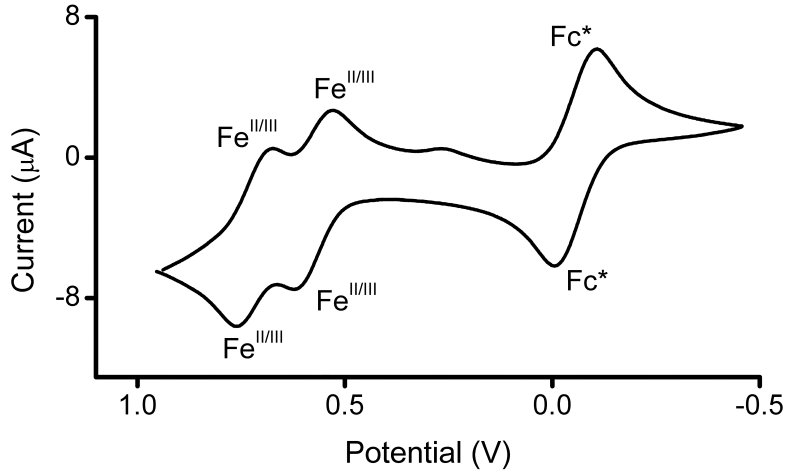

Figure B.3 CV of **2.1a** in CH_2Cl_2 with 0.1 M $[Bu_4N][PF_6]$ and Fc* internal standard.

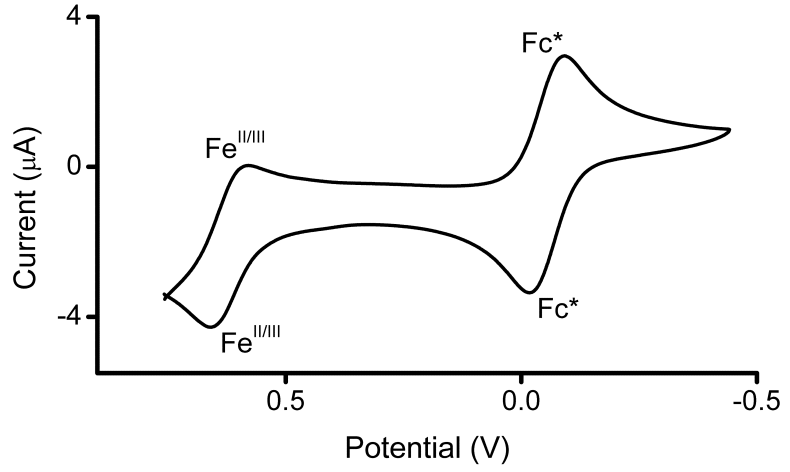

Figure B.4 CV of **2.3a** in CH_2Cl_2 with 0.1 M $[Bu_4N][PF_6]$ and Fc* internal standard.

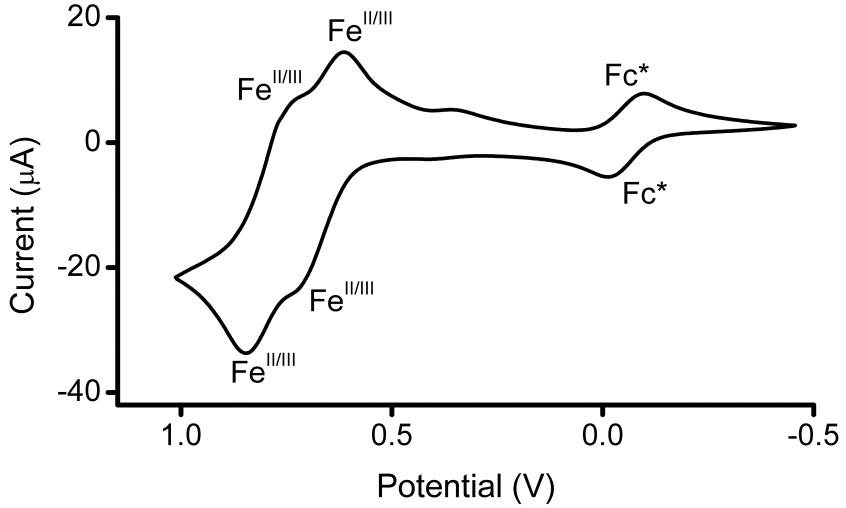

Figure B.5 CV of **2.1b** in CH_2Cl_2 with 0.1 M $[Bu_4N][PF_6]$ and Fc* internal standard.

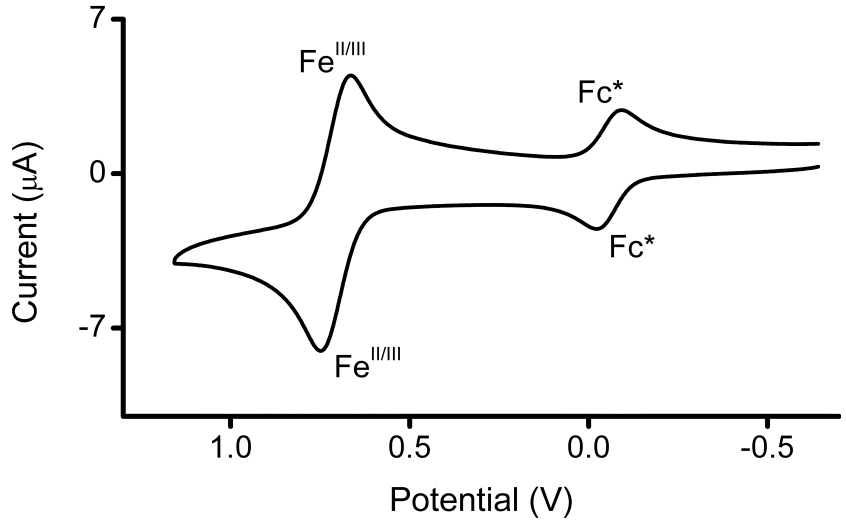

Figure B.6 CV of **2.3b** in CH_2Cl_2 with 0.1 M $[Bu_4N][PF_6]$ and Fc* internal standard.

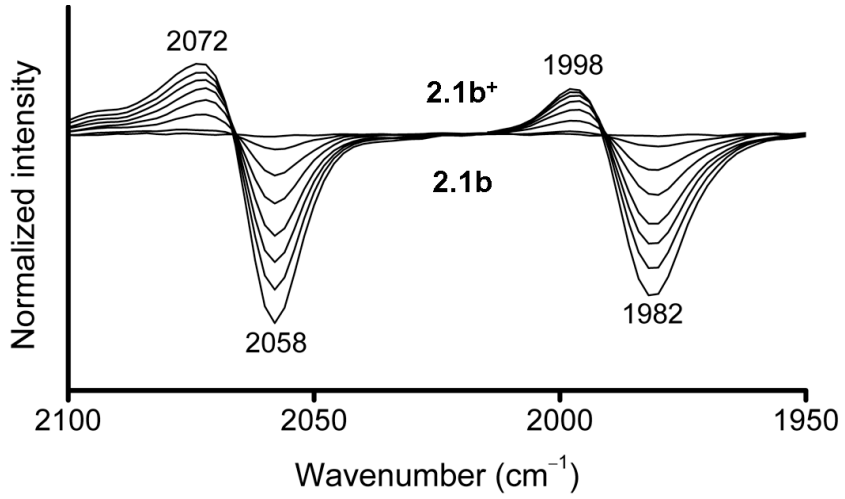

Figure B.7 Normalized IR difference spectra at 60 s intervals upon oxidation (E_{app} = +1.2 V) of **2.1b** in CH_2Cl_2 with 0.1 M $[Bu_4N][PF_6]$.

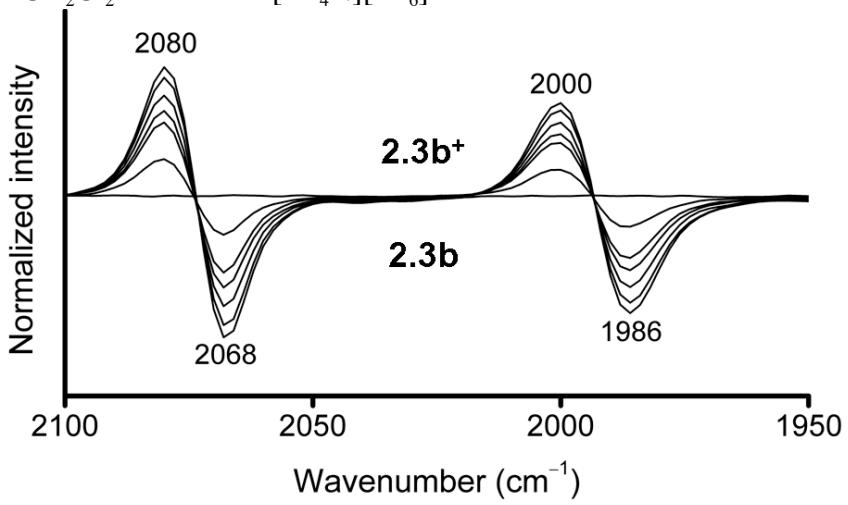

Figure B.8 Normalized IR difference spectra at 60 s intervals upon oxidation (E_{app} = +1.2 V) of **2.3b** in CH_2Cl_2 with 0.1 M $[Bu_4N][PF_6]$.

REFERENCES

(1) Noviandri, I.; Brown, K. N.; Fleming, D. S.; Gulyas, P. T.; Lay, P. A.; Masters, A. F.; Phillips, L. *J. Phys. Chem. B* **1999**, *103*, 6713–6722.

(2) Otwinowski, Z.; Minor, W. In *Macromolecular Crystallography, Part A*; Carter Jr., C. W., Sweets, R. M., Eds.; Academic Press: 1997; Vol. 276, p 307–326.

(3) Altomare, A.; Burla, M. C.; Camalli, M.; Cascarano, G. L.; Giacovazzo, C.; Guagliardi, A.; Moliterni, A. G. G.; Polidori, G.; Spagna, R. *J. Appl. Cryst.* **1999**, *32*, 115–119.

(4) Sheldrick, G. M. In *SHELXTL00: Program for Refinement of Crystal Structures*; University of Göttingen: Göttingen, Germany, 2000.

(5) Bildstein, B.; Malaun, M.; Kopacka, H.; Wurst, K.; Mitterböck, M.; Ongania, K.-H.; Opromolla, G.; Zanello, P. *Organometallics* **1999**, *18*, 4325–4336.

(6) Purecha, V. H.; Nandurkar, N. S.; Bhanage, B. M.; Nagarkar, J. M. *Tet. Lett.* **2008**, *49*, 1384–1387.

(7) Bildstein, B.; Malaun, M.; Kopacka, H.; Ongania, K.-H.; Wurst, K. *J. Organomet. Chem.* **1999**, *572*, 177–187.

Appendix C: Supporting Information for Chapter 4

Synthesis and Discussion of 4.19 4.20

(4.5)(PCy$_3$)Cl$_2$Ru=CHPh (4.19). A 6 mL glass vial equipped with a stir bar was charged with [**4.5**H][BF$_4$] (**4.12**) (56.1 mg, 0.164 mmol), NaHMDS (30.3 mg, 0.165 mmol) and toluene (4 mL), and then sealed with a Teflon lined cap. The reaction mixture was stirred for 5 min at ambient temperature. Subsequently, (PCy$_3$)$_2$Cl$_2$Ru=CHPh (**4.6**) (40.5 mg, 0.0492 mmol) was added and the vial was re-sealed with a Teflon lined cap. The solution was stirred at ambient temperature for 10 min. The resulting brown mixture was then loaded directly onto a chromatography column (media SiO$_2$, eluent 10:1 v/v hexanes/ethyl acetate). The column was washed with the aforementioned solvent ratio until unreacted **4.6** eluted as a bright purple solution. The column was then washed with ethyl acetate and the product eluted as a lime green solution. Evaporation of the solvent under reduced pressure yielded a lime green solid. A solution of hexanes/ethyl acetate (20:1 v/v, 10 mL) was then added which caused precipitation of a pale green powder which was collected by vacuum filtration to give the desired compound (22.4 mg, 57% yield). The compound was found to decompose in solution over a period of hours at room temperature; thus, NMR spectra were recorded at –80 °C. ^{1}H NMR (500 MHz, CD$_2$Cl$_2$, –80 °C)$^{):1}$ δ 19.61 (d, 1H, *J* = 4.5), 9.04 (s, 1H), 7.74 (s, 1H), 7.59 (t, 1H, *J* = 7.0), 7.36 (br s, 2H), 4.40 (s, 1H), 4.30 (s, 2H), 4.22–4.16 (m, 5H), 4.09 (s, 3H), 2.73 (s, 3H), 2.08–0.75 (m, 30H). ^{13}C NMR (125 MHz, CD$_2$Cl$_2$, -80 °C): δ 299.7, 223.6 (d, *J* = 76.6), 151.2, 130.8, 129.3, 128.7, 128.1, 127.8, 98.3, 97.21, 97.18, 71.7, 71.0, 70.4, 70.3, 66.5, 66.4, 66.3, 65.5, 49.8, 45.5, 31.2 (br), 28.3, 27.1 (br), 26.0. ^{31}P NMR (200 MHz, CD$_2$Cl$_2$, –80 °C): δ 35.86. HRMS: [M$^+$-Cl] Calcd. for C$_{38}$H$_{54}$N$_2$PClFeRu: 762.2106; Found 762.2098.

Anal. Calcd (%) for $C_{38}H_{53}Cl_2FeN_2PRu$: C, 57.29; H, 6.71; N, 3.52. Found: C, 57.43; H, 6.78; N, 3.67.

(4.5)(SIMes)Cl_2Ru=CHPh (4.20). A 6 mL glass vial equipped with a stir bar was charged with **4.12** (43.8 mg, 0.128 mmol), NaHMDS (23.2 mg, 0.127 mmol) and toluene (4 mL), and then sealed with a Teflon lined cap. The reaction mixture was stirred for 5 min at ambient temperature. (SIMes)(pyridine)$_2$$Cl_2$Ru=CHPh (46.5 mg, 0.064 mmol) was added and the vial was re-sealed with a Teflon lined cap. The solution was stirred at ambient temperature for 1 h and then concentrated under reduced pressure to afford a brown solid. The solid was then purified using column chromatography (media SiO_2, eluent 3:1 v/v hexanes/ethyl acetate). Removal of the solvent by evaporation under reduced pressure yielded the product as a lime green solid (26.5 mg, 50% yield). ^{1}H NMR (600 MHz, CD_2Cl_2): δ 19.04 (s, 1H), 7.45 (tt, J = 7.3, 1.1, 1H), 7.16 (t, J = 7.8, 2H), 7.01 (br s, 2H), 6.94 (br s, 1H), 6.19 (br s, 1H), 4.23–3.74 (br m, 12H), 3.08 (s, 3H), 2.82 (br s, 3H), 2.68 (br s, 3H), 2.45 (br s, 3H), 2.36 (s, 3H), 2.30 (s, 3H), 2.19 (s, 3H), 1.74 (br s, 3H). ^{13}C NMR (125 MHz, CD_2Cl_2): δ 303.4, 226.4, 219.6, 150.1, 138.7, 138.5, 138.3, 137.6, 137.1, 136.9, 136.6, 135.5, 130.2, 129.1, 128.9, 128.7, 128.6, 128.5, 127.5, 126.4, 98.1, 96.8, 71.4, 70.8, 69.7, 66.3, 66.2, 66.1, 64.9, 51.2, 50.5, 49.3, 43.7, 20.65, 20.59, 19.0, 18.8, 18.1, 17.2. HRMS: [M^+] Calcd. for $C_{41}H_{46}N_4Cl_2FeRu$: 822.1492; Found: 822.1493. Anal. Calcd (%) for $C_{41}H_{46}N_4Cl_2FeRu$•0.25(C_6H_{14}): C, 60.47; H, 5.91; N, 6.64. Found: C, 60.69; H, 5.91; N, 6.38.

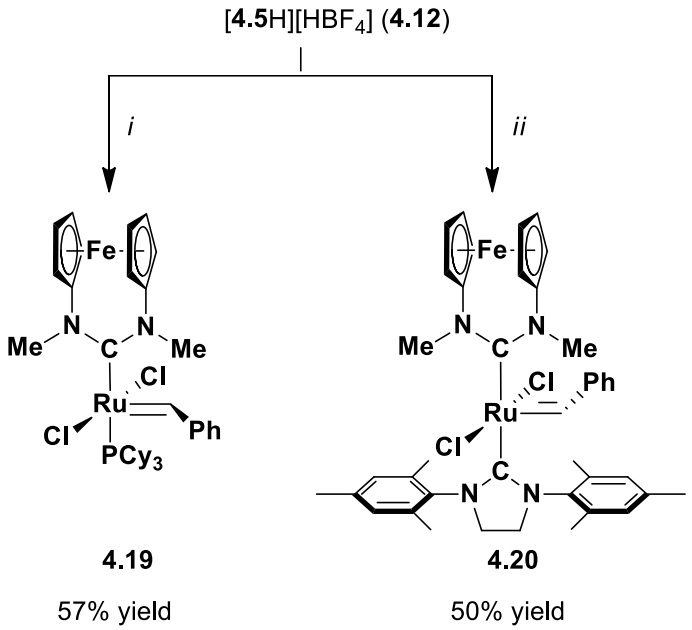

Scheme C.1 Synthesis of Ru complexes containing **4.5**. (*i*) (a) NaHMDS (1.0 equiv), toluene, ambient temperature, 5 min. (b) $(PCy_3)_2Cl_2Ru{=}CHPh$ (**4.6**) (0.30 equiv), toluene, ambient temperature, 10 min. (*ii*) (a) NaHMDS (1.0 equiv), toluene, ambient temperature, 5 min. (b) $(SIMes)(pyridine)_2Cl_2Ru{=}CHPh$ (0.50 equiv), toluene, ambient temperature, 1 h.

We attempted the synthesis of a complex of the type $(FcDAC)(PCy_3)Cl_2Ru{=}CHPh$, as the analogous SIMes containing complex **4.7** is well known to display high catalytic activities in a broad range of olefin metathesis reactions and is moderately stable in solution.[2] As summarized in Scheme C.1, treating a toluene solution of **4.12** with NaHMDS to form FcDAC **4.5** *in situ* followed by the addition of **4.6** afforded the expected complex **4.19** which was sufficiently stable to be isolated using column chromatography. The diagnostic low field benzylidene signal observed in the ^1H NMR spectrum of **4.19** was observed at 19.61 ppm (d, J = 4.5) in addition to a salient signal in the ^{31}P NMR spectrum at 35.86 ppm (CD_2Cl_2).[1] Although **4.19** was found to

have limited stability in solution and decomposed over a period of hours at ambient temperature, even in the absence of O_2 and water, the complex was stable in the solid state when stored at –30 °C.

Phosphine-free Ru complexes containing **4.5** were also investigated. Complexes of the type $(NHC)_2Cl_2Ru{=}CHPh$[3]and $(NHC)_a(NHC)_bCl_2Ru{=}CHPh$[4] often exhibit high catalytic activities at elevated temperatures and are typically stable due to the strong σ-donicity of their NHC ligands. The addition of $(SIMes)(pyridine)_2Cl_2Ru{=}CHPh$ to a toluene solution of **4.5** (generated *in situ* from **4.12**) resulted in the formation of mixed FcDAC-NHC Ru complex **4.20**, which was isolated in 50% yield after purification via column chromatography. To compare the solid-state structure of **4.20** to other Ru complexes and to determine if any isomerization had occurred during its synthesis or isolation (as was observed for **4.18**; see chapter 4), X-ray quality crystals were grown by slow evaporation of a concentrated hexanes solution of the complex (Figure S1 of original manuscript). The Ru–$C_{carbene}$ bond distances for previously reported bis-carbene Ru complexes span a relatively large range depending on the nature of the carbene ligands (2.052(9)–2.153(9) Å).[3,4a,c-e,f] The Ru–C_{FcDAC} and Ru–C_{SIMes} bond distances measured in the solid state structure of **4.20** (2.117(3) and 2.121(3) Å) were within the expected range and nearly identical to those reported for a mixed ADC–SIMes Ru complex (ADC = *N*,*N*'-dimesityl-*N*,*N*'-dimethylformamidin-2-ylidene) (Ru–C_{ADC} 2.112(3) Å; Ru–C_{SIMes} 2.132(3) Å).[4c] Additionally, the C1–Ru–C3 bond angle measured in the solid state structure of **4.20** (162.9(1)°) was comparable to that reported for related bis-carbene complexes (159.05(15)–166.9(4)°).[3,4a-c,f]

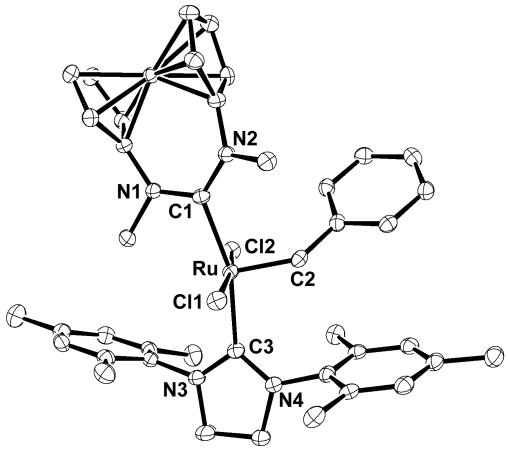

Figure C.1 ORTEP diagram of **4.20** showing ellipsoids at 50% probability. Hydrogen atoms have been omitted for clarity. Key atom distances (Å) and angles (°): Ru–C1, 2.117(3); Ru–C2, 1.846(3); Ru–C3, 2.121(3); C1–Ru–C3, 162.9(1); Cl1–Ru–Cl2, 171.92(2); N1–C1–N2, 120.0(2); N3–C3–N4, 106.7(2).

After the synthesis and characterization of **4.19** and **4.20**, a preliminary investigation of their catalytic activities was conducted. An exchange experiment was first employed to determine which ligand preferentially dissociated in **4.20**, which can be studied by heating a solution of the complex in the presence of excess PCy_3.[3d,4c] Heating a solution of **4.20** in benzene (15 mg in 0.8 mL of C_6D_6) in the presence of a 10-fold molar excess of PCy_3 at 100 ºC for 3 h resulted in a color change from lime green to brownish-red, which was consistent with the formation of **4.6** (note: complex **4.19** is green). ^{1}H and ^{31}P NMR spectroscopic analysis of the crude revealed new signals at δ 19.62 and 30.54 ppm, which were nearly identical to those NMR signals observed for an independent solution of **4.6** recorded in the same solvent (19.63 and 30.53 ppm). This experiment revealed that the FcDAC ligand dissociates in preference to SIMes. As such, complex **4.20** would yield the same catalytically-active intermediate as commercially-available catalysts **4.6** or **4.7**, and thus its activity was not further studied, although the electrochemical properties of **4.20** were still measured (see below). The activity of

complex **4.19** was evaluated in two representative olefin metathesis reactions (see Scheme C2).

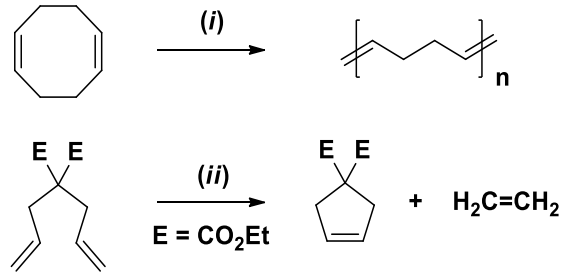

Scheme C.2 Olefin metathesis reactions studied using **4.19** as the catalyst. (*i*) 0.1 mol% [Ru], CD_2Cl_2 or toluene-d_8, 30 or 80 ºC. (*ii*) 1 mol% [Ru], CD_2Cl_2 or toluene-d_8, 30 or 80 ºC.

Table C.1 Summary of catalytic activities displayed by 19 in ROMP and RCM reactions.[a]

Entry	Substrate	Solvent	Temperature (°C)	Reaction Time (h)	Conversion (%)
1	COD	CD_2Cl_2	30	1	58
2	COD	CD_2Cl_2	30	24	93
3	COD	Toluene-d_8	80	0.5	100
4	DDM	CD_2Cl_2	30	1	10
5	DDM	CD_2Cl_2	30	24	30
6	DDM	toluene-d_8	80	1	37
7	DDM	toluene-d_8	80	24	45

[a] $[COD]_0$ = 0.5 M; $[DDM]_0$ = 0.1 M; $[\mathbf{4.19}]_0$ = 0.1 mol%. Conversions were determined by ^{1}H NMR spectroscopy. See text for additional details.

Under the standardized conditions reported by Grubbs and co-workers,[5] **4.19** showed relatively low catalytic activity in representative ring-opening metathesis polymerization (ROMP) of *cis*,*cis*-1,5-cyclooctadiene (COD) and the ring-closing

metathesis (RCM) of diethyl diallylmalonate (DDM). Significantly enhanced catalytic activities were observed at elevated temperatures as **4.19** gave complete conversion of COD to poly(1,4-butadiene) in 30 min at 80 °C. The highest conversion measured using **4.19** to catalyze the RCM of DDM was 45%.

The electrochemical properties of **4.19** and **4.20** were studied by CV (Table C.2; Figures S6 and S7 of the original manuscript, respectively). Complex **4.19** exhibited two irreversible oxidations at E_{pa} = 0.71 and 0.86 V versus SCE, which indicated that reversible control over catalytic activity would be precluded. Complex **4.20** exhibited two reversible[6] oxidations that were well-resolved with the first oxidation event occurring at a lower potential ($E_{1/2}$ = 0.57 V versus SCE) than that measured for **4.18** or **4.19** under otherwise identical conditions. These observations suggested to us that the presence of two strongly donating carbene ligands increased the overall electron density in the complex and stabilized the corresponding oxidation product. Consistent with this trend, the bis-PPh_3 complex **4.9** (i.e., $(PPh_3)_2Cl_2Ru$=(3-phenylindenylid-1-ene)) underwent oxidation at $E_{1/2}$ = 0.84 V versus SCE,[7] which is a potential higher than that measured for complexes containing one or two NHCs.

Table C.2 Summary of the electrochemical properties of complexes **4.19** and **4.20**.[a]

Compound	E_{pa} or $E_{1/2}$ (V) [b]
4.19	0.71 (ir),[c] 0.86 (ir)[c]
4.20	0.57 (r),[d] 0.98 (r)[d]

[a] Conditions: CH_2Cl_2 solution containing 1 mM analyte and 0.1 M $[Bu_4N][PF_6]$ as supporting electrolyte. Abbreviations; ir = irreversible; r = reversible. [b] Values are reported relative to SCE through the addition of Fc* as an internal standard adjusted to –0.057 V.[8] [c]Anodic peak potential (E_{pa}). [d] Half wave potential ($E_{1/2}$).

In light of the well-resolved redox-processes observed for **4.20**, subsequent attention was directed toward studying the electrochemical properties of this complex in more detail to discern the Fe and Ru oxidation processes. To do so, we employed UV/vis spectroscopy which is a useful technique for the characterization of the electrochemical properties of compounds containing ferrocene derivatives as a diagnostic ferrocenium ligand-to-metal-charge-transfer (LMCT) transitions occur at approximately 620 nm upon oxidation.[9] We selected 2,3-dichloro-5,6-dicyanoquinone (DDQ) ($E_{1/2}$ = 0.58 V versus SCE in $CH_2Cl_2/[Et_4N][ClO_4]$) as a one electron oxidant for **4.20** as numerous reports have characterized analogous oxidation products of Fc and Fc-substituted derivatives.[10] An equimolar solution of **4.20** and DDQ was studied by UV/vis spectroscopy, which revealed diagnostic absorptions attributed to a $DDQ^{\bullet -}$ species at λ_{max} = 586, 542, 455, 430, and 346 nm (Figure C.2). Collectively, these results suggested to us that DDQ underwent reduction; however, the strong absorbance in the expected region for ferrocenium transitions prevented assignment of the corresponding oxidation process to a Fe versus Ru center.[11] Upon the addition of two equivalents of DDQ, no increase in

absorbance attributed to $DDQ^{\bullet -}$ was observed which suggested to us that only oxidation of one metal center had occurred.

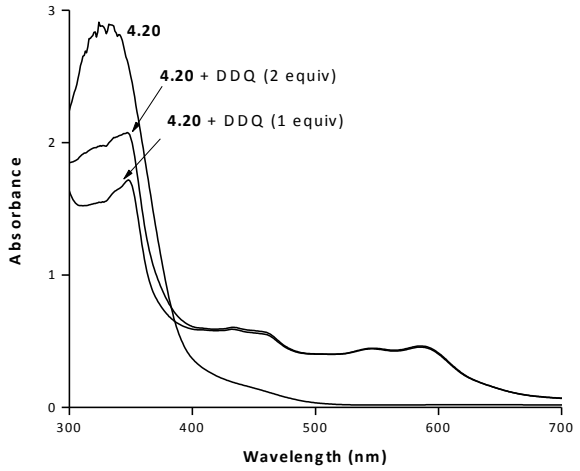

Figure C.2 UV/vis absorption spectra of **4.20** (1.2×10^{-4} M) treated with DDQ (1.2×10^{-4} M or 2.4×10^{-4} M) in CH_2Cl_2.

To identify the metal center undergoing oxidation in the aforementioned process, the EPR spectra for **4.20** treated with DDQ were recorded. When **4.20** and DDQ were combined (in a 1:1 molar ratio) in CH_2Cl_2, the resulting EPR spectrum showed two major features at g = 4.29 and 2.01 (see original manuscript). Given the high intensity and relative sharpness of the signal at g = 2.01, this peak was assigned to an organic-centered radical arising from $DDQ^{\bullet -}$. The weaker, broad signal observed at g = 4.29 was consistent with an Fe^{III}-centered radical. The Fe^{III} signal was comparable to a previously reported Ru^{II} complex incorporating a ferrocene-substituted pyridylamine ligand, where one electron oxidation using $[Ru(bpy)_3]^{3+}$ resulted in an EPR signal at g = 4.22, that was attributed to an Fe based process.[12] These data indicated that the oxidation of the Fe center occurred at a lower energy than that of the Ru center. However, when **4.20** was oxidized using excess DDQ (four equivalents), in addition to the expected signals at g =

4.29 and 2.01 a broad, low intensity signal was observed at g = 1.96 (overlapping with the signal at g = 2.01) which was consistent with the formation of a Ru^{III} species (Figure S14 of the original manuscript).[13] As a control experiment, an analogous sample was prepared using **4.6** (which contains only Ru) and DDQ (see original manuscript). One strong signal was observed, attributed to $DDQ^{\bullet -}$, found at g = 2.01, in addition to a broad signal attributed to Ru^{III}, occurring at g = 2.03 (overlapping with the former). Collectively, these results suggested to us that the oxidation of the Fe center occurred more readily than the oxidation of the Ru center, although DDQ appeared to oxidize both Fe and Ru in this particular complex when present in large excess.

CYCLIC VOLTAMMETRY

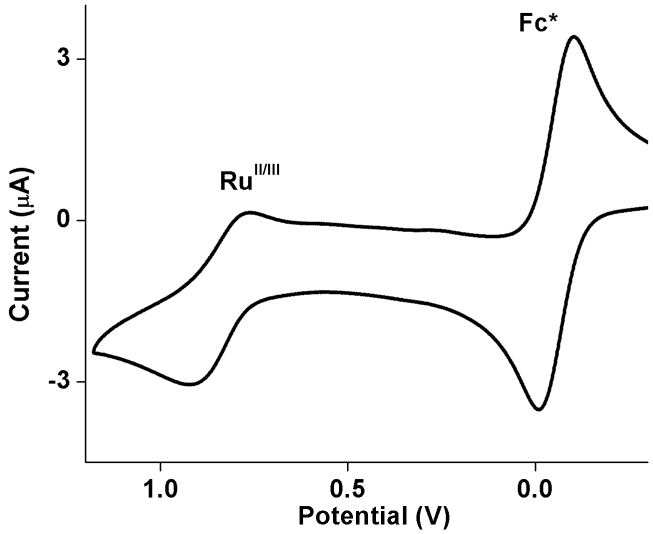

Figure C.3 CV of **4.9** in CH_2Cl_2 with 0.1 M $[Bu_4N][PF_6]$ and Fc* internal standard.

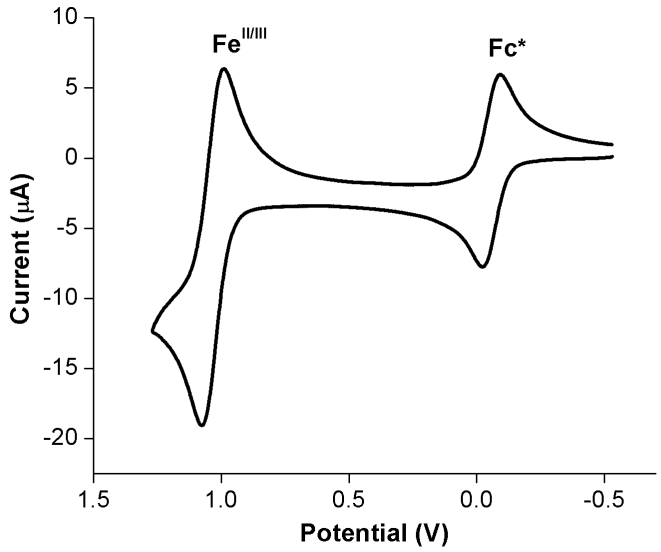

Figure C.4 CV of [**4.5**H][BF_4] (**4.12**) in CH_2Cl_2 with 0.1 M [Bu_4N][PF_6] and Fc* as the internal standard.

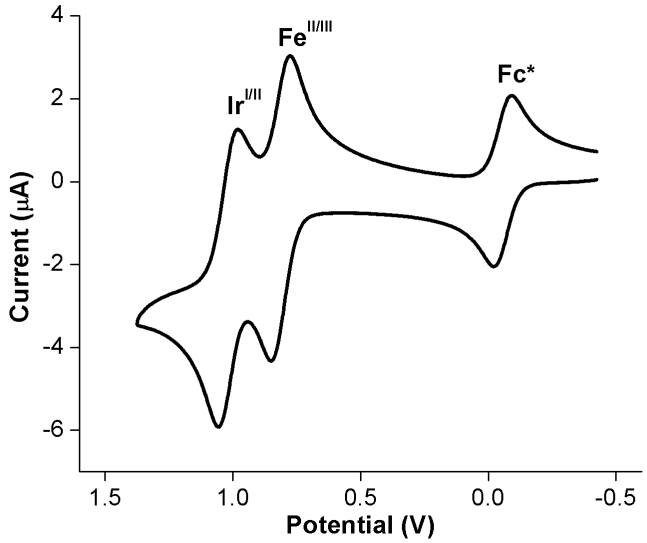

Figure C.5 CV of **4.13** in CH_2Cl_2 with 0.1 M [Bu_4N][PF_6] and Fc* as the internal standard.

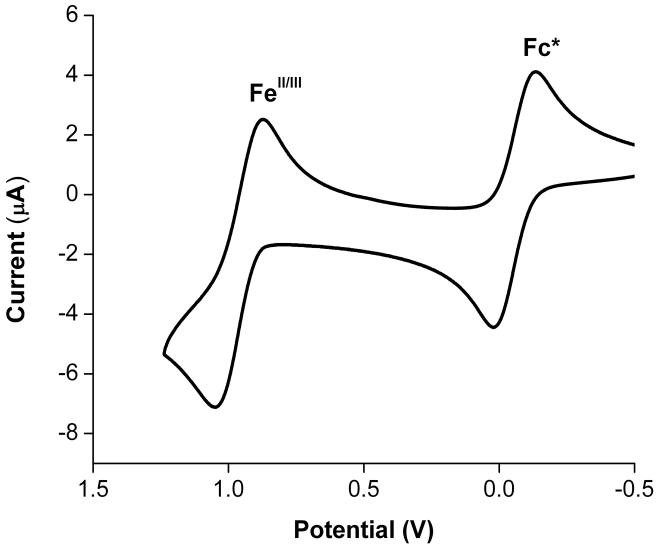

Figure C.6 CV of **4.15** in CH_2Cl_2 with 0.1 M $[Bu_4N][PF_6]$ and Fc* as the internal standard.

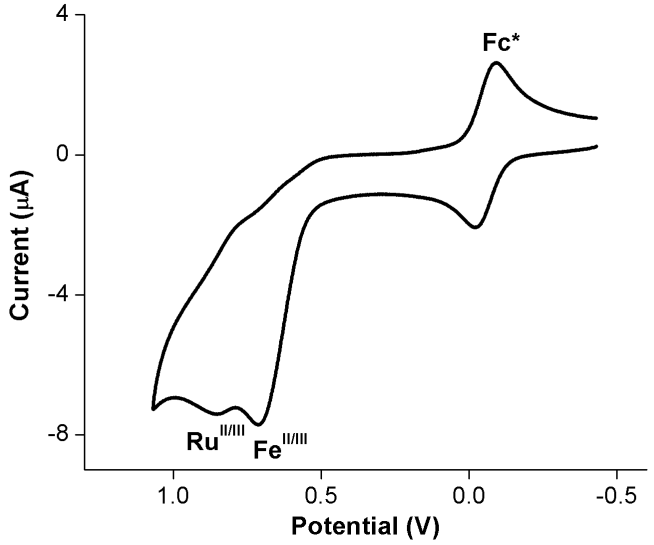

Figure C.7 CV of **4.19** in CH_2Cl_2 with 0.1 M $[Bu_4N][PF_6]$ and Fc* as the internal standard.

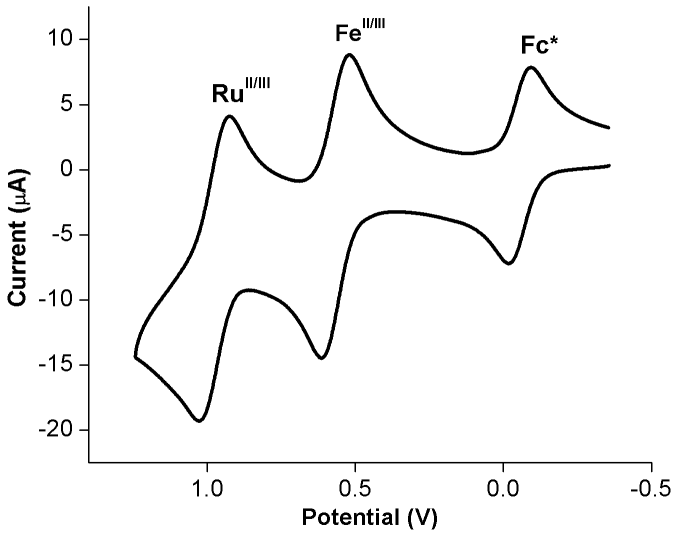

Figure C.8 CV of **4.20** in CH_2Cl_2 with 0.1 M $[Bu_4N][PF_6]$ and Fc* as the internal standard.

X-RAY CRYSTALLOGRAPHY

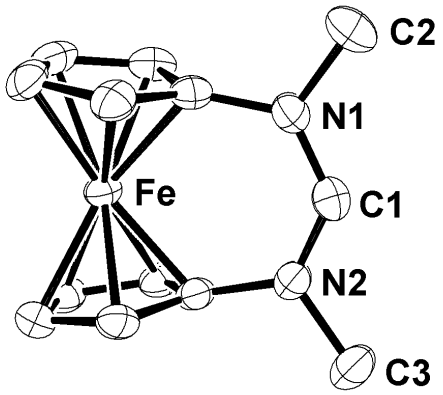

Figure C.9 ORTEP diagram of **4.12** showing ellipsoids at 50% probability. Hydrogen atoms and BF_4^- counterion have been omitted for clarity. Key atom distances (Å) and angles (°): N1–C1, 1.310(4); N2–C1, 1.314(4); Fe–C1, 3.272; N1–C1–N2, 129.4(3).

The data for 4.12 and 4.13 were collected on a Rigaku SCX-Mini diffractometer with a Mercury CCD using a graphite monochromator with MoKα radiation (l = 0.71073Å) at 223 K using a Rigaku Tech50 low temperature device. The data for 4.15 and 4.20 were collected on a Rigaku AFC12 diffractometer with a Saturn 724+ CCD using a graphite monochromator with MoKα radiation (1 = 0.71073Å) at 100 K using a Rigaku XStream low temperature device. The data for 4.18 were collected on a Nonius Kappa CCD diffractometer using a graphite monochromator with MoKα radiation (1 = 0.71073Å) at 153 K using an Oxford Cryostream low temperature device.

Details of crystal data, data collection and structure refinement are summarized in Table S4 of the original manuscript. Data reduction for **4.12**, **4.13**, **4.15**, and **4.20** were performed using Rigaku Americas Corporation's Crystal Clear program (version 1.40).[13] Data reduction for **4.18** were performed using DENZO-SMN. 14 For all crystals, the structure was solved by direct methods using SIR9715 and refined by full-matrix least-

squares on F2 with anisotropic displacement parameters for the non-H atoms using SHELXL-97. 16

For 4.12, 4.13, 4.15, and 4.18, the hydrogen atoms on carbon were calculated in ideal positions with isotropic displacement parameters set to 1.2xUeq of the attached atom (1.5×Ueq for methyl hydrogen atoms). For **4.18**, most hydrogen atoms on carbon were calculated in ideal positions with isotropic displacement parameters set to 1.2xUeq of the attached atom (1.5×Ueq for methyl hydrogen atoms). The hydrogen atom on C1a was observed in a ΔF map and refined with an isotropic displacement parameter. The data for 4.12, 4.15, and 4.18 were checked for secondary extinction effects but no correction was necessary. The data for 4.13 were corrected for secondary extinction taking the form: Fcorr = kFc/[1 + (1.02(19)×10-7)* Fc2l3/(sin2q)]0.25 where k is the overall scale factor. The tetrafluoroborate anion for 4.12 was disordered about two orientations. The disorder was modeled by assigning the variable x to the site occupancy factors for one component of the disorder consisting of atoms, B1, F1, F2, F3 and F4. The variable (1-x) was assigned to the atoms of the alternate component consisting of atoms, B1a, F1a, F2a, F3a and F4a. A common isotropic displacment parameter was refined for the fluorine atoms and a second isotropic displacement parameter was refined for B1 and B1a. While refining x, the geometry of the two anions was restrained to be approximately equal. In this way, the site occupancy factor for atoms, B1, F1, F2, F3 and F4 refined to 60(2)%. The atoms of the anion were refined anisotropically with their displacement parameters restrained to be approximately isotropic. Geometric restraints were applied throughout the refinement process. Neutral atom scattering factors and values used to calculate the linear absorption coefficient are from the International Tables for X-ray Crystallography (1992).[17]

Table C.3 Summary of Crystal Data, Intensity Collection, & Refinement Parameters for [**4.5**H][BF_4] (**4.12**), **4.13**, **4.15**, **4.18**, and **4.20**.

	4.12	**4.13**	**4.15**	**4.18**	**4.20**
CCDC No.	938913	938914	9389145	938916	938917
empirical formula	$C_{13}H_{15}BF_4FeN_2$	$C_{21}H_{26}ClFeIrN_2$	$C_{15}H_{14}ClFeIrN_2O_2$	$C_{52}H_{45}Cl_2FeN_2PRu$	$C_{41}H_{46}Cl_2FeN_4Ru$
formula weight	341.93	589.94	537.78	956.69	822.64
morphology and growth method[a]	Yellow prisms Vd pentane into CH_2Cl_2	Yellow prisms Slow evap. of hexanes	Yellow prisms Vd pentane into chloroform	Orange plates Vd hexanes into benzene	Green plates Slow evap. of hexanes
crystal system	Orthorhombic	Monoclinic	Triclinic	Monoclinic	Monoclinic
space group	Pbca	I2/a	P-1	P21/n	P21/n
a, Å	10.1257(10)	22.976(4)	7.8524(16)	16.7743(11)	14.5623(9)
b, Å	13.5984(14)	6.4866(10)	12.170(2)	15.8924(9)	19.3183(12)
c, Å	20.253(2)	26.186(5)	17.782(4)	17.3028(12)	13.9662(8)
α, deg	90.00	90.00	98.77(3)	90.00	90.00
β, deg	90.00	94.263(3)	91.41(3)	108.242(2)	112.9070(10)
γ, deg	90.00	90.00	108.35(3)	90.00	90.00
V, Å^3	2788.7(5)	3891.9(12)	1589.63(6)	4363.5(5)	3619.1(4)
T, K	233(2)	233(2)	120(2)	153(2)	100(2)
Z	8	8	4	4	4
D_{calc}, Mg/m^3	1.629	2.014	2.248	1.456	1.510
cryst size (mm)	0.13 x 0.15 x 0.20	0.04 x 0.10 x 0.25	0.04 x 0.08 x 0.14	0.04 x 0.11 x 0.12	0.05 x 0.12 x 0.16
reflections collected	27892	19094	28399	18025	58124
independent reflections	3187	4427	7264	9982	8165
R_1, wR_2 $\{I > 2\sigma(I)\}^b$	0.0408, 0.0994	0.0182, 0.0431	0.0348, 0.0841	0.0573, 0.0794	0.0388, 0.0868
goodness of fit	0.986	1.092	1.023	0.987	1.057

[a] Vd = vapor diffusion. [b] $R_1 = \Sigma (|F_o| - F_c|)/\Sigma|F_o|\}$; $wR_2 = \{\Sigma w(|F_o|^2 - |F_c|^2)^2/\Sigma w(|F_o|)^4\}^{1/2}$ where w is the weight given each reflection.

NOTES AND REFERENCES

(1) For comparison, the corresponding ^{1}H NMR (benzylidene) and ^{31}P NMR signals were recorded at 20.00 ppm (d, J = 5.10) and 35.22 ppm, respectively, at room temperature.

(2) (a) Scholl, M.; Trnka, T. M.; Morgan, J. P.; Grubbs, R. H.; *Tetrahedron Lett.* **1999**, *40*, 2247. (b) Morgan, J. P.; Grubbs, R. H. *Org. Lett.* **2000**, *2*, 3153. (c) Huang, J.; Stevens, E. D.; Nolan, S. P.; Peterson, J. L. *J. Am. Chem. Soc.* **1999**, *121*, 2674. (d) Hermann, W. A.; Köcher, C. *Angew. Chem. Int. Ed. Engl.* **1997**, *36*, 2162. (e) Chatterjee, A. K.; Morgan, J. P.; Scholl, M.; Grubbs, R. H. *J. Am. Chem. Soc.* **2000**, *122*, 3783. With selected examples with unsaturated imidazol-2-ylidenes, see: (f) Fürstner, A.; Thiel, O. R.; Ackermann, L.; Schanz, H. J.;

Nolan, S. P. *J. Org. Chem.* **2000**, *65*, 2204. (g) Briot, A.; Bujard, M.; Gouverneur, V.; Nolan, S. P.; Mioskowski, C. *Org. Lett.* **2000**, *2*, 1517.

(3) (a) Weskamp, T.; Schattenmann, W. C.; Spiegler, M.; Herrmann, W. A. *Angew. Chem., Int. Ed.* **1998**, *37*, 2490–2493; (b) Conrad, J. C.; Yap, G. P. A.; Fogg, D. E. *Organometallics* **2003**, *22*, 1986–1988; (c) Zhang, W.; Bai, C.; Lu, X.; He, R.; *J. Organomet. Chem.* **2007**, *692*, 3563–3567; (d) Ledoux, N.; Allaert, B.; Linden, A.; Van Der Voort, P.; Verpoort, F. *Organometallics* **2007**, *26*, 1052–1056.

(4) (a) Trnka, T. M.; Morgan, J. P.; Sanford, M. S.; Wilhelm, T. E.; Scholl, M.; Choi, T.-L.; Ding, S.; Day, M. W.; Grubbs, R. H. *J. Am. Chem. Soc.* **2003**, *125*, 2546. (b) Vorfalt, T.; Leuthäusser, S.; Plenio, H. *Angew. Chem., Int. Ed.* **2009**, *48*, 5191. (c) Rosen, E. L.; Sung, D. H.; Chen, Z.; Lynch, V. M.; Bielawski, C. W. *Organometallics* **2010**, *29*, 250. (d) Sashuk, V.; Peeck, L. H.; Plenio, H. *Chem.;Eur. J.* **2010**, *16*, 3983. (e) Bantreil, X.; Randall, R. A. M.; Slawin, A. M. Z.; Nolan, S. P. *Organometallics* **2010**, DOI: 10.1021/om100310f. (f) Peeck, L. H.; and Plenio, H. *Organometallics* **2010**, DOI: 10.1021/om1002717.

(5) Ritter, T.; Hejl, A.; Wenzel, A. G.; Funk, T. W.; Grubbs, R. H. *Organometallics* **2006**, *25*, 5740.

(6) The reversibility of the redox couples was confirmed by a scan rate dependency study; see Figure S9 of the original manuscript.

(7) See chapter 4 and Figure C.2.

(8) Noviandri, I.; Brown, K. N.; Fleming, D. S.; Gulyas, P. T.; Lay, P. A.; Masters, A. F.; Phillips, L. *J. Phys. Chem. B* **1999**, *103*, 6713–6722.

(9) (a) Lever, A. B. P. Inorganic Electronic Spectroscopy, 2nd ed., Elsevier, Amsterdam, 1984. (b) Prins, R. *J. Chem. Soc., Chem. Commun.* **1970**, 280.

(10) (a) Miller, J. S.; Krusic, P. J.; Dixon, D. A.; Reif, W. M.; Zhang, J. H.; Anderson, E. C.; Epstein, A. J. *J. Am. Chem. Soc.* **1986**, *108*, 4459. (b) Murphy, V. J.; O'Hare, D. *Znorg. Chem.* **1994**, *33*, 1833. (c) Salman, H. M. A.; Mahmoud, M. R.; Abou-El-Wafa, M. H. M.; Rabie, U. M.; Crabtree, R. H. *Inorg. Chem. Commun.* **2004**, *7*, 1209. (d) Pal, S. K.; Alagesan, K.; Samuelson, A. G.; Pebler, J. *J. Organomet. Chem.* **1999**, *575*, 108.

(11) (a) Hartmann, S.; Winter, R. F.; Brunner, B. M.; Sarkar, B.; Knödler, A.; Hartenbach, I. Eur. *J. Inorg. Chem.* **2003**, 876. (b) Das, N.; Arif, A. M.; Stang, P. *Inorg. Chem.* **2005**, *44*, 5798. (c) Kaim, W.; Sixt, T.; Weber, M.; Fiedler, J. *J. Organomet. Chem.* **2001**, *167*, 637. (d) Sohn, Y. S.; Hendrickson, D. N.; Gray, H. B. *J. Am. Chem. Soc.* **1971**, *93*, 3603.

(12) (a) S. Hartmann, R. F. Winter, B. M. Brunner, B. Sarkar, A. Knödler, Hartenbach, I. Eur. *J. Inorg. Chem.*, 2003, 876–891; (b) N. Das, A. M. Arif, P. Stang, *Inorg. Chem.*, 2005, **44**, 5798–5804; (c) W. Kaim, T. Sixt, M. Weber, J. Fiedler, *J.*

Organomet. Chem., 2001, **637**, 167–171; (d) H. B. Gray, Y. S. Sohn, D. N. Hendrickson, *J. Am. Chem. Soc.*, 1971, **93,** 3603–3612.

(13) Kojima, T.; Noguchi, D.; Nakayama, T.; Inagaki, Y.; Shiota, Y.; Yoshizawa, K.; Ohkubo, K.; Fukuzumi, S. *Inorg. Chem.*, **2008**, *47*, 886–895.

(14) CrystalClear 1.40 (2008). Rigaku Americas Corporation, The Woodlands, TX.

(15) DENZO-SMN. (1997). Z. Otwinowski and W. Minor, Methods in Enzymology, **276**: Macromolecular Crystallography, part A, 307 – 326, C. W. Carter, Jr. and R. M. Sweets, Editors, Academic Press.

(16) SIR97. (1999). A program for crystal structure solution. Altomare A., Burla M.C., Camalli M., Cascarano G.L., Giacovazzo C. , Guagliardi A., Moliterni A.G.G., Polidori G.,Spagna R. J. Appl. Cryst. 32, 115-119.

(17) Sheldrick, G. M. (1994). SHELXL97. Program for the Refinement of Crystal Structures. University of Gottingen, Germany.

(18) International Tables for X-ray Crystallography (1992). Vol. C, Tables 4.2.6.8 and 6.1.1.4, A. J. C. Wilson, editor, Boston: Kluwer Academic Press.

Appendix D: Supporting Information for Chapter 5

MATERIALS AND METHODS

The following compounds were prepared according to literature procedures: 1-mesitylimidazole,[1] $[Ir(COD)Cl]_2$ (COD = 1,5-cyclooctadiene),[2] $[Fe(\eta^5\text{-}C_5H_4COMe)Cp]$ (Cp = cyclopentadienyl),[3] $[Fe(\eta^5\text{-}C_5H_4COMe)Cp][BF_4]$,[4] $[Fe(Cp)_2][BF_4]$[4] and (1,3-bis-(2,4,6-trimethylphenyl)-2-imidazolylidene)dichloro(o-isopropoxyphenylmethylene)ruthenium (IMes-HG2).[5] All other reagents were purchased from commercial sources and used as received, including: $[((CH_3)_3Si)_2N]Na$ (NaHMDS), $[(Cp_2Fe)CH_2N(CH_3)_3][I]$, $(PCy_3)Cl_2Ru(=CH\text{-}o\text{-}O\text{-}i\text{-}Pr(C_6H_4))$. CD_2Cl_2, $CDCl_3$, DMSO-d_6 and C_6D_6 (99.9%) were purchased from Cambridge Isotope Laboratories, dried over 3 Å molecular sieves and degassed using three consecutive freeze-pump-thaw cycles prior to use. Solvents were either dried with a solvent purification system from the Vacuum Atmosphere Company (CH_2Cl_2, Et_2O and toluene) or freshly distilled over 3 Å molecular sieves (*n*-pentane) and degassed using three consecutive freeze-pump-thaw cycles prior to use. All reactions and manipulations were conducted under an atmosphere of nitrogen unless otherwise indicated. UV-vis spectra (molar absorptivities reported in M^{-1} cm^{-1}) were obtained at ambient temperature with a Perkin-Elmer Lambda 35 spectrometer, while IR spectra were recorded with a Perkin-Elmer Spectrum BX instrument in the absorption mode. ^1H and ^{13}C NMR spectra were recorded on either a Varian 300, 400, 500 or 600 MHz spectrometer. Spectra were referenced to the solvent residual as an internal standard, for ^1H NMR: $CDCl_3$, 7.24 ppm; C_6D_6, 7.15 ppm; CD_2Cl_2, 5.32 ppm; DMSO-d_6, 2.50 ppm; for ^{13}C NMR: $CDCl_3$, 77.0 ppm; C_6D_6, 128.0 ppm, CD_2Cl_2, 54.00 ppm; DMSO-d_6, 39.5 ppm. Coupling constants (*J*) are expressed in hertz (Hz). Melting points were obtained with an Opti-Melt Automated Melting Point System MPA100

apparatus and are uncorrected. High-resolution mass spectra (HRMS) were obtained with a VG analytical ZAB2-E or a Karatos MS9 instrument (ESI or CI) and are reported as m/z (relative intensity). Gas chromatography (GC) was performed on an Agilent 6850 gas chromatograph (HP-1 column (J&W Scientific), L = 30 m, I.D. = 0.32 mm, film = 0.025 m). Electrochemical measurements were performed on a CHI660D electrochemical workstation using a silver wire quasi-reference electrode, a platinum disk working electrode and a Pt wire auxiliary electrode in a gas tight three-electrode cell under an atmosphere of nitrogen. Unless specified otherwise, the measurements were performed using 1.0 mM solutions of the analyte in dry CH_2Cl_2 with 0.1 M $[N(nBu)_4][PF_6]$ as the electrolyte and decamethylferrocene (Fc*) as the internal standard. Differential pulse voltammetry measurements were performed with 50 mV pulse amplitudes and 2 mV data intervals. All potentials listed herein were determined by cyclic voltammetry at 100 mV s^{-1} scan rates and referenced to a saturated calomel electrode (SCE) by shifting decamethylferrocene$^{0/+}$ to –0.057 V (CH_2Cl_2).[6] Electronic absorption spectra were determined from the spectroelectrochemical measurements on a Hewlett-Packard 8453 diode-array spectrophotometer (range 200 – 1100 nm). X-band EPR spectra were recorded on a Bruker ELEXSYS 500 spectrometer and simulations were performed using XSOPHE.[7] Mössbauer spectra were recorded on an alternating constant-acceleration spectrometer. The minimum experimental linewidth was 0.24 mm s^{-1} (full width at half-height). A constant sample temperature was maintained with an Oxford Instruments Variox cryostat. Reported isomer shifts (δ) are referenced versus iron metal at 300 K. Elemental analyses were performed by Midwest Microlab, LLC in Indianapolis, IN.

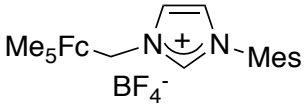

1-(1′,2′,3′,4′,5′-Pentamethylferrocenylmethyl)-3-mesityl-imidazolium tetrafluoroborate (5.9). A 50 ml flame-dried Schlenk flask was charged with 1,2,3,4,5-pentamethylferrocenylmethanol (222 mg, 0.78 mmol) and a stir bar. Dry CH_2Cl_2 (5 mL) was added followed by hydrogen tetrafluoroborate etherate (105 µl, 0.78 mmol) which resulted in the darkening of the solution. After stirring for 1 min, N-mesitylimidazole (300 mg, 1.6 mmol) was added in one portion and the resulting solution was stirred for 12 h. The solution was poured into Et_2O (50 mL) which resulted in the formation of a yellow precipitate which was purified by column chromatography (SiO_2, eluent: 19:1 v/v dichloromethane/methanol, R_f = 0.37). A concentrated dichloromethane solution of the crude product was layered with 100 mL ether to give yellow crystals. The crystals were collected by filtration and dried under vacuum to afford the desired compound (176 mg, 41% yield). ^{1}H NMR ($CDCl_3$): 8.65 (s, 1H), 7.50 (s, 1H), 7.05 (s, 1H), 6.94 (s, 2H), 4.95 (s, 2H), 3.98 (s, 2H), 3.84 (s, 2H), 2.30 (s, 3H), 1.94 (s, 6H), 1.60 (s, 15H). ^{13}C NMR ($CDCl_3$): 141.3, 136.1, 134.4, 130.7, 129.8, 123.0, 122.3, 82.8, 65.8, 49.7, 45.8, 21.1, 17.2, 11.0. ^{19}F NMR ($CDCl_3$): –151.8. HRMS (ESI): $[M]^+$ calcd for $C_{28}H_{35}N_2Fe$, 455.21445; found, 455.21513. Anal. calcd for $C_{28}H_{35}BF_4FeN_2$: C, 62.02; H, 6.51; N, 5.17; found: C, 61.74; H, 6.39; N, 5.26.

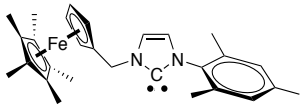

1-(1′,2′,3′,4′,5′-Pentamethylferrocenylmethyl)-3-mesityl-imidazol-2-ylidene (5.10). A 20 mL scintillation vial was charged with a stir bar, **5.9** (43 mg, 0.079 mmol), $NaN(SiMe_3)_2$ (14 mg, 0.070 mmol) and dry C_6D_6 (2 mL). The resulting mixture was stirred at 25 °C for 1 h and then filtered through a PTFE filter into a 20 mL scintillation vial. The desired compound (**5.10**) was found to decompose in

solution over the course of hours and therefore not isolated. Analysis by ^{1}H NMR spectroscopy showed quantitative formation of the desired compound. ^{1}H NMR (δ, C_6D_6): 6.74 (br, 2H), 6.72 (br, 1H), 6.32 (br, 1H), 5.02 (s, 2H), 3.62 (br, 2H), 3.55 (br, 2H), 2.11 (m, 9H), 1.75 (s, 15H).

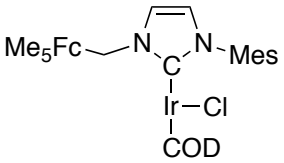

Chloro(η^4-1,5-cyclooctadienyl){1-(1′,2′,3′,4′,5′-pentamethylferrocenylmethyl)-3-mesitylimidazol-2-ylidene}iridium(I) (5.11). A 20 mL scintillation vial was charged with **5.9** (100 mg, 0.18 mmol), $NaN(SiMe_3)_2$ (45 mg, 0.22 mmol), $[Ir(COD)Cl]_2$ (62.5 mg, 0.093 mmol), THF (5 mL), and a stir bar. After stirring at ambient temperature for 16 h, removal of the solvent under reduced pressure afforded a brown residue. The residue was purified via column chromatography (SiO_2, hexanes:EtOAc 4/1 v/v, R_f = 0.65) to yield the desired compound as a yellow powder (58 mg, 79%). ^{1}H NMR ($CDCl_3$): 6.98 (s, 1H), 6.86 (s, 1H), 6.81 (d, J = 2 Hz, 1H), 6.58 (d, J = 2, 1H), 5.62 (d, J = 14, 1H), 5.34 (d, J = 14, 1H), 4.57 (m, 1H), 4.44 (m, 1H), 3.99 (m, 1H), 3.83 (m, 1H), 3.78 (m, 2H), 3.11 (m, 1H), 2.72 (m, 1H), 2.34 (s, 3H), 2.31 (s, 3H), 2.28-2.13 (m, 2H), 1.99 (s, 15H), 1.84 (s, 3H), 1.88-1.82 (m, 1H), 1.65-1.58 (m, 1H), 1.45-1.39 (m, 1H), 1.23-1.18 (m, 1H). ^{13}C NMR ($CDCl_3$): 178.6, 138.4, 137.0, 135.9, 134.3, 129.4, 128.0, 122.5, 119.4, 82.9, 82.8, 80.9, 80.2, 77.6, 73.2, 73.0, 72.6, 71.9, 51.2, 50.63, 50.61, 34.7, 32.6, 29.5, 29.0, 21.1, 19.6, 17.9, 11.3. HRMS (ESI): $[M–Cl]^+$ calcd for $C_{36}H_{46}N_2FeIr$, 755.2640; found, 755.2630. Anal. calcd for $C_{36}H_{46}N_2ClIr$: C, 54.71; H, 5.87; N, 3.54; found: C, 54.91; H, 5.92; N, 3.57.

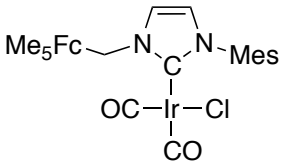

Chloro(dicarbonyl){1-(1′,2′,3′,4′,5′-Pentamethylferrocenylmethyl)-3-mesitylimidazol-2-ylidene}iridium(I) (5.12). A 20 mL scintillation vial was charged with **5.11** (50 mg, 0.063 mmol), CH_2Cl_2 (5 mL), and a stir bar. The solution was stirred under CO (1 atm) for 3 h and then concentrated under reduced pressure. The yellow residue was triturated with pentane (3 × 5 mL) and then dried under vacuum to yield the desired compound as a yellow solid (38 mg, 82%). IR (CH_2Cl_2): 2065, 1981 cm^{-1}. ^1H NMR ($CDCl_3$): 6.95 (s, 2H), 6.95 (s, 1H), 6.75 (s, 1H), 5.29 (s, 2H), 3.88 (br, 2H), 3.75 (br, 2H), 2.33 (s, 3H), 2.03 (s, 6H), 1.93 (s, 15H). ^{13}C NMR ($CDCl_3$) 181.0, 173.8, 186.0, 139.4, 135.1, 129.1, 122.7, 120.7, 81.0, 79.8, 73.2, 72.0, 50.5, 21.5, 18.3, 11.3. HRMS (ESI): $[M+HCl]^+$ calcd for $C_{30}H_{34}N_2O_2FeIr$, 702.1520; found, 702.1518. Anal. calcd for $C_{30}H_{34}N_2O_2FeIr$: C, 48.82; H, 4.64; N, 3.80; found: C, 49.15; H, 4.44; N, 3.48.

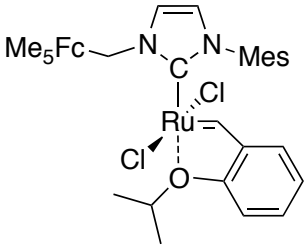

(1-(1′,2′,3′,4′,5′-Pentamethylferrocenylmethyl)-3-mesitylimidazol-2-ylidene)-Cl_2Ru(□CH-*o*-O*i*PrC_6H_4) (5.13). A 20 mL scintillation vial was charged with **5.9** (77 mg, 0.14 mmol), C_6H_6 (5 mL) and a stir bar. After adding $NaN(SiMe_3)_2$ (28 mg, 0.14 mmol), the resulting solution was stirred for 15 min before being filtered through a PTFE filter into a solution of HG-1 in benzene (2 mL). The resulting brown solution was stirred for 3 h and an aliquot was examined by ^1H NMR spectroscopy which showed that a mixture consisting of the desired product along with a by-product in which the isoproxy group was not coordinated to the metal center had formed. To facilitate phosphine deligation, the reaction mixture

was charged with S_8 (10 mg, 0.039 mmol) and stirred for 12 h. Flash chromatography (SiO_2, hexanes:EtOAc 4/1 v/v, R_f = 0.29) yielded the desired complex as a yellow microcrystalline solid (31 mg, 48%). ^{1}H NMR ($CDCl_3$): 16.46 (s, 1H), 7.50 (m, 1H), 7.07 (s, 2H), 6.96 (m, 3H), 6.89 (d, *J* = 2, 1H), 6.66 (d, *J* =2, 1H), 5.83 (s, 2H), 5.2 (m, 1H), 3.96 (s, 2H), 3.82 (s, 2H), 2.48 (s, 3H), 1.99 (s, 15H), 1.96 (s, 6H), 1.88 (d, *J* = 6, 6H). ^{13}C NMR (C_6D_6) 283.4, 172.1, 152.9, 144.8, 139.2, 138.3, 137.8, 136.3, 129.2, 123.2, 122.5, 121.8, 121.1, 113.2, 80.9, 75.0, 73.5, 72.8, 50.9, 22.5, 21.1, 18.2, 11.5 HRMS (ESI): $[M–2HCl]^+$ calcd for $C_{38}H_{45}N_2OFeRu$, 703.1925; found, 703.1929. Anal. calcd for $C_{38}H_{45}N_2OFeRu$: C, 58.92; H, 5.99; N, 3.62; found: C, 59.08; H, 5.89; N, 3.33.

RCM of 5.7: Single Redox Switching Experiment Using **5.13**. Inside a glove box, an NMR tube with a screw-cap septum was charged with **5.7** (20 μL, 0.080 mmol; $[7]_0$ = 0.1 M) and CD_2Cl_2 (750 μL). After equilibrating the sample at 30 °C in the NMR probe, the stock catalyst solution was added via syringe (100 μL, 1.3 μmol, 1.6 mol%). After collecting data points over the next 12 min using the Varian array function, the oxidant $[Fc][BF_4]$ was added (0.02 M, 75 μL, 1.5 μmol, 1.9 mol%). An immediate color change (yellow to dark brown) was observed along with a decreased reaction rate constant. After collecing data points for over the next 30 min using the Varian array function, the stock solution of decamethylferrocene (0.02 M, 100 μL, 2 μmol, 2.5 mol%) was added to the reaction mixture. The conversion of 7 to 8 was determined by comparing the ratio of the integrals of the methylene protons in the starting material at δ 2.61 (d) with those observed in the product at δ 2.98 (s).

X-RAY CRYSTALLOGRAPHY

Yellow single crystals of **5.9** were obtained by the slow diffusion of diethyl ether into a saturated CH_2Cl_2 solution. Orange single crystals of **5.12** were obtained by the slow diffusion of pentane into a saturated $CHCl_3$ solution. All crystals were coated with either Paratone or mineral oil and mounted onto a nylon cryoloop attached to a goniometer. Data for **5.9**, **5.12** and **5.13** were collected on a Rigaku AFC12 diffractometer with a Saturn 724+ CCD using a graphite monochromator with MoKα radiation (α = 0.71073Å) equipped with Oxford Cryostream cooling system (100 K). Data were collected under control of the Rigaku Americas Corporation's Crystal Clear version 1.40.[8] Structure solutions were obtained by direct methods for all compounds using SIR 97.[9] Refinements were accomplished by full-matrix least-squares procedures using the SHELXL-97[10] software suite. All hydrogen atoms were added in calculated positions and included as riding contributions with isotropic displacement parameters tied to those of the atoms to which they were attached. Additional crystallographic details may be found in the respective CIFs, which were deposited at the Cambridge Crystallographic Data Centre (CCDC), Cambridge, UK.

Table D.1 Crystal and refinement data.

	5.9	**5.12**	**5.13**
CCDC	898592	898593	937925
solvent	none	none	none
formula	$C_{28}H_{35}FeN_2BF_4$	$C_{30}H_{34}ClFeIrN_2O_2$	$C_8H_{46}Cl_2FeN_2ORu$
fw	542.24	738.09	774.59
xtl system	monoclinic	orthorhombic	monoclinic
space grp	P21/n	*P*bcn	P21/n
color, habit	yellow block	orange needle	Red needle
a, Å	15.781(2)	23.6684(9)	12.3311(30)
b, Å	11.9337(12)	17.2204(7)	21.6791(52)
c, Å	16.257(2)	13.7827(3)	14.4914(36)
α, deg.	90.00	90	90
β, deg.	117.850(3)	90	112.5191(32)
γ, deg.	90.00	90	90
V, Å^3	2707.0(6)	5617.5(4)	3578.6(16)
T, K	150	150	173
Z	4	8	4
R1[a], wR2[b]	0.0708, 0.1799	0.0380, 0.066	0.0447, 0.0925
GoF on F^2	1.040	1.106	1.188

[a]$R1 = \Sigma||F_o| - |F_c||/\Sigma|F_o|$. [b]$R_w = \{[\Sigma w(F_o^2 - F_c^2)/\Sigma w(F_o^2)^2\}^{1/2}$; $w = 1/[\sigma^2(F_o^2) + (xP)^2]$, where $P = (F_o^2 + 2F_c^2)/3$.

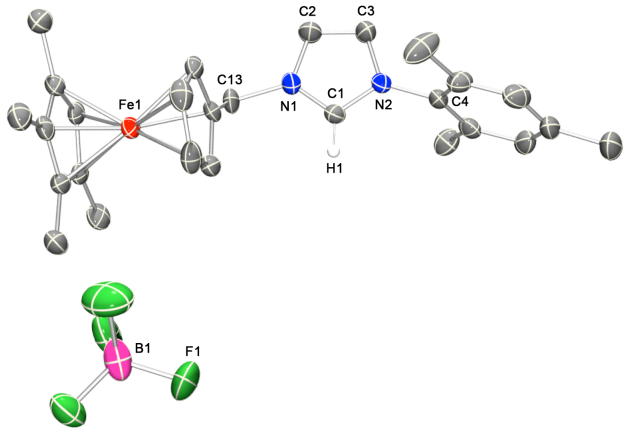

Figure D.1 ORTEP diagram of **5.9** rendered using POV-Ray. Thermal ellipsoid plots were drawn at the 50% probability level. Hydrogen atoms are omitted for clarity. Selected bond lengths (Å) and angles (°): C1–N1, 1.328(6); C1–N2, 1.335(6); C2–N1, 1.368(6); C3–N2, 1.373(6); C2–C3, 1.341(7); C4–N2, 1.453(6); C13–N1, 1.496(5); N1–C1–N2, 108.7(4); N1–C13–C14, 110.7(4).

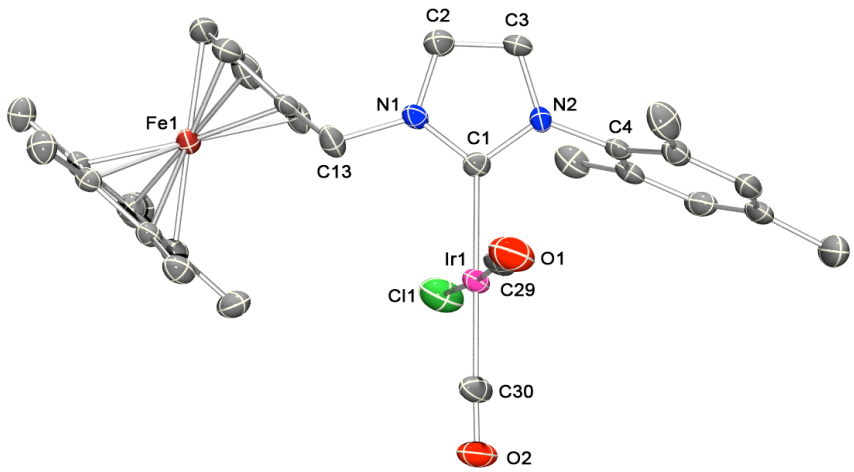

Figure D.2 ORTEP diagram of **5.12** rendered using POV-Ray. Thermal ellipsoid plots were drawn at the 50% probability level. Hydrogen atoms are omitted for clarity. Selected bond lengths (Å) and angles (°) C1–N1, 1.342(6); C1–N2, 1.366(6); C2–N1, 1.386(6); C3–N2, 1.378(6); C2–C3, 1.342(7); C4–N2, 1.453(6); C13–N1, 1.479(6); C1–Ir1, 2.070(4); Cl1–Ir1, 2.072(4); N1–C1–N2, 104.6(4); N1–C13–C14, 110.2(4).

ELECTROCHEMISTRY

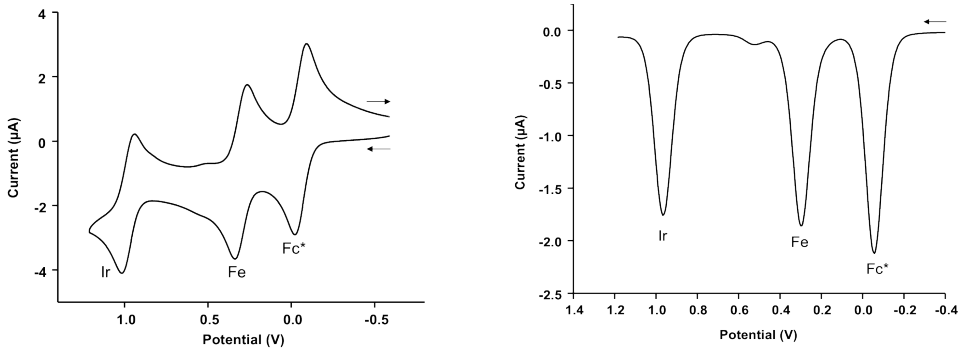

Figure D.3 CV (100 mV s^{-1} scan rate) and DPV (50 mV pulse amplitude) of **5.11** in CH_2Cl_2 with 1 mM analyte and 0.1 M $[N(nBu)_4][PF_6]$ as referenced to decamethylferrocene (Fc*) (internal standard, adjusted to –0.057 V vs SCE).

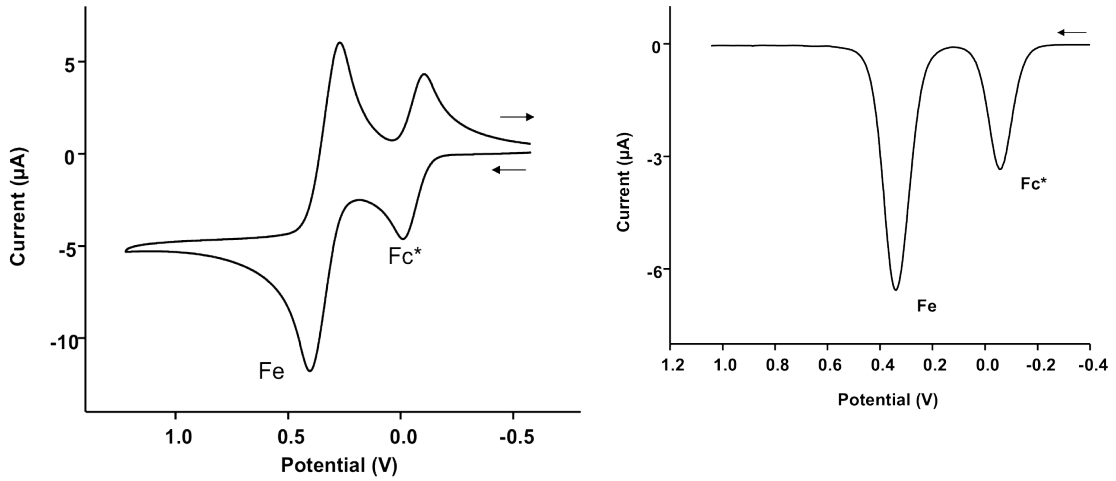

Figure D.4 CV (100 mV s^{-1}) and DPV (50 mV pulse amplitude) of **5.12** in CH_2Cl_2 with 1 mM analyte and 0.1 M $[N(nBu)_4][PF_6]$ as referenced to decamethylferrocene (Fc*) (internal standard, adjusted to –0.057 V vs SCE).

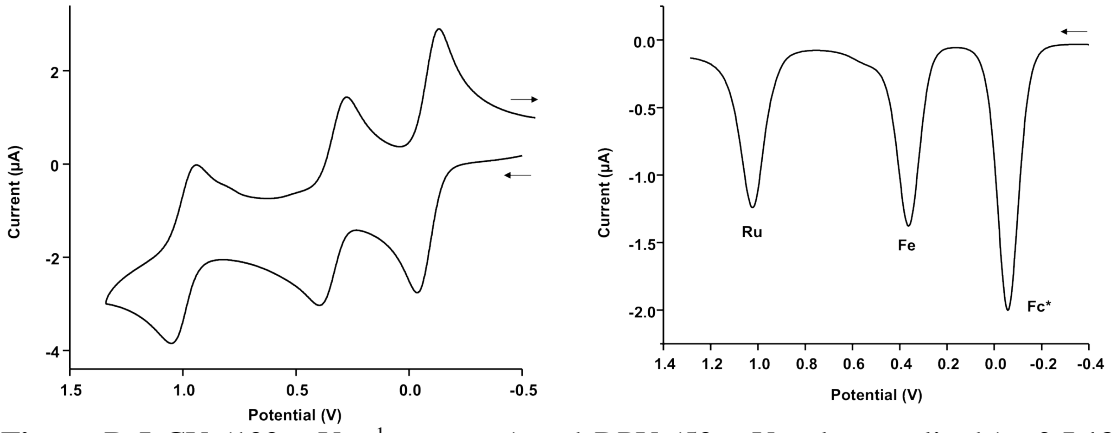

Figure D.5 CV (100 mV s^{-1} scan rate) and DPV (50 mV pulse amplitude) of **5.13** in CH_2Cl_2 with 1 mM analyte and 0.1 M $[N(nBu)_4][PF_6]$ as referenced to decamethylferrocene (Fc*) (internal standard, adjusted to –0.057 V *vs*. SCE).

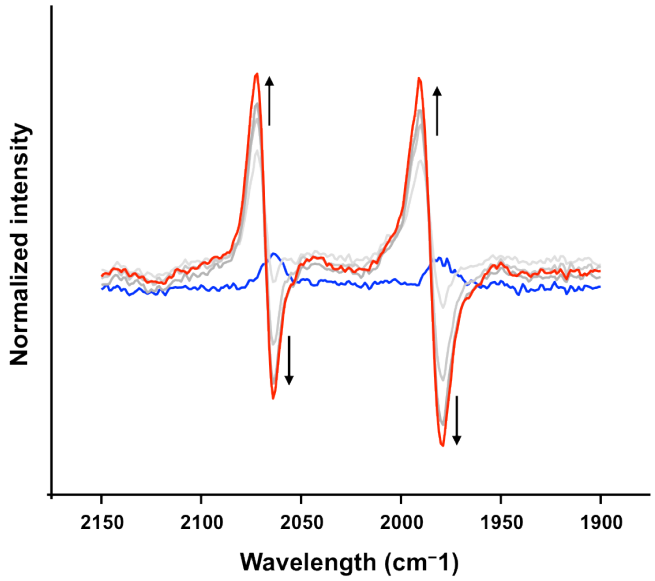

Figure D.6 Normalized IR difference spectra showing the shift in the υ_{CO}s upon oxidation (E_{app} = +0.60 V) of **5.12** ([**5.12**]$_0$ = 1 mM) in CH_2Cl_2 with 0.1 M [N(*n*Bu)$_4$][PF$_6$] as the supporting electrolyte.

References

(1) Occhipinti, G.; Jensen, V. R.; Trnroos, K. W.; Frystein, N. G.; Bjrsvik, H. –R. *Tetrahedron* **2009**, *65*, 7186.

(2) Komiya, S. *Synthesis of organometallic compounds: A practical guide*; J. Wiley & Sons., 1997.

(3) Graham, P. J.; Lindsey, R. V.; Parshall, G. W.; Peterson, M. L.; Whitman, G. M. *J. Am. Chem. Soc.* **1957**, *79*, 3416.

(4) Connelly, N. G.; Geiger, W. E. *Chem. Rev.* **1996**, *96*, 877.

(5) Merino, E.; Poli, E.; Díaz, U.; Brunel, D. *Dalton Trans.* **2010**, *41*, 10913.

(6) Noviandri, I.; Brown, K. N.; Fleming, D. S.; Gulyas, P. T. ; Lay, P. A.; Masters, A. F.; Phillips, L. *J. Phy. Chem. B* **1999**, *103*, 6713.

(7) Hanson, G. R.; Gates, K. E.; Noble, C. J.; Griffin, M.; Mitchell, A.; Benson, S. J. *Inorg. Biochem.* **2004**, *98*, 903.

(8) Rigaku Americas Corporation, 2008.

(9) A. Altomare, M. C. Burla, M. Camalli, G. L. Cascarano, C. Giacovazzo, A. Guagliardi, A. G. G. Moliterni, G. Polidori, R. Spagna R. *J. Appl. Cryst.* **1999**, *32*, 115.

(10) Sheldrick, G. M. *SHELXL/PC package (version 5.1), program for the refinement of crystal structures, University of Gottingen*, 2003; Sheldrick, G. M. *Acta. Cryst.* **2008**, *A-64*, 112.

Appendix E: Miscellaneous Bis(carbene) Design

Figure E.1 A bis(carbene) designed by C. Daniel Varnado Jr.

References

Abernethy, C. D.; Clyburne, J. A. C.; Cowley, A. H.; Jones, R. A. *J. Am. Chem. Soc.* **1999**, *121*, 2329.

Ackermann, L.; Fürstner, A.; Weskamp, T.; Kohl, F. J.; Herrmann, W. A. *Tetrahedron Lett.* **1999**, *40*, 4787.

Ajamian, A.; Gleason, J. L. *Angew. Chem. Int. Ed.* **2004**, *43*, 3754.

Alder, R. W.; Allen, P. R.; Murray, M.; Orpen, A. G. *Angew. Chem.* **1996**, *108*, 1211-1213.

Alder, R. W.; Blake, M. E.; Chaker, L.; Harvey, L.; Paolini, F.; Schütz, J. *Angew. Chem. Int. Ed.* **2004**, *43*, 5896.

Alder, R.W.; Blake, M. E.; Chaker, L.; Harvey, J. N.; Paolini, F.; Schötz, J. *Angew. Chem.*, **2004**, *116*, 6020–6036.

Allen, L. C. *J. Am. Chem. Soc.* **1989**, *111*, 9003-9114.

Allgeier, A. M.; Mirkin, C. A. *Angew. Chem. Int. Ed.* **1998**, *37*, 894-908.

Allgeier, A. M.; Slone, C. S.; Mirkin, C. A.; Liable-Sands, L. M.; Yap, G. P. A.; Rheingold, A. L. *J. Am. Chem. Soc.* **1997**, *119*, 550-559.

Allred, A. L. *J. Inorg. Nucl. Chem.* **1961**, *17*, 215-221.

Altenhoff, G.; Goddard, R.; Lehmann, C. W.; Glorius, F. *J. Am. Chem. Soc.* **2004**, *126*,15195-15201.

Altomare, A.; Burla, M. C.; Camalli, M.; Cascarano, G. L.; Giacovazzo, C.; Guagliardi, A.; Moliterni, A. G. G.; Polidori, G.; Spagna, R. *J. Appl. Cryst.* **1999**, *32*, 115-119.

AMagenau, J. D.; Strandwitz, N. C.; Gennaro A.; Matyjaszewski, K. *Science* **2011**, *332*, 81–84.

Arduengo III, A. J.; Bannenberg, T. P.; Tapu, D.; Marshall, W. J. *Chem. Lett.* **2005**, *34*, 1010-1011.

Arduengo III, A. J.; Bannenberg, T. P.; Tapu, D.; Marshall, W. J. *Tet. Lett.* **2005**, *46*, 6847-6850.

Arduengo III, A. J.; Dias, H. V. R.; Dixon, D. A.; Harlow, R. L.; Klooster, W. T.; Koetzle, T. F. *J. Am. Chem. Soc.* **1994**, *116*, 6812-6822.

Arduengo III, A. J.; Dias, H. V. R.; Harlow, R. L.; Kline, M. *J. Am. Chem. Soc.* **1992**, *114*, 5530-5534.

Arduengo III, A. J.; Harlow, R. L.; Kline, M. *J. Am. Chem. Soc.* **1991**, *113*, 361-363.

Arduengo III, A. J.; Iconaru, L. I. *Dalton Trans.* **2009**, 6903-6914.

Arduengo III, A. J.; Tapu, D.; Marshall, W. J. *Angew. Chem.* **2005**, *117*, 7406-7410.

Arduengo III, A. J.; Tapu, D.; Marshall, W. J. *Angew. Chem. Int. Ed.* **2005**, *44*, 7240-7244.

Arduengo III, A. J.; Tapu, D.; Marshall, W. J. *J. Am. Chem. Soc.* **2005**, *127*, 16400-16401.

Arduengo, A. J., III; *Acc. Chem. Res.* **1999**, *32*, 913–921

Arduengo, I. I. I. A. J.; Bannenberg, T. P.; Tapu, D.; Marshall, W. J. *Chem. Lett.* **2005**, *34*, 1010.

Arnold, P. L.; Casely, I. J. *Chem. Rev.* **2009**, *109*, 3599.

Arumugam, K.; Varnado, C. D., Jr.; Sproules, S.; Lynch, V. M.; Bielawski, C. W. *Chem. Eur. J.* **2013**, *19*, 10866.

Back, O.; Donnadieu, B.; Parameswaran, P.; Frenking, G.; Bertrand, G. *Nat. Chem.* **2010**, *2*, 369.

Balof, S. L., Yu, B., Lowe, A. B., Ling, Y., Zhang, Y., Schanz, H.-J. Eur. J. *Inorg. Chem.* **2009**, 1717.

Bandoli, G.; Dolmella, A. *Coord. Chem. Rev.* **2000**, *209*, 161.

Banks, R. L. *Chemtech* **1986**, *16*, 112-117.

Bantreil, X.; Poater, A.; Urbina-Blanco, C. A.; Bidal, Y. D.; Falivene, L.; Randall, R. A. M.; Cavallo, L.; Slawin, A. M. Z.; Cazin, C. S. J. *Organometallics* **2012**, *31*, 7415–7426.

Bantreil, X.; Randall, R. A. M.; Slawin, A. M. Z.; Nolan, S. P. *Organometallics* **2010**, *29*, 3007-3011.

Beer, P. D. *Chem. Soc. Rev.* **1989**, *18*, 409-450.

Bellec, N.; Massue, J.; Roisnel, T.; Lorcy, D. *Inorg. Chem. Commun.* **2007**, *10*, 1172-1176.

Bertogg, A.; Camponovo, F.; Togni, A. *Eur. J. Inorg. Chem.* **2005**, 347-356.

Biedermann, F.; Rauwald, U.; Cziferszky, M.; Williams, K. A.; Gann, L. D.; Guo, B. Y.; Urbach, A. R.; Bielawski, C. W.; Scherman, O. A. *Chem. Eur. J.* **2010**, *16*, 13716.

Bieniek, M.; Michrowska, A.; Usanov, D. L.; Grela, K. *Chem. Eur. J.* **2008**, *14*, 806–818.

Bieniek, M.; Samojłowicz, C.; Sashuk, V.; Bujok, R.; Śledź, P.; Lugan, N. l.; Lavigne, G.; Arlt, D.; Grela, K. *Organometallics* **2011**, *30*, 4144.

Bildstein, B. *J. Organomet. Chem.* **2001**, 617-618, 28.

Bildstein, B.; Hradsky, A.; Kopacka, H.; Malleier, R.; Ongania, K.-H. *J. Organomet. Chem.* **1997**, *540*, 127.

Bildstein, B.; Malaun, M.; Kopacka, H.; Ongania, K.-H.; Wurst, K. *J. Organomet. Chem.* **1998**, *552*, 45-61.

Bildstein, B.; Malaun, M.; Kopacka, H.; Ongania, K.-H.; Wurst, K. *J. Organomet. Chem.* **1999**, *572*, 177-187.

Bildstein, B.; Malaun, M.; Kopacka, H.; Wurst, K.; Mitterböck, M.; Ongania, K.-H.; Opromolla, G.; Zanello, P. *Organometallics* **1999**, *18*, 4325-4336.

Binobaid, A.; Iglesias, M.; Beetstra, D. J.; Kariuki, B.; Dervisi, A.; Fallis, A. A.; Cavell, K. J. *Dalton Trans.* **2009**, 7099–7112.

Blackmore, K. J.; Lal, N.; Ziller, J. W.; Heyduk, A. F. *Eur. J. Inorg. Chem.* **2009**, 735-743.

Blackmore, K. J.; Lal, N.; Ziller, J. W.; Heyduk, A. F. *J. Am. Chem. Soc.* **2008**, *130*, 2728–2729.

Blackmore, K. J.; Ziller, J. W.; Heyduk, A. F. *Inorg. Chem.* **2005**, *44*, 5559–5561.

Boeda, F.; Bantreil, X.; Clavier, H.; Nolan, S. P. *Adv. Synth. Catal.* **2008**, *350*, 2959–2966.

Boeda, F.; Clavier, H.; Nolan, S. P. *Chem. Commun.* **2008**, 2726–2740.

Boller, T. M.; Murphy, J. M.; Hapke, M.; Ishiyama, T.; Miyaura, N.; Hartwig, J. F. *Journal of the American Chemical Society* **2005**, *127*, 14263-14278.

Bolm, C.; Kesselgruber, M.; Raabe, G. *Organometallics* **2001**, *21*, 707-710.

Borguet, Y.; Zaragoza, G.; Demonceau, A.; Delaude, L. *Dalton Trans.* **2013**, *42*, 7287-7296.

Bourissou, D.; Guerret, O.; Gabbaï, F. P.; Bertrand, G. *Chem. Rev.* **2000**, *100*, 39-91.

Boydston, A. J., Williams, K. A.; Bielawski, C. W. *J. Am. Chem. Soc.* **2005**, *127*, 12496.

Boydston, A. J.; Bielawski, C. W. *Dalton Trans.* **2006**, 4073.

Boydston, A. J.; Khramov, D. M.; Bielawski, C. W. *Tetrahedron Lett.* **2006**, *47*, 5123;

Boydston, A. J.; Pecinovsky, C. S.; Chao, S. T.; Bielawski, C. W. *J. Am. Chem. Soc.* **2007**, *129*, 14550.

Boydston, A. J.; Rice, J. D.; Sanderson, M. D.; Dykhno, O. L.; Bielawski, C. W. *Organometallics* **2006**, *25*, 6087.

Boydston, A. J.; Vu, P. D.; Dykhno, O. L.; Chang, V.; Wyatt, A. R. II; Stockett, A. S.; Ritschdorff, E. T.; Shear, J. B.; Bielawski, C. W. *J. Am. Chem. Soc.* **2008,** *130*, 3143.

Boyer, J. L.; Cundari, T. R.; DeYonker, N. J.; Rauchfuss, T. B.; Wilson, S. R. *Inorg. Chem.* **2009**, *48*, 638-645.

Boyer, J. L.; Cundari,T. R.; DeYonker, N. J.; Rauchfuss, T. B.; Wilson, S. R. *Inorg. Chem.***2008**, *48*, 638–645.

Boyer, J. L.; Rochford, J.; Tsai, M.-K.; Muckerman, J. T.; Fujita, E. *Coord. Chem. Rev.* **2010**, *254*, 309–330.

Breslow, R. *J. Am. Chem. Soc.* **1957**, *79*, 1762-1763.

Breslow, R. *J. Am. Chem. Soc.* **1958**, *80*, 3719–3726.

Briot, A.; Bujard, M.; Gouverneur, V.; Nolan, S. P.; Mioskowski, C. *Org. Lett.* **2000**, *2*, 1517–1519.

Broderick, E. M.; Guo, N.; Vogel, C. S.; Xu, C.; Sutter, J.; Miller, J. T.; Meyer, K.; Mehrkhodavandi, P.; Diaconescu, P. L. *J. Am. Chem. Soc.* **2011**, *133*, 9278–9281.

Broderick, E. M.; Guo, N.; Wu, T.; Vogel, C. S.; Xu, C.; Sutter, J.; Miller, J. T.; Meyer, K.; Cantat, T.; Diaconescu, P. L. *Chem. Commun.* **2011**, **47**, 9897–9899.

Broggini, D.; Togni, A. *Helv. Chim. Acta* **2002**, *85*, 2518.

Brown, H. C.; Baude, E. A.; Nachod, F. C. Determination of Organic Structures by Physical Methods. Academic Press: New York, 1955.

Buchmeiser, M. R. *Chem. Rev.* **2000**, *100*, 1565–1604; (g) Trnka, T. M.; Grubbs, R. H. *Acc.Chem. Res.* **2001**, *34*, 18–29.

Cardin, D. J.; Cetinkaya, B.; Cetinkaya, E.; Lappert, M. F. *J. Chem. Soc., Dalton Trans.* **1973**, 514-522.

Carrette, L.; Friedrich, K. A.; Stimming, U. *Fuel Cells* **2001**, *1*, 5. Development and Understanding of New Membranes Based on Aromatic Polymers and Heterocycles for Fuel Cells. Ph.D. Dissertation, The University of Texas at Austin, August 2009.

Cavell, K. J.; McGuiness, D. S. *Coord. Chem. Rev.* **2004**, *248*, 671–681.

Çetinkaya, E.; Hitchcock, P. B.; Küçükbay, H.; Lappert, M. F.; Al-Juaid, S. *J. Organomet. Chem.* **1994**, *481*, 89.

Chang, Y.; Lee, H. H.; Kim, S. H.; Jo, T. S.; Bae, C. *Macromolecules* **2013**, *46*, 1754-1764.

Chatterjee, A. K.; Morgan, J. P.; Scholl, M.; Grubbs, R. H. *J. Am. Chem. Soc.* **2000**, *122*, 3783–3784.

Chauvin, Y. *Adv. Synth. Catal.* **2007**, 349, 27.

Chen, D.; Banphavichit, V.; Reibenspies, J.; Burgess, K. *Organometallics* **2007**, *26*, 855-859.

Chi, Y.; Chou, P.-T. *Chem. Soc. Rev.* **2010**, *39*, 638.

Chianese, A. R.; Kovacevic, A.; Zeglis, B. M.; Faller, J. W.; Crabtree, R. H. *Organometallics* **2004**, *23*, 2461.

Chianese, A. R.; Li, X.; Janzen, M. C.; Faller, J. W.; Crabtree, R. H. *Organometallics* **2003**, *22*, 1663-1667.

Chianese, A. R.; Mo, A.; Datta, D. *Organometallics* **2009**, *28*, 465.

Cho, J.-Y.; Tse, M. K.; Holmes, D.; Maleczka, R. E.; Smith, M. R. *Science* **2002**, *295*, 305-308.

Choi, B. G.; Hong, J.; Park, Y. C.; Jung, D. H.; Hong, W. H.; Hammond, P. T.; Park, H. *ACS Nano* **2011**, *5*,5167-5174.

Chotana, G. A.; Rak, M. A.; Smith, M. R. *J. Am. Chem. Soc.* **2005**, *127*, 10539-10544.

Clavier, H.; Broggi, J.; Nolan, S. P. *Eur. J. Org. Chem.* **2010**, 937-943.

Clavier, H.; Correa, A.; Escudero-Adán, E. C.; Benet- Buchholz, J.; Cavallo, L.; Nolan, S. P. *Chem. Eur. J.*, **2009**, *15*, 10244–10254.

Clavier, H.; Nolan, S. P. *Chem. Eur. J.* **2007**, *13*, 8029–8036.

Clavier, H.; Petersen, J. L.; Nolan, S. P. *J. Organomet. Chem.* **2006**, *691*, 5444–5477.

Clavier, H.; Urbina-Blanco, C. A.; Nolan, S. P. *Organometallics*, **2009**, *28*, 2848–2854.

Coady, D. J.; Khramov, D. M.; Norris, B. C.; Tennyson, A. G.; Bielawski, C. W. *Angew. Chem. Int. Ed.* **2009**, *48*, 5187.

Colacino, E.; Martinez, J.; Lamaty, F. *Coord. Chem. Rev.* **2007**, *251*, 726–764.

Coleman, K. S.; Turberville, S.; Pascu, S. I. Green, M. L. H. *J. Organomet. Chem.* **2005**, *690*, 653.

Collins, M. S.; Rosen, E. L.; Lynch, V. M.; Bielawski, C. W. *Organometallics*, **2010**, *29*, 3047–3053.

Connelly, N. G.; Geiger, W. E. *Chem. Rev.* **1996**, *96*, 877.

Connelly, N. G.; Geiger, W. E. *Chem. Rev.* **1996**, *96*, 877; (b) Aranzaes, J. R.; Daniel, M. C.; Astruc, D. *Can. J. Chem.* **2006**, *84*, 288.

Conrad, J. C.; Yap, G. P. A.; Fogg, D. E. *Organometallics* **2003**, *22*, 1986–1988.

Correa, A.; Marion, N.; Fensterbank, L.; Malacria, M.; Nolan, S. P.; Cavallo, L. *Angew. Chem. Int. Ed.* **2008**, *47*, 718.

Cotton, F. A. *Chemical Applications of Group Theory*; 3rd ed.; John Wiley & Sons: New York, 1990.

Cotton, F. A.; Kraihanzel, C. S. *J. Am. Chem. Soc.* **1962**, *84*, 4432-4438.

Crabtree, R. H. *The Organometallic Chemistry of Transition Metal*; 3rd ed., Wiley Sons: New York, 2001.

Crudden, C. M.; Allen, D. P. *Coord. Chem. Rev.* **2004**, *248*, 2247–2273.

CrystalClear 1.40 (2008). Rigaku Americas Corporation, The Woodlands, TX.

Curran, D. P. *Angew. Chem.* **1998**, *110*, 1230–1255; *Angew. Chem. Int. Ed.* **1998**, *37*, 1174-1196.

Dallas, A.; Kuhtz, H. A.; Farrell, B. Quilty; and Nolan, K. *Tetrahedron Lett*. **2007**, *48*, 1017.

Das, N.; Arif, A. M.; Stang, P. *Inorg. Chem.* **2005**, *44*, 5798–5804.

Debono, N.; Labande, A.S.; Manoury, E.; Daran, J.-C.; Poli, R. *Organometallics* **2010** *29*, 1879.

DeLuca, N. W.; Elabd, Y. A. *J. Polym. Sci., Part B: Polym. Phys*. **2006**, *44*, 2201-2225.

Demirhan, F.; Yildirim, Ö.; Çetinkaya, B. *Transition Met. Chem.* **2003**, *28*, 558.

DENZO-SMN. (1997). Z. Otwinowski and W. Minor, Methods in Enzymology, **276**: Macromolecular Crystallography, part A, 307 – 326, C. W. Carter, Jr. and R. M. Sweets, Editors, Academic Press.

Dias, E. L.; Grubbs, R. H. *Organometallics* **1998**, *17*, 2758-2767.

Dias, E. L.; Nguyen, S. T.; Grubbs, R. H. *J. Am. Chem. Soc*. **1997**, *119*, 3887-3897.

Díaz Requejo, M. M.; Pérez, P. J. *Angew. Chem. Int. Ed.* **2005**, *44*, 5284.

Díez-González, S.; Marion, N.; Nolan, S. P. *Chem. Rev.* **2009**, *109*, 3612–3676.

Díez-González, S.; Nolan, S. P. *Topics Organomet. Chem*. **2007**, *21*, 47-82.

Dinger, M. B.; Nieczypor, P.; Mol, J. C. *Organometallics* **2003**, *22*, 5291–5296.

Dobereiner, G. E.; Nova, A.; Schley, N. D.; Hazari, N.; Miller, S. J.; Eisenstein, O.; Crabtree, R. H. *J. Am. Chem. Soc.* **2011**, *133*, 7547.

Donahue, J. P. *Chem. Rev.* **2006**, *106*, 4747.

Dorta, R.; Kelly, R. A.; Nolan, S. P. *Adv. Synth. Catal.* **2004**, *346*, 917–920.

Downs, H. H.; Buchanan, R. M.; Pierpont, C. G. *Inorg. Chem.* **1979**, *18*, 1736–1740.

Doyle, M. P.; Bryker, W. J. *J. Org. Chem*. **1979**, *44*, 1572-1574.

Dragutan, V.; Dragutan, I.; Verpoort, F. *Platinum Met. Rev.* **2005**, *49*, 33–40.

Dunbar, M. A., Balof, S. L., LaBeaud, L. J., Yu, B., Lowe, A. B., Valente, E.J., Schanz, H.-J. *Chem. Eur. J.* **2009**, *15*, 12435.

Dunbar, M. A., Balof, S. L., Roberts, A. N., Valente, E. J., Schanz, H.-J. *Organometallics* **2011**, *30*, 199.

Dunitz, J. D.; Orgel, L. E. *Nature* **1953**, *171*, 121.

Dunitz, J. D.; Orgel, L. E.; Rich, A. *Acta Cryst.* **1956**, *9*, 373.

Eiland, P. F.; Pepinsky, R. J. *Am. Chem. Soc*. **1952**, *74*, 4971.

Eleuterio, H. *Chemtech*, **1991**, *21*, 92-95.

Eleuterio, H. S. *Journal of Molecular Catalysis* **1991**, *65*, 55-61.

Elschenbrolch, C.; Bilger, E. *Organometallics* **1985**, *4,* 2068–2071.

Enders, D.; Niemeier, O.; Henseler, A. *Chem. Rev.* **2007**, *107*, 5606.

Er, J. A. V.; Tennyson, A. G.; Kamplain, J. W.; Lynch, V. M.; Bielawski, C. W. *Eur. J. Inorg. Chem.* **2009**, 1729.

Farrugia, L. J. *J. Appl. Cryst.* **1999**, *32*, 837.

Feldman, J.; Schrock, R. R. *Prog. Inorganic Chem.* **1991**, *39*, 1.

Fernández, I.; Lugan, N.; Lavigne, G. *Organometallics* **2012**, *31*, 1155.

Fogg, D. E.; dos Santos, E. N. *Coord. Chem. Rev.* **2004**, *248*, 2365.

Fraser, C. Grubbs, R. H. *Macromolecules* **1995**, *28*, 7248–7255.

Frey, G. D.; Öfele, K.; Krist, H. G.; Herdtweck, E.; Herrmann, W. A. *Inorg. Chim. Acta* **2006**, *359*, 2622-2634.

Frey, G. D.; Rentzsch, C. F.; von Preysing, D.; Scherg, T.; Mühlhofer, M.; Herdtweck, E.; Herrmann, W. A. *J. Organomet. Chem.* **2006**, *691*, 5725.

Fructos, M. R.; Belderrain, T. R.; de Frémont, P.; Scott, N. M.; Nolan, S. P.

Fu, Y. Z.; Manthiram, A. *Journal of Power Sources* **2006**, *157*, 222-225.

Fu, Y.; Manthiram, A. Guiver, M. D. *Electrochem. Commun.* **2007**, *9*, 905-910.

Fu, Y.; Manthiram, A.; Guiver, M. D. *Electrochem. Commun.* **2006**, *8*, 1386-1390.

Fu, Y.; Manthiram, A.; M. D., Guiver *Electrochem. Commun.* **2006**, *8*, 1386-1390.

Furstner, A. *Angew. Chem.* **2000**, *112*, 3140–3172.

Fürstner, A. *Angew. Chem. Int. Ed.* **2000**, *39*, 3012.

Fürstner, A.; Grabowski, J.; Lehmann, C. W. *J. Org. Chem.* **1999**, *64*, 8275–8280.

Fürstner, A.; Thiel, O. R.; Ackermann, L.; Schanz, H. J.; Nolan, S. P. *J. Org. Chem.* **2000**, *65*, 2204–2207.

Garber, S. B.; Kingsbury, J. S.; Gray, B. L.; Hoveyda, A. H. *J. Am. Chem. Soc.* **2000**, *122*, 8168–8179.

Gessler, S.; Randl, S.; Blechert, S. *Tetrahedron Lett.* **2000**, *41*, 9973.

Ghassemi, H.; McGrath, J. E. *Polymer* **2004**, *45*, 5847-5854.

Gibby, J. L. J. E.; Farnworth, M. V.; Tekavec, T. N. *J. Am. Chem. Soc.* **2002**, *124*, 15188-15189.

Gimeno, A.; Medio-Simon, M.; de Arellano, C. R.; Asensio, G.; Cuenca, A. B. *Org. Lett.* **2010**, *12*, 1900.

Gischig, S.; Togni, A. *Eur. J. Inorg. Chem*. **2005**, 4745.

Gischig, S.; Togni, A. *Organometallics* **2004**, *23*, 2479-2487.

Gischig, S.; Togni, A. *Organometallics* **2005**, *24*, 203.

Glorius, F. In *N-Heterocyclic Carbenes in Transition Metal Catalysis*; Springer Berlin Heidelberg: 2007; Vol. 21, p 1.

Gourdoupi, N.; Kallitsis, J. K.; Neophytides, S. *Journal of Power Sources* **2008**, *195*, 170-174.

Gourdoupi, N.; Papadimitriou, K.; Neophytides, S.; Kallitsis, J. K. *Fuel Cells* **2008**, *8*, 200-208.

Graham, P. J.; Lindsey, R. V.; Parshall, G. W.; Peterson, M. L.; Whitman, G. M. *J. Am. Chem. Soc*. **1957**, *79*, 3416.

Gray, H. B.; Sohn, Y. S.; Hendrickson, D. N. *J. Am. Chem. Soc.* **1971**, *93*, 3603–3612.

Gregson, C. K. A.; Gibson, V. C.; Long, N. J.; Marshall, E. L.; Oxford, P. J.; White, A. J. P. *J. Am. Chem. Soc*. **2006**, *128*, 7410-7411.

Grubbs R. H.; Chang, S. *Tetrahedron* **1998**, *54*, 4413–4450.

Grubbs, R. H. *Adv. Synth. Catal*. **2007**, *349*, 34;

Grubbs, R. H. *Handbook of Metathesis*; Wiley-VCH: Weinheim, Germany, 2003.

Grubbs, R. H. *Tetrahedron* **2004**, *60*, 7117–7140.

Grubbs, R. H.; Trnka, T. M. *Ruthenium-Catalyzed Olefin Metathesis*; Wiley VCH, Weinheim, Germany, **2005.**

Guerret, O.; Sole, S.; Gornitzka, H.; Teichert, M.; Trinquier, G.; Bertrand, G. *J. Am. Chem. Soc*. **1997**, *119*, 6668.

Guerro, M.; Pham, N. H.; Massue, J.; Bellec, N.; Lorcy, D. *Tetrahedron* **2008**, *64*, 5285-5290.

Guiver, M. D.; Apsimon, J. W.; Kutowy, O. *Journal of Polymer Science Part C: Polymer Letters* **1988**, *26*, 123-127.

Guiver, M. D.; Croteau, S.; Hazlett, J. D.; Kutowy, O. *British Polymer Journal* **1990**, *23*, 29-39.

Guiver, M. D.; Kutowy, O.; ApSimon, J. W. *Polymer* **1989**, *30*, 1137-1142.

Guiver, M. D.; Robertson, G. P. *Macromolecules* **1995**, *28*, 294-301.

Gülcemal, S. G.; Labande, A.; Daran, J.-C.; Çetinkaya, B. Poli, R. *Eur. J. Inorg. Chem*. **2009**, 1806.

Gusev, D. G. *Organometallics* **2009***, 28,* 763.

Hadei, N.; Kantchev, E. A. B.; O'Brien, C. J.; Organ, M. G. *Org. Lett.* **2005**, *7*, 1991.

Hahn, E.; Radloff, C.; Pape T.; Hepp, A. *Organometallics* **2008**, *27*, 6408.

Hahn, F. E. *Angew. Chem. Int. Ed.* **2006**, *45*, 1348.

Hahn, F. E.; Foth, M. *J. Organomet. Chem.*, **1999**, *585*, 241.

Hahn, F. E.; Jahnke, M. C. *Angew. Chem., Int. Ed.* **2008**, *47*, 3122–3172.

Hahn, F. E.; Langenhahn, V.; Lügger, T.; Pape, T.; Le Van, D. *Angew. Chem. Int. Ed.* **2005**, *44*, 3759;

Hahn, F. E.; Langenhahn, V.; Meier, N.; Lügger, T.; Fehlhammer, W. P. *Chem. Eur. J.* **2003**, *9*, 704-712.

Hahn, F. E.; Langenhahn, V.; Pape, T. *Chem. Commun.* **2005**, 5390-5392.

Hahn, F. E.; Paas, M.; Van, D. L.; Fröhlich, R. *Chem. Eur. J.* **2005**, *11*, 5080-5085.

Hahn, F. E.; Plumed, C. G.; Münder, M.; Lügger, T. *Chem. Eur. J.* **2004**, *10*, 6285-6293.

Hahn, F. E.; Wittenbecher, L.; Boese, R.; Bläser, D. *Chem. Eur. J.* **1999**, *5*, 1931.

Hahn, F. E.; Wittenbecher, L.; Le Van, D.; Fröhlich, R. *Angew. Chem., Int. Ed.* **2000**, *39*, 541.

Hanson, G. R.; Gates, K. E.; Noble, C. J.; Griffin, M.; Mitchell, A.; Benson, S. J. *Inorg. Biochem.* **2004**, *98*, 903.

Harlow, K. J.; Hill, A. F.; Wilton-Ely, J. D. E. T. *J. Chem. Soc., Dalton Trans.* **1999**, 285–291.

Harrison, W. L.; Hickner, M. A.; Kim, Y. S.; McGrath, J. E. *Fuel Cells* **2005**, 5, 201-212.

Hartl, F.; Vlcek, A. *Inorg. Chem.* **1991**, *30*, 3048–3053.

Hartmann, S.; Winter, R. F.; Brunner, B. M.; Sarkar, B.; Knödler, A.; Hartenbach, I. *Eur. J. Inorg. Chem.* **2003**, 876–891.

Hayashi, T.; Konishi, M.; Kobori, Y.; Kumada, M.; Higuchi, T.; Hirotsu, K. *J. Am.* Kelly, R. A., III; Clavier, H.; Giudice, S.; Scott, N. M.; Stevens, E. D.; Bordner, J.; Samardjiev, I.; Hoff, C. D.; Cavallo, L.; Nolan, S. P. *Organometallics* **2008**, *27*, 202.

He, M.; Bode, J. W. *J. Am. Chem. Soc.* **2007**, *130*, 418.

Hermann, W. A.; Köcher, C. *Angew. Chem. Int. Ed.* **1997**, *36,* 2162–2187.

Herrmann, W. A. *Angew. Chem. Int. Ed.* **2002**, *41*, 1290-1309.

Herrmann, W. A.; Baskakov, D.; Herdtweck, E.; Hoffmann, S. D.; Bunlaksananusorn, T.; Rampf, F.; Rodefeld, L. *Organometallics* **2006**, *25*, 2449-2456.

Herrmann, W. A.; Elison, M.; Fischer, J.; Köcher, C.; Artus, G. R. J. *Angew. Chem. Int. Ed.* **1995**, *34*, 2371.

Herrmann, W. A.; Goossen, L. J.; Artus, G. R. J.; Köcher, C. *Organometallics* **1997**, *16*, 2472-2477.

Herrmann, W. A.; Köcher, C. *Angew. Chem., Int. Ed.* **1997**, *36*, 2163–2187.

Herrmann, W. A.; Kocher, C.; Gooßen, L. J.; Artus, G. R. J. *Chem. Eur. J.* **1996**, *2*, 1627-1636.

Herrmann, W. A.; Köcher, K. *Angew. Chem. Int. Ed.* **1997**, *36*, 2163-2187.

Herrmann, W. A.; Mihalios, D.; Ofele, K.; Kiprof, P.; Belmedjahed, F. *Chem. Ber. Recl.* **1992**, *125*, 1795-1799.

Herrmann, W. A.; Öfele, K.; Preysing, D. V.; Herdtweck, E. *J. Organomet. Chem.* **2003**, *684*, 235–248.

Herrmann, W. A.; Roesky, P. W.; Elison, M.; Artus, G.; Öfele, K. *Organometallics* **1995**, *14*, 1085-1086.

Hickner, M. A.; Ghassemi, H.; Kim, Y. S.; Einsla, B. R.; McGrath, J. E. *Chemical Reviews* **2004**, *104*, 4587-4612.

Higuchi, M.; Ikeda, I.; Hirao, T. *J. Org. Chem.* **1997**, *62*, 1072-1078.

Hillier, A. C.; Grasa, G. A.; Viciu, M. S.; Lee, H. M.; Yang, C.; Nolan, S. P. *J. Organomet. Chem.* **2002**, *653*, 69-82.

Hillier, A. C.; Lee, H. M.; Stevens, E. D.; Nolan, S. P. *Organometallics* **2001**, *20*, 4246.

Hino, T.; Wada, T.; Fujihara, T.; Tanaka, K. *Chemistry Letters* **2004**, *33*, 1596–1597.

Hong, S. H.; Grubbs, R. H. *J. Am. Chem. Soc.* **2006**, *128*, 3508.

Hopffgarten, M.; Frenking, G. *Eur. J. Inorg. Chem.* **2009**, *2009*, 4607.

Horsfield, A.; Wassermann, A. *J. Chem. Soc., Dalton Trans.* **1972**, 187.

Huang, J. K. ; Schanz, H. J. ; Stevens, E. D.; Nolan, S. P. *Organometallics*, **1999**, *18*, 2370−2375.

Huang, J.; Stevens, E. D.; Nolan, S. P.; Peterson, J. L. *J. Am. Chem. Soc.* **1999***, 121*, 2674–2678.

Hunter; C. A.; Sanders, J. K. M. *J. Am. Chem. S*oc. **1990**, *112*, 5525.

Iglesias, M.; Beetstra, D. J.; Stasch, A.; Horton, P. N.; Hursthouse, M. B.; Coles, S. J.; Cavell, K. J.; Dervisi, A.; Fallis, I. A. *Organometallics* **2007**, *26*, 4800-4809.

International Tables for X-ray Crystallography (1992). Vol. C, Tables 4.2.6.8 and 6.1.1.4, A. J. C. Wilson, editor, Boston: Kluwer Academic Press.

International Tables for X-ray Crystallography. Vol. C, Tables 4.2.6.8 and 6.1.1.4, A. J. Wilson, Ed., Kluwer Academic Press, Boston, MA, 1992.

Iojoiu, C.; Maréchal, M.; Chabert, F.; Sanchez, J. Y. *Fuel Cells* **2005**, *5*, 344-354.

Ishiyama, T.; Takagi, J.; Ishida, K.; Miyaura, N.; Anastasi, N. R.; Hartwig, J. F. *Journal of the American Chemical Society* **2001**, *124*, (3), 390-391.

Iulianelli, A.; Basile, A. *International Journal of Hydrogen Energy* **2012**, *37*, 15241-15255.

Ivin, K. J.; Mol, J. C. *Olefin Metathesis and Metathesis Polymerization*, Acedemic Press, San Diego, **1997**.

Ivin, K. J.; Mol, J. C. *Olefin Metathesis and Metathesis Polymerization*, 1st ed.; Academic Press: San Diego, CA, 1997; (c) Ivin, K. J. *J. Mol. Catal. A.: Chem.* **1998**, *133*, 1–16.

Jackstell, R.; Frisch, A.; Beller, M.; Röttger, D.; Malaun, M.; Bildstein, B. *J. Mol. Catal. A: Chem.* **2002**, *185*, 105.

Jafarpour, L.; Stevens, E. D.; Nolan, S. P. *J. Organomet. Chem.* **2000**, *606*, 49-54.

Jahnke, M. C.; Hahn, F. E. *Top. Organomet. Chem* **2010**, *30*, 95.

Jeletic, M. S.; Jan, M. T.; Ghiviriga, I.; Abboud, K. A.; Veige, A. S. *Dalton Trans.* **2009**, 2764-2776.

Jo, T. S.; Kim, S. H.; Shin, J.; Bae, C. *J. Am. Chem. Soc.* **2009**, *131*, 1656-1657.

Jones, N. D.; Wolf, M. O. *Organometallics* **1997**, *16,* 1352–1354.

Jørgensen, M.; Lee, S.; Liu, X.; Wolkowski, J. P.; Hartwig, J. F. *J. Am. Chem. Soc.* **2002**, *124*, 12557-12565.

Kaim, W.; Sixt, T.; Weber, M.; Fiedler, J. *J. Organomet. Chem.* **2001**, *637*, 167–171.

Kamber, N. E.; Jeong, W.; Waymouth, R. M.; Pratt, R. C.; Lohmeijer, B. G. G.; Hedrick, J. L. *Chem. Rev.* **2007**, *107*, 5813.

Kamplain, J. W.; Bielawski, C. W. *Chem. Commun.* **2006**, 1727.

Kamplain, J. W.; Lynch, V. M.; Bielawski, C. W. O*rg. Lett.* **2007**, *9*, 5401.

Kantchev, E. A. B.; O'Brien, C. J.; Organ, M. G. *Angew. Chem. Int. Ed.* **2007**, *46*, 2768-2813.

Kealy, T. J.; Pauson, P. L. *Nature* **1951**, *168*, 1039.

Kelly III, R. A.; Clavier, H.; Giudice, S.; Scott, N. M.; Stevens, E. D.; Bordner, J.; Samardjiev, I.; Hoff, C. D.; Cavallo, L.; Nolan, S. P. *Organometallics* **2008**, *27*, 202-210.

Kerres, J. A. *Fuel Cells* **2005**, *5*, 230-247.

Kerres, J.; Ullrich, A.; Häring, T.; Baldauf, M.; Gebhardt, U.; Preidel, W. *Journal of New Materials for Electrochemical Systems* **2000,** *3*, 229.

Kerres, J.; Ullrich, A.; Meier, F.; Häring, T. *Solid State Ionics* **1999,** *125*, 243-249.

Khramov, D. M.; Bielawski, C. W. *J. Org. Chem.* **2007**, *72*, 9407-9417.

Khramov, D. M.; Boydston, A. J.; Bielawski, C. W. *Angew. Chem. Int. Ed.* **2006**, *45*, 6186-6189.

Khramov, D. M.; Boydston, A. J.; Bielawski, C. W. *Org. Lett.* **2006**, *8*, 1831.

Khramov, D. M.; Lynch, V. M.; Bielawski, C. W. *Organometallics* **2007**, *26*, 6042.

Khramov, D. M.; Rosen, E. L.; Er, J. A. V.; Vu, P. D.; Lynch, V. M.; Bielawski, C. W. *Tetrahedron* **2008**, *64*, 6853–6862.

Khramov, D. M.; Rosen, E. L.; Lynch, V. M.; Bielawski, C. W. *Angew. Chem., Int. Ed.* **2008**, *47*, 2267–2270.

Kim, S.; Choi, S. Y.; Lee, Y. T.; Park, K. H.; Sitzmann, H.; Chung, Y. K. *J. Organomet. Chem.* **2007**, *692*, 5390-5394.

Kinder, R. E.; Zhang, Z.; Widenhoefer, R. A. *Org. Lett.* **2008**, *10*, 3157.

Kingsbury, J. S.; Harrity, J. P. A.; Bonitatebus, P. J.; Hoveyda, A. H. *J. Am. Chem. Soc.* **1999**, *121*, 791.

Kleiner, K. *Nature* **2006**, *441*, 1046-1047.

Knox, G. R.; Pauson, P. L.; Willison, D. *Organometallics* **1990**, *9*, 301–306.

Kojima, T.; Noguchi, D.; Nakayama, T.; Inagaki, Y.; Shiota, Y.; Yoshizawa, K.; Ohkubo, K.; Fukuzumi, S. *Inorg. Chem.* **2008**, *47*, 886–895.

Kojima, T.; Noguchi, D.; Nakayama, T.; Inagaki, Y.; Shiota, Y.; Yoshizawa, K.; Ohkubo, K.; Fukuzumi S. *Inorg. Chem.* **2008**, *47*, 886–895.

Komiya, S. *Synthesis of organometallic compounds: A practical guide*; J. Wiley & Sons, **1997.**

Kotz, J. C.; Nivert, C. L.; Lieber, J. M.; Reed, R. C. *J. Organomet. Chem.* **1975**, *91*, 87-95.

Kownacki, I.; Kubicki, M.; Szubert, K.; Marciniec, B. *J. Organomet. Chem.* **2008**, *693*, 321-328.

Krahulic, K. E.; Enright, G. D.; Parvez, M.; Roesler, R. *J. Am. Chem. Soc.* **2005**, *127*, 4142-4143.

Krejcik, M.; Danek, M.; Hartl, F. *J. Electroanal. Chem.* **1991**, *317*, 179.

Ku, R.-Z.; Huang, J.-C.; Cho, J.-Y.; Kiang, F.-M.; Reddy, K. R.; Chen, Y.-C.; Lee, K.-J.; Lee, J.-H.; Lee, G.-H.; Peng, S.-M.; Liu, S.-T. *Organometallics* **1999**, *18*, 2145-2154.

Kühl, O.; Saravanakumar, S.; Ullah, F.; Kindermann, M. K.; Jones, P. G.; Köckerling, M.; Heinicke, J. *Polyhedron* **2008**, 27, 2825.

Labande, A.; Daran, J.-C.; Manoury, E.; Poli, R. *Eur. J. Inorg. Chem.* **2007**, 1205-1209.

Lappert, M. F.; *J. Organomet. Chem.* **2005**, *690*, 5467.

Ledoux, N., Allaert, B., Linden, A., Van Der Voort, P., Verpoort, F., *Organometallics*, 2007, **26**, 1052–1056.

Lee, H. M.; Jiang, T.; Stevens, E. D.; Nolan, S. P. *Organometallics* **2001**, *20*, 1255.

Lee, J. K., Li, W., Manthiram, A., Guiver, M. D. *J. Electrochem. Soc.* **2009**, *156*, B46-B50.

Lee, J. K.; Li, W.; Manthiram, A. *J. Electrochem. Soc.* **2009**, *156*, B46-B50.

Lee, J. M.; Na, Y.; Han, H.; Chang, S. *Chem. Soc. Rev.* **2004**, *33*, 302.

Leibfarth, F. A.; Mattson, K. M.; Fors, B. P.; Collins, H. A.; Hawker, C. J. *Angew. Chem. Int. Ed.* **2013**, *52*, 199.

Leuthäußer, S.; Schmidts, V.; Thiele, C. M.; Plenio, H. *Chem. Eur. J.* **2008**, *14*, 5465-5481.

Leuthäusser, S.; Schwarz, D.; Plenio, H. *Chem. Eur. J.* **2007**, 13, 7195–7203.

Lever, A. B. P. *Inorganic Electronic Spectroscopy*, 2nd ed., Elsevier, Amsterdam, **1984**.

Li, W. Devlopment and Understanding of New Membranes Based on Aromatic Polymers and Heterocycles for Fuel Cells. Univesity of Texas at Austin, **2009**.

Li, W., Fu, Y.-Z., Manthiram, A., Guiver, M. D. *J. Electrochem. Soc.* **2009**, *156*, B258-B263.

Li, W.; Manthiram, A.; Guiver, M. D. *Electrochemical and Solid-State Letters* **2009**, *12*, B180-B184.

Li, W.; Manthiram, A.; Guiver, M. D. *Journal of Membrane Science* **2010**, *362*, 289-297.

Li, W.; Manthiram, A.; Guiver, M. D.; Liu, B. *Electrochemistry Communications* **2010**, *12*, 607-610.

Lin, J. C. Y.; Huang, R. T. W.; Lee, C. S.; Bhattacharyya, A.; Hwang, W. S.; Lin, I. J. B. *Chem. Rev.* **2009**, *109*, 3561.

Linnell, R. *The Journal of Organic Chemistry* **1960**, *25*, 290-290.

Liu, B.; Robertson, G. P.; Kim, D.-S.; Guiver, M. D.; Hu, W.; Jiang, Z. *Macromolecules* **2007**, *40*, 1934-1944.

Liu, G.; He, H.; Wang, J. *Adv. Synth. Catal.* **2009**, *351*, 1610–1620.

Liu, Z.; Yasseri, A. A.; Lindsey, J. S.; Bocian, D. F. *Science* **2003**, *302*, 1543-1545.

Lorkovic, I. M.; Duff Jr., R. R.; Wrighton, M. S. *J. Am. Chem. Soc.* **1995**, *117*, 3617-3618.

Lorkovic, I. M.; Wrighton, M. S.; Davis, W. M. *J. Am. Chem. Soc.* **1994**, *116*, 6220-6228.

Louie, J.; Gibby, J. E.; Farnworth, M. V.; Tekavec, T. N. *J. Am. Chem. Soc.* **2002**, *124*, 15188–15189.

Luján, C. Nolan, S. P. *Catal. Sci. Technol.* **2012**, *2*, 1027–1032.

Lüning, U. *Angew. Chem. Int. Ed.* **2012**, *51*, 8163.

Maishal, T. K.; Mondal, B.; Puranik, V. G.; Wadgaonkar, P. P.; Lahiri, G. K.; Sarkar, A. *J. Organomet. Chem.* **2005**, *690*, 1018–1027.

Marion, N.; de Fremont, P.; Lemiere, G.; Stevens, E. D.; Fensterbank, L.; Malacria, M.; Nolan, S. P. *Chem. Commun.* **2006**, 2048.

Marion, N.; Navarro, O.; Mei, J.; Stevens, E. D.; Scott, N. M.; Nolan, S. P. *J. Am. Chem. Soc.* **2006**, *128*, 4101-4111.

Marsella, M. J.; Maynard, H. D.; Grubbs, R. H. *Angew. Chem. Int. Ed.* **1997**, *36*, 1101-1103.

Martin, D.; Melaimi, M.; Soleilhavoup, M.; Bertrand, G. *Organometallics* **2011**, *30*, 5304.

Mas-Marzá, E.; Mata, J. A.; Peris, E. *Angew. Chem. Int. Ed.* **2007**, *46*, 3729-3731.

Masuda, J. D.; Schoeller, W. W.; Donnadieu, B.; Bertrand, G. *J. Am. Chem. Soc.* **2007**, *129*, 14180.

Mata, J. A.; Poyatos, M.; Peris, E. *Coord. Chem. Rev.* **2007**, 251, 841.

Matsushita, H.; Lee, S.-H.; Joung, M.; Clapham, B.; Janda, K. D. *Tet. Lett.* **2004**, *45*, 313.

McNitt, K. A.; Parimal, K.; Share, A. I.; Fahrenbach, A. C.; Witlicki, E. H.; Pink, M.; Bediako, D. K.; Plaisier, C. L.; Le, N.; Heeringa, L. P.; Griend, D. A. V.; Flood, A. H. *J. Am. Chem. Soc.* **2009**, *131*, 1305-1313.

Mercs, L.; Neels, A.; Albrecht, M. *Dalton Trans.* **2008**, 5570.

Merino, E.; Poli, E.; Díaz, U.; Brunel, D. *Dalton Trans.* **2010**, *41*, 10913.

Metallinos C.; Du, X. *Organometallics* **2009**, *28*, 1233.

Miller, J. S.; Krusic, P. J.; Dixon, D. A.; Reif, W. M.; Zhang, J. H.; Anderson, E. C.; Epstein, A. J. *J. Am. Chem. Soc.* **1986**, *108*, 4459–4466.

Miller, S. A.; Tebboth, J. A.; Tremaine, J. J. *J.Chem. Soc. (Resumed)* **1952**, 632.

Miller, T. M.; Ahmed, K. J.; Wrighton, M. S. *Inorg. Chem.* **1988**, *27*, 4326.

Miller, T. M.; Ahmed, K. J.; Wrighton, M. S. *Inorg. Chem.* **1989**, *28*, 2347–2355.

Min, S.; Kim, D. *Solid State Ionics* **2010**, *180*, 1690-1693.

Miyaura, N.; Suzuki, A. *Chem. Rev.* **1995**, *95*, 2457-2483.

Monsaert, S.; Canck, E. D.; Drozdzak, R.; Voort, P. V. D.; Verpoort, F.; Martins, J. C.; Hendrickx, P. M. S. *Eur. J. Org. Chem.* **2009**, 655–665.

Monsaert, S.; Drozdzak, R.; Dragutan, V.; Dragutan, I.; Verpoort, F. *Eur. J. Inorg. Chem.* **2008**,432–440.

Morgan, B. P.; Galdamez, G. A.; Gilliard, R. J., Jr.; Smith, R. C. *Dalton Trans.* **2009**, 2020.

Morgan, J. P.; Grubbs, R. H. *Org. Lett.* **2000**, *2*, 3153–3155.

Mori, H.; Miyoshi, E. *J. Theor. Comp. Chem.* **2005**, *4*, 333-344.

Muckerman, J. T.; Polyansky, D. E.; Wada, T.; Tanaka, K.; Fujita, E. *Inorg. Chem.* **2008**, *47*, 1787–1802.

Muddana, H. S.; Varnado, C. D.; Bielawski, C. W.; Urbach, A. R.; Isaacs, L.; Geballe M.T.; Gilson, M. K. *J. Comput. Aided Mol. Des.* **2012**, *26*, 475.

Murphy, V. J.; O'Hare, D. *Inorg. Chem.* **1994**, *33*, 1833–1841.

Navarro, O.; Marion, N.; Oonishi, Y.; Kelly III, R. A.; Nolan, S. P. *J. Org. Chem.* **2006**, *71*, 685-692.

N-Heterocyclic Carbenes in Synthesis, S. P. Nolan, ed., Wiley-VCH, Weinheim, **2006**.

N-Heterocyclic Carbenes in Transition Metal Catalysis, ed. F. Glorius, Springer-Verlag, Berlin, Germany, 2007; (c) *N-Heterocyclic Carbenes in Synthesis*; ed. S. P. Nolan, Wiley-VCH: Weinheim, 2006.

N-Heterocyclic Carbenes in Transition Metal Catalysis, F. Glorius, ed., Springer-Verlag, Berlin, Germany, **2007**

Nonnenmacher, M.; Kunz, D.; Rominger, F.; Oeser, T. *J. Organomet. Chem.* **2005**, *690*, 5647-5653.

Normand, A. T.; Cavell, K. J. *Eur. J. Inorg. Chem.* **2008**, 2781.

Norris, B. C.; Bielawski, C. W. *Macromolecules* **2010**, *43*, 3591.

Noviandri, I.; Brown, K. N.; Fleming, D. S.; Gulyas, P. T.; Lay, P. A.; Masters, A. F.; Phillips, L. *J. Phys. Chem. B* **1999**, *103*, 6713–6722.

O'Brien, C. J.; Kantchev, E. A. B.; Chass, G. A.; Hadei, N.; Hopkinson, A. C.; Organ, M. G.; Setiadi, D. H.; Tang, T.-H.; Fang, D.-C. *Tetrahedron* **2005**, *61*, 9723.

O'Brien, C. J.; Kantchev, E. A. B.; Valente, C.; Hadei, N.; Chass, G. A.; Lough, A.;. Hopkinson, C.; Organ, M. G. *Chem. Eur. J.* **2006**, *12*, 4743–4748.

Occhipinti, G.; Jensen, V. R.; Trnroos, K. W.; Frystein, N. G.; Bjrsvik, H. –R. *Tetrahedron* **2009**, *65*, 7186.

Öfele, K. *J. Organomet. Chem.* **1968**, *12*, P42-P43.

Öfele, K.; Herrmann, W. A.; Mihalios, D.; Elison, M.; Herdtweck, E.; Scherer, W.; Mink, J. *J. Organomet. Chem.* **1993**, *459*, 177-184.

Öfele, K.; Roos, E.; Herberhold, M. *Z. Naturforsch. B* **1976**, *31*, 1070-1077.

Organ, M. G.; Abdel-Hadi, M.; Avola, S.; Hadei, N.; Nasielski, J.; O'Brien, C. J.; Valente, C. *Chem. Eur. J.* **2007**, *13*, 150.

Otwinowski, Z.; Minor, W. In *Macromolecular Crystallography, Part A*; Carter Jr., C.; W., Sweets, R. M., Eds.; Academic Press: 1997; Vol. 276, p 307

Otwinowski, Z.; Minor, W. *Methods in Enzymology in Macromolecular Crystallography*, Part A, *276*, 307–326, C. W. Carter, Jr. and R. M. Sweets, Eds., Academic Press, 1997.

Özcubukcu, S.; Schmitt, E.; Leifert, A.; Bolm, C. *Synthesis* **2007**, 389.

Pal, S. K.; Alagesan, K.; Samuelson, A. G.; Pebler, J. *J. Organomet. Chem.* **1999**, *575*, 108–118.

Pauling, L. *The Nature of the Chemical Bond*; 3rd ed.; Cornell University Press: Ithaca, 1960.

Peeck, L. H.; Leuthaüsser, S.; Plenio, H. *Organometallics* **2010**, *29*, 4339–4345.

Peeck, L. H.; Plenio, H. *Organometallics* **2010**, *29*, 2761-2766.

Pefkianakis, E. K.; Morfopoulou, C.; Deimede, V.; Kallitsis, J. K. *Macromolecular Symposia* **2009**, *279*, 183-190.

Peng, H. M.; Webster, R. D.; Li, X. *Organometallics* **2008**, *27*, 4484-4493.

Peris, E. *Topics Organomet. Chem.* **2007**, *21*, 83-116.

Peris, E.; Crabtree, R. H. *Coord. Chem. Rev.* **2004**, *248*, 2239-2246.

Phillips, E. M.; Wadamoto, M.; Chan, A.; Scheidt, K. A. *Angew. Chem. Int. Ed.* **2007**, *46*, 3107.

Poater, A.; Cosenza, B.; Correa, A.; Giudice, S.; Ragone, F.; Scarano, V.; Cavallo, L. *Eur. J. Inorg. Chem.* **2009**, *2009*, 1759.

Poater, A.; Ragone, F.; Giudice, S.; Costabile, C.; Dorta, R.; Nolan, S. P.; Cavallo, L. *Organometallics*, **2008**, *27*, 2679.

Prins, R. *J. Chem. Soc., Chem. Commun.* **1970**, 280b–281.

Prins, R.; Korswagen, A. R. *J. Organomet. Chem.* **1970**, *25*, C74.

Prins, R.; Reinders, F. J. *J. Am. Chem. Soc.* **1969**, *91*, 4929.

Prühs, S.; Lehmann, C. W. ; Fürstner, A.; *Organometallics*, 2004, **23**, 280-287.

Purecha, V. H.; Nandurkar, N. S.; Bhanage, B. M.; Nagarkar, J. M. *Tet. Lett.* **2008**, *49*, 1384-1387.

Read de Alaniz, J.; Rovis, T. *J. Am. Chem. Soc.* **2005**, *127*, 6284.

Ren, X.; Springer, T. E.; Zawodzinski, T. A.; Gottesfeld, S., *Journal of The Electrochemical Society* **2000**, *147*, 466.

Ringenberg, M. R.; Kokatam, S. L.; Heiden, Z. M.; Rauchfuss, T. B. *J. Am. Chem. Soc.* **2008**, *130*, 788-789.

Ritter, T.; Hejl, A.; Wenzel, A. G.; Funk, T. W.; Grubbs, R. H. *Organometallics* **2006**, *25*, 5740–5745.

Robertson, N.; McGowan, C. A. *Chem. Soc. Rev.* **2003**, *32*, 96.

Rosen, E. L. PhD Thesis, University of Texas at Austin, 2009.

Rosen, E. L.; Sanderson, M. D.; Saravanakumar, S.; Bielawski, C. W. *Organometallics*, **2007**, *26*, 5774–5777.

Rosen, E. L.; Sung, D. H.; Chen, Z.; Lynch, V. M.; Bielawski, C. W. *Organometallics* **2010**, *29*, 250–256.

Rosen, E. L.; Varnado, C. D., Jr.; Tennyson, A. G.; Khramov, D. M.; Kamplain, J. W.; Sung, D. H.; Cresswell, P. T.; Lynch, V. M.; Bielawski, C. W. *Organometallics* **2009**, *28*, 6695–6706.

Sakurai, H.; Sugitani, K.; Moriuchi, T.; Hirao, T. *J. Organomet. Chem.* **2005**, *690*, 1750-1755.

Salman, H. M. A.; Mahmoud, M. R.; Abou-El-Wafa, M. H. M.; Rabie, U. M.; Crabtree, R. H. *Inorg. Chem. Commun.* **2004**, *7*, 1209–1212.

Samojłowicz, C.; Bieniek, M.; Grela, K. *Chem. Rev.* **2009**, *109*, 3708–3742.

Sanderson, M. D.; Kamplain, J. W.; Bielawski, C. W. *J. Am. Chem. Soc.* **2006**, *128*, 16514–16515.

Sanford, M. S.; Love, J. A.; Grubbs, R. H. *Organometallics* **2001**, *20*, 5314–5318.

Saravanakumar, S.; Kindermann, M. K.; Heinicke, J.; Kockerling, M. *Chem. Commun.* **2006**, 640.

Sashuk, V.; Peeck, L. H.; Plenio, H. *Chem. Eur. J.* **2010**, *16*, 3983–3993.

Sassano, C. A.; Mirkin, C. A. *J. Am. Chem. Soc.* **1995**, *117*, 11379-11380.

Scheiring, T.; Fiedler, J.; Kaim, W. *Organometallics* **2001**, *20*, 1437.

Scherer, G. N.; Maier, G.; Meier-Haack, J. Sulfonated Aromatic Polymers for Fuel Cell Membranes. In *Fuel Cells II*, Springer Berlin Heidelberg: 2008; Vol. *216*, pp 1 62.

Scheschkewitz, D. *Angew. Chem. Int. Ed.* **2008**, *47*, 1995.

Scholl, M.; Ding, S.; Lee, C. W.; Grubbs, R. H. *Org. Lett.* **1999**, *1*, 953–956.

Scholl, M.; Trnka, T. M.; Morgan, J. P.; Grubbs, R. H. *Tetrahedron Lett.* **1999**, *40*, 2247-2250.

Scholl, M.; Trnka, T.M.; Morgan, J.P.; Grubbs, R.H. *Tet. Lett.* **1999**, *40*, 2674.

Schrock, R. R. *Adv. Synth. Catal.* **2007**, *349*, 41.

Schrock, R. R. *Science* **1983**, *219*, 13-18.

Schrock, R. R.; Depue, R. T.; Feldman, J.; Schaverien, C. J.; Dewan, J. C.; Liu, A. H. *J. Am. Chem. Soc.* **1988**, *110*, 1423-1435.

Schrock, R. R.; Depue, R. T.; Feldman, J.; Yap, K. B.; Yang, D. C.; Davis, W. M.; Park, L.; Dimare, M.; Schofiled, M.; Anhaus, J.; Walborsky, E.; Evitt, E.; Kruger, C.; Betz, P. *Organometallics*, **1990**, *9*, 2262-2275.

Schrock, R. R.; Murdzek, J. S.; Bazan, G. C.; Robbins, J.; Dimare, M.; Oregan, M. *J. Am. Chem. Soc.* **1990**, *112*, 3875-3886.

Schubert, U.; Friedrich, P.; Orama, O. *J. Organomet. Chem.* **1978**, *144*, 175-179.

Schwab, P.; France, M. B.; Ziller, J. W.; Grubbs, R. H. *Angew. Chem. Int. Ed.* **1995**, *34*, 2039-2041.

Schwab, P.; France, M. B.; Ziller, J. W.; Grubbs, R. H. *Angew. Chem.* **1995**, *107*, 2179-2181.

Schwab, P.; Grubbs, R. H.; Ziller, J. W. *J. Am. Chem. Soc.* **1996**, *118*, 100-110.

Scott, N. M.; Clavier, H.; Mahjoor, P.; Stevens, E. D.; Nolan, S. P. *Organometallics* **2008**, *27*, 3181-3186.

Scott, N. M.; Nolan, S. P. *Eur. J. Inorg. Chem.* **2005**, *10*, 1815−1828.

Seo, H.; Kim, B. Y.; Lee, J. H.; Park, H.-J.; Son, S. U.; Chung, Y. K. *Organometallics* **2003**, *22*, 4783-4791.

Seo, H.; Park, H.-J.; Kim, B. Y.; Lee, J. H.; Son, S. U.; Chung, Y. K. *Organometallics* **2003**, *22*, 618.

Seo, H.; Roberts, B. P.; Abboud, K. A.; Merz, K. M.; Hong, S. *Org. Lett.* **2010**, *12*, 4860.

Shafir, A.; Power, M. P.; Whitener, G. D.; Arnold, J. *Organometallics* **2000**, *19*, 3978-3982.

Sharp, P. R.; Holmes, S. J.; Schrock, R. R.; Churchill, M. R.; Wasserman, H. J. *J. Am. Chem. Soc.* **1981,** *103*, 965-966.

Sheldrick, G. M. (1994). SHELXL97. Program for the Refinement of Crystal Structures. University of Gottingen, Germany.

Sheldrick, G. M. *Acta. Cryst.* **2008**, *A-64*, 112.

Sheldrick, G. M. In *SHELXTL00: Program for Refinement of Crystal Structures*; University of Göttingen: Göttingen, Germany, **2000.**

Sheldrick, G. M. SHELXL97, program for the refinement of crystal structures, University of Gottingen, Germany, 1994.

Shi, J.-C.; Yang, P.-Y.; Tong, Q.; Wu, Y.; Peng, Y. *J. Mol. Catal. A* **2006**, *259*, 7.

Shi, Z.; R. P. Thummel, *J. Org. Chem.* **1995**, *60*, 5935.

Shu, C.-F.; Wrighton, M. S. *Inorg. Chem.* **1988**, *27*, 4326-4329.

Sibert, J. W.; Forshee, P. B.; Lynch, V. *Inorg. Chem.* **2005**, *44*, 8602-8609.

Siemeling, U.; Auch, T. C.; Kuhnert, O.; Malaun, M.; Kopacka, H.; Bildstein, B. *Z. Anorg. Allg. Chem.* **2003**, *629*, 1334.

Siemeling, U.; Färber, C.; Bruhn, C. *Chem. Commun.* **2009**, 98-100.

Siemeling, U.; Farber, C.; Bruhn, C.; Leibold, M.; Selent, D.; Baumann, W.; von Hopffgarten, M.; Goedecke, C.; Frenking, G. *Chemical Science*, 697.

Siemeling, U.; Färber, C.; Leibold, M.; Bruhn, C.; Mücke, P.; Winter, R. F.; Sarkar, B.; Hopffgarten, M. V.; Frenking,G. *Eur. J. Inorg. Chem.* **2009**, 4607–4612.

SIR97. (1999). A program for crystal structure solution. Altomare, A.; Burla, M.C.; Camalli, M.; Cascarano, G.L.; Giacovazzo, C.; Guagliardi, A.; Moliterni, A.G.G.; Polidori, G.; Spagna, R. *J. Appl. Cryst.* **1999**, *32*, 115-119.

Sixt, T.; Fiedler, J.; Kaim, W. *Inorg. Chem. Commun.* **2000**, *3*, 80–82.

Slone, C. S.; Mirkin, C. A.; Yap, G. P. A.; Guzei, I. A.; Rheingold, A. L. *J. Am. Chem. Soc.***1997**, *119,* 10743–10753.

Slugovc, C.; Perner, B.; Stelzer, F.; Mereiter, K. *Organometallics*, **2004**, *23,* 3622-3626.

Sluis, P. V. D.; Spek, A. L. *Acta Cryst. A* **1990**, *46*, 194.

Sohn, Y. S.; Hendrickson, D. N.; Gray, H. B. *J. Am. Chem. Soc.* **1971**, *93*, 3603.

Sommer, W. J.; Weck, M. *Coord. Chem. Rev.* **2007**, *251*, 860.

Song, G.; Zhang, Y.; Li, X. *Organometallics* **2008**, *27*, 1936.

Spek, A. L. PLATON, a multipurpose crystallographic tool, Utrecht University, The Netherlands, **2000**.

Staub, B. F. *Angew. Chem., Int. Ed.* **2005**, *44*, 5974–5978.

Stevens, D.; Bordner, J.; Samardjiev, I.; Hoff, C. D.; Cavallo, L.; Nolan, S. P. *Organometallics* **2007**, *27*, 202.

Strohmeier, W.; Müller, F.-J. *Chem. Ber.* **1967**, *100*, 2812-2821.

Süßner, M.; Plenio, H. *Angew. Chem.* **2005**, *117*, 7045.

Sußner, M.; Plenio, H. *Angew. Chem. Int. Ed.* **2005**, *44*, 6885–6888.

Süßner, M.; Plenio, H. *Chem. Commun.* **2005**, 5417–5419.

Suzuki, A. *Journal of Organometallic Chemistry* **1999**, *576*, 147-168.

Szesni, N.; Drexler, M.; Maurer, J.; Winter, R. F.; de Montigny, F.; Lapinte, C.; Steffens, S.; Heck, J.; Weibert, B.; Fischer, H. *Organometallics*, **2006**, *25*, 5774.

Tafipolsky, M.; Scherer, W.; Öfele, K.; Artus, G.; Pedersen, B.; Herrmann, W. A.; McGrady, G. S. *J. Am. Chem. Soc.* **2002**, *124*, 5865-5880.

Tang, C. M.; Zhang, W.; Kerres, J. *Journal of New Materials for Electrochemical Systems* **2004**, *7*, 287-298.

Taton, T. A.; Chen, P. *Angew. Chem. Int. Ed.* **1996**, *35*, 1011.

Tennyson, A. G.; Kamplain, J. W.; Bielawski, C. W. *Chem. Commun.* **2009**, 2124.

Tennyson, A. G.; Lynch, V. M.; Bielawski, C. W. *J. Am. Chem. Soc.*, **2010**, *132*, 9420-9429.

Tennyson, A. G.; Ono, R. J.; Hudnall, T. W.; Khramov, D. M.; Er, J. A. V Kamplain, J. W.; Lynch, V. M.; Bielawski, C. W. *Chem. Eur. J.* **2009**.

Tennyson, A. G.; Ono, R. J.; Hudnall, T. W.; Khramov, D. M.; Er, J. A. V.; Kamplain, J.W.; Lynch, V. M.; Sessler, J. L.; Bielawski, C. W. *Chem. Eur. J.* **2010**, *16*, 304–315.

Tennyson, A. G.; Rosen, E. L.; Collins, M. S.; Lynch, V. M.; Bielawski, C. W. *Inorg. Chem.* **2009**, *48*, 6924-6933.

Thomas, J.-L.; Howarth, J.; Hanlon, K.; McGuirk, D. *Tetrahedron Lett.* **2000**, *41*, 413.

Thomas, K. R. J.; Lin, J. T.; Lin, H.-M.; Chang, C.-P.; Chuen, C.-H. *Organometallics* **2001**, *20,* 557–563.

Tolman, C. A. *Chem. Rev.* **1977**, *77*, 313-348.

Tolman, C. A. *J. Am. Chem. Soc.* **1970**, *9*, 2953; Strohmeier, W.; Müller, F.-J. *Chem. Ber.* **1967**, *100*, 2812.

Tonner, R.; Heydenrych, G.; Frenking, G. *Chemistry – An Asian Journal* **2007**, *2*, 1555.

Traill, P. R.; Bond, A. M.; Wedd, A. G. *Inorg. Chem.* **1994**, *33*, 5754-5760.

Trnka, T. M.; Grubbs, R. H. *Accounts Chem. Res.* **2001**, *34*, 18-29.

Trnka, T. M.; Morgan, J. P.; Sanford, M. S.; Wilhelm, T. E.; Scholl, M.; Choi, T.-L.; Ding, S.; Day, M. W.; Grubbs, R. H. *J. Am. Chem. Soc.* **2003**, *125*, 2546–2558.

Ulman, M.; Grubbs, R. H. *J. Org. Chem.* **1999**, *64,* 7202–7207.

Urbina-Blanco, C. A.; Bantreil, X.; Clavier, H.; Slawin, A. M.; Nolan, S. P. *Beilstein J. Org. Chem.* **2010**, *6*, 1120-1126.

Urbina-Blanco, C. A.; Leitgeb, A.; Slugovc, C.; Bantreil, X.; Clavier, H.; Slawin, A. M. Z.; Nolan, S. P. *Chem Eur. J.* **2011**, *17*, 5045–5053.

Varnado, C. D., Jr.; Lynch, V. M.; Bielawski, C. W. *Dalton Trans.* **2009**, 7253–7261.

Varnado, C. D., Jr.; Rosen, E. L.; Collins, M. S.; Lynch, V. M.; Bielawski, C. W. *Dalton Trans*. **2013**, DOI: 10.1039/c3dt51278a

Vazquez-Serrano, L. D.; Owens, B. T.; Buriak, J. M. *Chem. Commun.* **2002**, 2518.

Vazquez-Serrano, L. D.; Owens, B. T.; Buriak, J. M. *Inorg. Chim. Acta* **2006**, *359*, 2786.

Vernersson, T.; Lafitte, B.; Lindbergh, G.; Jannasch, P., A *Fuel Cells* **2006**, *6*, 340-346.

Vicent, C.; Viciano, M.; Mas-Marzá, E.; Sanaú, M.; Peris, E. *Organometallics* **2006**, *25*, 3713-3720.

Viciano, M.; Poyatos, M.; Sanaú, M.; Peris, E.; Rossin, A.; Ujaque, G.; Lledós, A. *Organometallics* **2006**, *25*, 1120-1134.

Vorfalt, T.; Leuthäusser, S.; Plenio, H. *Angew. Chem., Int. Ed.* **2009**, *48*, 5191–5194.

Vu, P. D. ; Boydston, A. J. ; Bielawski, C. W. ; *Green Chem.* **2007**, *9*, 1158-1159.

W. A. *Angew. Chem., Int. Ed.* **2002**, ***41***, 1290–1309.

Wada, T.; Fujihara, T.; Tomori, M.; Ooyama, D.; Tanaka, K. *Bull. Chem. Soc. Jpn.* **2004**, *77*, 741–749.

Wang, H. M. J.; Lin, I. J. B. *Organometallics* **1998**, *17*, 972-975.

Wanzlick, H.-W. *Angew. Chem.* **1962**, *74*, 129.

Wanzlick, H.-W.; Schönherr, H.-J. *Angew. Chem. Int. Ed.* **1968**, *7*, 141-142.

Ward, M. D.; McCleverty, J. A. *J. Chem. Soc., Dalton Trans*. **2002**, 275-288.

Warshawsky, A.; Kahana, N.; Deshe, A.; Gottlieb, H. E.; Arad-Yellin, R. *Journal of Polymer Science Part A: Polymer Chemistry* **1990**, *28*, 2885-2905.

Weinberger, D. A.; Higgins, T. B.; Mirkin, C. A.; Liable-Sands, L. M.; Rheingold, A. L. *Angew. Chem. Int. Ed.* **1999**, *38*, 2565.

Werner, H. *Angew. Chem. Int. Ed.* **2012**, *51*, 6052.

Wertheim, G. K.; Herber, R. H. *The Journal of Chemical Physics* **1963**, *38*, 2106.

Weskamp T., W. C. Schattenmann, M. Spiegler, W. A. Herrmann, *Angew. Chem., Int. Ed.*, **1998**, 37, 2490–2493.

Weskamp, T.; Kohl, F. J.; Hieringer, W.; Gliech, D.; Herrman, W. A. *Angew. Chem. Int. Ed.* **1999**, *38*, 2416–2419.

Williams, K. A.; Boydston, A. J.; Bielawski, C. W. *Chem. Soc. Rev.* **2007**, *36*, 729.

Willms, H.; Frank, W.; Ganter, C. *Chem. Eur. J.* **2008**, *14*, 2719.

Winberg, H. E.; Coffman, D. D. *J. Am. Chem. Soc.* **1965**, *87*, 2776-2777.

Winberg, H. E.; Downing, J. R.; Coffman, D. D. *J. Am. Chem. Soc.* **1965**, *87*, 2054.

Winter, R. F.; Hornung, F. M. *Organometallics* **1999**, *18,* 4005–4014.

Wolf, R.; Uhl, W. *Angew. Chem. Int. Ed.* **2009**, *48*, 6774.

Wolf, S.; Plenio, H. *J. Organomet. Chem.* **2009**, *694*, 1487-1492.

Yang, B.; Manthiram, A. *Electrochemical and Solid-State Letters* **2003**, *6*, A229-A231.

Yang, K.; Bott, S. G. Richmond, M. G. *Organometallics* **1995**, *14*, 2387–2394.

Yeung, L. K.; Kim, J. E.; Chung, Y. K.; Rieger, P. H.; Sweigart, D. A. *Organometallics*, **1996**, *15*, 3891-3897.

Yuan, Y.; Raabe, G.; Bolm, C. *J. Organomet. Chem.* **2005**, 690, 5747; Gischig, S.; Togni, *Organometallics*, **2004**, *23*, 2479.

Zanardi, A.; Corberán, R.; Mata, J. A.; Peris, E. *Organometallics* **2008**, *27*, 3570-3576.

Zanello, P.; Corsini, M. *Coord. Chem. Rev.* **2006**, *250*, 2000-2022.

Zhang, H.; Shen, P. K. *Chem. Rev.* **2012**, *112*, 2780-2832.

Zhang, W.; Bai, C.; Lu, X.; He, R. *J. Organomet. Chem.* **2007**, *692*, 3563–3567.

Zuo, Z.; Fu, Y.; Manthiram, A. *Polymers* **2012**, *4*, 1627-1644.

Vita

Charles Daniel Varnado Jr. was born in Baton Rouge, Louisiana to parents Danny and Dana Varnado. After graduating from Live Oak High School, he did construction work in refineries and power plants along the gulf coast for a couple years. In 2004 he migrated to Nacogdoches, Texas where he decided to study chemistry. After completing a B.S. at Stephen F. Austin State University in May 2007, he moved further west to Austin, Texas. Soon after he arrived, he joined the group of Prof. Christopher W. Bielawski. He completed an M.A. in December 2009 on novel ditopic ligands and their transition metal complexes. He then continued research in the Bielawski group to pursue a PhD focusing primarily on the design of redox-switchable olefin metathesis catalysts and new polymer electrolyte membranes for methanol fuel cells.

Permanent email: cdvarnado@gmail.com

This dissertation was typed by Charles Daniel Varnado Jr.